Studies on Catalysis by Vanadia Supported on Metal Oxides

Thesis submitted to the
Cochin University of Science & Technology
in partial fulfilment of the requirements for the degree of

Doctor of Philosophy
In
Chemistry
In the Faculty of Science

By
Sreejarani K.

Department of Applied Chemistry
Cochin University of Science And Technology
Kochi-22

August - 2002

CERTIFICATE

This is to certify that the thesis herewith is an authentic record of the research work carried out by Ms. Sreejarani K. under our supervision, in partial fulfilment of the requirements for the Degree of Doctor of Philosophy of Cochin University of Science and Technology, and further that no part thereof has been submitted before for the award of any other degree.

Dr. S. Prathapan,
(Supervising Guide)
Department of Applied Chemistry,
Cochin University of Science
and Technology,
Kochi-22,
India

Dr. S.Sugunan,
Professor and Head
(Supervising Co-Guide)
Department of Applied Chemistry,
Cochin University of Science
and Technology,
Kochi-22
India.

Kochi-22.
28-08-2002

CONTENTS

Chapter 1 : General Introduction and Literature Survey

Chapter 2 : Materials and Methods

Chapter 3 : Physico-Chemical Characterization

Chapter 4 : Friedel-Crafts Alkylation of Arenes

SECTION 2 : OXIDATIVE DEHYDROGENATION OF ETHYLBENZENE

Chapter 7 : Summary and Concluding Remarks

Preface

The drive to develop increasingly active and selective heterogeneous catalysts continues with considerable vigour. In the case of large and medium scale production processes particularly pharmaceutical and agrochemical areas, where high throughput synthesis and screening of potentially active compounds has become an economic imperative, the stimulation remains the need to increase profitability, process environmental acceptability and to develop more efficient and faster methods for synthesizing essential new products.

Vanadia based catalysts have attracted much attention in industry which play a key role in oxidation catalysis. In fact, almost all heterogeneous oxidation catalysts used on industrial scale for the production of fine chemicals contain vanadium as one of the major component of the active phase. Supported vanadium oxide catalysts are found to be superior to pure vanadia for its selective oxidation capacity. The interaction of the support is believed to modify the properties of the active surface vanadia species suitably so as to tune the system in an economically and industrially attractive mode.

It is well known that upon proper treatment with sulfuric acid or ammonium sulfate, many metal oxides develop a remarkable increase in surface acidity. These catalysts when calcined exhibit strong acid sites, which have opened new perspectives in the use of these environmental friendly solid catalysts for carrying out, industrially important reactions involving strong acid sites under milder conditions.

The present work is oriented to obtain a comparative evaluation of the physicochemical properties and catalytic activity of vanadia supported on metal oxide like SnO_2 and ZrO_2 and its sulfate modified compositions. Some reactions of industrial importance such as Friedel-Crafts reaction, Beckmann rearrangement of cyclohexanone oxime and selective oxidation reactions of aromatics have been selected for catalytic activity study in the present venture.

The work is presented in seven chapters, the last chapter giving the summary and conclusions of the results presented in the previous chapters. Our systems prove as potential catalysts for the benzylation of aromatics, where truly heterogeneous catalysts are rare and for Beckmann rearrangement reaction for the production of ε-caprolactam. Furthermore, the materials show considerable selective oxidation activities during oxidative dehydrogenation of ethylbenzene and cyclohexanol. There is plenty of scope for further research in this field, especially in the development of environmentally benign catalysts for alkylation, rearrangement and selective oxidation reactions of other aromatic substrates.

Chapter 1

General Introduction and Literature Survey

ABSTRACT

Heterogeneous catalysis is an interdisciplinary area, which has become the basis of industrial and environmental chemistry during this century. There is much renowned interest in the field of metal oxides since they are microporous materials with interesting physical as well as catalytic properties. Supported metal oxides exhibit interesting catalytic behaviour depending on the kind of support, the kind of active components and the preparation method. In particular, vanadium oxide catalysts in combination with various promoters are widely used for several reactions having industrial importance. In recent years, considerable interest has been focused on heterogeneous catalysis of organic reactions by sulfated metal oxides. In the present fundamental innovative research on supported vanadia systems reported in this thesis, a significant deviation is made by using SnO_2 and ZrO_2 as metal oxide supports with the investigation of the acidity generation by the sulfate anion modification. This chapter deals with the general introduction and literature review of the different components of the newly developed systems and the various reactions undertaken for the present investigation.

1.1 GENERAL INTRODUCTION

Catalysis is an essential but under-exploited technology in the manufacture of 'fine' or 'speciality' chemicals: typically end products and intermediates for pharmaceuticals, agrochemicals, electronics chemicals, consumer goods and food additives. Whilst there is much excellent and potentially valuable homogenous

catalytic chemistry in the academic literature, its application manufacturing scale is often restricted by economic, environmental, re and safety considerations. Heterogeneous systems, on the other hand, attractions like easier catalyst recovery, higher product selectivity, disposal of the used catalyst, design of continuous flow reactors and g they are accepted in the much versatile chemistry they offer.

Nearly eighty percentage of the heavy industrial chemicals is obt heterogeneous catalytic process. Commonly the heterogeneous cata solid and the reactants are either gases or liquids. A heterogeneous cat by providing an alternate reaction path with a lower energy of activati to global and domestic compulsions catalytic scientists have to dr strategies and plans relevant to basic research that would help developing and producing competitive heterogeneous catalysts and technologies in the global market. Using a catalytic material in indus requires a compromise in the properties of the catalysts to produce a which meets the contradictory demands imposed by industrial processe

Heterogeneous catalysts are classified into several ways. Based physico-chemical characteristics they can be divided as metal oxide metal oxides, mixed metal oxides, supported metal oxides and modifi oxides), supported metals/bimetallic catalysts, zeolites/ molecular siev hydrotalcites and solid supported heteropolysacids. Apart from this, also be classified on the basis of their functions as shape selective transfer, redox and acid-base catalysts. Another mode of classification on their behaviour in a particular reaction, as structure sensitive and s insensitive. Rates of structure sensitive catalytic reactions alter marked the crystallite size of the system is changed, whereas rate is independe crystallite size in structure insensitive reactions.

1.2 SOLID ACID CATALYSIS

Solid acid catalysis is one of the most important areas of resea has assumed great relevance as an economic alternative to

homogeneously catalyzed, industrially important reactions. The solid acid catalysts have many advantages over liquid Brönsted and Lewis acid catalysts. They are non-corrosive, environmentally benign, easily separable from the reaction mixture and pose few problems of disposal. The solid acid catalysts can also be designed to give higher activity, selectivity, regenerability and longer catalyst life. In the last two decades, substantial progress has been made and several industrial processes that use solid acid catalysts have been introduced successfully[1].

In recent years, a large variety of organic transformations have been reported using catalysts like zeolites and other microporous materials like clays, oxides and mixed oxides. Almost all acid catalyzed reactions, many of which require very corrosive acids in homogeneous conditions, have been achieved using solid acid catalysts[2]. Metal oxides, mixed oxides and supported oxides form a highly versatile class of catalysts due to their easily manipulated properties and/or a wide range of preparation variables. Titanium and vanadium based microporous materials have been accepted as efficient catalysts for oxidation reactions[3]. Cationic and anionic clays constitute another class of solid acids finding wide applications as ceramics, building materials, paper coatings, fillers, pharmaceuticals, etc[4].

1.3 METAL OXIDES IN HETEROGENEOUS CATALYSIS

Most of the solid acid-base catalysts used in various chemical transformations are based on inorganic oxides. In most cases these oxides are to be modified chemically or physically so as to get desired catalytic activity for a particular reaction. Oxides, because of their ability to take part in the exchange of electrons, protons or oxide ions, are used as catalysts in both redox and acid base catalysis[5]. In metal oxides, coordinative unsaturation is principally responsible for the ability towards the adsorption and catalysis of various reactions. The exposed cations and anions of the metal oxide surfaces form acidic and basic sites as well as acid-base pairs. Besides this, the variable

valency of the cation results in the ability of the oxides to undergo oxidations and reductions.

Generally these metal oxides are divided into four main categories, simple, mixed, modified and supported. Simple or single oxides usually offer poor catalytic activity and selectivity when compared to the multi-component systems. The major advantage of multi-component systems is that it is possible to tune oxygen sorption properties by meticulously choosing the required metal components so as to crystallize in a particular structural pattern. The reactivity of oxygen in this case is strongly dependent on the kind of neighbouring metal ions as well as M-O bonding distance and bond strength. According to Fuller *et al.*[6], the correlation between the catalytic activity and acid-base properties of the metal oxides can be explained by the strength of acid-base interaction between the reacting molecules and the catalyst surface. The generation of the new acid sites on mixing two oxides was first proposed by Thomas[7] and further developed by Tanabe and co-workers[8]. There seems to be a common view in these reports that the generation of new sites is associated with the charge imbalance at locally formed M_1-O-M_2 bonding, where M_1 is the host metal ion and M_2 is the doped or mixed metal ion. Some of the important reactions, which require metal oxides as catalysts are oxidations, oxidative dehydrogenations, dehydrodimerizations, and several acid-base catalyzed reactions.

1.4 TIN OXIDE AS CATALYST

Tin oxide has been widely used for inorganic materials. For instance, it has been studied regarding its ion-exchange properties[9]. Recently, there has been some interest in its properties as a semiconductor[10]. In its use as a catalyst, tin oxide is often used in the form of a mixed oxide. In the presence of tin oxide catalyst alone a few reactions are known, such as the oxidation of CO[11,12], the reduction NO_x[11,13], the oxidation of olefin[14], and isomerization of alkanes[15,16]. The systems prepared by depositing SnO_2 on SiO_2 or Al_2O_3 is of great interest because of the use of SnO_2 as gas sensor and conductive

coating[17]. Moreover, there is a great interest in SnO_2-based catalysts because of their wide range of applications in promoting various reactions. Tin oxide catalysts may exhibit different catalytic properties depending on the nature of the oxide carrier, since the metal-oxide support interaction affects both the redox properties and the dispersion of the active phase, the latter depending also on the tin content[18].

Pure SnO_2 is impractical as a heterogeneous catalyst because of its low activity. However, the mixed oxide system with some other metal oxides are known to be very effective for certain industrially important reactions[19]. There have already been several reports on partial oxidations using tin oxide containing binary catalysts such as SnO_2-MoO_3[20] SnO_2-P_2O_5[21], SnO_2-Sb_2O_5[22] and SnO_2-Bi_2O_3[23]. These combinations seem to induce an unexpectedly great change in the catalytic behaviour of the single tin oxide catalysts. Above all, the characteristic features of the selectivity become completely different as different sorts of metal oxides are incorporated into SnO_2[24]. Pt-SnO_2 and Pd-SnO_2 are found to be interesting catalysts for CO oxidation because of the synergic effects[11]. Catalytic property of tin oxides in benzene formation is highly enhanced by the addition of basic oxides whereas acrolien formation is promoted by acidic oxides[14].

Tin oxide, much like TiO_2, Fe_2O_3, UO_3, etc., is a metal oxide included in Group B, which is intermediate between the acidic metal oxides like V_2O_5, MoO_3 and WO_3 (Group A) and basic metal oxides such as NiO, MnO_2, CuO and Cr_2O_3 (Group C)[25]. It is reported that the acid-base property of the tin oxide system is significantly varied by the introduction of a small quantity of acidic or basic elements[24]. The IR spectra of adsorbed pyridine and ammonia revealed that tin oxide exhibit weak Lewis acidity, but does not show Brönsted acidity even in the presence of moisture.

Itoh *et al.*[16] showed that tin (IV) oxide evacuated above 400°C gave an ESR signal at 'g' value equal to 1.9, which was assigned to Sn^{3+}. The signal intensity varied with the evacuation temperature, showing a maximum at

500°C. The intensity of the signal decreased upon exposure to oxygen and on exposure to nitrobenzene, anion radicals were formed and the signal at 1.9 disappeared. These facts indicate that the paramagnetic centers are electron-donating sites and most of them are located on the surface of SnO_2. The acidity of SnO_2 calcined at 500°C was reported to be 0.133mmol g^{-1} as determined by the butylamine titration using methyl red indicator. However, acid sites stronger than $H_0 \leq 4.0$ were not detected[26].

The hydrous tin oxide efficiently catalyzed the reduction of carboxylic acid with 2-propanol in the vapour-phase at temperature ranging from 300-430°C, to give the corresponding alcohols. The partial oxidation of methanol over MoO_3-SnO_2 has been reported by Reddy *et al.*[27] and Murakami *et al.*[28] while the dimerization of formaldehyde was observed by Ai *et al.*[29] on SnO_2-WO_3 catalyst. Reductive halogenation of alkyl halides also proceeds over this catalyst[30]. Fuller *et al.*[6] reported the reduction of nitrous oxide by carbon monoxide over tin oxide catalyst. The reaction occurs principally by a redox mechanism involving CO chemisorption, CO_2 desorption *via* lattice oxygen abstraction and reduction of the catalyst by N_2O, the last being the rate-determining step. Oxidative dehydrogenation of ethylbenzene is also reported for catalysts containing SnO_2 as primary components[31,32].

1.5 ZIRCONIUM OXIDE AS CATALYST

Zirconium oxide is currently attracting considerable scientific interest due to its potential use as a catalyst support or promoter for a variety of catalyst systems. In recent years zirconium dioxide has become very important in the field of high technology ceramics with improved mechanical properties (particularly in wear parts, i.e., engine applications). Zirconia is modified by the addition of other oxides (Y_2O_3, MgO and CaO), which stabilizes the crystallographic phase and the microstructure required for a good performance as ceramic material[33].

The surface properties of zirconia catalysts have been extensively studied. Surface acidity and basicity of zirconium and its mixed oxide with

samarium was estimated by Hammett indicator technique[34]. Acid-base characteristics of binary oxides of Zr with Ce and La were examined by Sugunan *et al.*[35-37] and that of mixed oxides of ZrO_2 with SiO_2[38], SnO_2[26], TiO_2[39] and Y_2O_3[40] have also been reported. Shimokawabe *et al.*[41] carried out characterization of copper-zirconia catalysts prepared by impregnation method using tetramminecopper (II) nitrate solution. These precursors were transformed into bulky copper (II) oxide through highly dispersed copper (II) oxide depending on calcination temperature. Calafat *et al.*[42] reported the influence of preparation conditions on the surface area and phase changes of MoO_3-ZrO_2 catalysts. Addition of Mo preserves the metastable phase and increases the surface area of ZrO_2. The effects of tungsten precursor and preparation conditions on the properties of platinum free or platinum containing WO_x promoted zirconia have been studied[43]. Boyce *et al.*[44] investigated the crystallization behaviour of tungstate supported on zirconia and its relationship to acidic properties. Addition of silica stabilizes zirconia-tungstate against sintering by heat treatment. Spectroscopic studies on tetragonal ZrO_2 supported MoO_3 and NiO systems were conducted by Liu *et al.*[45] For tetragonal ZrO_2 supported MoO_3 system, LRS and UV-VIS DRS results indicate the formation of monomolybdate and polymolybdate species in samples with low and high Mo loadings respectively. In ZrO_2 supported NiO-MoO_3 binary oxide systems, the loading order of the oxides is critical for the species formed on the surface. No trace of $NiMoO_4$ phase could be detected after inversion of the loading sequence.

The catalytic activity of hydrous zirconium oxide calcined at different temperatures has been reported. Oppenauer oxidation of primary and secondary alcohols proceeded efficiently over hydrous zirconium oxide[46,47]. Convenient preparation of acetals over hydrous zirconium oxide is also reported[48]. Acetalization of carbonyl compounds occurred easily over hydrous zirconium oxide. Because of the low acidity of zirconium oxide, dehydration to methyl vinyl ketone was suppressed and the acetalization of the α,β-unsaturated ketone proceeded mainly at room temperature. Liquid-phase reduction of aldehydes and

ketones with 2-propanol was carried out over hydrous zirconium oxide[49]. The reaction is analogous to the well-known MPV reduction in which aldehydes and ketones are reduced with isopropanol in the presence of aluminum isopropoxide. *n*-Butane isomerization over tungsten oxide supported on zirconia was investigated by Yori *et al.*[42] Liquid-phase reduction of cyclohexanone in 2-propanol over ZrO_2-Y_2O_3[40] and mixed oxides of Zr, La and Al[37] have also been reported. The acid-base and surface electron properties and the catalytic activity of cerium-zirconium mixed oxides at various compositions towards the liquid-phase esterification of acetic acid with *n*-butanol were also tested[36].

1.6 VANADIUM OXIDE AS CATALYST

Vanadium oxide has an age-old history in the vast area of heterogeneous catalysis as the catalyst used for contact process. Vanadium (V) oxide compounds exists in a number of coordinations and structures[50]. The easy oxidation and reduction and the existence of cations of different oxidation states in the intermediate oxides have been proved to be important factors for vanadia to possess a prominent role in redox catalysis. Vanadium-based oxides are widely used as catalysts in oxidation reactions. However, for pure vanadia the selectivity to a desired product is too low, which often exhibits complete oxidation activity. It is accepted that addition of other metal oxides can significantly improve the catalytic activity and selectivity of single vanadium oxide catalyst. This is usually achieved by dispersing vanadium oxide on suitable support of required physical properties. The fine dispersion of active species on the support makes supported vanadia dominate over bulk vanadia. Thus supported vanadium oxide systems are drawing much attention nowadays as potential heterogeneous catalysts in selective oxidation reactions.

1.7 SUPPORTED VANADIA CATALYSTS

The catalytic properties of vanadium oxides are strongly influenced by the method of preparation, nature of the support and the type of promoters. In many cases, they are doped with promoters to improve their activity and /or selectivity, the supports being used to improve mechanical strength, thermal

stability and lifetime. Supports were believed to be inert in catalytic reactions; it is known now, however, the structure and composition of the materials used as supports can influence the activity and selectivity of the active vanadia phase to a marked degree[51-54]. The supports that are generally used for the preparation of these systems are Al_2O_3, TiO_2, Nb_2O_5 and SiO_2. Supported vanadia catalysts are renowned for their activity towards various types of partial or selective oxidation reactions, e.g., the oxidation of sulfur dioxide, carbon monoxide and hydrocarbons[55-59]. These systems have also been found to be effective catalysts for the oxidation of methanol to methyl formate[60,61]. Vanadia catalysts supported on titania-alumina mixed oxide were found to exhibit superior activities in selective catalytic reduction of NO_x[62-65].

Oxidative dehydrogenation of alkanes has been carried out over supported vanadia catalysts in presence of oxygen under suitable reaction conditions[66-68]. The catalytic behaviour of silica supported vanadia catalysts is observed to be superior to that of bulk V_2O_5 in oxidative dehydrogenations since the vanadium oxide species are mostly in tetrahedral coordination below the monolayer coverage and the vanadium ion in the bulk V_2O_5 are in octahedral coordination[69]. The rate of alkane conversion increases with vanadia content within the monolayer coverage for Al_2O_3-V_2O_5 systems[70] whereas titania supported vanadia catalysts[71] are observed to be very poor catalyst for this reaction. Wachs *et al.*[72] have studied the partial oxidation of methane over well dispersed vanadia systems on SiO_2, TiO_2, etc. where the highest formaldehyde selectivity was shown by V_2O_5-SiO_2 catalyst. Centi *et al.*[73] have reviewed the work on the nature of active layer in vanadium oxide supported on TiO_2 and control of its reactivity in the selective oxidation and ammoxidation of alkyl aromatics. Okuhara *et al.*[74] have shown that the over layers of vanadia species on SiO_2 and Al_2O_3 have highly pronounced influence on oxidation of alcohols.

An important application of supported vanadia is the selective catalytic reduction (SCR) of NO with ammonia[71,75]. Recently, highly active SCR catalysts

have been prepared[76,77] by a specific reaction of vanadyl alkoxides with the surface hydroxy groups of a TiO_2 support. Mixed oxide gels, in particular TiO_2-SiO_2 supports are being developed[76,78,79] to enhance further the activity, selectivity and stability of these catalysts.

Vanadium oxide catalysts in combination with various promoters are widely used for the selective oxidation of organic molecules. As a commercial catalyst, for selective oxidation of benzene, naphthalene and *o*-xylene, vanadium oxide has been watched for a long time. Recently it is also used in the preparation of maleic anhydride from 1-butene or *n*-butane. According to many studies, the partial oxidation on vanadium oxides was considered to be based on a redox mechanism[80-83] and the active sites were reported to be the V=O species[84-87]. The V=O bonds are known to be in the (010) plane of vanadium oxides[88]. Gasior and Machej[89] investigated the influence of the grain morphology of vanadium oxide on its activity and selectivity for the partial oxidation of *o*-xylene to phthalic anhydride. They found that the selectivity to phthalic anhydride could be correlated with the relative contribution of the (010) planes.

The catalysts used in ammoxidation of aromatic hydrocarbons are usually promoted and supported vanadium oxides. Propane ammoxidation was investigated by Nilsson *et al.*[90] using Al-Sb-V catalysts. Murakami *et al.*[28] used pure V_2O_5 and V_2O_5/ Al_2O_3 for ammoxidation of toluene. With VO_x/ TiO_2, benzaldehyde and benzylamine are the initial products at low ammonia and oxygen pressure[91]. Unsupported vanadium oxides are also active for ammoxidation of 3-picoline. VO_x/ TiO_2 (anatase and rutile) catalysts have been recently examined for the dehydration of N-ethyl formamide[92].

1.8 STRUCTURE OF SURFACE VANADIUM OXIDE SPECIES

In recent years, there has been growing emphasis on the study of the structure of the catalytically active surface phases containing vanadium in the case of supported vanadia catalysts. The existence of different surface vanadia species on various supports has been the subject of a number of studies. The actual structure present will depend amongst other things, on the chemical nature and

crystal structure of the support, the vanadium loading and on the presence of adventitious impurities. Metal-support interactions lead to several physical and morphological changes of the support as well as the active vanadia species.

Dispersion of vanadia on various support systems is reported by Schart *et al.*[93] and Sohn *et al.*[94] A rapid formation of a multilayered structure has also been observed on ZrO_2/ V_2O_5, as a consequence of weak interaction between the support and the dispersed vanadium oxide. If vanadium loading exceeds the theoretical monolayer, $Zr_2V_2O_7$ is formed[95]. Dependence of surface species formation on the acid-base behaviour of the support has been proved by various studies[93,96].

A series of investigations have shown that, depending on the vanadia coverage, various surface species are formed on the support materials. Isolated mono-oxo vanadyl groups and two-dimensional vanadium oxide clusters correspond to low coverages, whereas a separate V_2O_5 phase and polyvanadates are observed at higher coverages[97]. Wokaun *et al.*[93] have detected tetrahedral structures of vanadium oxide species at very low vanadia contents over TiO_2 by Raman spectroscopy. At higher vanadia loadings, a distorted two-dimensional surface bound vanadia phase is identified. The vanadium oxide species spontaneously form or self assemble by thermal treatments of physical mixtures of V_2O_5 on oxide supports[98-100]. This suggests that the vanadium oxide species possess thermodynamically preferred molecular structures that cannot be altered by preparation methods.

Deo and Wachs[101] have shown that a low surface coverage of vanadia on SiO_2 is due to somewhat lower density and reactivity of the silica surface hydroxyl groups with vanadia relative to the other oxide supports like Nb_2O_5, TiO_2 and Al_2O_3. However, Vogt *et al.*[102] have reported that dispersion of vanadia on silica can be improved by using special techniques other than the conventional impregnation methods. Scholten *et al.*[103] suggested that reducibility of the vanadium oxide structures increases with increase in surface coverage of V_2O_5/ γ-Al_2O_3 catalysts.

On MgO, isolated VO_4 tetrahedra without bridging V-O-V oxygen ions forming $Mg_3V_2O_8$ like structure, appeared within a large range of vanadium loading. Dimeric VO_4 tetrahedra of the type $Mg_3V_2O_7$ and mixed ortho and pyro magnesium vanadates have also been observed depending on the catalyst preparation procedure or vanadium loading[104-107]. Formation of the dispersed species at lower coverages and formation of crystalline vanadates are also observed in the case of metal oxides like La_2O_3, Sm_2O_3 and Bi_2O_3[108]. Characterization studies on V_2O_5/ SiO_2 by Eckert *et al.*[109] have shown the existence of the isolated tetrahedral structure of the type $(SiO)_3$-V=O in the dehydrated catalysts. At higher vanadia percentage, VO_4 tetrahedral units form aggregates leading to chains or bidimensional arrays where the V^{5+} ions become increasingly six coordinated. Vanadia crystallites appeared above 60% of monolayer coverage in the case of Al_2O_3 while for TiO_2, the crystalline vanadia appeared above 100% of the theoretical monolayer[110].

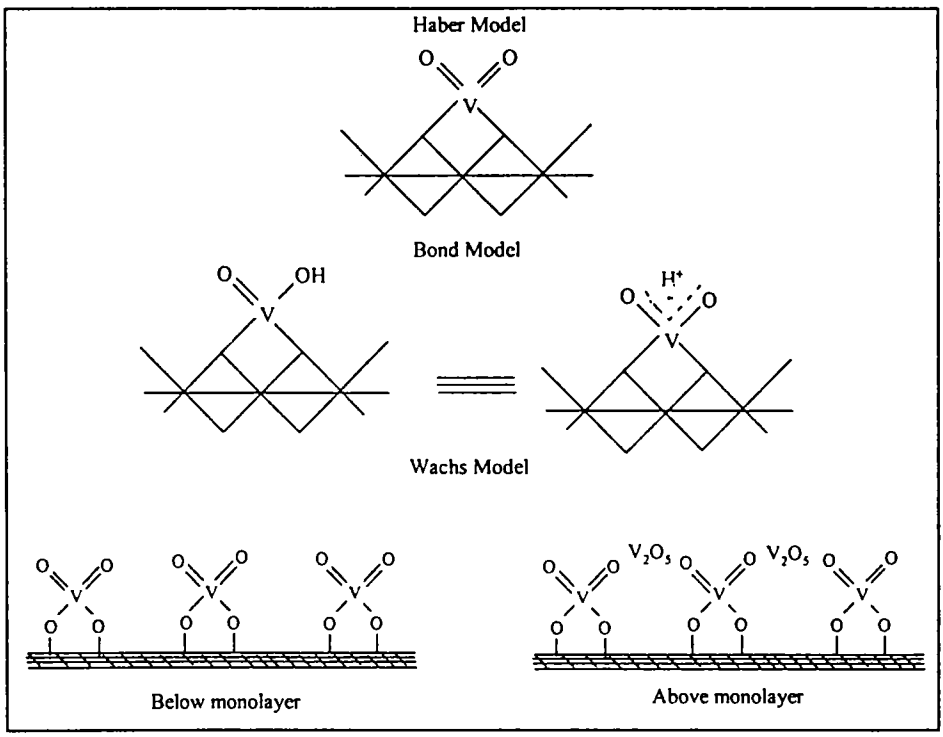

Figure 1.1
Structural models for the surface vanadia species.

Several authors have proposed various models for the molecular structure of surface vanadium oxide catalyst on different metal oxide supports[71,111-118]. The important ones are those proposed by Haber[71], Bond[111] and Wachs[112], which are shown in Figure 1.1. The Haber model shows isolated tetrahedral vanadate species and presents dioxo species containing two V=O groups on the support surface. This structure cannot explain the functionalities of catalysts with monolayer coverage. Bond model is the oxo hydroxy vanadium species or a structure in which the electrons are delocalized. It explains both the redox and acidic properties of surface vanadia species below monolayer coverages. The Wachs model identifies isolated vanadate species up to saturation coverage above which vanadia shows small-distorted crystallites in addition to the surface vanadate species.

1.9 SELECTIVE OXIDATION ACTIVITY AND ACIDITY GENERATION BY VANADIA LOADING

The most important aspect of supported vanadia systems is the selective oxidation activity towards partial oxidation products. The complete oxidation of organics is minimized in the case of supported vanadia systems, which thereby enhances selective oxidation products that are industrially important. The selective oxidation activity is attributed to the lattice oxygen mobility. Isotopic oxygen exchange reaction conducted on supported vanadia call attention to the significance of lattice oxygen mobility of the systems in oxidation reactions[119]. Two vacancies are required for the exchange and it is available on the catalyst surface of pure V_2O_5 indicating high oxygen mobility. All layers in the crystals can participate, because diffusion of oxygen is much faster. This will result in over oxidation. In the case of supported system, either one or two exchange may take place due to low diffusion rate since no bulk oxygen is available in supported V_2O_5, where the vanadia species are bound to the support. This inference can be applied to the activity of the catalysts for partial oxidation reactions.

Deo *et al.*[101] determined the reactivity of several supported systems in the partial oxidation of methanol. The selectivity towards acetaldehyde followed the same trend in oxygen exchange reaction. The above-mentioned order for supported system was also observed for the partial oxidation of butane to maleic anhydride[120].

The oxidation on supported vanadia catalysts are known to take place through Mars and Krevelen mechanism. In this mechanism, the reactant is first oxidized by lattice oxygen. The catalyst in turn is oxidized by gaseous oxygen to regenerate the system. According to Sachtler *et al.*,[121,122] the selectivity in partial oxidation reactions is determined by the intrinsic activity of oxygen species and their availability. On the supported metal oxides there is no large reservoir of bulk oxygen, which is able to abstract large number of hydrogen atoms. Hence the oxidation stops at a desired level of partially oxidized products, without leading to the complete oxidation. Thus the locally limited oxygen atoms may be responsible for the high selectivity of supported vanadia catalysts in oxidation reactions.

Vanadia addition increases both Lewis and Brönsted acidity. It is believed that the surface Brönsted sites are located at the bridging V-O-support bond. At lower percentage of vanadia, Brönsted acidity is found to increase while at higher composition, the number of both Lewis and Brönsted acid sites are enhanced[123]. Studies of Hatayama *et al.*[124] also suggest that the Brönsted acid sites increase with increase in vanadium oxide component in the supported systems. According to Miyata *et al.*[125] the vanadium ions act as the center for Lewis acidity.

2.0 SULFATED METAL OXIDES AS CATALYSTS

Acid catalysis plays a key role in many important reactions of the chemical and petroleum industries. Conventional industrial catalysts, such as H_2SO_4, $AlCl_3$ and BF_3, have unavoidable drawbacks because of its severe corrosivity and high susceptibility to water. The search for environmentally benign heterogeneous catalysts have driven the world wide ongoing research of

new materials as substitutes for current liquid acids and halogen-based solid acids[126]. Among them, sulfated zirconia and related materials displaying higher thermal stability, very strong acidity and high catalytic activity have aroused increasing interest[127-131]. These materials were long believed to be superacids with acidity stronger than 100% sulfuric acid[127]. The term has become quite contentious nowadays claiming that the acidity is not exceeding that of 100% sulfuric acid[132]. Again the acid type is also controversial[129]. There are reports that the catalytic activity derives mainly or completely, from protonic (Brönsted) acid sites. Other authors are equally convinced that the acid sites are aprotic (Lewis sites). Whatever may be the fact, the significantly higher activities of these oxides for carbocationic reactions have shown that the introduction of sulfate groups can generate very strong acid sites on the metal oxide surfaces[133]. The catalytic activity of these materials also depends on the sulfur content. Acylation of toluene with acetic and benzoic acids catalyzed by solid superacid was reported by Hino *et al.*[134] Acid sites stronger than H_o= -15 are needed for the formation of the acyl cation from a carboxylic acid. Metal oxides other than zirconia that show enhanced acidity on sulfation include Fe_2O_3[127], TiO_2[135], SnO_2[136], Al_2O_3[137] and HfO_2[138]. In addition, sulfation of binary oxides such as ZrO_2-TiO_2, ZrO_2-Al_2O_3, Cr_2O_3-ZrO_2, ZrO_2-SiO_2, ZrO_2-HfO_2 and ZrO_2-SnO_2 are also reported in literature.

In comparison with pure metal oxides, sulfate promoted metal oxides show a higher surface area after calcination at high temperature in air. Arata *et al.*[127,139] observed finer particles in sulfated zirconia than in pure zirconia. The larger surface area of sulfated zirconia can be attributed to the retardation of crystallization and the resistance to sintering at high temperatures[140-144]. The extraordinary activity of these catalysts is caused by a good stabilization of the surface intermediates in presence of the surface sulfate species. The mechanism of sulfate ions adsorption in the solid is an anionic exchange between the OH groups of the solid surface and HSO_4^- from the solution[145]. The acidity induced by the sulfate anion is then controlled by

the presence of OH groups on the original material, the number of which can be changed by the conditions of preparation and pretreatment. Many theories have been put forward to explain the strong acidity, the exact nature of which remains still controversial[146].

Different structures have been postulated for sulfate-doped metal oxides systems from time to time depending on various experimental observations. Arata and co-workers[127,139] proposed a bidentate sulfate structure for sulfated zirconia in which the sulfate group bridges across two Zr atoms. The IR data of adsorbed pyridine show the existence of both Brönsted and Lewis acid sites with easy conversion of Lewis to Brönsted acid sites by adsorption of water molecules. Arata pointed out that the S=O bond in the sulfate complex of the sulfated oxide is much stronger than that of simple metal sulfates. Thus the Lewis acid strength of Zr^{4+} sites becomes remarkably greater by the inductive effect of S=O in the complex. The Lewis acid sites predominate in the absence of water and after high temperature calcination. In presence of water, Lewis sites are converted into Brönsted acid sites *via.* proton transfer. The following models are proposed for the structure of surface sulfates on sulfated zirconia (Figure 1.2)

Models 1 and 2 are proposed by Tanabe and co-workers[127,139] for the sulfate modified zirconia in the absence and presence of moisture respectively. Models 3-5 are suggested by Lavalley *et al.*[147-149] for the same catalyst. Model 3 corresponds to a low sulfate loading, 4 to a high sulfate loading and 5 to low sulfate loading in presence of moisture. These sulfated oxides are important catalysts for the skeletal isomerization of *n*-alkanes and alkylation of aliphatics by olefins to produce high octane number gasoline in petroleum industry[127,140,146,150-155]. Sulfated metal oxides are also found to be effective for acylation and alkylation reactions[156,157]. These are also potential catalysts for the hydrocracking of hydrocarbon polymer waste materials to C_4-C_{20} liquids with gasoline components exceeding 75%[158].

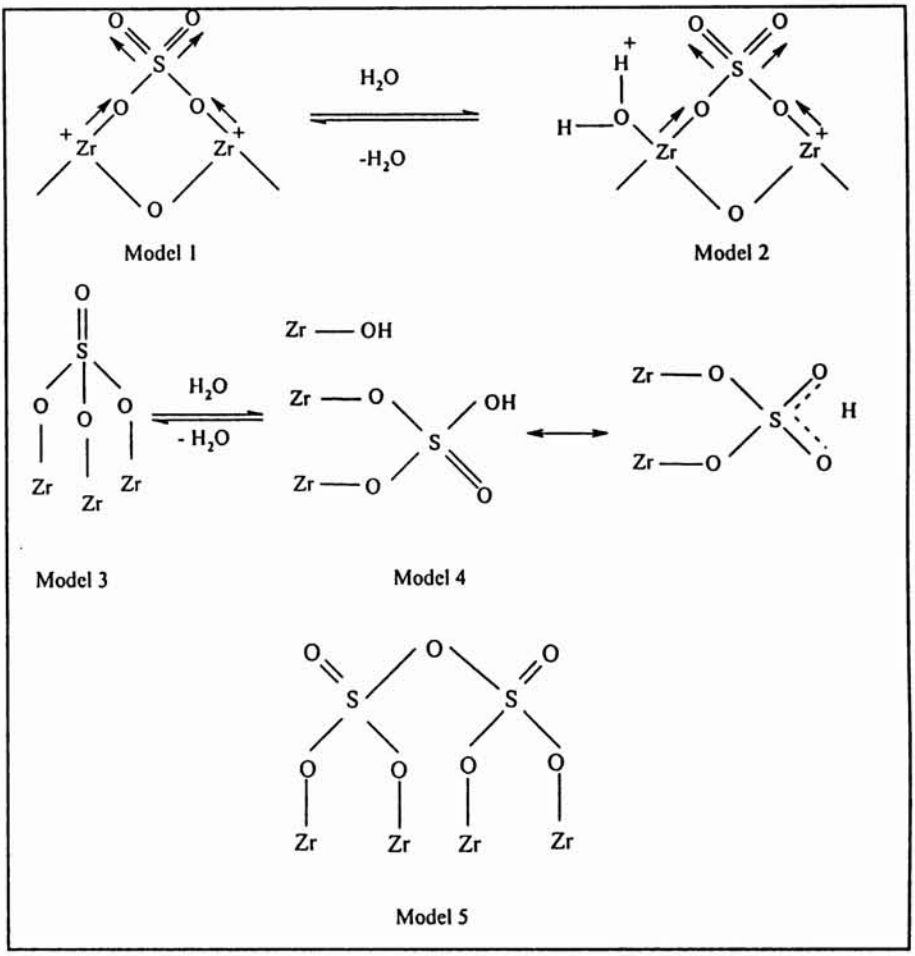

Figure 1.2

Different structural models for sulfated metal oxides

2.1 METAL PROMOTED SULFATED METAL OXIDES

In spite of their high activity, the sulfated metal oxide systems suffer from the major drawback of rapid deactivation. Several reasons have been proposed for this rapid deactivation such as change in sulfur oxidation state[159], sulfur leaching or decomposition during the reaction[160], coke deposition at high temperatures,[161] etc. Constant efforts are on the way to improve the stability and reusability of the systems. Incorporation of transition metal oxides has

been reported to enhance the stability of the surface sulfate species and the thermal stability. However, the nature of such an enhancement is vague. The processes involved when a support is impregnated with a solution of a metal salt are generally very complex. Metal distribution depends on the diffusion into the pore and the adsorption of the salt. Pore blocking can occur when big molecules of adsorbate diffuse into the small pores of the adsorbent and this will affect the distribution of the metal over the solid surface. Incorporation of the second or third component may affect the acidity and the catalytic activity of the oxides either positively or negatively, depending on the nature of the metal components.

Sulfated zirconia catalysts containing noble metals, most often platinum, has been the widely studied[127,162-165]. Wen *et al.*[164] suggested a bifunctional role of Pt whereas Ebitani *et al.*[166-169] considered that Pt induces a promoting effect of hydrogen by dissociation of the latter, which is followed by spill over and generation of strong Brönsted acid sites. It has been pointed out that presence of Pt, Rh and Ni on sulfated zirconia superacid catalysts improves the performance in skeletal isomerization of alkanes[166]. Hino[170] carried out preparation of iron-supported zirconia for the reaction of butane to isobutane.

Miao *et al.*[171] undertook a study on the sulfate promoted mixed oxide superacids. Among the sulfated binary oxides, the addition of Cr increases the catalytic activity most evidently. The addition of V, Ti, Al, Fe, Ni, or Co enhances the catalytic activity only slightly while the addition of Mo, W, Mn or Sn diminishes the catalytic activity. Comparing the data of sulfated ternary oxides, it is clear that the combination of Mn or V and Cr cannot further improve the catalytic activity of the Cr-Zr binary oxide system, but the addition of a third metal component to the Fe-Zr binary oxide system may increase the catalytic activity remarkably.

The promoting effect of Al on various types of sulfated metal oxide catalysts has been investigated[172]. Incorporation of appropriate amount of Al_2O_3 to sulfated titania and iron oxide before sulfation was found to increase

the acidity, activity and stability of the catalysts for the isomerization of *n*-butane and *n*-pentane significantly. The addition of Al_2O_3 stabilizes the surface sulfate complex on the oxides and increases the number of catalytically active acid sites on the catalysts. The high catalytic activity and slow deactivation are attributed to the increase in the number of intermediate strong acid sites providing long-term activity.

Sohn and Jang[173], who investigated the activity of sulfate modified and unmodified ZrO_2-SiO_2 towards 2-propanol dehydration and cumene dealkylation reactions, observed an enhancement of catalytic activity with the sulfated samples. Salmones *et al.*[174] determined the catalytic performance of $Pt/SO_4^{2-}/ZrO_2$-SiO_2 in the hydroisomerization of *n*-pentane and the catalytic activity was found to be dependent on the zirconia content. Catalytic properties of ZrO_2-SiO_2 for cyclohexene conversion (skeletal isomerization and hydrogen transfer) have also been studied[175]. XRD, TG-DTA, surface area measurement, FTIR and acidity determination by pyridine and dimethylpyridine chemisorption were used to characterize the samples. The effect of the sulfation on the surface structure and catalytic activity/selectivity was also studied. The characterization and catalytic activity studies of sulfated ZrO_2-TiO_2 mixed oxides were attempted by Lonyi *et al.*[176] Addition of titania as a second oxide to zirconia hinders its aggregation. It modifies the extensive properties, but not the intensive, acidic properties of the sulfated catalysts. The surface area of the sulfated mixed oxide was controlled by the titania rather than by the sulfate content.

Sulfated zirconia supported on alumina and silica was investigated by Lei *et al.*[177] Zirconyl nitrate was used as precursor for the preparation. In the case of SZ/Al_2O_3 series, the tetragonal phase was stabilized after supporting; the acid strength and the amount of strong acid sites also increased. However, for SZ/SiO_2 series, although the tetragonal phase of zirconia was stabilized, the lower number of strong acid sites probably limited the increase in catalytic activity for butane isomerization. Grau *et al.*[178] observed that the crystallization

temperature shifts to a higher value after supporting ZrO_2 on γ-alumina and SiO_2 carriers. However, the shift of the former is much larger than that of the latter, which implies a stronger interaction between ZrO_2 and γ-alumina. The interaction between zirconia and carriers limits the agglomerization of zirconia particles and thereby suppresses the tetragonal to monoclinic transformation. The catalytic activity of zirconia improved when it was combined with high surface area materials like SiO_2 or Al_2O_3[179]. Increased activity was obtained only when the additives and zirconia were mixed as hydroxides before calcinations, indicating that some mixed oxide formation occurs. Alumina is weakly acidic and displays strong interaction with zirconia, while silica is nonacidic and only weakly interacts with zirconia.

The effect of the preparation method and the nature of the sulfated mixed oxide catalysts on the acid strength distribution were examined by Vijayanand *et al*[180]. The supports were prepared by ammonia hydrolysis and precipitation from homogeneous solutions. The amorphous nature of the sulfated samples at 620°C may be due to the retardation of crystallization due to the presence of amorphous alumina or silica. Microcalorimetric measurements of ammonia adsorption indicate that the sulfation of metal oxides caused the enhancement of acid sites with $\Delta H>130$ kJ/mol. The microcalorimetric data suggest that the mixed oxides are strong acids but not superacids.

2.2 SURFACE ACIDITY OF METAL OXIDES AND ITS MEASUREMENT

The acid-base properties of metal oxide carriers can significantly affect the final selectivity of heterogeneous catalysts[181]. In acid catalysis, the activity, selectivity and stability of solid acids are determined to a large extent by their surface acidity, i.e., the number, nature, strength and density of acid sites. The acidity required for catalyzing the transformation of reactants into valuable products or into byproducts is quite different. Certain reactions demand strong acid sites, while some others are catalyzed by weak acid sites[182]. The rate of certain bimolecular reactions depends on the space between acid sites probably because their catalysis requires several acid sites[183,184]. For skeletal transformations of

hydrocarbons, the rate depends essentially on the Brönsted acidity of the catalysts[182,185]. Good correlation has been obtained between the concentration of Brönsted sites and the rate of cumene dealkylation[186,187], xylene isomerization[188], disproportionation of toluene[189] and ethylbenzene[190,191], *n*-hexane cracking[192], etc. Lewis sites in the vicinity of protonic sites increase the Brönsted acid strength and consequently their activity[193]. The dependence of the catalytic properties on the acid properties of solid catalysts is often more complex for the reactions of functional compounds. The acid sites (Lewis and/or Brönsted) and base sites, which co-exist in adjacent positions on the surface of acid catalysts, participate together in most of these reactions (acid-base bifunctional catalysis)[181]. The rate and selectivity of reactions that do not occur by acid catalysis can also be affected by acidity. This is evident from the oxidation of hydrocarbons on transition metal oxides. Acid-base properties of these oxides either influence the adsorption and the desorption rates of the reactants and products or initiate side reactions[194]. The acidity of solids plays a significant role when these are used as supports. Interaction of the support with the active component can influence their catalytic properties. Thus, characterization of the acidity of catalysts is an important step in the prediction of their catalytic utility[195].

Benesi method (*n*-butylamine titration) has been widely employed as a conventional method for determining the acid strength distribution of solid acid surfaces[196,197]. This involves the titration of the solid acid suspended in a non-aqueous medium like benzene with *n*-butylamine. When suspended in non-aqueous medium in presence of the indicator, the solid develops a colour depending on the pK_a value of the indicator as well as that of the solid acid. If the colour developed is that of the acid form of the indicator, then H_o of the acid is less than or equal to the pK_a of the conjugate acid of the indicator. The lower the pK_a of the indicator, the higher the acid strength of the solid. It is assumed that the adsorption equilibrium of both amine and indicator molecules with acid sites is attained on the solid surface. This assumption has been questioned on the basis of the heterogeneity and anisotropy of solid surfaces. The establishment of adsorption equilibrium needs the adsorption-

readsorption cycles of basic molecules once adsorbed on the surface. According to Take *et al.*[198] it is very difficult for either *n*-butylamine or indicators, particularly the former, to reach adsorption equilibrium with acid sites under the usual conditions in the *n*-butylamine titration method. This was also confirmed by Deeba and Hall[199] and Adeeva *et al.*[200] by independent works. Disregard of this difficulty might lead to an overestimation of the acid strength. Some serious limitations are also associated with the experimental procedure like the uncertainty in observing the colour changes of indicators by naked eyes, possible interaction between solvents and catalysts, etc. This method is also not suitable for coloured materials and may have some problems when the pores of solids are too small for the large molecules of the indicators to get adsorbed and if there exists any interactions between indicators and any sites (basic or redox sites) other than acidic sites.

Another method most frequently used is based on the chemisorption of basic compounds[181,185,194]. Adsorption of bases followed by calorimetry or thermodesorption of stable bases followed by gravimetry or volumetry gives the total number of acid sites (Lewis and Brönsted) and their distribution according to their strength but do not differentiate between Lewis and protonic acid sites. The temperature programmed desorption (TPD) of an adsorbed base like pyridine[201-203], NH_3[203-208], benzene,[203,205,209] etc. can be used for characterizing the acid strength distribution and amount. The method, when applied to sulfated systems, however, suffers from the major drawback associated with the strong interaction between the adsorbate molecules and the surface sulfate species leading to oxidative decomposition of the adsorbed species during heating.

IR spectroscopy of a solid on which pyridine or ammonia is adsorbed can be employed to distinguish between Lewis and Brönsted acid sites. The nature of acid sites contributes to hinder the pyridine chemisorption. While no specific configuration is required for the formation of the pyridinium ion on Brönsted sites, coordinated pyridine interacts with its electron pair on Lewis centers in a configuration perpendicular to the surface sites implying larger diffusion restrictions in the case of microporous solids. There are IR bands characteristic of pyridine adsorbed on Brönsted acid sites (1545 cm^{-1}) and pyridine adsorbed

on Lewis site (1440-1465 cm^{-1}). The existence of both Brönsted and Lewis acid sites on sulfated zirconia is confirmed by the diffuse reflectance IR spectra of adsorbed pyridine[210]. Kustov *et al.*[211] determined the Brönsted acidity of sulfated zirconia by adsorption of a weak base like benzene. The band shift of OH groups to lower frequency due to hydrogen bonding with the benzene molecules was taken as a measure of Brönsted acid strength. The larger the shift, the stronger is the acid strength. Pyridine (Py) and dimethylpyridine (DMP), which specifically adsorb on Lewis and Brönsted sites, have been used as probe molecules to investigate the surface acidic properties. Pyridine is adsorbed on the Lewis acid sites by donation of lone pair of nitrogen to the acid site (donation to a coordinatively unsaturated cation) whereas pyridinium ions are adsorbed on Brönsted acid sites. DMP is specifically adsorbed on Brönsted sites due to steric effect and due to its higher basic strength it will detect even the weakest acid centers[212,213]. IR spectroscopic investigation after pyridine adsorption reveals quasi-identical concentration of Lewis and Brönsted sites at low calcination temperatures (below 600°C). For higher calcination temperatures, Lewis acidity increased at the expense of Brönsted acidity[214].

Hall and co-workers[132,215] developed a UV-visible spectroscopic method for the measurement of acidity of solid catalysts. They pointed out that, due to red shifts of bands of unprotonated indicators, the visual observation of an yellow colour on adsorption can be misleading, and the spectroscopic determination of peak maxima is essential for correct determination of the acid strength using Hammett indicators. Electron paramagnetic resonance (EPR) is able to detect paramagnetic carbocations formed by the charge transfer between surface sites and organic molecules. This has been used to characterize strong ionizing sites on solid acid catalysts using probe molecules, which are difficult to ionize, such as benzene. Coster *et al.*[216] used aniline as a probe molecule and obtained signals for the corresponding radical cation. Yamaguchi *et al.* reported that the adsorption of perylene on sulfated zirconia gave the typical EPR signal corresponding to a radical cation whereas no signal was observed for the nonsulfated ZrO_2 indicating that the oxidizing property of ZrO_2 is generated by the introduction of the sulfate ion[217].

Acid strength of metal oxide catalysts can also be measured by NMR technique[218]. The ^{31}P solid magic angle spinning (MAS) NMR spectroscopy of adsorbed trimethyl phosphine (TMP) is an effective method for probing the acidity of heterogeneous catalysts[216, 219-222]. The method has the advantage over infrared spectroscopy of adsorbed pyridine in that the amount of TMP bound in a particular state can be readily quantified[221]. The acidity of a catalyst surface can also be determined by using appropriate test reactions. The most widely used examples include decomposition of alcohols,[24,223,224] cracking of aromatic hydrocarbons and isomerization of alkenes[225].

2.3 CUMENE CRACKING REACTION

The cracking of alkyl aromatic hydrocarbons is a very specific reaction. Cumene is a conventional model compound for testing the catalytic acidity since it undergoes different reactions over different types of acid sites. The cumene conversion reaction can be schematically represented as shown in Figure 1.3.

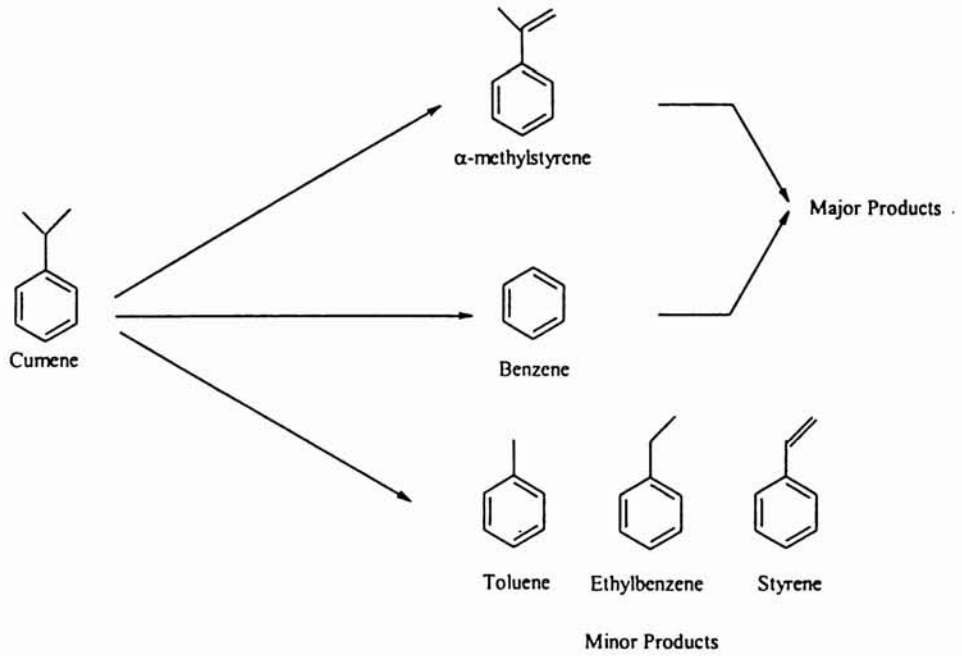

Figure 1.3
General scheme for cumene cracking reaction.

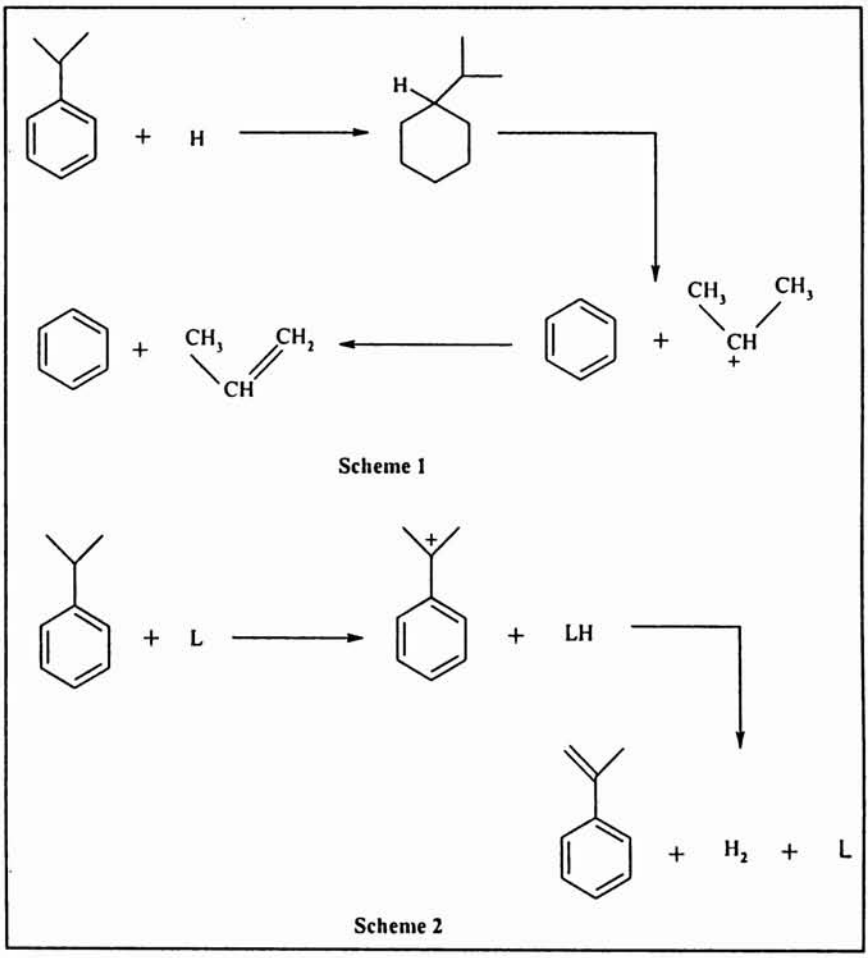

Figure 1.4
Mechanism of cumene conversion reaction.

The major reactions occurring during cumene conversion may be grouped into dealkylation (cracking) and dehydrogenation. Another possibility is the cracking of the alkyl chain to give ethylbenzene. Ethylbenzene on dehydrogenation gives styrene. Cracking of cumene to benzene (Scheme 1) is generally attributed to the action of Brönsted sites by a carbonium ion mechanism[226-229] while dehydrogenation of cumene yields α methylstyrene as the major product (Scheme 2), the formation of which

has been ascribed to the Lewis acid sites[226]. Mechanism of cumene conversion may be represented as in Figure 1.4.

Boorman *et al.* prepared a series of catalysts containing fluoride, cobalt and molybdenum as additives to γ-alumina, both individually and in combination. The surface acidity of these systems was correlated with their reactivity for cumene conversion[230,231]. Sohn and Jang[173] correlated the activity for cumene dealkylation with both acidity and acid strength distribution of sulfated ZrO_2-SiO_2 catalysts.

2.4 REACTIONS SELECTED FOR THE PRESENT STUDY

The best method for characterization of industrial catalysts is through model reactions[182,194]. The operating conditions being similar to those of industrial processes, they provide a more correct evaluation of the catalytic utility. The literature survey on supported vanadia systems revealed that they form a technologically important class of solid catalysts that are extensively used in chemical industry. They are widely used as catalysts for various oxidations, ammoxidation and selective catalytic reductions in general. The sulfated metal oxides are well known for its acidity and are extensively used in various industrially important acid-catalyzed reactions. Therefore we have selected reactions from both the domains, such as Friedel Crafts alkylation of aromatics and Beckmann rearrangement representing the acid catalyzed reactions; oxidation of cyclohexanol and oxidative dehydrogenation of ethylbenzene representing the oxidation reactions.

I. Friedel-Crafts Alkyaltion of Aromatics

Friedel-Crafts alkylation constitutes the most important method for the introduction of alkyl chains to the aromatic rings. A wide range of homogeneous catalysts like $FeCl_3$, $AlCl_3$ and BF_3 and protonic acids like HF and H_2SO_4 have been found to be well suited for the reaction[232,233]. These catalysts, however, suffer from the inherent drawback of extreme corrosivity, high susceptibility to water and difficulty in catalyst recovery. The

stoichiometric amounts of the catalyst with respect to the benzylating agent required for the reaction make the work-up procedure tedious. The moisture sensitivity of these homogeneous catalysts demand moisture-free solvents and reactants, anhydrous catalyst and dry atmosphere for its handling. The high Lewis acidity of these homogeneous catalysts also results in several undesirable side reactions leading to secondary reaction products. The general scheme of the reaction can be represented as in Figure 1.5.

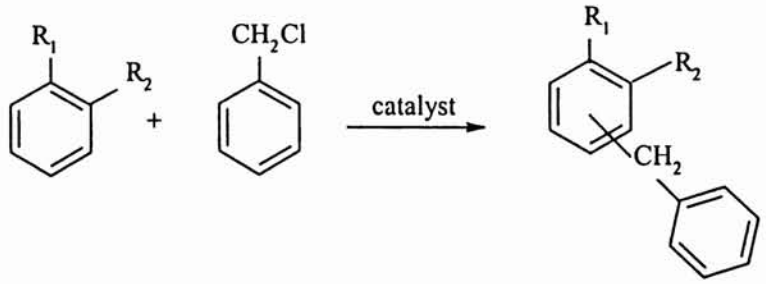

Arene Benzyl chloride Monoalkylated product (MAP)

R_1, R_2= H: Benzene;
R_1=H, R_2=CH_3: Toluene
R_1, R_2= CH_3 : *o*-Xylene

Figure 1.5
Scheme for Friedel-Crafts benzylation of arenes.

The development of solid acid catalysts has been a breakthrough in this field. The environmental concerns and the drive towards a "clean technology" prompt the replacement of the liquid acids by eco-friendly solid acid catalysts. Strongly acidic reagents are generally required for the efficient catalysis of Friedel-Crafts reactions. A wide range of solid acid catalysts from clays[234-236] and zeolites[237-241] to heteropolyacids[242-244] has been widely tested for their applicability towards this reaction.

Ga_2O_3 and In_2O_3 supported on mesoporous Si-MCM-41 or even on micro- or macroporous inert catalyst carriers were found to be efficient for the catalysis of benzylation of benzene and alkylation of aromatics even in

presence of moisture[245]. Catalytic activity of mesoporous molecular sieves has also been tested for the alkylation of benzene[246,247], toluene and *m*-xylene[246]. Lanthanum trichloride supported on silica acted as an active catalyst for the alkylation and acylation[248,249]. $LaCl_3$ deposited on K-10 montmorillonite was recovered quantitatively on the support after use whereas for analogous scandium catalyst only 12% of the scandium salt was recovered.

Shape selectivity and high acidity comparable to that of liquid acids render zeolites a good option for the Friedel-Crafts reactions[250]. Botella *et al.*[251] investigated the influence of reaction conditions and physico-chemical properties on the acylation of toluene with acetic anhydride over β-zeolite. Liquid-phase benzoylation and benzylation of *o*-xylene using various zeolite catalysts was carried out by Singh *et al.*[240,241]. Reaction time, xylene to benzyl/ benzoyl chloride molar ratio, reaction temperature, SiO_2/Al_2O_3 ratio, etc. were found to have a great influence on the percentage conversion and selectivity. Benzylation of naphthalene over H-β and H-Y zeolites using benzyl chloride as the benzylating agent has also been investigated[252].

Acid treated[253], pillared[254-256] and transition metal containing clays[257-259] also find wide use as Friedel-Crafts catalysts. A comparative study on H_2SO_4, HNO_3 and $HClO_4$ treated metakaolinite as Friedel-Crafts alkylation catalyst has been reported[260]. The effect of impregnating $ZnCl_2$, $FeCl_3$, $MnCl_2$, $SnCl_2$ and $AlCl_3$ on the catalytic activity of natural kaolinite and its activated form for the Friedel-Crafts alkylation of benzene with benzyl chloride is examined[261]. The process leads to catalysts with improved activity, the maximum activity being associated with $FeCl_3$. Montmorillonite supported zinc and nickel chlorides were proposed to be highly active and selective for Friedel-Crafts alkylation[257]. Lenarda *et al.*[262] investigated the catalytic activity of montmorillonite pillared with aluminium or aluminium-gallium polyoxycations and their respective repillared derivatives for the liquid-phase alkylation of benzene with ethylene to produce ethylbenzene.

Reports of superacidity in the sulfated metal oxides prompted several researchers to investigate on its application to different industrially important reactions, of which Friedel-Crafts reactions need special mention. Several reports are available in literature concerning the utility of these catalysts for Friedel-Crafts reactions[263,264]. James Clark[265] investigated the use of sulfated zirconia as catalysts for the alkylation of benzene with long chain linear alkenes to form linear alkylbenzenes. Samantaray[266] studied the physico-chemical properties and catalytic activity of sulfated titania for the gas-phase alkylation of benzene and substituted benzenes using isopropanol as alkylating agent. Catalytic activity was found to be dependent on the sulfate ion concentration in the catalyst and also benzene to alcohol molar ratio. Promoting effect of Al on sulfated oxide catalysts was subjected to investigation[267]. Introducing small amounts of alumina into sulfated zirconia, titania and iron oxide enhances the activity for the benzoylation of toluene with benzoyl chloride considerably. The enhanced long-term activity of Al-promoted catalysts is associated with an increase in acid sites of intermediate strength, which is caused by the formation of Al-O-Zr and Al-O-Ti bonds in the mixed oxides.

Inversion of relative reactivities and selectivities of benzyl chloride and benzyl alcohol in Friedel-Crafts alkylation with toluene using different solid acid catalysts was also investigated[268,269]. When reacted separately, benzyl chloride is more reactive than benzyl alcohol. It is proposed that when present together; benzyl alcohol is preferentially and strongly adsorbed on the catalytic sites and prevents any adsorption of benzyl chloride thereby blocking it from reacting with toluene. Only when some sites are vacant due to complete depletion of alcohol by reaction, benzyl chloride molecules get a chance to adsorb and react.

II. Beckmann Rearrangement of Cyclohexanone Oxime

ε-Caprolactam is an important starting material for nylon-6 synthesis. It is conventionally produced by the liquid-phase Beckmann rearrangement catalyzed by concentrated sulfuric acid. However, the reaction suffers several drawbacks

due to the corrossive nature of the sulfuric acid and by the large amount of ammonium sulfate formed. To avoid these problems vapour-phase Beckmann rearrangement has been attempted using various solid acid catalysts. The major product of the reaction is ε-caprolactam, while minor quantities of 5-cyanopentane, 5-cyanopent-1-ene, cyclohexanone and 2-cyclohexene-1-one are also formed as side products[270]. The reaction scheme is presented in Figure 1.6.

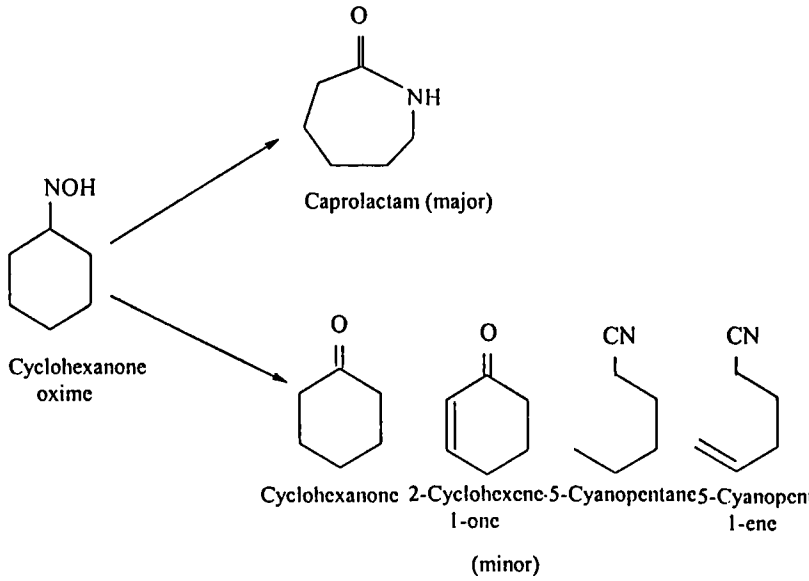

Figure 1.6
Reaction scheme for Beckmann rearrangement.

Silica-alumina[271] and H-Y zeolites[272] exhibit relatively low ε-caprolactam selectivity and short catalytic life while high ε-caprolactam selectivity is exhibited by SiO_2- and Al_2O_3 supported B_2O_3 prepared by chemical vapour deposition (CVD)[273,274], high siliceous H-ZSM-5 zeolies[275,276], titanium silicate[277], SiO_2 supported Ta_2O_5[278] and SAPO-11 zeolite[279]. However, the catalytic lifetimes of these catalysts are too short to be used in industry.

Corma *et al.*[280,281] reported that ε-caprolactam is converted to 5-cyanopent-1-ene on H-Na-Y zeolite. Sato *et al.*[275, 276] found that on high siliceous ZSM-5, a catalyst with low acidity leads to high selectivity of ε-caprolactam due to the

smooth desorption of ε-caprolactam. Dai *et al.*[282-285] found that on mesoporous-silica (MCM-41 and FSM-16) and zeolite (H-β, H-LTL, H-OFF-ERI and H-USY) catalysts, ε-caprolactam selectivity and catalyst's lifetimes are improved in the presence of alcohol. These results imply that the smooth desorption of ε-caprolactam from the catalyst surface is an important factor for improving ε-caprolactam selectivity.

Ushikubo *et al.*[286,287] reported that hydrated tantalum oxides having strong acidic properties in its amorphous forms catalyze Beckmann rearrangement, but the yields of ε-caprolactam and catalyst life was insufficient. Silica supported tantalum oxide[288] prepared by the reaction between tantalum alkoxide and silica showed high catalytic effiency when compared to that of Ta/ SiO_2 prepared by impregnating acidic aqueous $TaCl_5$ solution on SiO_2.

After the possibility of heterogeneously catalyzed reaction was reported, considerable attention has been paid to the potential of zeolites to act as a catalyst in the vapour-phase Beckmann rearrangement of cyclohexanone oxime[277,280,284,289-292]. Solvent effect has been investigated in the liquid-phase Beckmann rearrangement over H-Beta catalyst[293]. It is revealed that the performance of the reaction is strongly dependent on the nature of the solvent. The facility of protonation of oxime is primarily dependent upon the competitive adsorption between substrate and the solvent.

Catalytic performance of titania-zirconia- supported boria catalysts is reported by Mao *et al* [294]. The acidic and catalytic properties of boria supported on binary oxide were found to be affected by the boria loading. It was suggested that the medium strength acid sites, which were characterized by ammonia TPD, are responsible for the selective formation of ε-caprolactam. As the boria loading increases, the strength and concentration of acid sites on the catalyst increases and the optimum boria loading of 12 wt% contained the maximum

number of medium strength acid sites. The trigonal coordinated boron species is responsible for the enhanced acidity and hence the catalytic activity.

In the reaction of cyclohexanone oxime over B_2O_3/ Al_2O_3, the activity diminished with process time, whereas the ε-caprolactam selectivity remained constant during the first five hours. The catalyst decay was attributed to the coke formed on the surface and the caprolactam selectivity was associated with the concentration of intermediate strength acid sites[295].

Molecular sieves like H-MCM-41[296], H-FSH-16[297], Al-MCM-41[298], SAPO-5[279], SAPO-11[299], etc. have been studied for the vapour-phase Beckmann rearrangement. For the reaction over H-MCM-41 and H-FSH-16 during six hour process time, the former exhibited better performance with 1-hexanol as diluent. Al-MCM-41 with Si/ Al mole ratio of 25 exhibited high catalytic activity using ethanol as solvent.

III. Cyclohexanol Oxidation

The selective oxidation of primary and secondary alcohols is extensively studied over vanadia-based catalysts. It has been reported recently that methyl formate can be directly formed with high selectivity and yield by catalytic methanol oxidation on V-Ti oxides[300-303]. High selectivity to formaldehyde in methanol oxidation was also reported with VO_x/SiO_2 and VO_x/SnO_2 catalysts[27,304]. Oxidative dehydrogenation of isopropanol over a number of metal oxide systems was studied by Gervasini *et al.*[305] and correlated the activity with the acid strength. The participation of V=O in determining the partial oxidation activity in ethanol oxidation was emphasized by several authors[306,307].

Various liquid-phase oxidation reactions have been studied using supported vanadia catalysts. Partial oxidation of cyclohexanol to cyclohexanone is an important commercial process, for the production of polyamides, nylon 6,6, urethane foams, adipic acid, in lubricating additives, etc[308]. The general scheme of the reaction is represented in Figure 1.7.

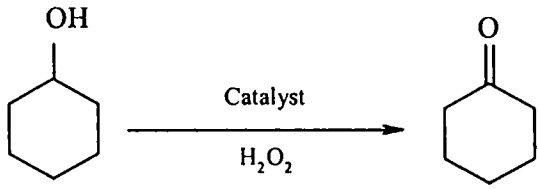

Figure 1.7
Selective oxidation of cyclohexanol to cyclohexanone.

The dehydrogenation reaction involved in alcohol oxidation usually competes with dehydration of the starting compound to olefin, which is produced in variable proportions depending on the particular catalyst and reaction conditions. Deo *et al.*[309] have suggested that in the case of vanadia-based systems, an active catalyst in selective oxidation reactions possesses a molecularly dispersed vanadium oxide phase, which is more active and selective than the bulk V_2O_5. The selective oxidation reactions over V-Ti oxides have suggested that the active catalytic species is likely to be a solid solution on V^{4+} in the TiO_2. The promoting effect of the vanadia has been explained as the effective dispersion of V_2O_5 on the titania surface and the weakening of V=O bonds.

The oxidation of cyclohexanol to cyclohexanone using hydrogen peroxide ad co-oxidant over vanadium and molybdenum containing heteropolyacids (HPA)[310] is recently reported. From the investigations, it was clear that the catalytic oxidation of cyclohexanol could be accelerated if the degree of vanadium substitution of the HPA catalyst is increased. The catalytic conversion is also observed to be dependant on the amount of hydrogen peroxide co-oxidant. It has been observed that as the number of vanadium atoms increases, the corresponding amount of V^{4+} also increases which is oxidized by hydrogen peroxide to V^{5+}. The results point to fact that vanadium in +5 oxidation state is the catalytically active center and the vanadium centers are more active than the corresponding molybdenum ions. However, only a limited number of literature reports are seen on the cyclohexanol oxidation activity of vanadia-based catalysts.

IV. Oxidative Dehydrogenation (ODH) of Ethylbenzene

Styrene is an important monomer used for industrial production of many synthetic polymers. It is commercially manufactured by the catalytic dehydrogenation of ethylbenzene[311,312]. Oxidative dehydrogenation involves the removal of hydrogen from the reactant molecules by oxygen from the feed to form the corresponding olefins without parallel or consecutive oxidation reactions giving carbon monoxide or dioxide as non- selective products.

Most work on the oxydehydrogenation of ethylbenzene has been devoted to the selection of suitable catalyst and appropriate reaction conditions for improved styrene yield and selectivity. The dehydrogenation of ethyl benzene was carried out over a variety of catalysts and reaction conditions of temperature, diluents and catalyst promoter. The general catalysts reported for the ODH of ethylbenzene includes metal oxides3[11,312], phosphates[319-322] and organic polymers[323,324]. The schematic representation of the reaction is given in Figure 1.8.

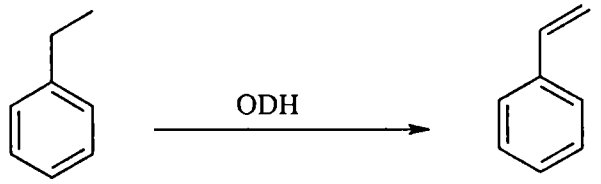

Figure 1.8
Oxidative dehydrogenation of ethylbenzene to styrene.

The oxydehydrogenation activity of various acidic catalysts has received increasing attention in recent years. Tagawa *et al.*[325,326] studied silica - alumina, tin oxides, and phosphates and concluded that moderate acid strength is the key factor for the reaction. Removal of strong acid sites by addition of sodium acetate improved the selectivity, but excessive sodium deactivated the catalyst. Fiedorow *et al.*[327]also obtained a similar result with alumina where small amounts of sodium did not affect activity even though strong acid sites would

have been removed. Echigoya *et al.*[328] found that introducing acidity into silica by addition of either magnesium or zirconium correlated well with oxydehydrogenation activity. Alumina is reported to be an active catalyst for the oxidative dehydrogenation of ethylbenzene and other alkylbenzenes[329-331]. Kania *et al.*[332] investigated the effect of incorporation of Fe_2O_3, Cr_2O_3, NiO, MoO_3 and MgO on the oxydehydrogenation activity of γ- alumina and observed that introduction of Fe_2O_3 and Cr_2O_3 leads to a considerable increase in the catalytic activity.

Jyothi *et al.* investigated the catalytic activity of rare earth promoted sulfated tin oxide for the oxidative dehydrogenation of ethylbenzene and found that these systems exhibits better oxidation activity when compared to the non-sulfated analogues and sulfated tin oxide[333]. Kim *et al.*[317] studied the influence of lanthana, ceria, praseodymia and neodymia incorporation on the activity of molybdena-alumina systems and among the four lanthanides used praseodymia showed the maximum promoting effect.

Oxidative dehydrogenation of alkanes has been carried out over various vanadia-based systems in presence of oxygen under suitable reaction conditions[66-68]. Silica supported vanadia catalysts showed considerable activity in the oxidative dehydrogenation of alkanes[334-339]. At very low surface coverage of vanadium oxide, the catalyst exhibited very high activity which was attributed to the highly dispersed species of $(Si\text{-}O)_3V{=}O$ formed on the silica surface. These species were shown to be more easily reducible than bulk vanadia. These findings proved that the redox properties are operative during ODH of lower alkanes. Similar effect of vanadia loading was also observed with Al_2O_3/V_2O_5 catalysts[340,341]. Le Bars *et al.*[342] have observed that V_2O_5 / γ-Al_2O_3 catalysts with the vanadia content ranging from 3 to 10 wt% have exhibited increased activity and selectivity above which the properties decreased. Mamedov *et al.*[343] have prepared active MVSb (M=Ni, Co, Bi, Sn) oxides supported on alumina for ethylbenzene oxidative dehydrogenation. The ethylbenzene conversion is observed to increase with increase in vanadium site

concentration at the surface of SnV, SbV and SnVSb oxide catalysts. Blasco *et al.*[344] studied and summarized the general factors, which affect the oxidative dehydrogenation activity of vanadia supported systems. According to them, apart from the extent of vanadia loading, there are some other factors, which control the activity and selectivity in the reactions. The selectivity is found to be dependant on the nature and size of the reactant fed. Aggregate forms of vanadia and its coordination number are the other factors, which influences the activity and selectivity of these systems. Both isolated and dimeric V^{5+} species are found to be active and selective towards the partial oxidation products. The reducibility plays a major role in selectivity; the more reducible the catalyst, the less selective the supported system towards the reaction.

2.5 OBJECTIVES OF THE PRESENT WORK

The recent advances made on the application of vanadia catalysts in a host of industrially important reactions prompted us to draw an ambitious programme of work on fundamental research on the development of new supported vanadia systems for oxidation and acid catalyzed reactions. Very interesting results have been reported in studies on the use of supported vanadia catalysts in various reactions to produce fine chemicals, olefins and to transform toxic molecules into environmental friendly species. In a bid to invent novel supports that would give more active and selective vanadia catalysts, metal oxides like SnO_2 and ZrO_2 were selected as the supports for the present investigation. The choice of these metal oxides was made on the literature information about the suitability as supports for preparing other catalysts. The sulfate modification of the supported systems were also tried to enhance the acidity of the catalyst surface. The aim was to combine the two significant features, i.e., selective oxidation capacity and acidity in the same system. Different vanadia loadings are attempted to modify the properties of the support and to get an understanding of the active species of vanadia on the support. A systematic investigation of the influence of vanadia loading on the properties of the supports has been carried out by various physico-chemical

characterization techniques. Vanadia addition as well as sulfate modification are expected to enhance the acidity of the systems. The surface acidic property of the prepared systems was also investigated in detail. The catalytic activity of the systems was screened for various industrially important reactions. The main objectives of the present work are the following.

- To prepare metal oxide (SnO_2 and ZrO_2) supported vanadia catalysts with different vanadium oxide content and its sulfated analogues by the wet impregnation method.
- To examine the surface properties and to understand the nature of surface vanadia species of these systems employing different instrumental techniques like EDX, BET surface area and pore volume measurements, FTIR, ^{51}V NMR, DR UV-VIS, etc.
- To explore the acidic character of the catalysts using various independent techniques such as TPD of ammonia, perylene adsorption method and cumene conversion test reaction.
- To investigate the catalytic efficiency of the samples towards Friedel-Crafts benzylation of arenes.
- To evaluate the catalytic performance of these systems in Beckmann rearrangement of cyclohexanone oxime.
- To test the catalytic activity of the systems in selective oxidation reactions like oxidation of cyclohexanol and oxidative dehydrogenation of ethylbenzene.

ଌ ଌ ଌ

REFERENCES

1. K. Tanabe and W. F. Holdderich, *Appl. Catal. A. Gen.*, 181 (1999) 399-434.
2. W. F. H. Foelderich and H. V. Bekkum, *Stud. Surf. Sci. Catal.*, 58 (1991) 631.

3. P. Kumar, R. Kumar and B. Pandey, *Synlett* (1995) 289.

4. A. Vaccari, *Appl. Clay Sci.*, 14 (1999) 161.

5. J. Haber, "*Perspectives in Catalysis*", Blackwell scientific publications, 1992, 371.

6. M. J. Fuller and M. E. Warwick, *J. Catal.*, 39 (1975) 412.

7. C. L. Thomas, *Ind. Eng. Chem.*, 41 (1949) 2564.

8. K. Tanabe and T. Takeshita., in "*Advances in Catalysis*", Academic press, New York, 17 (1967) 315.

9. J. D. Donaldson and M. J. Fuller, *J. Inorg. Nucl. Chem.*, 32 (1970) 1703.

10. N. Yamazoe, *Catal. Soc. Jpn.*, 28, (1986) 555.

11. M. J. Fuller and M. E. Warwick, *J. Catal.*, 29 (1973) 441.

12. E. W. Thorton and P.G. Harrison, *J. Chem. Soc., Faraday Trans.*, 1, 71 (1975) 461.

13. F. Solymosi and J. Kiss, *J. Chem. Soc., Chem. Comm.*, 1974, 509.

14. T. Seiyama, M. Egashira, T. Sakamoto and I. Aso, *J. Catal.*, 24 (1972) 76.

15. C. Chemball, H. F. Leach and I. R. Shannon, *J. Catal.*, 29 (1973) 99.

16. M. Itoh, H. Hattori and K. Tanabe, *J. Catal.*, 43 (1976) 192.

17. V. M. Jimenez, J. A. Mejias, J. P. Espinos, and A. R. Gonzalez-Ellipe, *Surf. Sci.*, 366 (1996) 545.

18. A. Auroux, D. Sprinceana, and A. Gervasini, *J. Catal.*, 195 (2000) 140-150.

19. D. J. Hucknall "*Selective Oxidation of Hydrocarbons*", Academic press, London, 1974.

20. J. Builen, *J. Catal.*, 10 (1968) 188.

21. Y. Marakami, M. Inagaki, K. Iwayama and H. Uchida, *Shokubai.*, 12 (1970) 89.

22. K. Wakabayeshi, Y. Kamiya and N. Ohta, *Bull. Chem. Soc. Jpn.*, 40 (1967) 2172.

23. T. Seiyama, T. Uda, I. Mochida and M. Egashira, *J. Catal.*, 34 (1974) 29.

24. M. Ai, *J. Catal.*, 40 (1975) 318-326.

25. M. Ai, and S. Suzuki, *Shokubai.*, 15 (1973) 159.

26. G. W. Weng, H. Hattori and K. Tanabe, *Bull. Chem. Soc. Jpn.*, 56 (1983) 2407.

27. B. M. Reddy, K. Narsimha, C. Sivaraj and P. Kanta Rao, *Appl. Catal.*, 55 (1989) L1-L4.

28. M. Niwa, H. Yamada, and Y. Murakami, *J. Catal.*, 134 (1992) 331-377.

29. M. Ai, *Appl. Catal.*, 9 (1984) 371-377.

30. K. Takashi, M. Shibagaki, H. Kuno and H. Matsushita, *Bull. Chem. Soc. Jpn.*, 67 (1994) 1107.

31. S. Kito. T. Hattori and Y. Murakami, *Appl. Catal.*, 48 (1989) 107.

32. T. Hattori, H. Niwa and A. Satsuma, *Appl. Catal.*, 50 (1989) 11-15.

33. R. Stevens, "*Zirconia and Zirconia Ceramics*", 2nd Ed., Magnesium Elektron Ltd., Manchester (1986).

34. S. Sugunan, Sunitha Kurur and Anto Paul, *Ind. J. Chem.*, 33A, (1994) 1096.

35. S. Sugunan, G. V. Chemparathy and Anto Paul, *Ind. J. Engg. Mater. Sci.*, 3 (1996) 45.

36. S. Sugunan and Binsy Varghese, *Ind. J. Chem.*, 37A (1998) 806.

37. S. Sugunan and Anto Paul, *Ind. J. Chem.*, 36A (1997) 300.

38. H. Dzisko, *Proc. Inter. Cong. Catal.*, Amsterdam (1964) 19.

39. K. Shibata, T. Kiyoura, J. Kitagawa, T. Sumiyoshi and K. Tanabe, *Bull. Chem. Soc. Jpn.*, 46 (1973).

40. S. Sugunan and Anto Paul, *Ind. J. Chem.*, 36A (1997) 1068.

41. M. Shimokawabe, H. Asakawa and N. Takezawa, *Appl. Catal.*, 59 (1990) 45.

42. A. Calafat, L. Avilan and J. Aldana, *Appl. Catal. A. Gen.*, 201 (2000) 215.

43. S. R. Vaudagna, R. A. Comelli and N. S. Figoli, *Appl. Catal. A. Gen.*, 164 (1997) 265.

44. R. A. Boyse and E. I. Ko, *J. Catal.*, 179 (1998) 100.

45. Z. Liu and Y. Chen, *J. Catal.*, 177 (1998) 3.

46. H. Kuno, K. Takahashi, M. Shibagaki and H. Matsushita, *Bull. Chem. Soc. Jpn.*, 63 (1990) 1943.

47. H. Kuno, M. Shibagaki, K. Takahashi and H. Matsushita, *Bull. Chem.Soc.Jpn.*, 64 (1) (1991) 312.

48. M. Shibagaki, K. Takahashi, H. Kuno and H. Matsushita, *Bull. Chem. Soc. Jpn.*, 63 (4) (1990) 1258.

49. M. Shibagaki, K. Takahashi and H. Matsushita, *Bull. Chem. Soc. Jpn.*, 61 (1988) 3283.

50. G. Deo, I. E. Wachs and J. Haber, *Cri. Rev. Surf. Chem.*, 4 (1994) 141.

51. M. Akimoto and E. Echigoya, *J. Catal.*, 29 (1973) 91.

52. D. Vanhove and M. Blanchard, *J. Catal.*, 37 (1976) 6.

53. M. S. Wanwright and T. W. Hoffman, *Can. J. Chem. Soc.*, 55 (1977) 552.

54. K. Hauffe and H. Raveling, *Ber. Bunsenges. Phy. Chem.*, 84 (1980) 912.

55. Y. Nagakawa, T. Ono, H. Miyata and Y. Kubokawa, *J. Chem. Soc. Faraday Tans.*, 1, 79 (1983) 2929.

56. H. Miyata, M. Kohno, T. Ono, and F. Hatayama, *J. Chem. Soc. Faraday Tans.*, 1, 85 (1989) 3663.

57. B. M. Reddy, I. Ganesh and B. Chowdhary, *Catal. Today*, 49 (1999) 115.

58. L. J. Lakhshmi, Z. Ju and E. C. Alyea, *Langmuir*, 15 (1999) 3521.

59. I. J. Doh, Y. I. Pae and J. R. Sohn, *J. Ind. Eng. Chem.*, 5 (1999) 161.

60. P. Forzatti, E. Tronoconi, G. Busca and P. Titarellp, *Catal. Today*, 1 (1987) 209.

61. G. Busca, A. S. Elmi and P. Forzatti, *J. Phy. Chem.*, 91 (1987) 5263.

62. G. Centi, S. Militerno, S. Perathoner, A. Riva and G. Barambilla, *J. Chem. Soc. Chem. Comm.*, (1991) 88.

63. G. Centi, S. Perathoner, B. Kartheuser, D. Rohan and B. Hoidnett, *Appl. Catal. B.*, 1 (1992) 129.

64. H. M. Matralis, M. Ciardelli, M. Ruwett and P. Grange, *J. Catal.*, 157 (1995) 368.

65. V. M. Mastikhin, V. V. Terskikh, O. B. Lapina, S. V. Filiminova, M. Seidl and H. Knovinger, *J. Catal.*, 156 (1995) 1.

66. I. M. Welch, L. J. Croce and H. F. Christmann, "*Hydrocarbon Process*", 57 (1978) 131.

67. T. G. Alkhazhov and A. F. Lisovskei, "*Oxidative Dehydrogenation of Hydrocarbons*", (in Russian) Khimia, Moscow (1980).

68. F. Cavani and F. Trifiro, *Appl. Catal. A.*, 88 (1992) 115.

69. E. A. Mamedov and V. C. Carberan, *Appl. Catal. A.*, 127 (1995) 1.

70. J. G. Eon, R. Oliver and J. C. Volta, *J. Catal.*, 145 (1994) 318.

71. J. Haber, A. Kozilowska and R. Kozlowski, *J. Catal.*, 102 (1986) 255.

72. Q. Sun, J. Hehng, H. Hu, R. G. Hermann, I. E. Wachs and K. Klier, *J. Catal.*, 165 (1997) 91.

73. G. Centi, *Appl. Catal. A.*, 147 (1996) 267.

74. K. Inumaru, M. Misono and T. Okuhara, *Appl. Catal. A.*, 149 (1997) 133.

75. H. Bosch and F. Jansen, *Catal. Today.*, 2 (1998) 369.

76. A. Baiker, P. Dollenmeier, M. Glinski and A. Reller, *Appl. Catal.*, 35 (1987) 35.

77. M. Schrami-Marth, W. Fluhr, A. Wokoun and A. Baiker, *Ber. Bunsenges. Phy. Chem.*, 93 (1989) 852.

78. B. E. Handy, A. Baiker, K. L. Walther and A. Wokaun, in "*Synthesis and Properties of New Catalysts*", E. W. Corcoran and M. Ledoux Eds., Malen Res. Soc., Philadelphia, (1990) p. 107.

79. K. L. Walther, M. Schrami-Marth, A. Wokaun and A. Baiker, *Catal. Lett.*, 4 (1990) 27.

80. P. Mars and D. W. van Krevelen, *Chem. Eng. Spec. Suppl.*, 3 (1954) 41.

81. S. K. Bhatacharya and P. Mohanti, *J. Catal.*, 20 (1971) 10.

82. L. Gonzalez, J. P. Jolly and J. E. Germain, *J. Chem. Phys.*, 75 (1978) 324.

83. A. Bielaski, K. Dyrek and E. Serwicka, *J. Catal.*, 66 (1980) 316.

84. K. Tamara, S. Yoshida, S. Ishida and H. Kakioka, *Bull. Chem. Soc. Jpn.*, 41 (1968) 2840.

85. M. Nakamura, K. Kawai and Y. Fujiwara, *J. Catal.*, 34 (1974) 345.

86. D. J. Cole, C. F. Cullis and D. J. Hucknall, *J. Chem. Soc. Faraday Trans.*, 72 (1976) 2185.

87. M. Akimoto, M. Usami and E. Echigoya, *Bull. Chem. Soc. Jpn.*, 51 (1978) 2195.

88. A. Bystrom, K. A. Wilhemi and O. Brotzen, *Acta. Chem. Scand.*, 4 (1950) 1119.

89. M. Gasior and T. Machej, *J. Catal.*, 83 (1983) 472.

90. G. Busca, F. Cavani and F. Trinro, *J. Catal.*, 106 (1987) 471.

91. J. Nilson, A. R. L. Conovas, S. Hansen and A. Andresson, *J. Catal.*, 160 (1996) 244.

92. G. C. Bond and S. Flamerz Tahir, *Appl. Catal.* A., 71 (1991) 1-31.

93. U. Schart, M. Schrami-Marth, A. Wokaun and A. Baiker, *J. Chem. Soc. Faraday Trans.*, 87 (1991) 3299.

94. J. R. Sohn, S. G. Cho Y. I. Pae and S. Hayashi, *J. Catal.*, 159 (1996) 170.

95. M. Santai, A. Andersson, L. R. Wallenberg and B. Rebenstorf, *Appl. Catal. A.*, 106 (1993) 51.

96. G. Deo and I. E. Wachs, *J. Phys. Chem.*, 95 (1991) 5889.

97. M. Kantcheva, K. Hadjiivanov and D. klissurski, *J. Catal.*, 134 (1992) 299.

98. Y. C. Xie and Y. Q. Tang, *Adv. Catal.*, 37 (1990) 1.

99. T. Machej, J. Haber, A. M. Turek and I. E. Wachs, *Appl. Catal.*, 70 (1991) 115.

100. G. Deo, A. M. Turek, I. E. Wachs, T. Machej, J. Haber, N. Das, H. Eckert and A. M. Hirt, *Appl. Catal. A.*, 91 (1992) 27.

101. G. Deo and I. E. Wachs, *J. Catal.*, 145 (1994) 323.

102. E. T. C. Vogt, M. de Boer, A. J. van Dillen and J. W. Geus, *Appl. Catal.*, 40 (1988) 255.

103. A. W. Stobbe-Kreemers, G. C. van Leerdam, J. P. Jacobs, H. H. Brongersma and J. J. F. Scholten, *J. Catal.*, 152 (1995) 130.

104. M. Chaar, D. Patel, M. Kung and H. H. Kung, *J. Catal.*, 105 (1987) 483.

105. M. Chaar, D. Patel, M. Kung and H. H. Kung, *J. Catal.*, 109 (1988) 463.

106. T. Blasco, J. M. Lopez Neito, A. Dejoz and M. I. Vazquez, *J. Catal.*, 157 (1995) 271.

107. D. S. H. Sam, V. Soenen and J. C. Volta, *J. Catal.*, 123 (1990) 417.

108. A. Corma, J. M. Lopez Neito, N. Paredes, M. Perez, Y. Shen, H. Cao and S. L. Suib, *Stud. Surf. Sci. Catal.*, 72 (1992) 213.

109. N. Das, H. Eckert, H. Hu, I. E. Wachs, J. walker and F. Feher, *J. Phys. Chem.*, 97 (1993) 8240.

110. J. M. Lopez Neito, G. Kremenik and J. L. G. Fiero, *Appl. Catal.*, 61 (1990) 235.

111. G. C. Bond, J. P. Zurita, S. Flamerz, P. J. Gellings, H. Bosch, J. G. van Ommen and B. J. Kips, *Appl. Catal. A.*, 22 (1986) 261.

112. I. E. Wachs, R. Y. Saleh, S. S. Chan and C. C. Chersich, *Appl. Catal.*, 15 (1985) 339.

113. R. Y. Saleh, I. E. Wachs, S. S. Chan and C. C. Chersich, *J. Catal.*, 98 (1986) 102.

114. G. C. Bond, S. Flamerz and R. Shukri, *Faraday Disc. Chem. Soc.*, 87 (1989) 65.

115. G. C. Bond, J. P. Zurita and S. Flamerz, *Appl. Catal.*, 27 (1986) 353.

116. G. Busca and J. C. Lavelley, *Spectrochem. Acta.*, 42A (1986) 443.

117. R. Kozlowski, R. F. Pettifer and J. M. Thomas, *J. Phys. Chem.*, 87 (1983) 5176.

118. H. Eckert and I. E. Wachs, *J. Phys. Chem.*, 93 (1989) 6769.

119. C. Doornkamp, M. Clement, X. Gao, G. Deo, I. E. Wachs and V. Ponec, *J. Catal.*, 185 (1999) 415.

120. I. E. Wachs, J. Jehng, G. Deo, B. M. Weckuyson, V. V. Guliants, J. B. Benziger and S. Sundaresan, *J. Catal.*, 170 (1997) 75.

121. W. M. H. Sachtler and N. H. De Boer, "*Proceedings in 3rd International Congress on Catalysis*", Amsterdam, Wiley, New York, (1964) p. 240.

122. W. M. H. Sachtler, G. J. H. Dorgelo, J. Fahrenfort, and R. J. H. Voorhoev, "*Proceedings in 4th International Congress on Catalysis*", Moscow, Adler, New York, (1968) p. 454.

123. J. Le Bars, J. C. Vedrine, A. Aurox, S. Trautmann and M. Baerns, *Appl. Catal. A. Gen.*, 119 (1994) 341.

124. F. Hatayama, T. Ohno, T. Maruoka, T. Ono and H. Miyata, *J. Chem. Soc. Faraday Trans.*, 87 (16) (1991) 2629.

125. H. Miyata, K. Fujii and T. Ono, *J. Chem. Soc. Faraday Trans.*, 1 (84) (1988) 3121.

126. K. Tanabe, M. Misono, Y. Ono and H. Hattori, "*New Solid Acids and Bases*", Kodansha, Tokyo (1989).

127. K. Arata, *Adv. Catal.*, 37 (1990) 165.

128. F. Harin, D. Andriamasinoro, A. Abdulsamad and J. Sommer, *J. Catal.*, 131 (1991) 199.

129. B. H. Davis, R. A. Keogh and R. Srinivasan, *Catal. Today*, 20 (1994) 219.

130. Z. Gao, J. M. Chen and Y. Tang, *Acta. Chim. Sin.*, 52 (1994) 36.

131. C. Morterra, G. Cerrato, F. Pinna, M. Signoretto and G. Strukul, *J. Catal.*, 149 (1994) 181.

132. B. S. Umansky, J. Engelhardt and W. K. Hall, *J. Catal.*, 127 (1991) 128.

133. R. Barthos, F. Lonyi, J. Engelhardt and J. Valyon, *Top. Catal.*, 10 (2000) 79-87.

134. M. Hino and K. Arata, *J. Chem. Soc. Chem. Commun.*, 3 (1985) 112.

135. K. Tanabe, M. Misono, Y. Ono and H. Hattori, *Stud. Surf. Sci. Catal.*, 51 (1989) 199.

136. H. Matsuhashi, M. Hino and K. Arata, *Chem. Lett.*, (1988) 1027.

137. K. Arata and M. Hino, *Appl. Catal.*, 59 (1990) 197.

138. K. Arata and M. Hino, *React. Kinet. Catal. Lett.*, 25 (1984) 143.

139. K. Arata and M. Hino, *Mater. Chem. Phys.*, 26 (1990) 213.

140. F. R. Chen, G. Coudurier, J. F. Joly and J. C. Vedrine, *J.Catal.*, 143 (1993) 616.

141. M. S. Scurrell, *Appl. Catal.*, 34 (1987) 109.

142. T. Yamaguchi, K. Tanabe and Y. C. Kung, *Mater. Chem. Phys.*, 16 (1986) 67.

143. J. R. Sohn and H. W. Kim, *J. Mol. Catal.*, 52 (1989)361.

144. P. D. L. Mercera, J. G. Van Ommen, E. B. M. Doesburg, A. J. Burggraaf and J. R. H. Ross, *Appl. Catal.*, 57 (1990) 127.

145. T. Lopez, J. Navarrete and R. Gamez, *Appl. Catal. A. Gen.*, 125 (1995) 217.

146. E. Iglesia, S. L. Solid and G. M. Karmer, *J. Catal.*, 144 (1993) 238.

147. M. Bensitel, O. Saur, J. C. Lavalley and B. A. Morrow, *Mater. Chem. Phys.*, 19 (1988) 147.

148. O. Saur, M. Bensitel, A. B. M. Saad, J. C. Lavalley, C. P. Tripp and B. A. Morrow, J. Catal., 99 (1986) 104.

149. B. A. Morrow, R. A. Mc Farlane, M. Lion and J. C. Lavalley, J. Catal., 107 (1987) 232.

150. K. Arata, *Appl. Catal. A. Gen.*, 146 (1996) 3.

151. V. Adeeva, J. W.de Haan, J. Janchen, G. D. Lei, V. Schunemann, L. J. M. van de ven, W. M. H. Sachtler and R. A. van Santen, *J.Catal.*, 151 (1995) 364.

152. J. M. Parera, *Catal. Today*, 15 (1992) 481.

153. M. Y. Wen, I. Wender and J. Tierney, *Energy Fuels*, 4 (1990) 372.

154. M. -Trung Tran, N. S. Gnep, G. Szabo and M. Guisnet, *Appl. Catal. A. Gen.*, 171 (1998) 207.

155. C. Morterra, G. Cerrato, F. Pinna, M. Signoretto and G. Strukul, *J. Catal.*, 149 (1994) 181.

156. K. Tanabe, *Mater. Chem. Phys.*, 13 (1985) 347.

157. Y. Xia, W. Hua and Z. Gao, *Catal. Lett.*, 55 (1998) 101.

158. K. R. Venkatesh, J. Hu, J. W. Tierney and I. Wender, *Prepr. Am. Chem. Soc. Div. Fuel Chem.*, 40 (1995) 788.

159. J. C. Yori, J. C. Luy and J. M. Parera, *Appl. Catal.*, 46 (1989) 103.

160. R. A. Comelli, C. R. Vera and J. M. Parera, *J. Catal.*, 151 (1995) 96.

161. F. R. Chen, G. Coudurier, J. F. Joly and J. C. Vedrine, *J.Catal.*, 143 (1993) 616.

162. T. Yamaguchi, *Appl. Catal.*, 61 (1990) 1.

163. T. Yamaguchi, K. Tanabe and Y. C. Kung, *Mater. Chem. Phys.*, 16 (1986) 67.

164. M. Y. Wen, I. Wender and J. Tierney, *Energy Fuels*, 4 (1990) 372.

165. T. Hosoi, T. Shimadzu, S. Itoh, S. Baba, H. Takaoka, T. Imai and N. Yokoyama, *Prepr. Am. Chem. Soc. Div. Petrol. Chem.*, 33 (1988) 562.

166. K. Ebitani, J. Konishi and H.Hattori, *J. Catal.*, 130 (1991) 257.

167. K. Ebitani, T. Tsuji, H. Hattori and H. Kita, *J. Catal.*, 135 (1992) 609.

168. K. Ebitani, H. Konno, T. Tanaka and H. Hattori, *J. Catal.*, 135 (1992) 60.

169. K. Ebitani, H. Konno, T. Tanaka and H. Hattori, *J. Catal.*, 143 (1993) 322.

170. M. Hino, *Catal. Lett.*, 34 (1996) 125.

171. C. Miao, W. Hua, J. Chen and Z. Gao, *Catal. Lett.*, 37 (1996) 187.

172. W. Hua, Y. Xia, Y. Yue and Z. Gao, *J. Catal.*, 196 (2000) 104.

173. J. R. Sohn and H. J. Jang, *J. Mol. Catal.*, 64 (1991)349.

174. J. Salmones, R. Licona, J. Navarrete and P. Salas, *Catal. Lett.*, 36 (1996) 135.

175. J. A. Navio, G. Colon, M. Macias, J. M. Campelo, A. A. Romero and J. M. Marians, *J.Catal.*, 161 (1996) 605.

176. F. Lonyi, J. Valyon, J. Engelhardt and F. Mizukami, *J. Catal.*, 160 (1996) 279.

177. T. Lei, J. S. Xu, Y. Tang, W. M. Hua and Z. Gao, *Appl. Catal. A. Gen.*, 192 (2000) 181.

178. J. M. Grau, C. R. Vera and J. M.Parera, *Appl. Catal. A. Gen.*, 172 (1998) 311.

179. R. W. Bormett and S. A. Asher, *J. Appl. Phys.*, 77 (1995) 5916.

180. P. Vijayanand, N. Viswanadham, N. Ray, J. K. Gupta and T. S. R. Prasada Rao, "*Recent Advances in Basic and Applied Aspects of Industrial Catalysis*", T. S. R. Prasada Rao and G. Murali Dhar (Eds.), *Stud. Surf. Sci. Catal.*, Vol 113 (1998) p. 999.

181. K. Tanabe, "*Solid Acids and Bases and their Catalytic Properties*", Academic Press, New York (1970) 103-158.

182. M. Guisnet, "*Catalysis by Acids and Bases*", B. Imelik *et al.* (Eds.), *Stud. Surf. Sci. Catal.*, 20, Elsevier, Amsterdam, 1985, 283-297.

183. H. S. Bierenbaum, R. D. Partridge and A. H. Weiss, *Adv. Chem. Ser.*, 121 (1973) 605.

184. M. Guisnet, F. Avendano, C. Bearez and F. Chevalier, *J. Chem. Soc. Chem. Comm.*, (1985) 336.

185. H. A. Benesi and B. H. C. Winquist, *Adv. Catal.*, 27 (1978) 97.

186. J. Turkevich and Y. Ono, *Adv. Catal.*, 20 (1969) 135-152.

187. P. A. Jacobs, H. E. Leeman and J. B. Uytterhoeven, *J. Catal.*, 33 (1974) 17.

188. J. W. Ward and R. C. Hansford, *J. Catal.*, 13 (1969) 154.

189. T. Aonuma, M. Sato and T. Shiba, *Shokubai*, 5 (1963) 274.

190. H. G. Karge, J. Ladbeck, Z. Sarbak and K. Hatada, *Zeolites*, 2 (1982) 94.

191. H. G. Karge, K. Hatada, Y. Zhang and R. Fiedorow, *Zeolites*, 3 (1983) 13.

192. J. W. Ward, *J. Catal.*, 10 (1968) 34.

193. C. Mirodatos and D. Barthomeuf, *J. Chem. Soc. Chem. Comm.*, (1981) 39.

194. J. Kijenski and A. Baiker, *Catal. Today*, 5 (1989) 1.

195. M. R. Guisnet, *Acc. Chem. Res.*, 23 (11) (1990) 393.

196. H. A. Benesi, *J. Phys. Chem.*, 61 (1957) 970.

197. H. A. Benesi, *J. Am. Chem. Soc.*, 78 (1956) 5490.

198. J. Take, Y. Nomizo and Y. Yoneda, *Bull. Chem. Soc. Jpn.*, 46 (1973) 3568.

199. M. Deeba and W. K. Hall, *J. Catal.*, 60 (1979) 417.

200. V. Adeeva, J. W.de Haan, J. Janchen, G. D.Lei, V. Schunemann, L. J. M. van de ven, W. M. H. Sachtler and R. A. van Santen, *J.Catal.*, 151 (1995) 364.

201. K. Ebitani, J. Konishi, A. Horie, H. Hattori and K. Tanabe, "*Acid-base Catalysis*", K. Tanabe, H. Hattori, T. Yamaguchi and T. Tanaka (Eds), Tokyo (1989) p. 491.

202. H. Matsuhashi, H. Motoi and K. Arata, *Catal. Lett.*, 26 (1994) 325.

203. F. Arene, R. Dario and A. Parmaliana, *Appl. Catal. A. Gen.*, 170 (1998) 127.

204. A. Corma, V. Fornes, M. I. Juan Rajadell and J. M. Lopez Nieto, *Appl. Catal. A. Gen.*, 116 (1994) 151.

205. X. Song and A. Sayari, *Appl. Catal. A. Gen.*, 110 (1994) 121.

206. T. Okuhara, T. Nishimura, H. Watanabe and M. Misono, *J. Mol. Catal.*, 74 (1992) 247.

207. A. Corma, M. I. Juan-Rajadell, J. M. Lopez-Nieto and C. Martinez, *Appl. Catal., A. Gen.*, 111 (1994) 175.

208. A. Corma, A. Martinez and C. Martinez, *J. Catal.*, 149 (1994) 52.

209. C. H. Lin and C. Y. Hsu, *J. Chem. Soc. Chem. Comm.*, 20 (1992) 1479.

210. M. Hino, K. Arata and K. Yabe, *Shokubai*, 22 (1980) 232.

211. L. M. Kustov, V. B. Kazansky, F. Figueras and D. Tichit, *J. Catal.*, 150 (1994) 143.

212. A. Corma, C. Rodellas and V. Fornes, *J. Catal.*, 88 (19984) 374.

213. H. A. Benesi, *J. Catal.*, 28 (1973) 76.

214. M. -Trung Tran, N. S. Gnep, G. Szabo and M. Guisnet, *Appl. Catal. A. Gen.*, 171 (1998) 207.

215. B. S. Umansky and W. K.Hall, *J. Catal.*, 124 (1990) 97.

216. D. J. Coster, A. Bendada, F. R. Chen and J. J. Fripiat, *J. Catal.*, 140 (1993) 497.

217. R. Srinivasan, D. Taulbee and B. H. Davis, *Catal. Lett.*, 9 (1991) 1.

218. V. Semmer, P. Batamack, C. Doremieux-Morin, R. Vincent and J. Fraissard, *J. Catal.*, 161 (1996) 186.

219. W. P. Rothwell, W. X. Shen and J. H. Lunsford, *J. Am. Chem. Soc.*, 106 (1984) 2452.

220. J. H. Lunsford, W. P. Rothwell and W. X. Shen, *J. Am. Chem. Soc.*, 107 (1985) 1540.

221. J. H. Lunsford, P. N. Tutunjian, P. Chu, E. B. Yah and D.J. Zalewski, *J. Phys. Chem.*, 93 (1989) 2590.

222. J. H. Lunsford, H. Sang, S. M. Campbell, C.H. Liang and R. G. Anthony, *Catal. Lett.*, 27 (1994) 305.

223. M. A. Barteau, *Chem. Rev.*, 96 (1996) 1413.

224. M. Ai, *Bull. Chem. Soc. Jpn.*, 50 (1977) 2597.

225. J. Sabati, F. E. Massoth, M. Tokarz, G. M. Tsai and J. Mc Cauley, *Proc. 8th Int. Cong. in Catal.*, Berlin, (1984) Vol. IV, p. 735.

226. A. Corma and B. W. Wojciechowski, *Catal. Rev. Sci. Eng.*, 24 (1982) 1.

227. J. W. Ward, *J. Catal.*, 9 (1967) 225.

228. W. Przystajko, R. Fieddorow and I. G. Dalla Lana, *Appl. Catal.*, 15 (1985) 265.

229. H. Pines, "*The Chemistry of Catalytic Hydrocarbon Conversions*", Academic Press, New York (1981) p.85.

230. P. M. Boorman, R. A. Kydd, Z. Sarbak and A. Somogyvari, *J. Catal.*, 96 (1985) 115.

231. P. M. Boorman, R. A. Kydd, Z. Sarbak and A. Somogyvari, *J. Catal.*, 100 (1986) 287.

232. G. A. Olah, "*Friedel-Crafts and Related Reactions*", Vols.1-4, Wiley-Interscience, New York, London (1963-1964).

233. G. A. Olah, "*Friedel-Crafts Chemistry*", Wiley-Interscience, New York, London, Sydney, Toronto (1973).

234. A. Cornelis, C. Dony, P. Laszlo and K. M. Nsunda, *Tetrahedron Lett.*, 34 (1993) 529.

235. R. Stroh, J. Ebersberger, H. Haberland and W. Hahn, *Ger. Patent* (1959) 1 051 271.

236. R. van Helden, C. F. Koht and H. D. Scharf, *Brit. Patent* (1968) 1 110 029.

237. V. R. Choudhary, S. K. Jana and B. P. Kiran, *Catal. Lett.*, 59 (1999) 217.

238. A. P. Singh and D. Bhattacharya, *Catal. Lett.*, 32 (1995) 327.

239. A. P. Singh, D. Bhattacharya and S. Sarma, *J. Mol. Catal. A. Chem.*, 102 (1995) 139.

240. B. Jacob, S. Sugunan and A. P. Singh, *J. Mol. Catal. A. Chem.*, 139 (1999) 43.

241. A. P. Singh, B. Jacob and S. Sugunan, *Appl. Catal. A. Gen.*, 174 (1998) 51.

242. Y. Izumi and K. Urabe, *Stud. Surf. Sci. Catal.*, 90 (1994) 1.

243. I. Yusuke, O. Mayumi and U. Kazuo, *Appl. Catal. A. Gen.*, 132 (1995) 127.

244. Y. Isumi, N. Natsuma, H. Takamine, J. Tamaoki and K. Urabe, *Bull. Chem. Soc. Jpn.*, 62 (1989) 2159.

245. V. R. Choudhary, S. K.Jana and B. P. Kiran, *J. Catal.*, 192 (2000) 257.

246. S. Jun and R. Ryoo, *J. Catal.*, 195 (2000) 237.

247. N. He, S. Bao and Q. Xu, *Appl. Catal. A. Gen.*, 169 (1998) 29.

248. D. B-Barbier, A. Dormond and F. D-Montagne, *J. Mol. Catal. A. Chem.*, 149 (1999) 215.

249. D. Baudry, A. Dormond and F. D-Montagne, *New J. Chem.*, 18 (1994) 871.

250. U. Freese, F. Heinrich and F. Roessner, *Catal. Today*, 49 (1999) 237.

251. P. Botella, A. Corma, J. M. Lopez Nieto, S. Valencia and R. Jacquot, *J. Catal.*, 195 (2000) 161.

252. D. Bhattacharya, A. K. Pandey and A. P. Singh, *Recent Advances in Basic ana Applied Aspects of Industrial Catalysts*, T.S.R.Prasada Rao and G. Murali Dhar (Eds.) *Stud. Surf. Sci. Catal.*, Vol. 113 (1998) p. 737.

253. C. N. Rhodes and D. R. Brown, *J. Chem. Soc. Faraday Trans.*, 88 (15) (1992) 2269.

254. J. R. Butruille and T. J. Pinnavaia, *Catal. Today*, 14 (1992) 141.

255. A. Geatti, M. Lenarda, L. Storaro, R. Ganzerla and M. Perissinotto, *J. Mol. Catal. A. Chem.*, 121 (1997) 119.

256. B. M. Choudary, M. L. Kantam, M. Sateesh, K. K. Rao and P. L. Santhi, *Appl. Catal. A. Gen.*, 149 (1997) 257.

257. J. H. Clark, A. P. Kybett, D. J. Macquarrie, S. J. Barlow and P. Landon, *J. Chem. Soc. Chem. Comm.*, (1989) 1353.

258. K. R. Sabu, R. Sukumar and M. Lalithambika, *Bull. Chem. Soc. Jpn.*, 66 (1993) 3535.

259. T. Cseri, S. Bekassy, F. Figueras and S. Rizner, *J. Mol. Catal. A. Chem.*, 98 (1995) 101.

260. K. R. Sabu, R. Sukumar, R. Rekha and M. Lalithambika, *Catal. Today*, 49 (1999) 321.

261. R. Sukumar, K. R. Sabu, L. V. Bindu and M. Lalithambika in "*Recent Advances in Basic and Applied Aspects of Industrial Catalysts*", T.S.R.Prasada Rao and G.Murali Dhar (Eds.) *Stud. Surf. Sci. Catal.*, Vol. 113 (1998) p. 557.

262. M. Lenarda, L. Storaro, G. Pellegrini, L. Piovesan and R. Ganzerla, *J. Mol. Catal. A. Chem.*, 145 (1999) 237.

263. P. M. Price, J. H. Clark, K. Martin, D. J. Macquarrie and T. W. Bastock, *Org. Process. Res. Dev.*, 2 (1998) 221.

264. G. D. Yadav and A. A. Pujari, *Green Chem.*, 1 (1999) 69.

265. J. H. Clark, G. L. Monks, D. J. Nightingale, P. M. Price and J. F. White, *J. Catal.*, 193 (2000) 348.

266. S. K. Samantaray, T. Mishra and K. M. Parida, *J. Mol. Catal. A. Chem.*, 156 (2000) 267.

267. W. Hua, Y. Xia, Y. Yue and Z. Gao, *J. Catal.*, 196 (2000) 104.

268. G. D. Yadav, T. S. Thorat and P. S. Kumbhar, *Tetrahedron Lett.*, 34 (3) (1993) 529.

269. G. D. Yadav and T. S. Thorat, *Tetrahedron Lett.*, 37 (30) (1996) 5405.

270. D. Shouro, Y. Ohya, S. Mishima and T. Nakajima, *Appl. Catal. A. Gen.*, 214 (2001) 59-67.

271. Y. Murakami, V. Saeki and K. Ho, *Nippon Kagaku Kaishi*, 1978 (1978) 2.

272. P. S. Landis and P. B. Venuto, *J. Catal.*, 6 (1966) 245.

273. S. Sato, K. Urabe and Y. Izumi, *J. Catal.*, 102 (1986) 99.

274. S. Sato, K. Urabe and Y. Izumi, *Appl. Catal.*, 29 (1987) 107.

275. H. Sato, K. Hirose and M. Kitamura, *Nippon Kagaku Kaishi*, 1989 (1989) 548.

276. H. Sato, K. Hirose and Y. Nakamura, *Chem. Lett.*, 1993 (1993) 1987.

277. A. Thankaraj, S. Sivasanker, and P. Ratnasamy, *J. Catal.*, 137 (1992) 252.

278. T. Ushikubo and K. Wada, *J. Catal.*, 148 (1994) 138.

279. P. S. Singh, R. Bandyopadhyay, H. G. Hegde and B. S. Rao, Appl. Catal. A. Gen., 136 (1996) 249.

280. A. Corma, H. Garcia and J. Primo, *Zeolites*, 11 (1991) 593.

281. A. Aucejo, M. C. Burguet, A. Corma and V. Fornes, *Appl. Catal. A. Gen.*, 22 (1986) 187.

282. L. –X. Dai, K. Koyama and T. Tatsumi, *Catal. Lett.*, 53 (1998) 211.

283. L. –X. Dai, Y. Iwaki, K. Koyama and T. Tatsumi, *Appl. Surf. Sci.*, 121/ 122 (1997) 335.

284. L. –X. Dai, R. Hayashide, Y. Iwaki, K. A. Koyano and T. Tatsumi, *J. Chem. Soc., Chem. Comm.*, (1996) 1071.

285. L. –X. Dai, K. Koyama, M. Miyamoto and T. Tatsumi, *Appl. Catal. A. Gen.*, 189 (1999) 237.

286. T. Ushikubo and K. Wada, *Appl. Catal.*, 67 (1990) 25.

287. K. Wada and T. Ushikubo, *Japanese Unexamined Patent Publication No. 63-51945.*

288. T. Ushikubo, H. Yanai and K. Wada, *"Catalytic Science and Technology"*, Vol. 1 (1991) p. 509.

289. H. Sato, K. Hirose and S. Nakamura, *Stud. Surf. Sci. Catal.*, 49 (1989) 1213.

290. J. S. Reddy, R. Ravisankar, S. Sivasankar and P. Ratnasamy, *Catal. Lett.*, 17 (1994) 139.

291. W. F. Holderich and G. Heitmann, *Catal. Today*, 38 (1997) 227.

292. W. F. Holderich and G. Dahlhoff, *Chem. Innov.*, 31 (2) (2001) 29.

293. Y.-M. Chung and H. –K. Rhee, *J. Mol. Catal. A. Chem.*, 175 (2001) 249.

294. D. Mao, G. Lu, Q. Chen, Z. Xie and Y. Zhang, *Catal. Lett.*, Vol. 77, No. 1-3 (2001) 119.

295. T. Curtin, J, B. Mc Monagle and B. K. Hodnett, *Appl. Catal. A.*, 93 (1992) 75.

296. G. P. Heitmann, G. Dahlhoff and W. F. Holderich, *Appl. Catal. A.*, 185 (1999) 99.

297. H. P. Lin, S. Cheng and C. -Y. Mou, *J. Chin. Chem. Soc.*, 43 (1996) 375.

298. A. N. Ko, C. C. Hung, C. W. Chen and K. H. Ouyang, *Catal. Lett.*, Vol. 71, No. 3-4 (2001) 219.

299. K. V. V. S. B. S R. Murthy, M. Chandrakala, S. J. Kulkarni and K. V. Raghavan, *Ind. J. Chem. Tech.*, Vol. 8 (2001) 368.

300. E. R. S. Winter, *J. Catal.*, 22 (1971) 158.

301. E. R. S. Winter, *J. Catal.*, 15 (1969) 144.

302. E. R. S. Winter, *J. Catal.*, 34 (1974) 431.

303. E. R. S. Winter, *J. Catal.*, 19 (1970) 32.

304. K. Kijenski, A. Baiker, M. Glinski, P. Dollenmeier, and A. Wokaun, *J. Catal.*, 101 (1986) 1.

305. A. Gervasini and A. Auroux, *J. Catal.*, 131 (1991) 190.

306. P. M. Michalatos, M. C. Kung, I. Jahan and H. H. Kung, *J. Catal.*, 140 (1993) 226.

307. J. Le Bars, A. Auroux, M. Forisier and J. C. Vedrine, *J. Catal.*, 162 (1996) 250.

308. K U. Ingold, *Aldrichimica*, 22 (1989) 69.

309. G. Deo and I. E. Wachs, *J. Catal.*, 146 (1994) 323.

310. V. Indira, P. A. Joy, N. Alekar, S. Gopinatahn and C. Gopinathan, *Ind. J. Chem.*, 36A (1997) 687-692.

311. W. W. Kaeding, *Catal. Rev.*, 8 (1973) 307.

312. E. H. Lee, *Catal. Rev.*, 8 (1973) 285.

313. A. Cortes and J. L. Seoane, *J. Catal.*, 34 (1974) 7.

314. A. Joseph, R. L. Mednick, M. L. Shorr, S. W. Weller and P. Rona, *Israel J. Chem.*, 12 (1974) 739.

315. W. Kania and K. Jurezyk, *Appl. Catal.*, 61 (1990) 35.

316. Z. Dziewiecki and A. Makowski, *React. Kinet. Catal. Lett.*, 13 (1980) 51.

317. J. J. Kim and S. W. Weller, *Appl. Catal.*, 33 (1987) 15.

318. G. V. Shakhnovich, I. P. Belomestnykh, N. V. Nekrasov, M. M. Kostyukovsky and S. L. Kiperman, *Appl. Catal.*, 12 (1984) 23.

319. G. Emig and H. Hofmann, *J. Catal.*, 84 (1983) 15.

320. Y. Murakami, K. Iwayama, H. Uchida, T. Hattori and T. Tagawa, *Appl. Catal.*, 2 (1982) 67.

321. G. E. Vrieland, *J. Catal.*, 111 (1988) 1.

322. E. Vriel and P. G. Menon, *Appl. Catal.*, 77 (1991) 1.

323. J. Iwasawa, H. Nobe and S. Ogasawara, *J. Catal.*, 31 (1973) 444.

324. G. C. Grunewald and R. S. Drago, *J. Mol. Catal.*, 58 (1990) 227.

325. T. Tagawa, T. Hattori, Y. Murakami, K. Iwayama, Y. Ishida and H. Uchida, *J. Catal.*, 75 (1982) 56.

326. T. Tagawa, T. Hattori, Y. Murakami, K. Iwayama, Y. Ishida and H. Uchida, *J. Catal.*, 75 (1982) 66.

327. R. Fiedorow, W. Przystajko, M. Sopa and I. G. Dalla Lana, *J. Catal.*, 68 (19812) 33.

328. E. Echigoya, H. Sano and M. Tanaka, *8th International Congress on Catalysis*, Berlin Dechema, Frankfurt-am-Main, Vol : 5 (1984) p. 623.

329. T. G. Alkhazov, A. E. Lisovskii, M. G. Safarov and A. M. Dadasheva, *Kinet. Katal.*, 13 (1972) 509.

330. P. Ciambelli, S. Crescitelli, V. De Simone and G. Russo, *Chim. Ind. Milan.*, 55 (1973) 634.

331. K. Tazaki, R. Kitahama, F. Nomura and T. Yokoji, *Japan Pat 74 39 246*; Chem. Abstr 83 44002 v (1975).

332. W. Kania and K. Jurczyk, *Appl. Catal.*, 61(1990) 35.

333. T. M. Jyothi, K. Sreekumar, M. B. Talawar, A. A. Belhekar, B. S. Rao and S. Sugunan, *Bull. Chem. Soc. Jpn.*, 73 (2000) 1.

334. S. T. Oyama and G. A. Somorjai, *J. Phys. Chem.*, 94 (1990) 5022.

335. L. Owens and H. H. Kung, *J. Catal.*, 144 (1993) 202.

336. A. Erdohelyi and P. Solymosi, *J. Catal.*, 123 (1990) 31.

337. S. T. Oyama, A. M. Middlebrook and G. A. Somorjai, *J. Phys. Chem.*, 94 (1990) 5094.

338. J. Le Bars, A. Auroux, J. C. Vedrine and M. Baerns, *Stud. Surf. Sci. Catal.*, 72 (1992) 81.

339. J. Le Bars, J. C. Vedrine, A. Auroux, S. Trautmann and M. Baerns, *Appl. Catal. A.*, 88 (1992) 179.

340. J. G. Eon, R. Oliver and J. C. Volta, *J. Catal.*, 145 (1994) 318.

341. J. Le Bars, J. C. Vedrine, A. Auroux and S. Trautmann, "*Proc. DGMK Conf. on Selective Oxidations in Petrochemistry*", M. Baerns and J. Weitkamp (Eds.), Goslar, Germany (1992) p. 59.

342. J. Le Bars, A. Auroux, M. Forisier and J. C. Vedrine, *J. Catal.*, 162 (1996) 250.

343. E. A. Mamedov, R. M. Talyshinski, R. G. Rizayev and V. C. Carberan, *Catal. Today*, 32 (1996) 177.

344. T. Blasco and Lopez Neito, *Appl. Catal. A. Gen.*, 157 (1997) 117.

Chapter 2

Materials And Methods

ABSTRACT

The materials and the experimental procedures used for catalyst preparation, characterization, surface acidity and catalytic activity measurements are described in this chapter. The techniques used for the surface characterization like EDX, XRD, BET surface area and pore volume measurements, TG, SEM, FTIR, solid-state ^{51}V NMR and DR UV-VIS are expected to be powerful tools to study the changes of the local environment and nature of surface vanadium species. Ammonia TPD, perylene adsorption and vapour-phase cumene cracking are the methods adopted for the surface acidity determination. Reactions of industrial importance such as Friedel-Crafts alkylation, Beckmann rearrangement of cyclohexanone oxime and selective oxidations are chosen for the catalytic activity measurements.

2.1 INTRODUCTION

Catalysis is a complex surface phenomenon occurring on the surface of a catalyst. The adsorption of the reactant molecules and their interaction to give the product on the active phase of the catalyst depend not only on the reaction variables, but also on the nature of sites on the catalyst surface, which in turn determines the 'quality' of the catalyst system. In the production of commercial catalysts, even a minute change in the conditions of preparation changes the

quality of the catalyst[1]. Hence utmost care should be taken during the preparation of the systems. The performance of a catalyst can be better appreciated if one knows as many of its physico-chemical properties as possible. Measuring the same parameters after use often helps in understanding the cause of catalyst deactivation.

Supported vanadia catalysts form a complex class of catalysts, which are used in various reactions of industrial importance. The nature of the active sites on vanadia phase in these catalysts is expected to vary over a wide range with the vanadia loading and with the nature of the support. To understand the phenomenon of adsorption and catalysis on a molecular basis, the nature of the molecular structure of the vanadium oxide species on these catalysts should be thoroughly investigated and it is essential that the adsorption and active sites are to be extremely probed.

With this background, we have prepared two series of supported vanadia catalysts with a wide range of vanadia loading and its sulfated analogues using SnO_2 and ZrO_2 as novel supports. The experimental procedure used to synthesize the pure, supported and the sulfated catalysts are given in this chapter. They were thoroughly characterized and tested for catalytic activity with various techniques. The materials used and the methodologies are described in the following sections.

2.2 CATALYST PREPARATION

The metal oxide supports were prepared *via* hydroxide method[2]. Various vanadia supported catalysts with different V_2O_5 contents were prepared by following the conventional wet impregnation (excess solvent) technique[3]. The sulfate modification of the samples was done by a second step wet impregnation using 0.5 M sulfuric acid. For a comparative evaluation of the properties, pure vanadia (V_2O_5) and sulfated vanadia were also synthesized.

2.2.1 Materials

The materials used for catalyst preparation are given below:

Materials	*Suppliers*
Stannous chloride	Qualigens
Zirconyl nitrate	CDH
Ammonium hydroxide	Merck
Ammonium metavanadate	Merck
Conc. H_2SO_4	Merck

2.2.2 Methods

A detailed discussion of the experimental procedures used to develop the catalyst systems for the present investigation is given in the following section.

I. Preparation of Single Oxides

i) Tin oxide (SnO_2)

Stannous chloride was taken in a china dish and conc. HNO_3 was added drop wise until a pasty material was formed. It was then dissolved in minimum amount of aqua-regia on a sand bath and diluted with water to get stannic chloride solution.

The precipitate of hydrous tin oxide was obtained by adding 1:1 ammonia solution slowly to the boiling stannic chloride solution with stirring until the pH of mother liquor was 4-5. The precipitate was coagulated for 15 minutes and allowed to stand overnight. The mother liquor was decanted off and the precipitate was washed several times with distilled water until it was completely free from chloride ions. The precipitate was filtered, dried at 110°C for 12 h in an air oven and powdered below 100 μ mesh size. The hydroxide obtained was calcined at 550°C in air for 5 h in a muffle furnace[4].

ii) Zirconium oxide (ZrO_2)

Hydrous zirconium oxide was prepared by the hydrolysis of zirconyl nitrate with 1: 1 ammonia. Zirconyl nitrate was dissolved in minimum amount of doubly distilled water. To a boiling solution of zirconyl nitrate in water, aqueous ammonia was added drop wise with constant stirring till complete precipitation was achieved. The pH of the final solution was in the range 10-11.The solution was solidified and was made into a colloidal state which was boiled for about 15 minutes and allowed to stand overnight. The aqueous portion was decanted from the precipitate; fresh water was added for washing the precipitate repeatedly until the precipitate was free of nitrate ions. The precipitate was filtered, oven dried at 110°C for 12 h, powdered and calcined for 5 h at 550°C in air[4].

iii) Vanadium oxide (V_2O_5)

To obtain pure vanadium oxide catalyst, ammonium metavanadate was dissolved in conc. HCl and then precipitated by adding ammonium hydroxide until pH = 7. The precipitate was washed until the solution was free from chloride ions, dried at 110°C and calcined at 550°C for 5 h [5].

II. Preparation of Supported Vanadia Catalysts

The catalysts with various vanadium oxide contents were prepared by wet impregnation of metal oxide supports in the hydroxide form with required amount of oxalic acid solution of ammonium metavanadate. The solution was evaporated to dryness with vigorous stirring. The precipitate obtained was oven dried at 110°C for 12 h, powdered and calcined at 550°C for 5 h [6].

III. Preparation of Sulfated Systems

The hydroxide form of the metal oxide (single and supported) was exposed to 0.5 M H_2SO_4 (5 mL g^{-1}) for 3 h with stirring. The precipitate was filtered without washing, dried at 110°C overnight, powdered and calcined at 550°C for 5 h [4,7].

2.3 CATALYST NOTATIONS

The catalyst systems developed for the present investigation and its designation are given below.

Notation	*System*
TX	V_2O_5/ SnO_2 with X (= 0,3,6,9,12 &15) weight % of vanadia loading
ZX	V_2O_5 / ZrO_2 with X (= 0,3,6,9,12 &15) weight % of vanadia loading
V	Vanadium oxide (V_2O_5)
STX	Sulfated V_2O_5/ SnO_2 systems
SZX	Sulfated V_2O_5/ ZrO_2 systems
SV	Sulfated vanadia

2.4 CHARACTERIZATION TECHNIQUES

The prepared catalyst samples were characterized by adopting a variety of physico-chemical methods. Before each characterization, the samples were activated at 550°C for 2 h.

2.4.1 Materials

The materials used for catalyst characterization are

Materials	*Suppliers*
Liquid nitrogen	Manorama Oxygen Pvt. Ltd.
Potassium bromide	Merck
Aluminium oxide	Merck
Magnesium oxide	Merck

2.4.2 Methods

A brief discussion of each method of characterization adopted along with its experimental aspects is presented in the following sections.

I. Energy Dispersive X-ray Fluorescence Analysis (EDX)

Energy dispersive X-ray fluorescence (EDX) analysis is a successful analytical technique that quantitatively and qualitatively identifies the elemental composition of solid samples. The method is practically nondestructive and is sensitive to very low concentrations (minimum detection limit being 0.1% in the best case). The principle of EDX is based on the strong interaction of electrons with matter. When electrons of appropriate energy impinge on a sample, they cause emission of X-rays whose energies and relative abundance depend on the composition of the sample[8].

The electron beam from a scanning electron micrograph used in this technique can eject an electron from the inner shell of the sample atom. The resulting inner shell electron vacancy is filled by another electron from a high-energy shell in the atom. While moving from a high-energy state to a lower one, this vacancy-filling electron gives up some of its energy (equal to the difference in the energy between the two electronic levels involved) in the form of electromagnetic radiation. Since this electronic energy is fairly large for inner shells, the radiation appears as X-rays. As all elements have a unique configuration of electronic energy levels, the X-ray pattern spectrum will be unique for a particular element. Furthermore, under the given analysis conditions, the number of X-rays emitted by each element will be directly proportional to the concentration of that element in the sample.

The X-ray peak position along with the energy scale identify the element present in the sample, while the integrated peak areas, after application of appropriate correction factors, can give us percentage composition of each of the elements. EDX spectra of the samples were recorded in a Stereoscan 440 apparatus.

II. BET Surface Area and Pore Volume Measurements

Surface area determination is an important factor in predicting the catalyst performance. Of the several techniques to estimate the surface area

and pore volume of porous materials, BET method [9] is the widely accepted procedure and this method is based on the extension of the Langmuir theory to multi-layer adsorption. The general form of BET equation can be written as

$$P / [V (P_o-P)] = [1 / (V_mC)] + [(C-1) / V_mC] (P/P_o)$$

where,

P - Adsorption equilibrium pressure

P_o - Saturated vapour pressure of the adsorbate

V - Volume occupied by molecules adsorbed at equilibrium pressure

V_m - Volume of the adsorbate required for monolayer coverage

C - Constant related to the heat of adsorption

A plot of $P/ [V (P_o-P)]$ against P/ P_o is a straight line with slope $(C-1)/ V_mC$ and intercept $1/ V_mC$. From the slope and intercept, V_m can be calculated and the specific surface area of the sample can be calculated using the relation,

$$A=V_mN_oA_m / W \times 22414$$

where,

N_o - Avagadro number

A_m - Molecular cross sectional area of the adsorbate (0.162 nm^2 for N_2)

W - Weight of the catalyst sample (g)

In BET method, adsorption of N_2 is carried out at liquid nitrogen temperature. Previously activated samples were degassed at 200°C under nitrogen for 2 h and then brought to -196°C using liquid nitrogen for adsorbing N_2 gas at various pressures. The pore volume is measured by the uptake of N_2 at a relative pressure of 0.9.

Simultaneous determination of surface area and total pore volume of the samples were achieved in a Micromeritics Gemini surface area analyzer by the low temperature N_2 adsorption method.

III. Scanning Electron Microscopy (SEM)

Scanning Electron Microscopy allows the imaging of the topography of a solid surface by using back scattered or secondary electrons with good resolution of about 5 nm. In this technique, a fine probe of electrons is scanned over the sample surface using deflection coils. The interaction between the primary beam and the specimen produces various signals, which are detected, amplified and displayed on a cathode ray tube screened synchronously with the beam. They can also be conveniently deflected and focused by electronic or magnetic field so that magnified real-space images can be formed. This makes the technique suitable for producing very impressive, in-focus images from a highly irregular structure, typical of catalyst specimens. This technique is of great interest in catalysis particularly because of its high spatial resolution[10].

SEM analysis of the samples was done using Stereoscan 440 Cambridge U.K Scanning Electron Microscope. The sample was dusted on alumina and coated with a thin film of gold to prevent surface charging and to protect the material from thermal damage by electron beam. A uniform film thickness of about 0.1 mm was maintained for all the samples.

IV. Thermogravimetric Analysis (TGA)

Thermogravimetry (TG), in which the catalyst sample is subjected to a controlled heating to higher temperatures at a specified heating rate is a well-established technique in heterogeneous catalysis. It finds widest applications in the determination of drying range, calcination temperature, phase composition, percentage weight loss and stability limits of a catalyst.

In TG, the loss of weight of a sample is being continuously recorded over a period of time under controlled heating rate. Changes in weight are due to the rupture and/or formation of various physical and chemical bonds at elevated temperatures, which lead to the evolution of volatile products or the formation

of heavier reaction products. From the thermogram, where we plot weight against temperature, information about dehydration, decomposition and various forms or products at various temperatures can be obtained. The first derivative of the thermogram (DTG) gives a better understanding of the weight loss and can also be used to determine the thermal stability of the samples.

Shimadzu TGA-50 instrument was used for carrying out thermogravimetric studies. About 20 mg of the sample was used at a heating rate of 20°C min^{-1} in N_2 atmosphere. The TG data were computer processed to get thermograms. Any decomposition of the sample is indicated by a dip in the curve. These dips correspond to the weight loss due to decomposition and hence provide an idea about the species lost during the heating step.

V. X-Ray Diffraction Analysis (XRD)

X-ray analysis is one of the most widely used techniques in heterogeneous catalysis, since it constitutes a powerful and readily available method for determining the atomic arrangements in solid substances, their composition and crystallinity. It is a versatile method for the qualitative and quantitative analysis of solid phases and can provide useful information about the crystallite size of specific components and the purity of the substance. Other uses include the identification of the structure of the substance, its allotropic transformation, transition to different phases, lattice constants and the presence of foreign atoms in the crystal lattice of an active component[11].

The principle of XRD is based on the interaction of X-rays with the periodic structure of a polycrystalline material, which acts as a diffraction grating. A fixed wavelength is chosen for the incident radiation and the diffraction pattern is obtained by observing the intensity of the scattered radiation as a function of scattering angle of 2θ. The relationship among the wavelength of X-ray beam λ, the angle of diffraction, θ and the interplanar distance or d-spacing d, is given by Bragg's equation,

$$n\lambda = 2d \sin\theta,$$

where, n is an integer called the order of diffraction

A rough estimate of crystallite size can be obtained from the line broadening using the Scherrer's equation[12],

$$t = \lambda / B \cos\theta$$

where, B is the Full Width at Half Maximum (FWHM) of the strongest peak, t is the crystal diameter and θ, the Bragg angle.

XRD patterns were recorded in a Rigaku D-max C X-ray diffractometer using Ni filtered Cu-K_α radiation (λ = 1.5406 Å). The crystalline phases were identified by comparison with the standard JCPDS (Joint Committee on Powder Diffraction Standards) data file[13].

VI. Fourier Transform Infrared Spectroscopy (FTIR)

Infrared spectroscopy is a well-accepted technique for the study of catalysts and surface reactions. Infrared spectra provide valuable information about the basic characteristics of a molecule, namely, the nature of atoms, their spatial arrangement and their chemical linkage, since it can identify the various functional groups, the adsorbed species and reaction intermediates on the catalyst surface. It is basically a bulk technique that takes advantage of the surface aspects of the catalyst and provides information about the structure of surface sites those are either directly observable or made observable by pre-adsorption of probe molecules. The frequencies and intensities of the IR bands can give abundant evidence on the state of supported metal dispersion, structure, metal-support interaction, metal-metal interaction, etc. It can also be used to measure the surface acidity of catalysts. FTIR offers higher sensitivity and higher resolution than conventional IR.

Infrared spectroscopy has a prominent role in identifying the surface aspects of supported vanadia catalysts, since it can discriminate between various vanadium oxide structures. Infrared spectroscopy also provides direct

information about the interaction of vanadium oxide with the surface hydroxyls of oxide supports[14-18]. In the case of sulfated metal oxide, from the position and intensity of the bands the structure and co-ordination behaviour of the sulfate groups present on the catalyst surface can be identified [19-21].

FTIR spectra of the powder samples were measured by the KBr disc method over the range 4000-400 cm^{-1} using Shimadzu DR 5001 instrument.

VII. Solid-State ^{51}V NMR Spectroscopy

Solid-State Nuclear Magnetic Resonance (NMR) techniques represent a novel and promising tool in the repertoire of methods for examining the molecular structure of amorphous and polycrystalline solid samples. In heterogeneous catalysis its principal use is to characterize the chemical and structural environment of atoms on the catalyst or in species adsorbed on the catalyst surface[22]. Since NMR only probes the local environment of a nucleus under study, this method is well suited for the structural analysis of disordered catalyst surfaces. In addition to the structural information provided, the direct proportionality of the signal intensity to the number of contributing nuclei makes NMR useful for quantitative studies[23,24].

Solid-state NMR studies of heterogeneous catalysts are usually carried out by 'Magic Angle Spinning' (MAS) i.e., rapid mechanical rotation of the sample about an axis subtended at an angle 54°44' with respect to the magnetic field. This technique removes line broadening from dipolar interactions, chemical shift anisotropy and quadrupolar interactions to the first order since all of the interactions contain the angular term $3\cos^2\theta - 1$ which is zero for $\theta = 54.7°$. The number of signals in the solid-state NMR spectrum gives the number of different structural environment of the observed nucleus in the sample while the relative signal intensities correspond to the relative occupancies of the different environments[25].

Solid-State ^{51}V NMR has been used to probe the local environment of vanadium at the surface and has provided insight into the types of sites present and their role in selective catalytic oxidations and reductions[26-28]. The ^{51}V isotope (I=7/2) has a large magnetic moment and short spin - lattice relaxation time due to the nuclear quadrupolar interactions. The solid-state NMR spectrum is produced by the interaction of this moment with the electrostatic gradients created by an asymmetric environment. Typical line shapes of distorted tetrahedral, distorted octahedral, regular tetrahedral and square pyramidal environments can often be identified and profitably used to characterize the different types of vanadia species on the catalysts surface qualitatively and quantitatively[29].

^{51}V NMR spectra of the prepared samples were measured by 300 DSX Brooker spectrometer with a static magnetic field of 8.5 T. The ordinary single pulse sequence was used and the number of scans was adjusted from 200 to 15,000 depending on the concentration of vanadium. The spectra were expressed with the reference signal of NH_4VO_3 at a chemical shift value of 0 ppm and the higher frequency shift from the standard was taken as positive.

VIII. Diffuse Reflectance UV-VIS Spectroscopy (DR UV-VIS)

Diffuse reflectance UV-visible spectroscopy allows the study of electronic transitions between orbitals or bands in the case of atoms, ions and molecules in gaseous, liquid or solid state. In catalysis, the informations given by DRS mainly include the active phase-supports interaction, the chemical changes during a modification procedure leading to the active phase and the nature of the co-ordination sphere of the active surface species.

Electronic transitions of transition elements are two types, metal-centered transitions [d-d or (n-1) d - ns] and charge-transfer (CT) transitions. d-d transitions give information about the oxidation state and co-ordination environment of transition metal ion. (n-1) d - ns transitions are often too high

in energy to be observed in the spectrum. The CT transitions are intense since they are Laporte–allowed and are sensitive to the nature of donor and acceptor atoms[30]. In DR measurements, the light emitted by the sample and the reference material is collected by an integration sphere and the detector of the double beam spectrometer gives the apparent absorbance.

Diffuse reflectance UV-VIS spectroscopy is widely used in the surface characterization of supported vanadia catalysts. The CT spectra of V^{+5} (d^0) are strongly influenced by the environment of the central vanadium ion in mono/multi layer phase[31]. The CT absorption band positions can differentiate between the monomeric and two dimensional vanadia species and their coordination geometries[32].

Diffuse reflectance UV-VIS spectra of the samples were recorded using a conventional spectrophotometer (Ocean Optics-2000) with CCD detector. Magnesium oxide (MgO) was used as the reference material.

2.5 SURFACE ACIDITY MEASUREMENTS

Surface acidity and basicity measurements have received considerable attention in recent years because they can provide significant information about the behaviour of solid surfaces. Determination of strength of the acid sites exposed on the solid surface as well as their distribution is a necessary requirement to understand the catalytic properties of acidic solids. The conversion and selectivity of acid catalyzed reactions are influenced not only by the nature of active sites but also by its number and strength.

A number of physico-chemical methods have been developed and widely accepted to evaluate the strength and amount of surface acid sites on catalysts and a large variety of probe molecules have been utilized to ascertain the acidity quantitatively as well as to provide an insight into the distribution of these acid sites[33]. However, the range of applicability of most of these methods is limited to a narrow domain of solids and to a given experimental procedure.

2.5.1 Materials

The materials used for surface acidity measurements are given below

Materials	*Suppliers*
H_2SO_4	Merck
NaOH	CDH
Perylene	Merck
Benzene	Qualigens
Cumene	Merck

2.5.2 Methods

A thorough investigation of the surface acidity of the prepared systems was done using three independent techniques namely,

I. Temperature programmed desorption of ammonia

II. Perylene adsorption followed by spectroscopic measurements

III. Vapour-phase cumene cracking reaction

The experimental procedures for these methods are as follows.

I. Temperature Programmed Desorption of Ammonia (TPD)

Among the various physico-chemical methods used to characterize acid sites, temperature programmed desorption is the most promising technique, facilitating the direct determination of the total acidity and the distribution of strength of acid sites. Ammonia is chosen as the gas-phase probe molecule, which by means of gas-solid interaction and their site titration describes the catalyst surface behaviour. When chemisorbed on a surface possessing acid properties, ammonia can interact with the acidic protons, electron acceptor sites and hydrogen from neutral or weakly acidic hydroxyls and thus can detect most of the different types of acid sites[34]. An ammonia molecule can be retained on the surface of oxides in different modes[35] viz.,

i. hydrogen bonding *via* one of its hydrogen atom to a surface oxygen atom or to the oxygen of surface hydroxyl group. It is the weakest mode of interaction.

ii. transfer of proton from surface hydroxyl to the adsorbate.

iii. co-ordination to an electron-deficient metal atom. It is the strongest mode of interaction.

Thus a fairly reliable interpretation of the TPD pattern of ammonia from solid acids can be attributed to ammonia chemisorbed on weak, medium and strong sites respectively, being yet not possible to discriminate between Brönsted and Lewis acidic sites[36,37].

Ammonia TPD measurements in the range 100-600°C were performed in a conventional flow-type apparatus using a steel reactor (30 cm length and 1 cm diameter), a heating rate of 10°C min^{-1} and in a nitrogen atmosphere. Pelletized catalyst was activated at 300°C inside the reactor under nitrogen flow for half an hour. After cooling to room temperature, it was saturated with ammonia, injected in absence of the carrier gas flow and allowed to attain equilibrium. The excess and physisorbed ammonia was purged out by a current of nitrogen for half an hour at 100°C at which the TPD was subsequently started. The temperature was then raised to 600°C in a stepwise manner at a linear heating rate. The ammonia evolved at intervals of 100°C was trapped in known volume of dilute sulfuric acid solution and estimated volumetrically by back titration with standard NaOH and is plotted as a function of catalyst temperature (desorption temperature). Frequently, the strength of the acidic sites from which ammonia molecule desorbs is simply characterized by the temperature of peak maxima of the desorption spectra. The different surface acidities were determined by quantifying the desorbed ammonia at various temperatures. The amount of ammonia desorbed in the temperature ranges 100-200, 200-400, 400-600°C was assigned as weak, medium and strong acid sites respectively.

II. Perylene Adsorption Studies

Adsorption studies using perylene as electron donor gives information regarding the Lewis acidity in presence of Brönsted acidity[38]. The principle is based on the ability of the catalyst surface acid sites (electron deficient centers) to accept electron from an electron donor, like perylene to form a charge-transfer complex. The amount of the adsorbed species can be measured by spectroscopic means[39]. Perylene has an electron affinity of 1.17 eV,[40] which accounts for the ease with which it can form cation radical in liquid solutions. The adsorption of the molecule on the metal oxide leads to the reduction of the molecule and implies the presence of sufficiently stronger electron acceptor sites (Lewis acid sites) on the catalysts surface[41].

In this method, adsorption experiment was carried out in a 50 mL stoppred U-shaped tube taking 10 mL each of freshly prepared perylene in benzene solution and stirring it with a weighed amount of the catalyst for 4 h. The concentration range of perylene was varied from 0.01 to 0.02 mol L^{-1} in benzene. After 4 h, the contents were filtered and the absorbance of the filtrate was measured at a particular wavelength. For all the cases, the sorption experiments were performed in the adsorbate concentration range where Beer-Lambert's law is valid. Since perylene is getting adsorbed on the catalyst surface, its concentration will be less in the solution after adsorption. The amount of perylene adsorbed was determined by measuring the absorbance of the solution before and after adsorption. From the Langmuir plots, the limiting amount of perylene adsorbed over the catalyst surface, which is a measure of the Lewis acidity of the system, is obtained. The chemical interaction between the adsorbate and the sample may be described by the Langmuir adsorption isotherm,

$$C/X = 1/BX_m + C/X_m$$

where, C is the concentration of perylene solution, B, a constant and X_m is the limiting amount of perylene adsorbed, which corresponds to the theoretical amount of the adsorbate required to cover all the active sites for base adsorption.

All the absorbance measurements were done in a UV-VIS spectrophotometer (Shimadzu UV-160 A) at a λ_{max} 439 nm using 10 mm quartz cell.

III. Vapour-Phase Cumene Cracking Reaction

Vapour-phase cumene cracking is a model reaction in identifying the Lewis/ Brönsted acidity of a catalyst. Cumene is cracked to benzene and propene over Brönsted sites as opposed to the dehydrogenation to α-methylstyrene over Lewis acid sites[42]. Thus the relative amount of benzene and α-methylstyrene in the product mixture is a good indication of the acidity possessed by the catalyst.

Cumene cracking reaction was carried out in the vapour-phase in a fixed bed, down-flow, vertical quartz reactor (2 cm diameter, 40 cm length) inside a double zone furnace. 0.5 g catalyst activated at the required temperature was placed inside the reactor immobilized using glass wool. Cumene was fed into the reactor at a flow rate of 6 mL h^{-1}. The reactor bed was maintained at 350°C. The product analysis was achieved gas chromatographically by comparison with authentic samples. Table 2.1 gives the analytical details of the reaction.

2.6 CATALYTIC ACTIVITY MEASUREMENTS

The catalytic activity of the prepared catalyst systems was tested for some well-known industrially important reactions. The reactions can be carried out either in liquid or vapour-phase. Liquid-phase reactions suffer from the limitation that the maximum temperature attainable is the refluxing temperature of the reaction mixture. This restriction is efficiently surmounted in the vapour-phase conditions.

For the present investigation, Friedel-Crafts benzylation of aromatics and cyclohexanol oxidation with H_2O_2 were carried out in liquid-phase whereas Beckmann rearrangement of cyclohexanone oxime and oxidative dehydrogenation (ODH) of ethylbenzene were done in vapour-phase.

2.6.1 Materials

The materials used for catalytic activity measurements are given below.

Materials	*Suppliers*
Benzene	Merck
Toluene	Merck
o-Xylene	Merck
Benzyl chloride	Merck
Cyclohexanol	S. d. Fine
H_2O_2 (30%)	Qualigens
Cyclohexanone oxime	Prepared in the Laboratory
Ethylbenzene	CDH

2.6.2 Methods

The experimental procedures adopted for catalytic activity measurements are described below:

I. Liquid-Phase Reactions

The liquid-phase reactions performed were benzylation of arenes (benzene, toluene and *o*-xylene) using benzyl chloride as the alkylating agent and the oxidation of cyclohexanol using hydrogen peroxide as co-oxidant.

All the reactions were carried out on a 100 mL/ 50 mL round bottomed (R.B) flask equipped with an oil bath, a magnetic stirrer and air/water condenser. The temperature of the oil bath was adjusted according to the requirement for a particular reaction and kept constant by means of a dimmerstat.

i) Benzylation Reaction

The liquid-phase benzylation of benzene, toluene and *o*-xylene using benzyl chloride was carried out in a 50 mL double-necked flask fitted with a spiral condenser. The temperature was maintained using an oil bath. In a

typical run, the aromatic substrate (benzene, toluene or *o*-xylene as the case may be) and benzyl chloride in the specific molar ratio was added to 0.1 g of the catalyst in the R.B flask and the reaction mixture was magnetically stirred. The product analysis was done using a Chemito 8610 Gas Chromatograph equipped with a flame ionization detector and SE-30 column. The GC analytical conditions are given in Table 2.1. The aromatic substrate being taken in excess, the yields were calculated based on the amount of alkylating agent. The selectivity for a product was expressed as the amount of the particular product divided by the total amount of products and multiplied by 100.

The influence of the reaction parameters like substrate to benzylating agent, molar ratio, reaction temperature, duration of run and the amount of the catalyst was investigated in detail. The present work also attempts a closer look into the metal leaching and deactivation of the systems under the reaction conditions for understanding the molecular aspects of the reaction. The susceptibility of the catalyst to the presence of moisture was also tested.

ii) Cyclohexanol Oxidation

The catalytic oxidation of cyclohexanol was conducted at atmospheric pressure in a 100 mL R.B flask equipped with a condenser and a magnetic stirrer. The reactants (cyclohexanol, 30% H_2O_2 and solvent) in the required ratio were stirred with 0.1 g of the catalyst. The products were identified by comparison with authentic samples in a Chemito 8610 Gas Chromatograph using Carbowax column the temperature programme of which is discussed in Table 2.1. The conversions and product selectivity were scanned for different H_2O_2/ phenol ratios and reaction temperatures. The solvent effect was also subjected to investigation.

II. Vapour-Phase Reactions

Applicability of the liquid-phase reaction is often limited by low temperature requirement below the boiling point of the least boiling

component of the reaction mixture. Reactions can be done at much higher temperatures in the vapour-phase set up where the reactants will be in the gas phase, which undergo reaction over the catalyst surface.

We have performed Beckmann rearrangement of cyclohexanone oxime and oxidative dehydrogenation of ethylbenzene as vapour-phase reactions. The vapour-phase reactions were conducted at atmospheric pressure in a fixed bed, vertical, down-flow quartz reactor inserted into a double-zone furnace. The catalyst in powdered form (0.5 g) was immobilized using glass wool and sandwiched between inert silica beads. The thermocouple positioned near the catalyst bed monitored the reaction temperature. The temperature was regulated using a temperature controller. The reactant was fed into the reactor with the help of a syringe pump at a controlled flow rate. The condensed reaction mixture was collected downstream from the reactor in a receiver connected through a cold water-circulating condenser. The products were collected at regular time intervals and analyzed gas chromatographically.

i) Beckmann Rearrangement of Cyclohexanone Oxime

Exactly 0.5 g of the activated catalyst was placed at the center of the reactor. The feed containing cyclohexanone oxime (5 wt%) in benzene (diluent) was introduced to the reactor using a syringe pump at the required flow rate. The reactor effluents including the products were collected at the end of a water condenser and analyzed by GC equipped with SE-30 column and FID detector. Table 2.1 reveals the analysis conditions of the product mixture.

The influence of feed rate and reaction temperature was also investigated. Deactivation studies were also conducted for the different catalyst systems.

Table 2.1
Analysis conditions for various catalytic reactions.

Catalytic Reaction	Analysis conditions			
	Column	Temperature Programme for the column	Injector Temperature (°C)	Detector Temperature (°C)
Cumene Cracking	SE-30	120°C-isothermal	230	230
Friedel-Crafts benzylation	SE-30	80°C-3-5°C-230°C*	250	250
Cyclohexanol Oxidation	Carbowax	70°C-3-5°C-170°C	200	200
Beckmann Rearrangement	SE-30	90°C-3-5°C-240°C	250	250
Oxidative dehydrogenation	FFAP	100°C-isothermal	150	150

*Initial temperature-Duration-Rate of increase-Final temperature.

ii) Oxidative Dehydrogenation of Ethylbenzene

Vapour-phase oxidative dehydrogenation reaction runs were carried out in a fixed bed reactor by passing 25 mL of air/ minute along with ethylbenzene in the temperature range 300-550°C. The products were analyzed using GC fitted with FFAP column and FID detector. The gas chromatographic analysis details are specified in Table 2.1. A detailed investigation on the effect of reaction parameters like temperature, feed rate and time on stream was done to obtain a better understanding of the nature and course of the reaction.

REFERENCES

1. K. Morikawa, T. shirasaki and M. Okada, *Adv. Catal.*, 20 (1969) 97.
2. F. D. Snell and L. S. Ettre, *"Encyclopedia of Industrial Chemical Analysis"*, Vol. 17, p. 475, Intersciences, New York, 1973.
3. K. V. Narayana, A. Venugopal, K.S. Rama Rao, V. Venketa Rao, S. Khaja Masthan and P. Kanta Rao, *Appl. Catal. A. Gen.*, 150 (1997) 269.
4. K. Arata, *Appl. Catal. A. Gen.*, 146 (1996) 3-32.
5. M. Ponzi, C. Duschatsky, A. Carraseull, E. Ponzi, *Appl. Catal. A. Gen.*, 169 (1998) 373.
6. J. R. Sohn, S. G. Cho, Y. I. Pae and S. Hayashi, *J. Catal.*, 150 (1996) 170-177.
7. H. Matsuhashi, M. Hino, K. Arata, *Chem. Lett.*, (1998) 1027.
8. Clive Whiston, *"X-ray methods-Analytical Chemistry by Open Learning"*, John Wiley, New York, 1991, p. 296.
9. S. Brunauer, P. H.. Emmette and E. Teller, *J. Am. Chem. Soc.*, 60 (1938) 309.
10. A. Howie, *"In Characterization of Catalysts"*, J. Thomas and R.M. Lambert Eds., John Wiley, New York, 1980, p. 89.
11. D. K. Chakrabarthy, *"Solid-state Chemistry"*, New Age International Ltd., New Delhi, 1996, p. 14.
12. Clive Whiston, *"X-ray methods-Analytical Chemistry by Open Learning"*, John Wiley, New York, 1987, Ch.3.
13. H. Lipson and H. Steeple, *"Interpretation of X-ray Powder Diffraction Patterns"*, Macmillan, London, 1970, p. 261.
14. L. D. Frederickson and D. M. Hausen, *Anal. Chem.*, 35 (1963) 818.
15. F. Hatayama, T. Ohno, T. Maruoka, T. Ono and H. Miyata, *J. Chem. Soc. Faraday Trans.*, 87 (1991) 235.
16. G. Ramis, C. Cristiani, P. Forzetti and G. Busca, *J. Catal.*, 124 (1990) 574.
17. G. Busca, Mater. Chem. Phy., 19 (1988) 157.

18. H. Miyata, M. Kohno, T. Ono, T. Ohno and F. Hatayama, *J. Mol. Catal.*, 63 (1990) 181.

19. R. L. Parfitt and R. S. C. Smart, *J. Chem. Soc. Faraday Trans.*, 1, 73 (1977) 796.

20. D. A. ward and E. I. Ko, *J. Catal.*, 150 (1994) 18.

21. N. B. Colthup, *J. Opt. Soc. Am.*, 40 (1950) 397.

22. G. Ertl, H. Knozinger and J. Weitkamp, "*Handbook of Heterogeneous Catalysis*", Vol.2, VCH, Weinheim, 1997, p. 256.

23. J. R. Sohn, M. Y. Park and Y. I. Pae, *Bull.Korean Chem. Soc.*, 17 (1996) 274-279.

24. E. H. Park, M. H. Lee and J. R. Sohn, *Bull.Korean Chem. Soc.*, 21, No.9 (2000) 913-918.

25. E. R. Andrew, *Intern. Rev. Phy. Chem.*, 1 (1981) 195.

26. H. Eckert and I. E. wachs, J. Phy. Chem., 93, 6 (1989) 796-805.

27. H. Eckert, G. Deo and I. E. wachs, *Coll. Surf.*, 45 (1990) 347-359.

28. V. M. Mastikhin, V. V. Terskikh, O. B. Lapina, S. V. Filimonova, M. Seidl and H. Knozinger, *Sol. St. Nucl. Mag. Res.*, 4 (1995) 369-379.

29. G. C. Bond, *Appl. Catal.*, 71 (1991) 1-31.

30. G. Ertl, H. Knozinger and J. Weitkamp, "*Handbook of Heterogeneous Catalysis*", Vol.2, VCH, Weinheim, 1997, p. 646.

31. M. Schrami-Marth and A. Wokaun, *J. Chem. Soc. Faraday Trans.*, 81, 16 (1991) 2635-2646.

32. U. Scharf, M. Schrami-Marth and A. Wokaun, *J. Chem. Soc. Faraday Trans.*, 87, 19 (1991) 3299-3307.

33. P. A. Jacobs, in "*Characterization of Heterogeneous Catalysts*", F. Delanney, Ed., Studies in Surface Science and Catalysis, 20., Elsevier, Amsterdam, 1985, p. 311.

34. T. Kijenski and A. Baiker, *Catal. Today*, 5 (1989) 1-120.

35. M. C. Kung and H. H. Kung, *Catal. Rev.-Sci. Eng.*, 27 (1985) 425-460.

36. A. Francesco, D. Roberto and P. Adolfo, *Appl. Catal. A. Gen.*, 170 (1998) 127-137.

37. H. G. Karge and V. Dondur, *J. Phy. Chem..*, 94 (1990) 765.

38. B. D. Flockart, J. A. N. Scott and R.C. Pink., *Trans. Faraday Soc.*, 62 (1966) 730.

39. J. J. Rooney and R. C. Pink, *Proc. Chem. Soc.*, (1961) 70.

40. A. Streitweser and I. Schwager, *J. Phy. Chem.*, 66 (1962) 2316.

41. B. D. Flockart, I. M. Sesay and R.C. Pink, *J. Chem. Soc. Faraday Trans.*, 79 (1983) 1009-1015.

42. S. M. Bradley and R. A. Kydd, *J. Catal.*, 141 (1993) 239.

Chapter 3

Physico-Chemical Characterization

ABSTRACT

Supported vanadia catalysts on SnO_2 and ZrO_2 and its sulfated analogues were successfully synthesized by the incipient wetness impregnation method. The catalyst samples prepared were characterized by adopting various physical methods such as EDX, XRD, BET surface area and pore volume measurements, Thermogravimetry, FTIR, ^{51}V NMR and DR-UV-VIS spectroscopy. TPD of ammonia, perylene adsorption method and vapour-phase cumene cracking reaction were employed to quantify the various types of acid sites on the surface of the catalysts. The characterization techniques established that vanadium oxide species are highly dispersed as two-dimensional over layers on the metal oxide supports. The surface vanadia species exist as isolated VO_4 tetrahedral units at low vanadia loadings, which polymerize to give octahedral VO_6 units and various disordered para-crystalline V_2O_5 phases at higher loadings. The basic structure of the active vanadia species is not affected by the surface modification by sulfate groups. In most cases, the supported systems and its sulfated series exhibited a remarkable heterogeneity in surface acidity.

3.1 INTRODUCTION

Heterogeneous catalysis deals with the transformation of molecules at the interface between a solid (catalyst) and the gaseous or liquid-phase carrying these molecules[1]. This transformation involves a series of phenomena, the understanding and control of which require the study of how the catalyst is constituted at its surface as well as in the bulk. Again, variation in the conditions of preparation and pretreatment very much alters the surface properties and catalytic behaviour of the catalysts[2]. Hence they must be thoroughly

characterized before use. The development of powerful characterization techniques therefore has been of major importance in recent years.

Physico-chemical characterization of the prepared catalysts is usually done to ensure the purity of the systems and to get an insight to the nature of the active sites on the catalyst surface. The preparation of supported vanadia catalysts with varying vanadium oxide content as well as its surface modification by sulfate addition were done by the conventional wet impregnation method. Following catalyst preparation, the chemical composition and surface area of the systems were determined by EDX analysis and BET surface area measurements respectively. Thermogravimetric analysis of the samples gave an idea about the thermal stability of the catalysts. Information on the chemical structure of the supported oxides could be obtained from vibrational and electronic spectroscopies such as FTIR, Diffuse Reflectance UV-VIS spectroscopy. XRD and solid–state ^{51}V NMR provided additional characterization techniques of the materials.

Since solid supported catalysts and the sulfated metal oxides are well known for its surface acidity, a more detailed investigation of the acidity of the prepared systems was desirable. Therefore, in the present study, three independent methods were dedicated to the problems of nature, amount and strength of acid sites. Ammonia TPD, where the strength and distribution of acid sites were evaluated in terms of the amount and nature of the sites from which the desorption of ammonia occurred, limiting amount of perylene adsorbed on the catalyst surface which was measured by spectroscopic means and the selectivity ratio obtained in acid-catalyzed test reaction of cumene cracking were employed to find the surface acidity of the prepared systems. The results of each characterization method and their interpretations are included in this chapter. The textural properties and acidity measurements are presented in two separate sections; (I) Physical characterization (II) Surface acidity measurements.

3.2 PHYSICAL CHARACTERIZATION

The catalyst samples prepared were characterized by adopting various physical methods such as Energy Dispersive X-ray (EDX) analysis, BET surface area and pore volume measurements, X-ray diffraction analysis and different spectroscopic techniques. The observations and the explanation of the results for each method are presented separately for V_2O_5-SnO_2 and V_2O_5-ZrO_2 under two sections.

3.2.1 V_2O_5-SnO_2 Systems

I. Energy Dispersive X-ray Fluorescence Analysis (EDX)

The elemental composition of the vanadia impregnated as well as the sulfate-doped samples were determined using EDX analysis and the results for a few samples are given in Table 3.1.

Table 3.1
Energy Dispersive X-ray analysis data for V_2O_5-SnO_2 systems.

Catalysts	Composition					
	Atom %			Oxide %		
	Sn	V	S	SnO_2	V_2O_5	SO_4
T0	100	-	-	100	-	-
T6	86.6	13.4	-	94.3	5.7	-
T9	82.7	17.3	-	91.2	8.8	-
ST0	98.1	-	1.9	98.9	-	1.1
ST6	88.6	8.7	2.3	93.0	5.5	1.5
ST9	81.2	11.9	6.9	88.7	8.5	2.8

Results:

The EDX data show the surface composition of the supported as well as the sulfated systems. From the results, the vanadium oxide content of T6 system is found to be 5.7% whereas for the sulfated analogue, it is 5.5%. In the case of high loaded systems with an expected vanadia loading of 9 wt%, the

values obtained are 8.7% and 8.5% respectively for T9 and ST9. The amount of sulfate retained in the sample shows a gradual increase from 1.1 to 2.5% as we increase the vanadium oxide content from 0 to 9 wt% though the same concentration of sulfuric acid solution was used for sulfate modification.

Discussion:

The elemental analysis of the prepared systems clearly indicates that the expected catalyst profile can be successfully achieved by the conventional wet impregnation method. This is evident from the EDX data, which show the amounts of vanadium oxide in the samples as very close to the expected values. Thus, by this method, it is possible to get desired loading of vanadium oxide either in more or less than the monolayer equivalent. The sulfate content of the vanadia promoted samples is considerably higher, when compared with simple sulfated system, which indicate that vanadium oxide doping brings about a considerable reduction in the extent of sulfate loss from the catalyst surface. The fact that the presence of vanadia stabilizes the sulfate overlayers on the catalyst surface is also apparent from the increase in the sulfate retaining capacity of the systems with increase in vanadia content.

II. BET Surface Area and Pore Volume Measurements

Table 3.2 presents the surface areas and pore volumes of the V_2O_5-SnO_2 systems measured using the BET method by nitrogen adsorption at –196°C. All the samples were calcined and activated at 550°C prior to each experiment.

Results:

Table 3.2 shows the effect of vanadium oxide content and sulfate modification on the surface properties of the catalysts. From the table, it is observed that the surface area of the support is increased from 25 to 49 $m^2 g^{-1}$ when we introduce 3 wt% vanadium oxide to the single oxide. In the supported systems, the surface area increases with vanadia content, reaches a maximum value for T9 system and then decreases with further increase in vanadium oxide content. The maximum surface area obtained for the

supported system is 83 $m^2 g^{-1}$. Crystalline vanadia (V_2O_5) is having very low surface area value (1.8 $m^2 g^{-1}$) compared to either pure tin oxide or the supported systems. The pore volumes measured by the same method show similar trend and the maximum value observed is 0.081 $cm^3 g^{-1}$ for T9 system.

Table 3.2
Surface area and pore volume of V_2O_5-SnO_2 systems.

Systems	BET Surface Area ($m^2 g^{-1}$)	Pore Volume ($cm^3 g^{-1}$)	Systems	BET Surface Area ($m^2 g^{-1}$)	Pore Volume ($cm^3 g^{-1}$)
T0	25	0.023	ST0	79	0.081
T3	49	0.054	ST3	87	0.086
T6	61	0.062	ST6	95	0.096
T9	83	0.081	ST9	118	0.110
T12	72	0.072	ST12	89	0.092
T15	67	0.064	ST15	74	0.072
V	1.8	0.002	SV	3.3	0.003

The surface area and pore volume of the sulfated samples are invariably higher than those of the oxides without sulfate treatment. Though the surface area and pore volumes are enhanced to a greater extent the trend is the same as in the case of unmodified systems. It gradually increases, reaches a maximum at 9 wt% loading and then declines. The surface area and pore volume of ST9 are 118 $m^2 g^{-1}$ and 0.11 $cm^3 g^{-1}$ respectively.

Discussion:

From Table 3.2, it is established that the presence of vanadium oxide on the support surface has an imperative effect on surface area and pore volume of V_2O_5-SnO_2 systems. It is found that the surface changes appreciably upon impregnation of vanadia, the change being more at high loading. According to Gopalan *et al.*[3], predominantly sintering and to some extent grain growth are the main mechanisms by which the surface area of a metal oxide decreases in

the temperature range 400-600°C. The presence of vanadium oxide reduces the sintering and grain growth by forming a two-dimensional layer on the surface of SnO_2 which reduces the mobility of defects on the grain surface or reduces the surface energy of the support metal oxide grain[3-5] thereby increasing the surface area. At high loading, the crystalline V_2O_5 formed can block up the pores of tin oxide support leading to the abatement of the surface area. The repartition of the pore volume at high loading also supports the dramatic plugging of pores with V_2O_5 particles[6]. The decrease in pore volume is due to the decrease in the number of pores as the crystallites agglomerize by virtue of sintering and enhanced crystallization of vanadium oxide.

The remarkable enhancement of surface area and pore volume by sulfate modification is attributed to the retardation of crystallization of the support oxides by the sulfate groups present on the surface[7]. The lowering of degree of crystallinity, as evident from the XRD patterns discussed below, supports the increase in surface area by sulfate treatment. The dispersed vanadia particles along with the sulfate species prevent the agglomerization of tin oxide particles leading to an enhanced surface area at low loading[8]. The blocking of pores again accounts for the decrease in surface area with increase in the vanadium oxide content in the sulfated systems also. From the EDX results given in Table 3.1, it is seen that, with increase in the vanadium oxide content, the sulfate retaining capacity of the tin oxide systems increases. The preferential attachment of these sulfate groups at the edges of the pores leading to the partial filling of the pores, which reduces their effective radii and volumes can be an additional factor in the reduction of surface area and pore volume of the sulfated sample with high vanadia content.

III. Scanning Electron Microscopy (SEM)

Scanning electron micrographs of the representative systems are shown in Figure 3.1. The effect of vanadia loading as well as sulfate modification is apparent from the SEM pictures of T0, T3, T6 and ST6 samples.

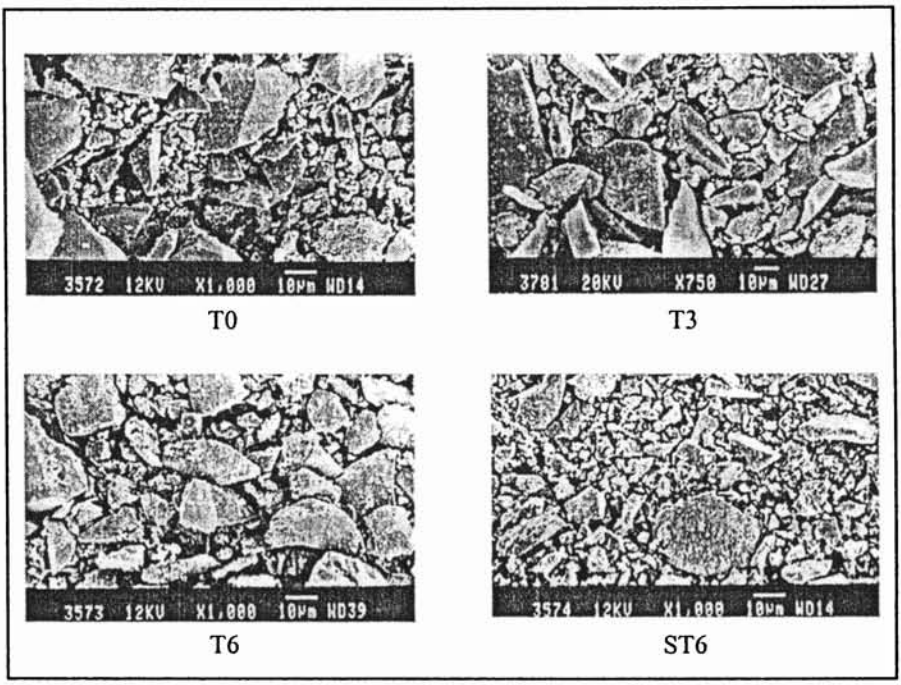

Figure 3.1
Scanning Electron Micrographs of V_2O_5-SnO_2 systems.

Results:

Bigger crystallites are found in the case of pure SnO_2. The particle size is observed to be decreasing with increase in the vanadium oxide content as evident from the SEM photographs of T3 and T6. Smaller particles with almost uniform size are seen in the case of ST6 showing the effect of introduction of sulfate anions to the catalyst surface.

Discussion:

From the results, it is found that vanadia loading to the single metal oxide surface reduces the particle or crystallite size considerably. Combining the SEM and surface area results, it is thus expected that the vanadia loading up to 9 wt% has a positive effect on the surface properties as well as catalytic activities. The sulfate modification of the surface leads to further reduction in the particle size

and makes the catalyst surface more uniform. These results support the observation that sulfate modification increases the surface area of the samples. The presence of vanadium oxide and surface sulfate groups prevent the agglomerization of SnO_2 particles, thereby increasing the surface area[8].

IV. Thermogravimetric Analysis (TGA)

To examine the thermal properties of the prepared samples, thermal analysis was carried out and Figure 3.2 illustrates the TG curves (dotted line) obtained for pure, supported and sulfate treated samples. Uncalcined samples of T0, T6 and ST6 were taken as the representatives and subjected to TG analysis. A more clear decomposition pattern is obtained by plotting the derivative of the curves, which is also displayed in Figure 3.2 (solid line).

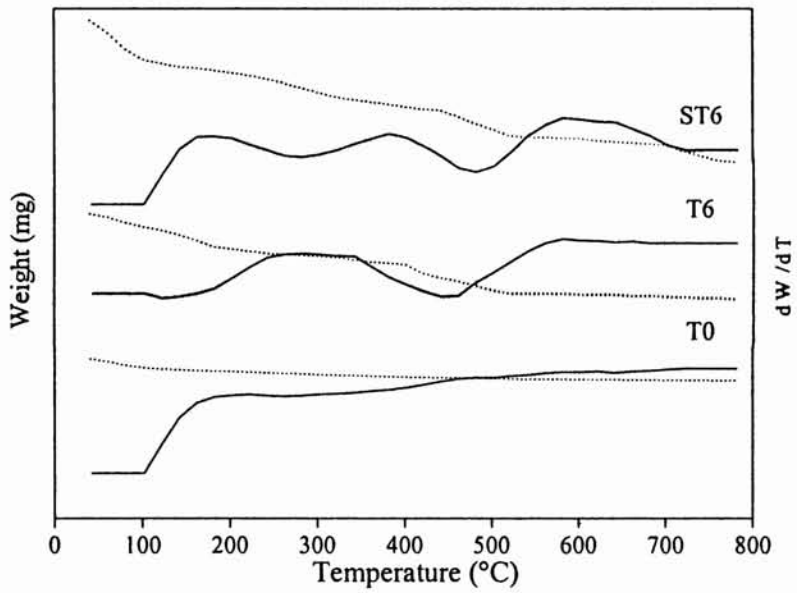

Figure 3.2
TG (....) DTG (—) curves of V_2O_5-SnO_2 systems.

Results:

The TG-DTG curve of pure tin oxide shows a dip near 100°C. In the case of vanadia promoted sample T6, two additional weight losses at about 180°C and 350 to 450°C temperature range are also observed. No other weight loss is noticed in the higher temperature region in this case. The sulfated samples showed an initial weight loss at around 100°C and in addition to those observed for T6, yet another decomposition is prominent above 700°C for this system.

Discussion:

The weight loss around 100°C for pure tin oxide is due to the removal of physisorbed water from the catalyst surface[9,10]. No phase transition is observed here indicating the stability of the tin oxide phase. In the case of T6, the additional dips in the thermogram at 180°C and between 350 and 450°C may be attributed to the evolution of NH_3 and H_2O decomposed from NH_4VO_3 used in the preparation of supported systems. According to Ponzi *et al.*,[11] during this temperature range (180-450°C), the NH_4VO_3 decomposition occurs with the release of two molecules of NH_3 and one of H_2O, giving rise to an intermediate $(NH_4)_2O(V_2O_5)_3$, which eventually transforms to V_2O_5. No other compound formation is noticed here since there is no additional weight loss at higher temperature. The melting of vanadia from the catalyst surface is reported to be at 674°C[11]. The absence of any weight loss at higher temperature range shows that the vanadia present on the support surface is more stable. Careful examination of the TG-DTG curve of the sulfated system ST6, reveals the commencement of decomposition of sulfate into SO_2/ SO_3 vapours above 700°C. The decomposition of surface sulfate groups above 700°C is reported in the case of sulfated metal oxides[12,13].

V. X-Ray Diffraction Analysis (XRD)

The powder X-ray diffractograms of the pure, supported and sulfate modified systems calcined at 550°C are given in Figure 3.3.

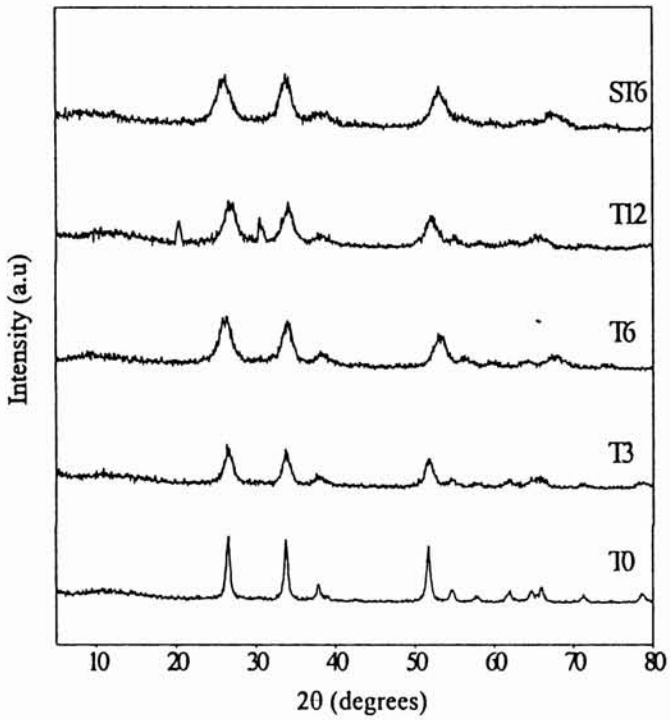

Figure 3.3
XRD profiles of V_2O_5-SnO_2 systems.

Results:

The XRD pattern of pure tin oxide gives sharp peaks. As vanadia is introduced to the support system, the intensity of peaks is found to be slightly reduced. No change in the peak intensities is observed as the weight percentage of vanadium oxide increases from 3 to 6. At high vanadium oxide content, additional peaks appear at 2θ values 20 and 31 as evident from the XRD profile of T12. The XRD profile of the sulfated system, ST6 shows only a trivial broadening of the peaks.

Discussion:

The sharp peaks in the XRD pattern of pure tin oxide show that it is highly crystalline and the position of the peaks reveals that the oxide is in tetragonal active phase[14]. The experimental data agree very closely with the standard values given in the JCPDS data cards for these systems. The crystalline phase of tin oxide in all the supported systems remains the same indicating that it is the stable-phase in the temperature region where the heat treatments were performed. The decrease in the intensity of the XRD peaks with vanadium oxide loading suggests that the surface of tin oxide is progressively getting covered by the vanadium-oxide structures. The interaction between the vanadia particle and the support oxide hinders the crystallization, which is reflected in the reduction of peak intensity. The absence of the known crystalline phases of V_2O_5 in the catalysts up to 6 wt% suggests that the deposited vanadia is finely dispersed on the catalyst surface in the form of VO_4 tetrahedra or in the form of two- dimensional oxovanadate structures, just as on Al_2O_3 and TiO_2 surfaces[15-19]. The additional peaks observed at 2θ values of 20 and 31 for high vanadia loaded samples may be attributed to the crystal planes of V_2O_5 crystallites[20]. The XRD pattern of the sulfated sample does not show differences from those of the unmodified samples. It has been reported that the degree of crystallization of the sulfated oxides is much lower than that of the oxides without sulfate treatment[21-23]. The absence of any change in the peak intensity after sulfate treatment indicates that the amount of sulfate retained on the surface is insufficient to cause any change in the diffraction pattern and it is well dispersed on the surface without entering into the bulk of the catalyst.

VI. Fourier Transform Infrared Spectroscopy (FTIR)

Figures 3.4 and 3.5 show the FTIR spectra of unmodified and sulfate modified V_2O_5-SnO_2 catalysts with various vanadium oxide content, calcined at 550°C.

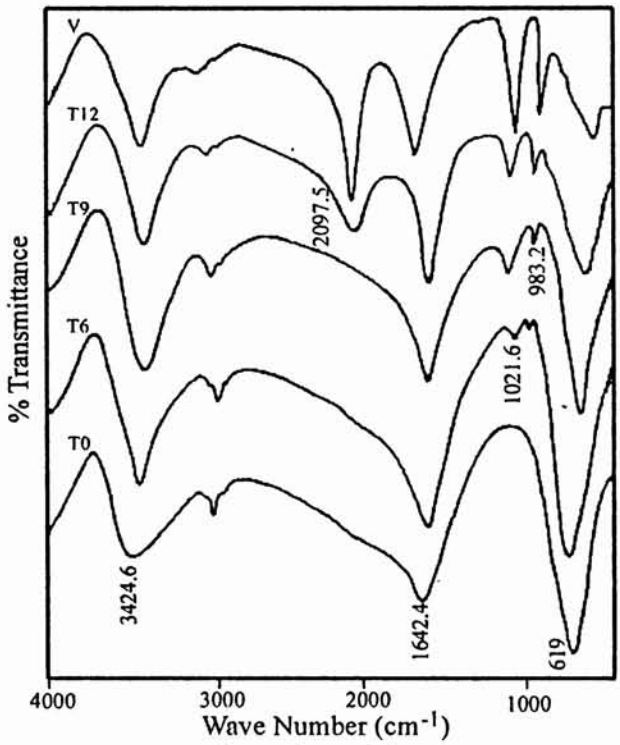

Figure 3.4
FTIR of unmodified V_2O_5-SnO_2 systems.

Results:

The IR spectrum of pure tin oxide contains three major absorption bands at 3424, 1642 and 619 cm^{-1}. As vanadia is introduced to the single oxide, the intensity of the first two bands increases whereas the third peak remains as such. IR spectrum of T6 shows additional weak bands at 1020 cm^{-1}, the intensity of which increases as the vanadia percentage increases. A new band at 983 cm^{-1} is also observed in the case of T9. Further accumulation of vanadium oxide gives rises to yet another band at 2057 cm^{-1} (IR spectrum of T12). The pure V_2O_5 shows intense IR absorption bands at 845, 1030, and 2046 cm^{-1} in addition to the broad bands at about 3500 and 1700 cm^{-1}. The IR spectra of all the sulfated samples show absorption bands at 960-980, 1060-1070, 1130-1150 and 1210cm^{-1}, apart from the bands present on the unmodified systems (Figure 3.5). High resolution of these bands shows three absorptions at 1174, 1062 and 976 cm^{-1}.

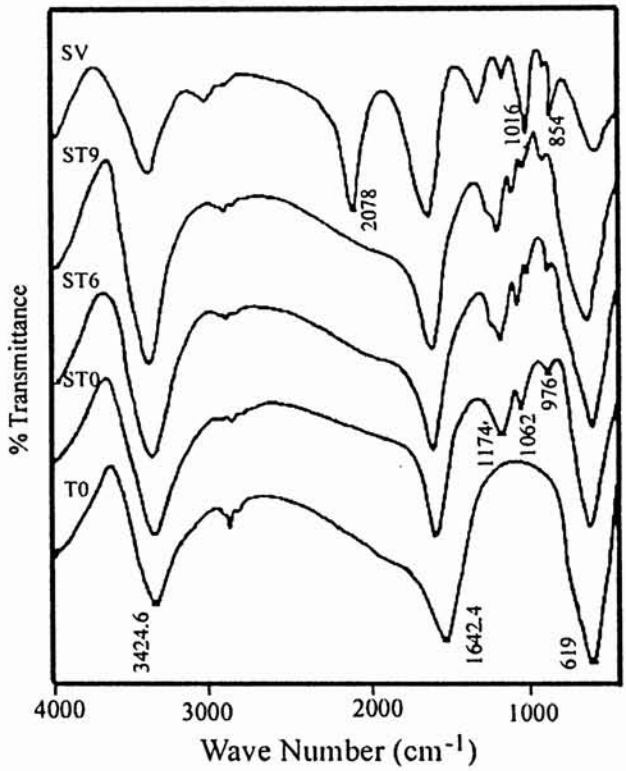

Figure 3.5
FTIR of sulfate modified V_2O_5-SnO_2 systems.

Discussion:

The bands at 3424 and 1624 cm^{-1} in the case of pure tin oxide may be attributed to the hydroxyl groups associated with the structural water[24] whereas the third band at 619 cm^{-1} is due to the Sn-O bonds of the support[25]. According to Bond *et al.*[26] an increase in the intensity of the bands at 3424 and 1624 cm^{-1} with vanadia addition may be related to the deformation of the vibration of adsorbed water and surface OH groups of the support. The band at 983 cm^{-1} in the supported systems is caused by the stretching vibrations of the terminal V=O bonds of amorphous bulk oxides[27-29] or by stretching modes of terminal V=O bonds of polyvanadate structure containing V-O-V bridges[30]. In the case of systems with high vanadium oxide content, the bands at 1020

and 2057 cm^{-1} correspond to the V=O stretching mode and its first overtone respectively[31,32]. These features are coincident with those observed with pure V_2O_5[33-35]. Baiker *et al.*[36] reported the presence of coordinated but distorted tetrahedral VO_4 species in the V_2O_5-TiO_2 system which is well dispersed as a monolayer at low vanadia loadings and multilayer having disordered VO_6 octahedra which has structural similarity to bulk V_2O_5 at high vanadia loading. Present observations are in line with these reported results. For our samples, it is found that up to 6 wt% of vanadia loading, crystalline vanadia is not observed suggesting that it is well dispersed as a monolayer on the SnO_2 surface. The vanadia loading exceeding the formation of monolayer above 6 wt% is well crystallized and the peaks are observed in the IR spectra.

The sulfate loading of the supported systems has been qualitatively confirmed from the additional absorption bands in the range 1200-1000 cm^{-1}. IR bands in the spectra of the sulfated systems (Figure 3.5) are characteristic of the bidentate sulfate group coordinated to the metal ion. The peak at 1210 cm^{-1} corresponds to the unsymmetrical vibrations of the chelate bidentate[37-39].

Infrared spectra of sulfated metal oxides, especially the superacidic sulfated ZrO_2, HfO_2, TiO_2, Fe_2O_3, TiO_2 and SnO_2 have been the subject of detailed study for explaining the superacidity and for proposing the structural model for the surface sulfate species[8,11,40,41]. A common feature of all super acidic sulfated oxides is the presence of a strong band near 1400 cm^{-1} representing the asymmetric stretching frequency of S=O[42-44]. The presence of this band and hence the super acidity, depends very critically on the water content of the sulfated oxides. Only sulfates at the surface of oxides brought *in vacuo* to medium-high dehydration showed a strong band around 1400 cm^{-1}. In presence of water vapour this band disappears and only low frequency bands persists[45]. The lack of IR band near 1400 cm^{-1} in the present case reveals that none of the sulfated samples under study possesses superacidic qualities. This is explained by the fact that though the calcination temperature is 550°C no special precautions other than that of keeping it in a desiccator are taken (like

keeping *in vacuo* in sealed tubes) to make the samples perfectly dry before various characterization studies. The IR spectral bands of the samples closely agree with the bidentate sulfate complex structure having bands around 1150, 1130, 1070 $cm^{-1}$and a shoulder at 980 cm^{-1}.

The observations of IR studies supplement the XRD results that vanadia is well dispersed on the support surface up to 6 wt% vanadium oxide content.

VII. Solid-State ^{51}V NMR Spectroscopy

The solid-state ^{51}V NMR spectra of V_2O_5-SnO_2 catalysts calcined at 550°C are shown in Figure 3.6. Ammonium metavanadate is taken as the reference where the signal is assigned to be at 0 ppm.

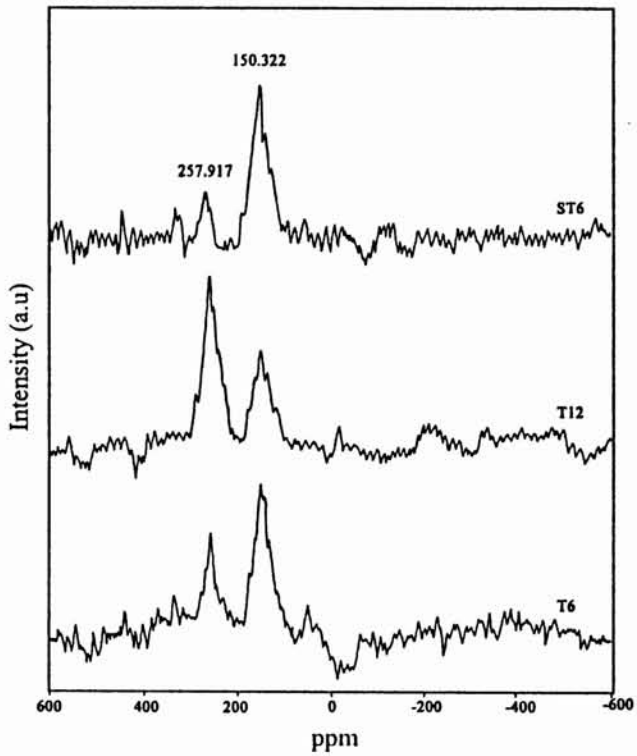

Figure 3.6
^{51}V NMR spectra V_2O_5-SnO_2 systems.

Results:

Figure 3.6 shows two types of major signals in the NMR spectra of the catalysts with varying intensities depending on the vanadium oxide content. For the sample T6, a shoulder peak at 257.9 ppm and an intense peak at 150.3 ppm are prominent. As the vanadia loading increases to 12 wt%, the situation reverses, a rather intense and sharp peak at 257.9 ppm and a broad and less intense peak at 150.3 ppm are observed. The NMR spectra of the sulfated sample ST6 is very much similar to that of its unmodified counterpart, T6.

Discussion:

The two types of signals in the ^{51}V NMR spectra of the V_2O_5-SnO_2 catalysts represent two different coordination spheres for the surface vanadium oxide species. Different peak positions normally indicate differences in spectral parameters and are observed due to different local environment of vanadium nuclei[46-50]. A low value for the chemical shift in the wide line NMR is characteristic of vanadium oxide in low coordination (tetrahedral), while a higher value is assigned to a higher (octahedral) coordination based on the spectra of various known vanadium oxide containing compounds[51-53]. In general, it is known that low surface coverages favour a tetrahedral coordination of vanadium oxide, but at higher surface coverages, vanadium oxide becomes increasingly octahedrally coordinated. Similar chemical shift for vanadium oxide species was previously observed on titania and alumina[51,54]. However, the surface vanadia structure is remarkably dependent on the metal oxide support material. Vanadium oxide on TiO_2 (anatase) displays the highest tendency to be 6-coordinated at low surface coverage[55], whereas in the case of Al_2O_3, a tetrahedral surface vanadium species is formed[46] at low vanadia content. At low vanadium loading, for TiO_2-ZrO_2, a tetrahedral vanadium species is exclusively dominant compared with an octahedral species[56].

Thus the signal at 257.9 ppm in the present case can be ascribed to the vanadium-oxygen structures surrounded by a distorted tetrahedron of oxygen atoms, whereas the other peak at 150.3 ppm to that of a distorted octahedron of oxygen atoms. From Figure 3.6, peak positions of the vanadium oxide species on

the SnO_2 surface indicate that the vanadia species are tetrahedrally coordinated at low vanadium oxide content and as the loading increases the coordination becomes predominantly octahedral. These observations are in very good agreement with the XRD and IR results described in the above sections. This implies that vanadia is well dispersed as a monolayer having isolated tetrahedral units at low vanadia content while for the loading exceeding the formation of monolayer, it is well crystallized on the catalyst surface. It is relevant to note that the peak positions of the sulfated sample remain as such when compared to the spectrum of unpromoted sample. This is symptomatic of the fact that the local environment of the vanadium oxide species in the supported systems does not change with the introduction of sulfate groups to the surface.

VIII. Diffuse Reflectance UV-VIS Spectroscopy (DR UV-VIS)

Figure 3.7 compares the DRS spectra of V_2O_5-SnO_2 systems with different wt% of vanadia and its sulfated analogue. All the samples were identically treated with magnesium oxide serving as the reference. The band maxima of DRS spectra of some reference compounds containing vanadium are given in Table 3.3 for comparison of the results.

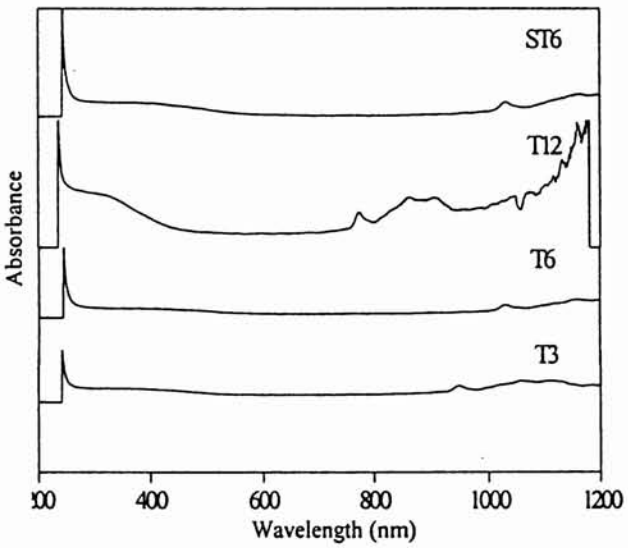

Figure 3.7
DRS of modified V_2O_5-SnO_2 systems.

Table 3.3

Band maxima in the DRS spectra of some reference compounds of vanadium.

Compound	DRS Absorption Max. (nm)	Oxidation-State of V	Molecular Structure of vanadium-oxygen species
NH_4VO_3	286, 219	5+	Tetrahedral and polymeric
Na_3VO_4	282, 228	5+	Tetrahedral and isolated
$Pb_2V_2O_7$	266, 217	5+	Tetrahedral and dimeric
V_2O_5	477, 325	5+	Octahedral and polymeric
V/USY	405	5+	Tetrahedral and some polymeric Octahedral
V/SiO_2	770, 625	4+	Octahedral
V/Al_2O_3	805, 580	4+	Octahedral

Results:

Although the spectra are quite similar, one can notice some important differences in the higher and lower wavelength regions (d-d region and UV region respectively). The DRS spectra of all the samples contain a sharp peak at the low wavelength region, the intensity of which increases first with vanadia loading and then remain almost the same at higher loading (DRS of T3 and T6). The high loaded sample, T12 is characterized by a weak absorption and a shoulder at about 700-900 nm range in addition to the intense band at the lower wavelength region. Yet another unresolved broad band is present at 1100-1200 nm region in the case of T12. The DRS spectrum of the sulfated sample ST6 is similar to that of the unmodified sample T6.

Discussion:

The DRS spectra of vanadium oxides are characterized by charge-transfer (CT) transitions of the type $O \rightarrow V^{n+}$ and d-d transitions of V^{n+}, and

their energies are dependent on the oxidation state and coordination environment[57]. From the Table 3.3 it is clear that the band maxima of V^{5+} shift to higher energy (lower wavelengths) with decreasing coordination number[58-60]. Thus the Figure 3.7 enables us to distinguish between the surface vanadia species on V_2O_5-SnO_2 systems. The intense band at the lower wavelength region is attributed to the tetrahedrally coordinated V^{5+} species in all the samples whereas the broad band at higher wavelength region (700-900 nm) is indicative of 6-fold coordination of the vanadium ion[61], which is prominent only in the high loaded system, T12. The red shift of this CT band is observed when the coordination of the central vanadium ion changes from tetrahedral to octahedral state. The broad band at the 1100-1200 nm in the case of T12 indicates the presence of crystalline V_2O_5[62]; the contribution of this species to the total intensity is appreciable showing that the surface species is well crystallized at high loading. The unraveled coordination geometry of the supported vanadia species obtained from DRS technique confirms the fact that the supported V^{5+} species on V_2O_5-SnO_2 systems prefers a tetrahedral environment in the low loading whereas it polymerizes to octahedral species and eventually to crystalline V_2O_5 at high loading. Here again, it is observed that the presence of the sulfate ions on the catalyst surface does not affect the local environment of the vanadium-oxygen species. The results are in perfect agreement with those obtained from XRD, FTIR and solid-state ^{51}V NMR suggesting that the combination of these techniques can be used to perform the surface characterization of supported vanadia systems.

3.2.2 V_2O_5-ZrO_2 Systems

I. Energy Dispersive X-ray Fluorescence Analysis (EDX)

The chemical composition data from EDX analysis for representative samples of V_2O_5-ZrO_2 systems are given in Table 3.4.

Table 3.4

Energy Dispersive X-ray analysis results for V_2O_5-ZrO_2 systems.

Catalysts	Composition					
	Atom %			Oxide %		
	Zr	V	S	ZrO_2	V_2O_5	SO_4
Z0	100	-	-	100	-	-
Z6	86.1	13.9	-	94.4	5.6	-
Z9	81.9	18.1	-	91.3	8.9	-
SZ0	97.2	-	2.8	98.1	-	1.9
SZ6	84.5	8.9	6.6	92.2	5.1	2.7
SZ9	79.3	9.8	10.9	85.0	8.6	6.4

Results:

Table 3.4 gives the elemental composition of the samples as oxide percentage and atomic percentage. The molar concentration of the supported oxide shows that the catalysts contain the expected loading of vanadium oxide. The amount of sulfate retained in the case of SZ6 is 2.7% whereas it is found to higher for SZ9 (6.4%). For ST6 and ST9 the values are 1.5 and 2.8 respectively.

Discussion:

The results indicate that effective loading of vanadium oxide is taking place on the ZrO_2 support. The amount of sulfate retained on the catalyst surface increases as the vanadia percentage increases. This is pinpointing that the incorporation of vanadia improves the sulfate retaining ability of the systems. Comparing the support effects (Table 3.1 and Table 3.4), it is clear that ZrO_2 is having a superior sulfate binding capacity than SnO_2. This may be due to comparatively stronger interaction of the sulfate group with ZrO_2 surface than that of SnO_2 surface.

II. BET Surface Area and Pore Volume Measurements

Table 3.5 shows the surface area and pore volume measured for V_2O_5-ZrO_2 systems by BET method and the effect of vanadia loading as well as sulfate modification on these surface properties.

Table 3.5
Surface area and pore volume of V_2O_5-ZrO_2 systems by BET method.

Systems	BET Surface Area ($m^2 g^{-1}$)	Pore Volume ($cm^3 g^{-1}$)	Systems	BET Surface Area ($m^2 g^{-1}$)	Pore Volume ($cm^3 g^{-1}$)
Z0	43	0.058	SZ0	126	0.120
Z3	78	0.083	SZ3	115	0.120
Z6	89	0.085	SZ6	136	0.132
Z9	72	0.081	SZ9	111	0.100
Z12	53	0.020	SZ12	69	0.072
Z15	47	0.020	SZ15	58	0.061
V	1.8	0.002	SV	3.3	0.003

Results:

From the above table, it is clear that the surface areas of vanadia-impregnated samples are higher than that of pure ZrO_2 calcined at the same temperature. It is also worth noting that the surface area increases gradually with vanadium oxide content up to 6 wt% loading (89 $m^2 g^{-1}$). On the contrary, the samples with high vanadia content, i.e., from 9 wt% loading onwards, it shows a reduction in the surface area. The crystalline vanadia (V_2O_5) is having very low surface area value (1.8 $m^2 g^{-1}$) compared to any of the systems. A similar trend is observed with the pore volume values in the supported systems. The sulfate modification of the samples remarkably enhances the surface area and pore volume and it is noticeable that the surface area and pore volume reach a maximum value in SZ6 among the sulfated systems. As the system goes from SZ6 to SZ9, a drastic drop off in the surface area and pore volume is observed.

Discussion:

The effect of the vanadia content on the surface area and pore volume of the V_2O_5-ZrO_2 systems indicates that vanadia in small amount stabilizes the microstructure of ZrO_2 and the wet impregnation method allows the preparation of high surface area samples with a broad range of vanadium oxide content[63]. The increase in surface area is attributed to the inhibition of sintering by the presence of vanadia dopant[64,65]. At high loaded systems blocking of the pores of zirconia by crystalline V_2O_5 or the strong Zr-V interaction may be the reason for the decrease in the surface area[66]. The low pore volume of high vanadia-loaded system also supports the pore plugging by the crystalline vanadia species.

Consistent with the earlier reports, the sulfated samples showed a higher surface area as compared to pure zirconia or the unmodified supported catalysts. Sulfation reduces the extent of surface area loss during high temperature calcination. This can be explained on the basis of higher resistance to sintering as well as the delayed transformation from amorphous to crystalline state acquired by doping with sulfate ions[67-71]. Sulfate doping suppresses particle growth and also facilitates the dispersion of the zirconia particles resulting in a higher surface area. However, the dramatic reduction in the surface area and pore volume of the high vanadium containing systems among the sulfate modified samples may be due the higher amount of sulfate retained on the surface which is evident from the EDX results. The sulfate groups adhering to the edges of the pores also lead to partial blocking of the pores. Thus it can be assumed that for low sulfate loadings the stabilizing effect of the sulfate ions gets the upper hand. At high sulfate loadings plugging of the pores may result in a reduction in the surface area[6].

III. Scanning Electron Microscopy (SEM)

To examine the effect of vanadia loading and surface sulfate modification on the particle size of the catalysts, SEM picture of the representative samples were taken and are presented in Figure 3.8.

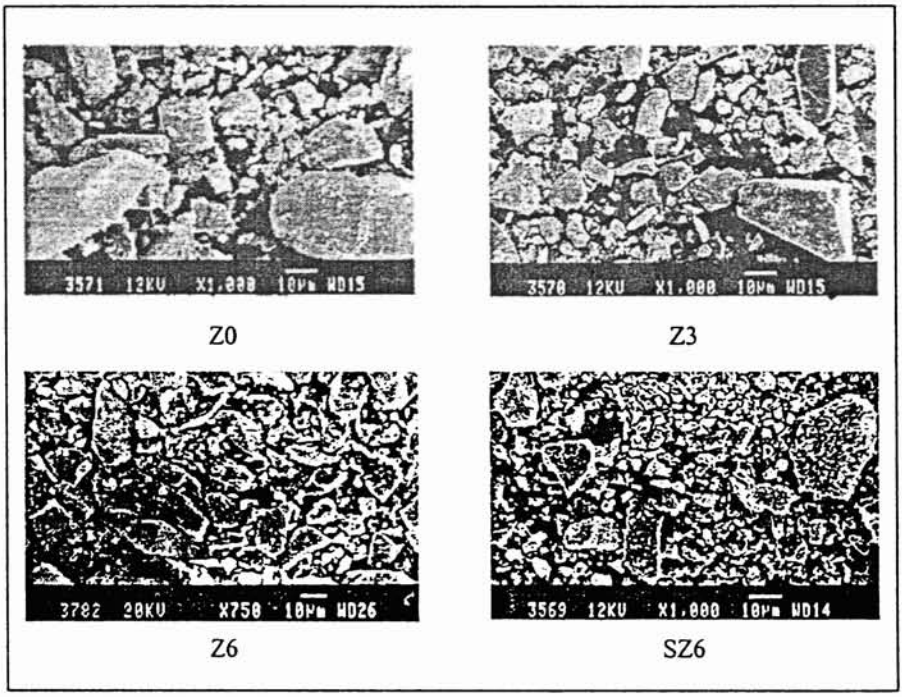

Figure 3.8
SEM photographs of V_2O_5-ZrO_2 systems.

Results:

The particle size is observed to be larger in the case of pure zirconia. The SEM pictures of Z3 and Z6 clearly show that the crystallite size is decreasing with vanadia addition. In comparison with pure zirconia, or the unmodified supported systems the sulfated samples give particles of still lower crystallite size as observed in the SEM picture of SZ6.

Discussion:

The SEM pictures agree well with the BET surface area results. Suppression of particle growth is evident from the decreased particle size, which leads to an enhanced surface area of vanadia-loaded zirconia in comparison with pure zirconia. Addition of sulfate anion species causes a

further setback to the crystallization and sintering process, which is manifested from the uniform particles on the surface, which in turn increases the surface area of the samples in comparison with the simple supported system. The metal oxide species along with the sulfate ions prevent the agglomerization of zirconia particles resulting in a lower crystallite size and higher surface area.

IV. Thermogravimetric Analysis (TGA)

The thermal stability of the samples was examined by TG analysis and Figure 3.9 illustrates the TG curves (dotted line) and its derivative (solid line) obtained for pure, supported and sulfate treated samples. To study the influence of vanadium and sulfate species on the structural change of the precursor during calcinations, thermal analysis was done with uncalcined samples of Z0, Z6 and SZ6.

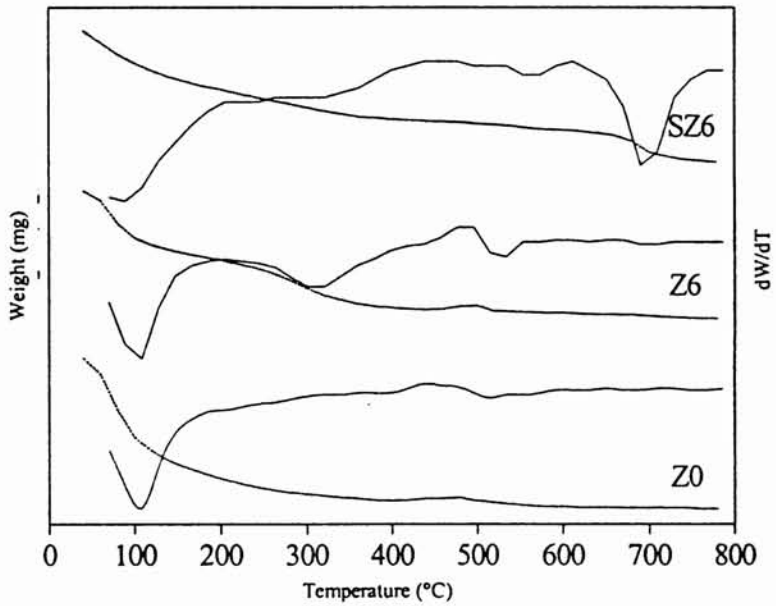

Figure 3.9
TG (....) DTG (—) curves of V_2O_5-ZrO_2 systems.

Results:

The TG pattern of pure zirconia indicates a continuous dehydration over the entire temperature range scanned. The TG-DTG curve of pure zirconia shows weight losses near 100°C and at about 420°C. In the case of vanadia promoted sample Z6, two additional dips are observed at about 180°C and 250°C. Here the weight loss observed at 420°C in pure zirconia is shifted to 490°C. No additional weight loss is noticed in the higher temperature region for Z6 system. The onset of another decomposition in the case of sulfated system SZ6 is visible at around 690°C.

Discussion:

The sharp weight loss at 420°C corresponds to the crystallization of hydrous zirconia from an amorphous into a crystalline form. Srinivasan *et al.*[72] observed that the exothermic peak appeared at the same temperature for samples after calcination lead to pure monoclinic or tetragonal zirconia. The weight loss around 100°C is due to the removal of physisorbed water from the surface[73]. A notable influence of V_2O_5 on the crystallization of hydrous zirconia has been observed in the case of Z6, as shown in Figure 3.9. The exothermic peak is shifted to a higher temperature indicating that the loading of vanadium oxide delays the crystallization of zirconia[74]. In the case of Z6, the additional peaks at 180°C and 250°C may be attributed to the evolution of NH_3 and H_2O decomposed from NH_4VO_3[75]. The absence of weight loss at high temperature region for Z6 due to the melting of V_2O_5 may provide the indirect evidence for the absence of bulk V_2O_5 phase in the sample. In the case of sulfated sample SZ6, the initial weight loss corresponds to the removal of surface adsorbed water of hydration. The high temperature weight loss peak observed at around 690°C can be ascribed to the decomposition of the sulfate species and the evolution of oxides of sulfur[76].

V. X-Ray Diffraction Analysis (XRD)

Figure 3.10 shows the XRD patterns for V_2O_5-ZrO_2 systems with different vanadium oxide contents. The figure also includes the XRD profiles of the pure zirconia as well as that of the sulfate-doped sample for comparison.

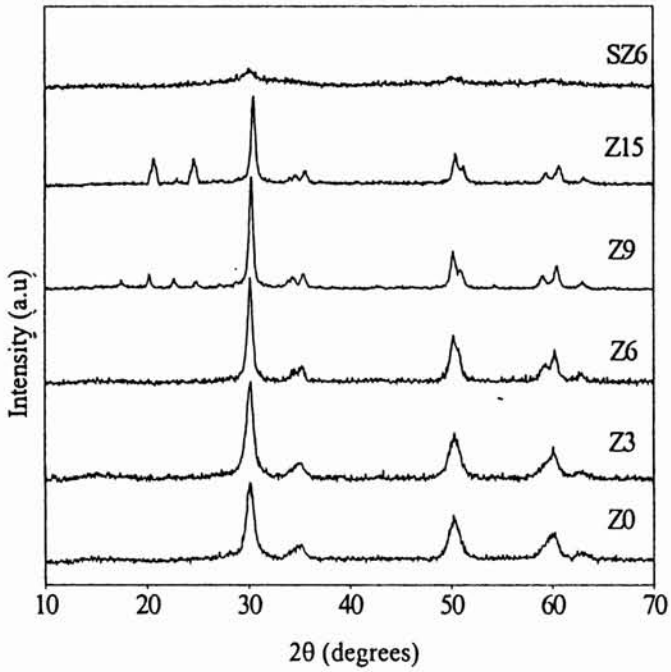

Figure 3.10
XRD patterns of V_2O_5-ZrO_2 systems.

Results:

The XRD pattern of pure zirconia shows only a single phase. As vanadia is introduced to the support system, improvement in the peak intensity is observed. The XRD patterns of Z3 and Z6 are appeared to be almost similar with no change in the peak intensities. From 9 wt% of vanadium oxide content onwards, small peaks appear at 2θ values 20 and 31 in addition to the main peaks of the support metal oxide. The intensity of these small peaks increases with further increase in vanadia percentage. The intensities of XRD peaks are severely reduced in the case of sulfated system SZ6, although the peak positions remain the same as in the case of pure zirconia.

Discussion:

The XRD pattern of pure zirconia shows the predominance of reflections of the tetragonal ZrO_2 phase, in agreement with the literature

reports[66,68,77]. In comparison with pure zirconia, the vanadium incorporated systems showed enrichment of the tetragonal phase. Incorporation of transition metal species thus results in the stabilization of tetragonal phase of zirconia by delaying the transformation of this metastable phase into the thermodynamically favoured monoclinic phase. Thus, the presence of these species on the surface prevents the zirconia from an undisturbed crystallization. The absence of characteristic peaks corresponding to the vanadium oxide species in the supported systems with vanadia loading up to 6 wt% implies that the added vanadia species are present in the form of solid solution or it is highly dispersed on the ZrO_2 surface, which can be accounted on the basis of the low vanadia loading studied[78]. However, the appearance of characteristic peak of vanadia at high surface concentrations of vanadium oxide suggests that the vanadia content is higher than that required for monolayer coverage and is well crystallized[21]. The lower intensities of reflections of the sulfated sample indicate a lesser crystallinity and higher sulfate retaining capacity of the zirconia samples. The bulk sulfate species that may be retained to a greater extent retards the transformation of amorphous hydrous zirconium oxide to the tetragonal phase. The sulfate content higher than that required for monolayer coverage in the high loaded systems implies the migration of the sulfate moieties into the bulk[79], which is also confirmed by the higher sulfate amount by EDX results and the lower surface area values.

VI. Fourier Transform Infrared Spectroscopy (FTIR)

Figures 3.11 and 3.12 present the FTIR spectra of different supported V_2O_5-ZrO_2 catalysts with various vanadium oxide contents, calcined at 550°C and its sulfated analogues respectively.

Results:

The IR spectrum of pure zirconia gives two strong absorption bands at 3429 and 1647 cm^{-1} in addition to the band at 456 cm^{-1}. For Z6, absorption bands at 896 cm^{-1} and 1023 cm^{-1} with a less intense shoulder at 2063 cm^{-1} also appear. The intensity of these bands increase as the vanadia percentage

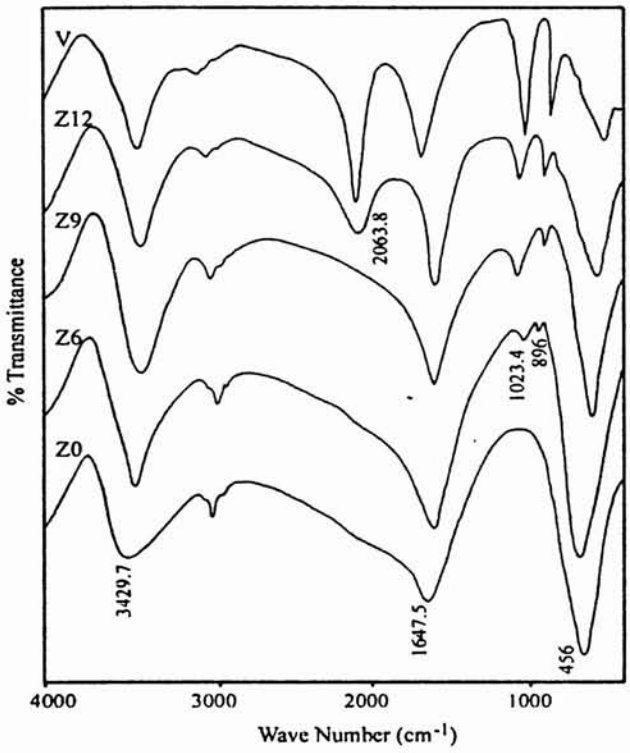

Figure 3.11
FTIR of supported V_2O_5-ZrO_2 systems.

increases gradually from 6 to 12. The IR spectrum of crystalline V_2O_5 shows strong absorption bands at 845, 1030, and 2046 cm^{-1} in addition to the broad bands at about 3500 and 1700 cm^{-1}. As shown in the figure, from 6 wt% vanadia loading onwards the bands due to crystalline V_2O_5 become prominent in the V_2O_5-ZrO_2 systems. The IR spectra of all the sulfated samples (Figure 3.12) show absorption bands at 960-980, 1060-1070, 1130-1150 and 1210 cm^{-1} apart from the bands present on the unmodified systems.

Discussion:

The oxide supports generally terminate with surface OH groups, which are quite polar and give strong IR bands in the 3000-4000 cm^{-1} and 1600-1700 cm^{-1}

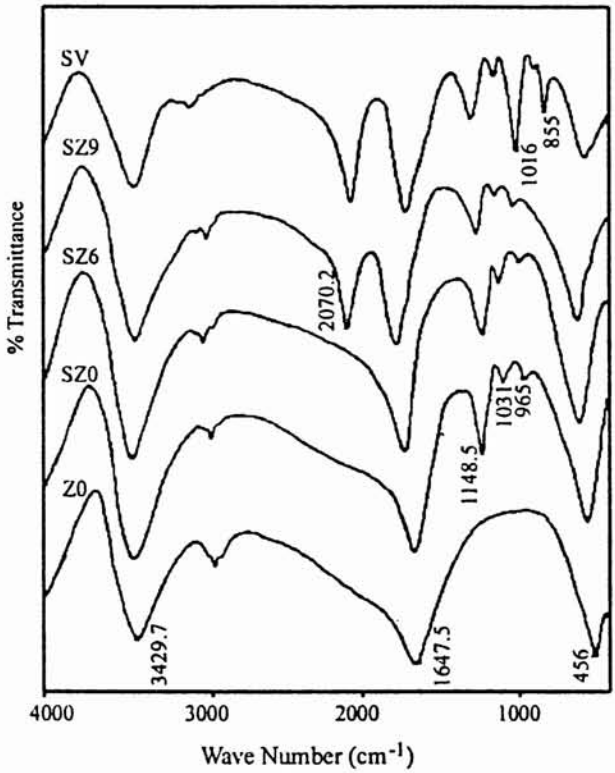

Figure 3.12
FTIR of sulfate modified V_2O_5-ZrO_2 systems

regions[80]. Thus the IR at 3429 and 1627 cm^{-1} in the case of pure zirconia may be attributed to the surface hydroxyl groups. The band at 456 cm^{-1} is characteristic of the surface metal-oxygen species, which usually vibrate in the 100-800 cm^{-1} region. The absorption band at 1023 cm^{-1} in the supported systems is assigned to the V=O stretching vibration, while that at 896 cm^{-1} is attributed to the coupled vibration between V=O and V-O-V[81]. Generally, the IR bands of V=O bonds of crystalline V_2O_5 are observed at 1020-1025cm^{-1} with an overtone band between 2060 and 2070 cm^{-1} and is confirmed by the IR spectrum of V in Figure 3.11[82]. It has been reported that the appearance of the IR bands at 1020 and 896 cm^{-1} is indicative of the fact that the vanadia content is above that which is necessary to cover all the support surface with one 'monolayer'[83].

The presence of coordinated but distorted tetrahedral VO_4 species as a monolayer at low loadings and multilayer having disordered VO_6 octahedra with traces of crystalline V_2O_5 at high vanadia loading has been observed in the case of various vanadia supported metal oxides[84-87]. The characteristic IR bands at 1023 and 896 cm^{-1} appearing at 6 wt% of vanadia in the present case indicate the completion of monolayer. Thus it is assumed that in the stable monolayer below 6 wt%, the vanadia forms isolated tetrahedral species, a disordered V_2O_5 like phase above the monolayer limit. Finally the octahedral and para-crystalline V_2O_5 have been recognized at very high loadings.

In comparison with pure and vanadia supported zirconia, the spectrum of sulfated samples (Figure 3.12) exhibits a broad peak with shoulders around 1200 cm^{-1}. The peaks at 1029, 1076 and 1222 cm^{-1} are typical of the S-O mode of vibration of a chelating bidentate sulfate ion coordinated to a metal cation[88].

The XRD results in the above section showed that the peaks due to crystalline vanadia appear from 9 wt% vanadium oxide content onwards. As shown in Figure 3.10, the crystalline V_2O_5 is not found in the case of Z6. However, the presence of V_2O_5 from 6 wt% vanadia onwards is apparent from the IR spectra of the samples calcined at the same temperature. This indicates that for Z6 calcined at 550°C, the V_2O_5 crystallites formed are less than 4 nm in size that is beyond the detection limit of XRD technique.

VII. Solid-State ^{51}V NMR Spectroscopy

Solid-state NMR methods represent a novel and promising approach to vanadium oxide catalytic materials. The solid-state ^{51}V NMR spectra of a few V_2O_5-ZrO_2 systems are shown in Figure 3.13.

Results:

Two different types of signals are obatined in the ^{51}V NMR spectra of V_2O_5-ZrO_2 catalysts. A powder pattern with an intense peak at about -95.4 ppm is observed in addition to the comparatively narrower and less intense signal near 83.9 ppm for Z6 system. Although the peak positions remain the

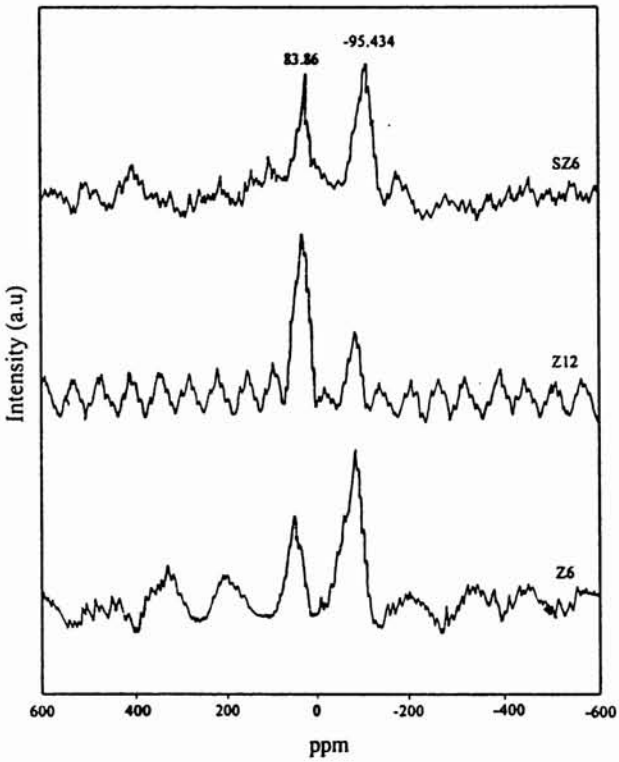

Figure 3.13
^{51}V NMR spectra V_2O_5-ZrO_2 systems.

same for a higher vanadia loaded system, Z12, the relative NMR intensities have been changed. In the case of Z12, the signal at higher chemical shift value (83.9 ppm) is exclusively dominant compared with the other signal at lower chemical shift value, -95.4 ppm. The NMR signals of SZ6 do not show any appreciable change from its unmodified counterpart Z6.

Discussion:

The ^{51}V NMR spectra of V_2O_5-ZrO_2 systems reveal two diverse vanadium environments for the surface vanadium oxide species. The resonances observed in the present case are similar to those observed previously and the lower and higher chemical shift values may be assigned to

vanadium in four fold and six fold coordination respectively[46-50]. While both four fold and six fold coordinate vanadium atoms are present in all the systems,[27,89] the current study shows that the tetrahedral or the four fold geometry of the surface vanadia species is prevalent at lower surface coverages and that the polymeric (octahedral) species increases with increasing vanadia content. This trend matches with that seen by Wach *et al.*[90] for the increase in the ratio of polymeric to isolated surface vanadia species. Since the NMR spectrum of the sulfated system remains similar to that of the unpromoted sample, it is assumed that the local environment of vanadium is not changed with surface modification by the sulfate groups. This finding namely, the amount of octahedral vanadium species increases with increasing vanadium oxide loading agree well with the results of previous characterization techniques such as XRD and FTIR.

VIII. Diffuse Reflectance UV-VIS Spectroscopy (DR UV-VIS)

The UV-VIS diffuse reflectance spectra were recorded for V_2O_5-ZrO_2 catalysts containing various weight percentages of vanadia with an identically treated magnesium oxide as reference material. The DR spectra of our samples are presented in Figure 3.14, which also includes the spectrum of sulfate-modified system, SZ6.

Results:

From Figure 3.14, it is observed that only a single charge transfer band is present at about 250 nm in the case of sample containing 3 wt% of vanadium oxide. For a higher vanadia loaded system Z6, a slight enhancement in the intensity of the band at 250 nm along with appearance of a broad band at higher wavelength region (above 800 nm) is recorded. Further increase of vanadia content to 12 wt%, intensifies the second band while the former remains the same. In addition to the band at 800 nm, the spectrum of Z12 possesses an unresolved broad band in the range 900-1100 nm. The surface modification by sulfate anions does not result in strong changes in the UV-VIS

spectrum, which is characterized by the bands quite similar to that of the unmodified sample with the same vanadia content, Z6.

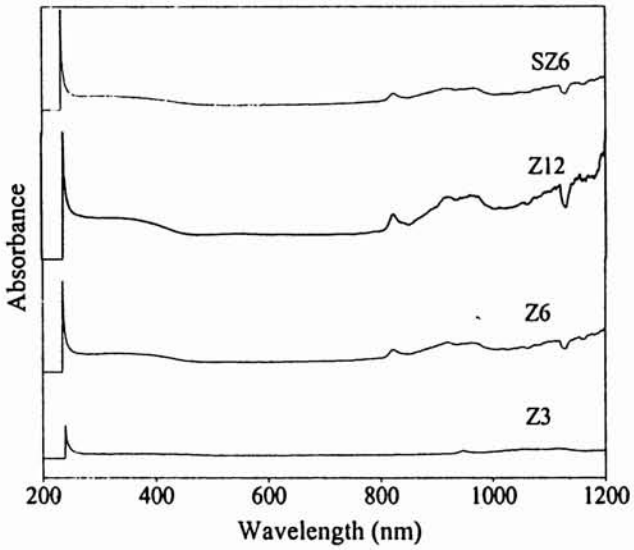

Figure 3.14
DR UV-VIS spectra of V_2O_5-ZrO_2 systems.

Discussion:

The energy of the oxygen→ vanadium charge-transfer (CT) absorption band, which is correlated with minimum diffuse reflectance, is strongly influenced by the number of ligands surrounding the central vanadium ion and may provide information on the coordination of the vanadium in the mono/ multilayer phase[91]. Several important investigations of supported vanadia catalysts with diffuse reflectance UV-VIS spectroscopy[91-95] have reported that tetrahedrally coordinated vanadium ions are identified by the charge-transfer absorptions between 300 and 200 nm. This class comprises monomeric (isolated) species well dispersed on the support surface as well as small clusters or linear chains. A charge transfer band at higher wavelength region, usually above 400 nm characterizes vanadium ion in an octahedral environment. In agreement with the proposed interpretations, the results of the present study

suggest that four fold coordinated isolated vanadium oxide species are observed at low vanadia loading up to 3 wt%. The appearance of the absorption band at higher wavelength region from 6 wt% onwards shows the development of the central vanadium ion from tetrahedral to octahedral coordination. At still higher concentrations of vanadia, weak signals that correspond to the crystalline vanadia are detected. The geometry of the surface vanadium oxide species is found to be unaltered even after the surface modification with sulfate anions as evident from the spectrum of SZ6.

The spectroscopic features observed in our catalysts discussed in sequence promote the understanding of the local structure of the surface V_2O_5. The comparison of the surface structure becomes meaningful since there is an absolute agreement with the results obtained from different spectroscopic methods. From the data, the presence of tetrahedrally coordinated V ions at low coverages (0-3 wt%), of polymeric arrays consisting of VO_6 octahedra at higher loading and of crystalline V_2O_5 at very high loading on the surface of V_2O_5-ZrO_2 systems is inferred.

3.3 SURFACE ACIDITY MEASUREMENTS

The acidic properties of the metal oxides are generally thought to play an important role in determining the adsorptive and catalytic properties of these materials. Moreover, it has been found that the acidic properties of the supported as well as the surface modified metal oxides are particularly important since the number, strength and nature of these acid sites can be controlled by varying the oxide compositions and the surface treatment of the sample[96-99]. The effect of vanadium oxide incorporation on the acidic properties of the metal oxides namely SnO_2, ZrO_2 and the disparity in the surface acidity by the surface sulfate modification of the samples were investigated in detail by employing three independent methods viz. temperature programmed desorption of ammonia, perylene adsorption studies and vapour-phase cumene cracking reaction.

Temperature programmed desorption (TPD) of ammonia enables the characterization of the acid strength distribution of the systems. This procedure is considered as a standardization method since ammonia allows the determination of both the protonic and cationic acidities by titrating acid sites of any strength. The acid site distribution profiles show the presence of weak (desorption in the temperature range 100-200°C), medium (200-400°C) and strong (400-600°C) acid sites. In adsoption studies, the limiting amount of the electron donor (perylene) adsorbed on the catalyst surface provides valuable information about the strength and amount of strong electron acceptor sites (Lewis acid sites). In vapour-phase cumene cracking reaction, the selectivity to the cracking product (benzene) is related to the Brönsted acidity whereas that for dehydrogenation product (α-methylstyrene) to the Lewis acidity. Thus, the main incentive to carry out the cumene conversion reaction in the present case is to correlate the presence of Brönsted and Lewis acid sites on the catalyst surface to the product distribution and other acidity data. Various conclusions derived from these investigations are presented in the following sections separately for the two series of catalyst systems.

3.3.1 V_2O_5-SnO_2 Systems

I. Temperature Programmed Desorption of Ammonia (TPD)

Table 3.6 gives the distribution of acid sites of pure tin oxide, vanadia supported tin oxide systems and its sulfated counter parts, determined by ammonia TPD. Total acidity is also shown as the sum of amount of ammonia desorbed from the entire temperature region.

Results:

Table 3.6 reveals that pure tin oxide possesses comparatively very small amount of acidity. Upon vanadia addition, it is observed that, the amount of ammonia desorbed from all the temperature region is increased considerably. The enhancement in the strength and amount of acid sites in the weak, medium and strong regions is rather gradual as we increase the vanadia content

Table 3.6

Ammonia TPD studies on V_2O_5-SnO_2catalysts-
A comparative evaluation of acid strength distribution

Catalyst	Amount of ammonia desorbed (mmol g^{-1})			
	Weak (100-200°C)	Medium (200-400°C)	Strong (400-600°C)	Total
T0	0.32	0.36	0.12	0.56
T3	0.35	0.37	0.16	0.72
T6	0.37	0.46	0.19	0.81
T9	0.49	0.55	0.20	0.94
T12	0.58	0.48	0.22	1.07
T15	0.98	0.74	0.26	1.26
ST0	0.55	0.45	0.18	0.85
ST3	0.56	0.64	0.29	1.07
ST6	0.63	0.66	0.25	1.19
ST9	0.63	0.67	0.31	1.37
ST12	0.57	0.65	0.26	1.06
ST15	0.43	0.61	0.15	0.99

from 0 to 15 wt%. Thus among the unmodified supported V_2O_5-SnO_2 catalysts, T15 is showing the maximum acidity. The TPD data of the sulfated V_2O_5-SnO_2 systems show a considerable enrichment of the amount of both strong and weak acid sites after incorporation of sulfate species on the supported as well as pure tin oxide surface. But, a regular increase in the acidity values as experienced in the case of unmodified samples is not observed with the vanadia content in the case of sulfated series. The acidity increases initially up to 9 wt% vanadia loading and then drastically reduces for the high loaded samples. Among the sulfated analogues therefore, ST9 is the one that has the maximum acidity value compared to other systems. The trend of different types of acidity can be summarized as :

Type of acid sites	Trend of acidity	
	Unmodified systems	Sulfated systems
Weak	T0<T3<T6<T9<T12<T15	ST0<ST3<ST6<ST9>ST12>ST15
Medium	T0<T3<T6<T9>T12<T15	ST0<ST3<ST6<ST9>ST12>ST15
Strong	T0<T3<T6<T9<T12<T15	ST0<ST3<ST6<ST9>ST12>>ST15
Total	T0<T3<T6<T9<T12<T15	ST0<ST3<ST6<ST9>ST12>ST15

Discussion:

The ammonia TPD results indicate that the number of acid sites on pure tin oxide is much less when compared with that of vanadia supported tin oxide systems. Table 3.6 suggests that new acid sites are created on the support surface by the addition of vanadia. The number and strength of all types of acid sites namely, weak, medium and strong, are increased by gradually increasing the vanadium oxide content. The steady increase in the acidity values with vanadia content has been already reported in the case of supported metal oxides[100,101]. The most general conceptual model available to predict the acidity generated by mixing two metal oxides is that of Tanabe *et.al.*[102] According to them, the acid sites are created due to the charge imbalance induced at the local M_1-O-M_2 bond structure of the supported oxide where, M_1 is the host metal and M_2 the second component. The increase in acidity therefore can be ascribed to the strong interaction of highly dispersed V_2O_5 on weakly or moderately acidic support oxide[103].

Considerable enhancement of both strong and weak acid sites is observed after sulfation where the total acidity gradually increase with an increase in vanadia loading up to 9 wt%, which then declines unexpectedly. A substantial difference is noticed in the distribution pattern in the high vanadia loaded systems. The initial enhancement of acidity can be attributed to the increase of the electron accepting properties of the three coordinated metal cations *via.* the inductive effect of the sulfate anions, which withdraw electron density through the bridging oxygen atom[39,104]. According to the dual

Brönsted-Lewis site model proposed by Clearfield[105] uncalcined catalyst contains protons as bisulfate and as hydroxyl groups bridging two metal ions. During calcination, either the bisulfate anion can react with an adjacent hydroxyl group resulting in a Lewis acid site or two adjacent hydroxyl groups can react keeping bisulfate ion intact thereby generating Brönsted acidity. The combination of these Brönsted sites with the adjacent Lewis sites can also generate strong acidity. However, the drastic reduction in the acidity values for high vanadia containing sulfated systems may be owing to the higher amount of sulfate retained on the surface. Elemental analysis by EDX revealed that amount of sulfate retained is higher for systems with high vanadium oxide content (Table 3.1). The decrease in surface acidity at high concentration of sulfate is probably due to the formation of polysulfate, which reduces the number of Brönsted sites and consequently that of the total acid sites[6].

II. Perylene Adsorption Studies

Electron acceptor adsorption studies gave information regarding the presence of Lewis acid sites in presence of Brönsted acid sites. The adsorption of perylene from a solution in benzene was done at room temperature. The limiting amount perylene adsorbed is a measure of the Lewis acidity or the electron accepting capacity. The results of the perylene adsorption studies on the different systems at calcination temperature 550°C are presented in Figure 3.15.

Results:

As evident from Figure 3.15, the limiting amount of perylene adsorbed is very low in the case of pure tin oxide and vanadium oxide when separately addressed. The introduction of vanadia to the surface significantly changes the adsorption properties. The amount of electron donor adsorbed increases gradually when we increase the vanadium oxide content from 3 to 15 wt% and is found to be maximum with the T15 system. The sulfated analogues exhibited higher perylene adsorption capacity than the simple vanadia impregnated systems. A regular gradation in the limiting amount is observed up to ST9 among the sulfated samples, which thereafter reduces for the samples containing higher amount of vanadia.

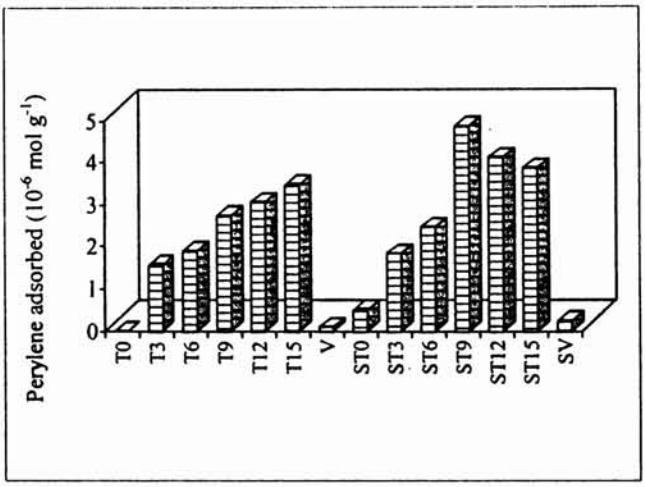

Figure 3.15
Variation in Lewis acidity of V_2O_5-SnO_2 systems
from perylene adsorption studies.

Discussion:

The lower value of limiting amount of perylene in the case of single oxides indicates comparatively lower electron accepting capacity and hence the lower Lewis acidity compared to the supported systems. Incorporation of vanadium ions influences the acid strength *via.* electronic interactions as evident from the higher values for the limiting amount in the vanadia loaded systems. Introduction of metal cation into the crystal lattice may result in the formation of some complex structures in some local areas on the surface, which results in an overall increase in the electronegativity of the surface complex[106]. As the electronegativity of the incorporated vanadium ions is higher than that of Sn, an increase in Lewis acidity is expected in all the cases, which is observed experimentally also. The results of adsorption studies given in Figure 3.15 clearly show a considerable enhancement of Lewis acidity on sulfation which can be attributed to the increase of the electron accepting properties of the surface metal cations by the sulfate anions[39,104]. The presence of sulfate on the surface can also thus result in the generation of strong coordinatively unsaturated Sn (IV) Lewis acid sites[107]. However, the reduction in the case of high vanadia

loaded samples in the sulfated sequence may be due to the high sulfate loading where sulfate groups mostly exist in the form of polynuclear pyrosulfates[108]. The perylene adsorption results are observed to be proportional with the variation of strong sites obtained from ammonia TPD method.

III. Vapour-Phase Cumene Cracking Reaction

Cumene cracking reaction was chosen as a test reaction for acidity where the cumene conversion and relative product selectivity could be correlated with the surface acidic properties. In vapour-phase cumene cracking, α-methylstyrene and benzene were obtained as the major products while ethylbenzene and styrene appeared in minor quantities. In some cases toluene is also detected in trace amounts. Cumene conversion reaction was carried out in vapour-phase at 350°C at a flow rate of 6 mL h^{-1} and with a time on stream of 2 h. In the present case the various cracking products such as benzene, toluene, styrene and ethylbenzene are considered together while calculating the selectivities. The conversion and product selectivity for the different metal incorporated systems are shown in Table 3.7.

Results:

The conversion and selectivity for various products furnished in Table 3.7 indicates that dehydrogenation of cumene to α-methylstyrene is the predominant reaction. Pure oxides exhibit very low conversions under the reaction conditions studied. In the case of vanadia loaded systems, the low loaded samples produce significant amount of cracking products, the selectivity of which decreases gradually with vanadium oxide content with a concomitant increase in the selectivity to the dehydrogenation product, α-methylstyrene. The cumene conversion percentage gradually increases with the addition of vanadia. In comparison with the simple loaded systems, sulfate promoted samples show higher conversion rates. Low vanadia loaded systems among the sulfated series seem to be more efficient in catalyzing the reaction. An increase in the vanadia loading above 9 wt% has a detrimental effect on the cumene

conversion. Incorporation of sulfate anions enhances the selectivity to α-methylstyrene generally. ST9 show the highest selectivity for α-methylstyrene for which the conversion is also maximum. Thereafter with further increase in vanadia loading, the cracking product selectivity increases while α-methylstyrene selectivity diminishes.

Table 3.7
Cumene cracking over V_2O_5-SnO_2 systems.

Catalyst	Conversion (wt%)	Selectivity (%)	
		Cracking products	α-methylstyrene
T0	4.29	36.1	63.9
T3	5.00	24.7	75.3
T6	5.76	20.2	79.8
T9	6.45	19.9	80.1
T12	7.38	13.7	86.3
T15	9.22	12.3	87.7
V	1.23	36.5	63.5
ST0	5.69	34.7	65.3
ST3	6.37	27.9	72.1
ST6	6.73	14.5	85.5
ST9	10.29	10.0	90.0
ST12	9.32	13.0	87.0
ST15	8.27	23.6	76.4
SV	2.78	28.8	71.2

[Amount of catalyst: 0.5 g, Temperature: 350°C, Flow rate: 6 mL h^{-1}, TOS: 2 h]

Discussion:

Cumene conversion is known to be catalyzed by strong[109] or moderate[110] acid sites. The major reactions occurring during cumene conversion may be grouped into dealkylation (cracking) and dehydrogenation. Cracking of cumene

is generally attributed to the action of Brönsted sites by a carbonium ion mechanism while dehydrogenation of cumene yields α-methylstyrene as the major product, the formation of which has been ascribed to the Lewis acid sites[111-114]. The selectivity towards dehydrogenated products may be thus related to the Lewis acidity of the systems and the generation of cracking products with the Brönsted acidity of the systems. Boorman *et al.* prepared a series of catalysts containing fluoride, cobalt and molybdenum as additives to γ-alumina, both individually and in combination and the surface acidity of these systems was correlated with their reactivity for cumene conversion[115,116]. Sohn *et al.*[43] correlated the activity for cumene dealkylation with both acidity and acid strength distribution of sulfated ZrO_2-SiO_2 catalysts.

In our case, the cumene conversion seemed to be dependent on the total amount of acid sites, which is clear from Table 3.7. Vanadia-doped systems are found to be more active when compared to the single oxide systems, suggesting the formation of new acid sites on the catalyst surface by the addition of the second component[110]. The increase in the α-methylstyrene selectivity with vanadia content on the supported systems can be attributed to the intrinsic Lewis acidity imparted to the support by vanadium ion. The trend is similar to that obtained for perylene adsorption studies. The enhanced rate of cumene conversion in the case of sulfated samples can be accounted by the sufficiently higher amount of acidity possessed by these systems. The selectivity towards dehydrogenation showed a marginal increase with sulfate loading and is in line with the increase in Lewis acidity of the systems by the electron withdrawing nature of the sulfate groups. The drop-off in the selectivity towards α-methylstyrene and the cumene conversion at high vanadia loadings may be explained on the basis of bulk polysulfate species present, which decreases the acidity of the systems to a greater extent[6].

The correlation between the limiting amount of perylene from the adsorption studies and the dehydrogenation selectivities are presented in Figure 3.16. The figure gives a proportional relationship between the two, supporting the fact that Lewis sites are responsible for the dehydrogenation. The results are

also in good agreement with the strong acidity trend from ammonia TPD method. Comparing the cumene conversion percentage with the total acidity of the system from ammonia TPD measurements (Figure 3.17), we can conclude that the conversion is related to the total acidity of the systems.

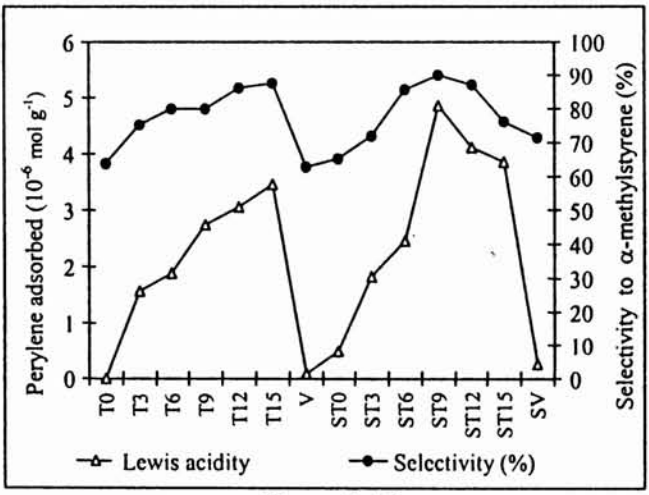

Figure 3.16
Correlation of Dehydrogenation selectivity with Lewis acidity obtained from perylene adsorption studies.

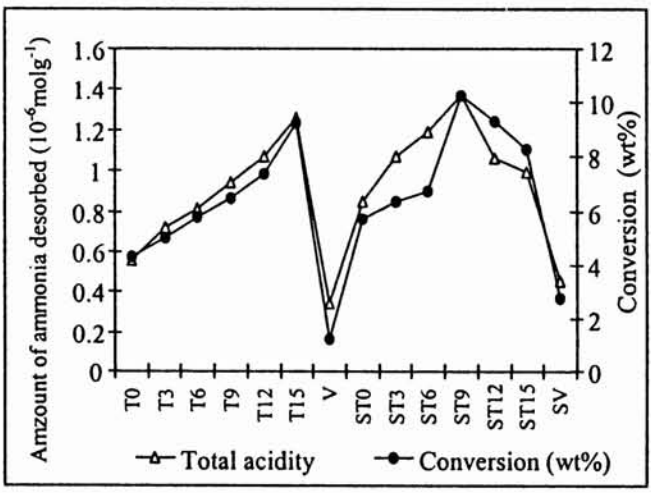

Figure 3.17
Cumene conversion correlated with total acidity of the systems obtained from ammonia TPD method.

3.3.2 V_2O_5-ZrO_2 Systems

I. Temperature Programmed Desorption of Ammonia (TPD)

The acidity of the V_2O_5-ZrO_2 and its sulfated analogues, as characterized by the desorption pattern of ammonia, spanned in the temperature range 100-600°C is given as the distribution of acid sites in Table 3.8.

Table 3.8
Ammonia TPD studies on V_2O_5-ZrO_2catalysts-
A comparative evaluation of acid strength distribution.

Catalyst	Amount of ammonia desorbed (mmol g^{-1})			
	Weak (100-200°C)	Medium (200-400°C)	Strong (400-600°C)	Total
Z0	0.12	0.13	0.07	0.25
Z3	0.19	0.21	0.11	0.28
Z6	0.35	0.46	0.25	0.75
Z9	0.28	0.36	0.17	0.61
Z12	0.19	0.28	0.07	0.42
Z15	0.19	0.23	0.05	0.33
SZ0	0.76	0.67	0.24	1.14
SZ3	0.23	0.28	0.11	0.45
SZ6	0.69	0.63	0.21	1.05
SZ9	0.59	0.55	0.18	0.97
SZ12	0.35	0.31	0.14	0.86
SZ15	0.30	0.27	0.12	0.48

Results:

As shown in Table 3.8, although pure zirconia shows some amount of acidity, the addition of vanadium oxide to the support results in a remarkable increase in acidity in almost all regions. The acidity increases slowly upon the addition of vanadia and reaches a maximum at 6 wt% and then decreases. Thus,

the most dramatic change of the over-all acidity by adding vanadia is observed in the case of Z6 system. Among the sulfated analogues, SZ0 is having the highest acidity values. The vanadia impregnated sulfated samples show the same trend in the acidity values as that of the unmodified counterparts. The trend of acidity for the simple and surface modified systems are given as :

Type of acid sites	Trend of acidity	
	Unmodified systems	Sulfated systems
Weak	Z0<Z3<Z6>Z9>Z12>Z15	SZ0>SZ3<SZ6>SZ9>SZ12>SZ15
Medium	Z0<Z3<Z6>Z9>Z12>Z15	SZ0>SZ3<SZ6>SZ9>SZ12>SZ15
Strong	Z0<Z3<Z6>Z9>Z12>Z15	SZ0>SZ3<SZ6>SZ9>SZ12>SZ15
Total	Z0<Z3<Z6>Z9>Z12>Z15	SZ0>SZ3<SZ6>SZ9>SZ12>SZ15

Discussion:

The ammonia thermodesorption results give clear evidence for the presence of surface acid sites of different strength going from weak to strong acidities. In view of the data from Table 3.8, it is apparent that the incorporation of vanadia modifies, to a significant extent, the acidity of ZrO_2 surface. The effect of vanadia on the acidic properties of ZrO_2 has been already reported[117,118]. Different proportions of the component oxides have been found to generate acid sites on the support surafce[130]. The combination of ZrO_2 and V_2O_5 probably generate stronger acid sites and more acidity as compared with the separate oxides. A mechanism for the generation of acid sites by mixing two oxides has been proposed by Tanabe *et al.*[102] They suggest that the acid generation is caused by an excess of negative or positive charge in a model structure related to the coordination number of the elements. However, at high vanadia loading the degree of polymerization of surface vanadyl species will be prominent with an enhanced formation of crystalline V_2O_5. It is reported that the vanadia as surface over layers imparts acidity, while the V_2O_5 crystallites hardly exhibit acidity[119,120]. This accounts for the reduction in the acidity values observed for high vanadia loaded systems.

The acidity of the sulfated zirconia system is considerably higher than that of pure ZrO_2. The pronounced enhancement in the amount of weak, medium and strong acid sites may be accounted for on the basis of the increase in the acidity induced by the sulfate groups on the surface. The electron withdrawing nature of the sulfate group increases the Lewis acidity of the systems[111]. Lunsford *et al.*[121] pointed out that Lewis sites adjacent to Brönsted acid sites results in enhancement of the Brönsted acidity due to the electron withdrawing inductive effect. The decrease in the acidity values from SZ9 onwards can be explained by the presence of V_2O_5 crystallites and polysulfate groups. The polysulfate together with crystalline V_2O_5 blocks the acid sites giving diffusive limitation to ammonia molecule[76]. The comparison of acidity values and surface area (Table 3.5) of the different V_2O_5-ZrO_2 systems suggest that the acidity runs parallel with the surface area.

II. Perylene Adsorption Studies

The limiting amounts of perylene adsorbed obtained from the Langmuir plots for V_2O_5-ZrO_2 systems are shown in Figure 3.18.

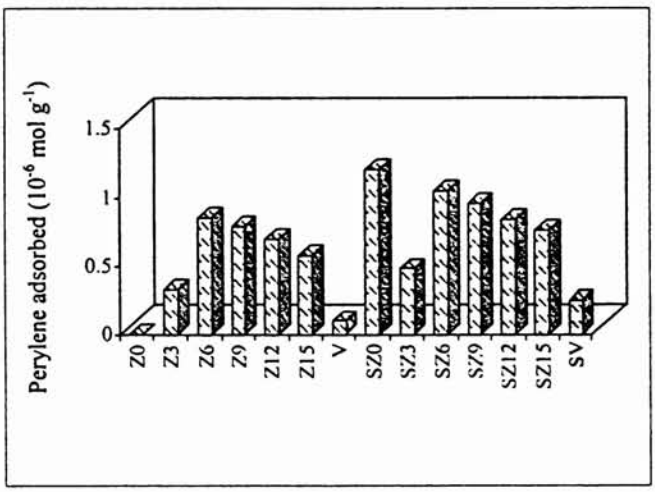

Figure 3.18
Variation in Lewis acidity of V_2O_5-ZrO_2 systems
from perylene adsorption studies.

Results:

From Figure 3.18, it is observed that the limiting amount of perylene adsorbed which gives a measure of the Lewis acidity or the electron accepting capacity, is higher for vanadia containing systems than for single oxide components. The limiting amount of perylene shows a steady increase with successive vanadium oxide addition up to 6 wt%, which thereafter reduces, with further addition of vanadia. Similar trend in the electron accepting capacity is observed with sulfate-doped samples with an exception of SZ0 that gives a comparatively higher value for the limiting amount.

Discussion:

A comparative evaluation of Lewis acidity obtained from perylene adsorption studies for V_2O_5-ZrO_2 systems suggests that the addition of vanadia substantially improves the Lewis acidity when present in small quantities. As discussed in the previous section, Zr^{4+} in the surface complex, becomes more positive when vanadia is introduced to the support, thereby resulting in enhanced Lewis acidity. At high vanadia loadings, a significant loss of Lewis acid sites is apparent from the perylene adsorption results. This may be due to the blocking of the surface acidic sites by crystalline V_2O_5, which hardly imparts acidity to any metal oxide systems. Here again, the enhanced electron accepting capacity of the sulfated system can be explained by the increase of number and strength of Lewis acid sites by the electron withdrawing inductive effect of S=O of the sulfur complex on the oxide surface. The abnormal value in the case of SZ0 can be attributed to the very high Lewis acidity imparted to the pure zirconia surface most probably by a monolayer of the sulfate group. Presence of vanadia enhances the sulfate retaining capacity (as evident from the EDX results), which will lead to the formation of multilayers of polysulfate and reduces the acidity of the system.

III. Vapour-Phase Cumene Cracking Reaction

Table 3.9 gives the conversion percentage and product distribution obtained in vapour-phase cumene cracking reaction for different vanadia loaded ZrO_2 systems and its sulfated analogues.

Table 3.9
Cumene cracking over V_2O_5-ZrO_2 systems

Catalyst	Conversion (wt%)	Selectivity (%)	
		Cracking products	α-methylstyrene
Z0	3.11	50.0	50.0
Z3	4.30	27.7	72.3
Z6	5.84	12.9	87.1
Z9	4.64	19.0	81.0
Z12	4.08	20.4	79.6
Z15	3.90	24.4	75.6
V	1.23	36.5	63.5
SZ0	14.04	22.1	77.9
SZ3	8.27	30.1	69.9
SZ6	8.66	9.6	90.4
SZ9	7.27	19.0	81.0
SZ12	4.39	24.9	75.1
SZ15	2.57	37.0	63.0
SV	2.78	28.8	71.2

[Amount of catalyst: 0.5 g,Temperature: 350°C, Flow rate: 6 mL h^{-1}, TOS: 2 h]

Results:

As in the case of V_2O_5-SnO_2 systems, here also, the single oxides show lower conversion compared to the supported or sulfate modified systems. The cumene conversion by the simple and sulfated systems shows the same trend. The conversion increases with increase in vanadia content, reaches a maximum for system with 6 wt% vanadia and declines thereafter. The highest conversion is shown by the SZ0 system where the selectivity to the cracking products is 50%. The α-methylstyrene selectivity is parallel to the cumene conversion, which is maximum for Z6 and SZ6 in the supported, and sulfate modified vanadia-containing systems respectively. The variation in the α-methylstyrene selectivity is concomitant with the selectivity to the cracking products in all the cases.

Discussion:

The results of cumene cracking reaction with V_2O_5-ZrO_2 systems shows that the conversion strongly depends on the amount of acid sites on the catalysts

surface. The cracking performance of the catalysts is found to be suppressed by the vanadia addition, which is compensated by the enhancement of dehydrogenation activity at the initial stage up to 6 wt%. Later on, at higher vanadia loading the trend is reversed where the selectivity to the cracking products increases with a corresponding decrease in the α-methylstyrene selectivity. This is indicative of the fact that vanadia in lower amounts can impart Lewis acidity to the system by creating new acid sites, while the crystalline vanadia formed after 6 wt% has little ability to activate cumene because the acidity of V_2O_5 crystallites are very low. The cracking activity of the sulfated systems has the similar tendency though the conversion obtained is much higher than those of the unpromoted samples. The results indicate an increase in acid strength by the introduction of the sulfate species. The increase in selectivity to α-methylstyrene is suggestive of the increase in concentration of Lewis acid sites by surface sulfate modification.

Supporting evidence for these conclusions is provided by the ammonia TPD and perylene adsorption studies. The correlation obtained among the results of the three independent methods is apparent from the following figures (Figures 3.19 to 3.21).

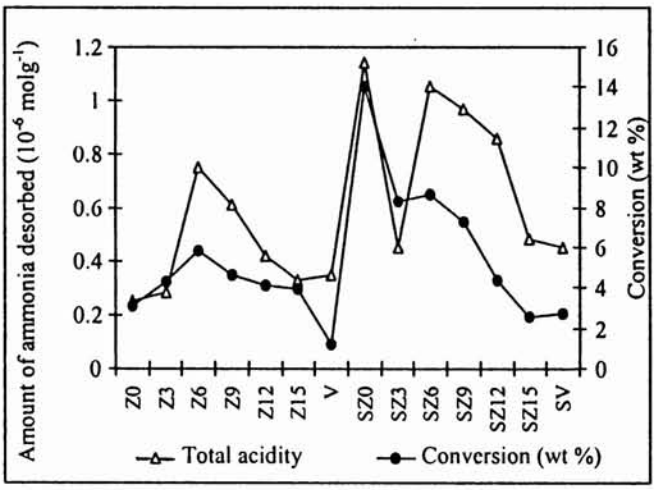

Figure 3.19
Conversion of cumene correlated with total acidity of the systems from ammonia TPD method.

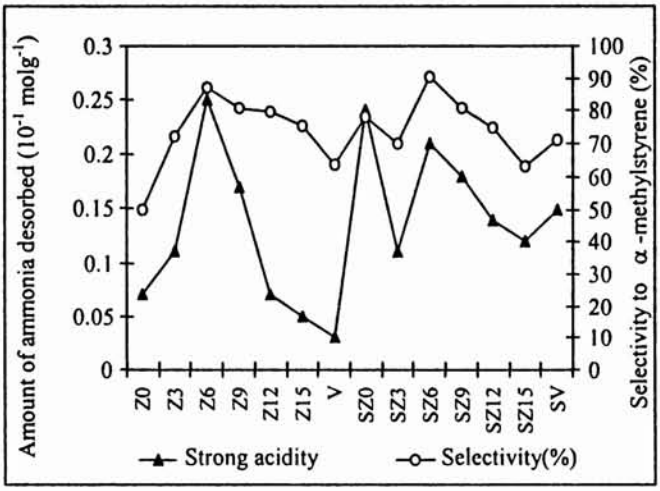

Figure 3.20
Correlation of dehydrogenation selectivity with strong acidity from ammonia TPD studies.

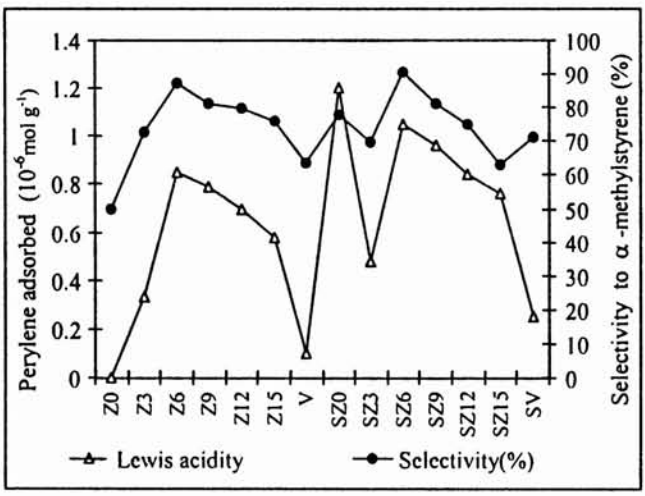

Figure 3.21
Correlation of dehydrogenation selectivity with Lewis acidity from perylene adsorption studies.

3.4 CONCLUSIONS

The following general conclusions can be drawn from the different surface characterization techniques as well as the surface acidity measurements of the supported vanadia systems and its sulfated analogues of SnO_2 and ZrO_2:

- The EDX results prove the wet impregnation method as a rather simple and efficient method to prepare supported vanadia system with desired loading of vanadium oxide and also for the preparation of surface modified systems with sulfate anions. The results also indicate that the sulfate retaining capacity of the supported system increases with vanadia loading.
- Surface area and pore volume measurements show that the presence of vanadia in small quantities stabilizes the microstructure of the systems leading to an increase in these properties, while large quantities of crystalline vanadia can lead to successive pore plugging. The surface area and pore volume of the sulfated systems are much higher than those of the unmodified samples. SEM analysis of the samples supports the observed trend in surface area and pore volume.
- The TG-DTG analysis of the pure and vanadia promoted samples reveal higher thermal stability of the catalyst system even after 700°C while the sulfated sample is stable only up to 700°C.
- The tetragonal phase of the single oxides is stabilized by the addition of vanadia as apparent from the XRD data. The sulfate anions hinder the crystallization of the oxide systems by preventing the agglomerization of surface particles.
- The combination of different spectroscopic characterization of the samples by XRD, FTIR, ^{51}V NMR and DR UV-VIS. concludes the presence of isolated tetrahedral surface vanadium species at the low surface coverages, which polymerizes to give octahedral units and eventually crystalline vanadia at high loadings. The monolayer coverage of the tetrahedral species appears to be complete at 6 wt% vanadia loading in

the case of V_2O_5-SnO_2 systems. Much faster formation of multilayer of vanadia is observed for V_2O_5-ZrO_2 samples with completion of monolayer coverage at 3 wt%. The presence of surface sulfate groups does not change the local structure of vanadium oxide species.

- The acidities of the systems measured by three independent techniques namely ammonia TPD, perylene adsorption and vapour-phase cumene cracking reaction give very good correlation of the results. The incorporation of vanadia substantially improves the acidity of the support oxide. Surface modification by the sulfate groups enhances the acidity of the systems to a considerable extent.

ꕥ ꕥ ꕥ

REFERENCES

1. K. Morikawa, T. Shirasaki and M. Okada, *Adv. Catal.*, 20 (1969) 97.
2. R. J. Poglar, F. H. Hambelton and J.H. Hockey, *J. Catal.*, 20 (1971) 309.
3. R. Gopalan, C. H. Chang and Y. S. Lin, *J. Mater. Sci.*, 30(1995) 3075.
4. P. D. L. Mercera, V. J. G Ommen, E. B. M. Doesberg, A. J. Burgraaff and J. R. H. Ross, *Appl. Catal.*, 78 (1991) 79.
5. B. Zhao, X. Xu, H. Ma, D. Sun and J. Gao, *Catal. Lett.*, 45 (1997) 237.
6. A. K. Dalai, R. Sethuraman, S. P. R. Katikeneni and R. O. Idem, *Ind. Eng. Chem. Res.*, 37 (1998) 3869.
7. A. Corma, *Chem. Rev.* 95 (1995) 559.
8. X. Song and A. Sayari, *Catal. Rev.-Sci. Eng.*, 38 (3) (1996) 329.
9. K. Morishige, K. Kittaka and T. Morimoto, *Bull. Chem. Soc. Jpn.*, 53 (1980) 2128.
10. H. P. Oliveira, F. J. Aaissi and H. E. Toma, *Mat. Res. Bull.*, 33(12) (1998) 1783-1792.
11. M. Ponzi, C. Duschatzky, A. Carrascull and E. Ponzi, *Appl. Catal. A. Gen.*, 169(1998) 373-379.
12. R. A. Keogh, R. Srinivasan and B.H Davis, *J. Catal.*, 151 (1995) 123.

13. O. Saur, M. Bensital, A. B. M. Saad, J. C. Lavalley, C. P. Tripp and B. A. Morrow, *J. Catal.*, 99 (1986) 104.
14. T. M. Jyothi, K. Sreekmar, M. B. Talwar, S. P. Mirajkar, B. S. Rao and S. Sugunan, *Polish J. Chem.*, 74 (2000) 123.
15. G. Deo and I. E. Wachs, *J. Catal.*, 129 (1991) 307.
16. G. Deo, I. E. Wachs and J. Haber, *Crit. Rev. Surf. Chem.*, 4 (1994) 141.
17. M. M. Kantcheva, K. I. Hadjiivanov and D. G. Klissurski, *J. Catal.*, 134 (1992) 299.
18. M. A. Vuurman and I. E. Wachs, *J. Phys. Chem.*, 96 (1992) 5008.
19. J. Haber, A. Kozlowska and R. Kozlowski, *J. Catal.*, 102 (1986) 52.
20. K. Jnumaru, M. Misono and T. Okuhara, *Appl. Cata. A. Genl.*, 149 (1997) 133-149.
21. M. M. Dubinin, *Chem. Rev.*, 60 (1960) 235.
22. M. P. Rosynek and P. T. Magnuson, *J. Catal.*, 46 (1977) 402.
23. S. K. Samantray, T. Mishra and K. M. Parida, *J. Mol. Catal. A. Gen.*, 156 (2000) 267-274.
24. K. Hadjiivanov, A. Davydov and D. Klissurski, *Kinet. Catal.*, 29 (1988) 161.
25. I. E. Wachs., *Catal. Today*, 27 (1996) 437-455.
26. G. C. Bond, A. J. Sarkani and G. D Parfitt, *J. Catal.*, 57 (1979)476.
27. G. C. Bond and S. Flamerz Tahir, *Appl. Catal.*, 71 (1991) 1-31.
28. L. Briand, L. Gambaro and H. Thomas, *J. Catal.*, 161 (1996) 839.
29. G. Fabbin and P. Baraldi, *Anal. Chem.*, 44 (1972) 1325.
30. G. Hausinger, H. Schemlz and H. Knozinger, *Appl. Catal.*, 39 (1988) 267.
31. G. Busca, G. Centi, L. Marchetti and F. Trifiro, *Langmuir.*, 2 (1989) 568.
32. N. Y. Topose, M. Topsoe and J. A. Dumesic, *J. Catal.*, 151 (1995) 226-240.
33. G. Busca, G. Ramis and V. Lorenzelli, *J. Mol. Catal.*, 50 (1989) 231.
34. G. Busca and J. C. Lavelley, *Spectrochim. Acta.*, 42A (1986) 443.
35. T. R. Gilson, O. F. Bizri and N. Cheetham, *J.Chem. Soc., Dalton Trans.*, (1973) 291.
36. M. Schrami Marth, A. Wokaun and A Baiker, *J. Catal.*, 124 (1990) 86.

37. K. Nakamoto, *Infrared and Raman Spectra of Inorganic and Co-ordination compounds*, 4th Edn., Wileny, New York, 1986.

38. F. Babou, G. Coudurier and J. C. Vedrine, *J. Catal.*, 152 (1995) 341-349.

39. T. Yamaguchi, *Appl. Catal.*, 61 (1990) 1-25.

40. B. A. Morrow, R. A. Mc Farlane, M. Lion and J. C. Lavalley, *J. Catal.*, 107 (1987) 232.

41. M. Bensitel, O. Saur, J. C. Lavalley and B. A. Morrow, *Mater. Chem. Phys., 19* (1988) 147.

42. M. Waquif, J. Bachelier, O. Saur and J. C. Lavalley, *J. Mol. Catal.*, 72 (1992) 127.

43. J. R. Sohn and H. J. Jang, *J. Mol. Catal.*, 64 (1991) 349.

44. C. Miao, W. Hua, J. Chen and Z. Gao, *Catal. Lett.*, 37 (1996) 187.

45. C. Monterra, G. Cerrato, F. Pinna, M. Signoretto and G. Strukul, *J. Catal.*, 149 (1994) 181.

46. H. Eckert and I. E. Wachs, *J. Phys. Chem.*, 93 (1989) 6769.

47. B. M. Reddy, E. P. Reddy, S. T. Srinivas, V. M. Mastikhin, N. V. Wosov and O. B. Lapina, *J. Phys. Chem.*, 96 (1992) 7070.

48. L. R. Le Costumer, B. Taouk, M. Lemeu, E. Payen, M. Guetton and J. Grimblot, *J. Phys. Chem.*, 92 (1988) 1230.

49. Z. Sobalik, O. B. Lapppina, O. N. Novgorodova and V. M. Mastikhn, *Appl. Catal.*, 63 (1990) 191.

50. A. Satsuma, H. Hattori, K. Mizutani, A. Furuta, A. Miyamoto, T. Hattori and Y. Murakami, *J. Phys. Chem.*, 92 (1988) 6065.

51. H. Eckert, G. Deo, I. E. Wachs and A. M. Hirt, *Coll. Surf.*, 45 (1995) 347.

52. G. Deo and I. E. Wachs, *J. Phys. Chem.*, 95 (1991) 5889.

53. F. Roozeboom, M. C. Mitteimeilijer, J. A. Moulijn, J. Medema, U. H. J. de Beer and P. J. Gellings, *J. Phys. Chem.*, 84 (1980) 2783.

54. L. J. Lakshmi, E. C. Alyea, S. T. Srinivas and P. K. Rao, *J. Phys. Chem.*, 101 (1997) 3324.

55. V. M. Mastikhin, V. V. Terskikh, O. B. Lapina, S. V. Filiminaova, M. Seidl and H. Knozinger, *Sol.State Nucl. Mag. Res.*, 70 (1995) 369.

56. E. H. Park, M. H. Lee and J. R. Sohn, *Bull. Chem. Soc.*, 21 (9) (2000) 913.
57. G. Catana, R. R. Rao, B. M. Weckhuysen, P. V. Der Voort, E. Vasant and R. A. Scoonhedyt, *J. Phys. Chem. B.*, 102 (1998) 8005.
58. C. J. Ballhausen and H. B. Gray, *Inorg. Chem.*, 1 (1962) 111.
59. A. B. P. Lever, "*Inorganic Electronic Spectroscopy*", 2nd Ed; Elsevier, Amsterdam.
60. N. N. Greenwood and A. Earnshaw, "*Chemistry of Elements*", Pergamon Press, Oxford, (1984).
61. M. Schrami-Marth and A. Wokaun, *J. Chem. Soc. Faraday Trans.*, 87 (16) (1991) 2635.
62. U. Scharf, M. Schrami-Marth and A. Wokaun, *J. Chem. Soc. Faraday Trans.*, 87 (19) (1991) 3299.
63. A. Calaf, L. Avilan and J. Aldana, *Appl. Catal. A. Gen.*, 201 (2000) 215.
64. D. A. Ward and E. I. Ko, *J. Catal.*, 150 (1994) 18.
65. R. A. Boyse and E. I. Ko, *Catal. Lett.*, 38 (1996) 225.
66. P. D. I. Mercera, V. I. G. Ommen, E. B. M. Doesburg, A. J. Burgraaf and J. R. H. Ross, *Appl. Catal.*, 57 (1990) 127.
67. F. R. Chen, G. Coudurier, J. F. Joly and J. C. Vedrine, *J. Catal.*, 143 (1993) 616.
68. K. Arata, *Adv. Catal.*, 37 (1990) 165.
69. M. S. Scurrell, *Appl. Catal.*, 34 (1987) 109.
70. T. Yamaguchi, K. Tanabe and Y. C. Kung, *Mater. Chem. Phys.*, 16 (1986) 67.
71. J. R. Sohn and H. W. Kim, *J. Mol. Catal.*, 52 (1989) 361.
72. R. Srinivasan, D. Taulbee and B. H. Davis, *Catal. Lett.*, 9 (1991) 1.
73. J. Livage, K. Doi and C. Mazïieres, *J. Phys. Chem.*, 93 (1989) 6769.
74. Z. Liu, W. Ji, L. Dong and Y. Chen, *Mat. Chem. Phy.*, 56 (1998) 134.
75. J. R. Sohn, S. G. Cho, Y. I. Pae and S. Hayashi, *J. Catal.*, 159 (1996) 170.
76. R. Srinivasan, R. A. Keogh, D. R. Milburn and B. H. Davis, *J. Catal.*, 153 (1995) 123.
77. T. Yamamoto, T. Tanaka, S. Takenaka, S. Yoshida, T. Onari, Y. Takahashi, T. Kusaka, S. Hasegawa and M. Kudo, *J. Phys. Chem.*, 103 (1999) 2385.
78. J. R. Sohn, M. Y. Park and Y. I. Pae, *Bull. Korean Chem. Soc.*, 17 (1996) 274.

79. D. Farcasiu, J. Q. Li and S. Cameron, *Appl. Catal. A: Gen.*, 154 (1997) 173.

80. H. P. Bochnm and H. Knozinger, "*Catalysis*", J. R. Anderson and M. Boudart, Eds., Vol.4, Springer, Berlin, (1983) Chapter 2.

81. K. Mori, A. Miyamoto and Y. Murakami, *J. Chem. Soc. Faraday Trans.*, 83 (1987) 3303.

82. T. R. Gilson, O. F. Bizri and N. Cheetham, *J. Chem. Soc. Dalton Trans.*, (1973) 291.

83. A. Andersson, *J. Catal.*, 76 (1982) 144.

84. G. C. Bond, J. Perez Zurita, S. Flamerz, P. J. Gellings, H. Bosch, J. G. van Ommen and B. J. Kep, *Appl. Catal.*, 22 (1986) 361.

85. A. J. van Hengstum, J. G. van Ommen, H. Bosch and P. J. Gellings, *Appl. Catal.*, 5 (1983) 3287.

86. R. Kozlowski, R. F. Pettifer and J. M. Thomas, *J. Phys. Chem.*, 87 (1983) 5176.

87. K. Kijenski, A. Baiker, M. Glinski, P. Dollenmeier and A. Wokaun, *J. Catal.*, 101 (1986) 7.

88. G. D. Yadav and J. J. Nair, *Microporous and Mesoporous Materials*, 33 (1999) 1.

89. G. T. went, L-J. Lei, S. J. Lombardo and A. T. Bell, *J. Phys. Chem.*, 96 (1992) 2235.

90. I. E. Wachs, G. Deo and B. M. Weckhuysen, *J. Catal.*, 161 (1996) 211.

91. M. Schrani-Marth, W. Fluhr, A. Wokaun and A. Baiker, *Ber. Bunsenges Phs. Chem.*, 93 (1989) 852.

92. F. Roozeboom, P. D. Cordingely and P. J. Gellings, *J. Catal.*, 68 (1981) 464.

93. W. Hanke, R. Bienert and H. G. Jerschkewitz, *Z. Anorg. Allg. Chem.*, 414 (1975) 109.

94. I. E. Wachs, *J. Catal.*, 124 (1990) 570.

95. C. Cristiani, F. Forazati and G. Busca, *J. Catal.*, 116 (1989) 586.

96. G. Connel and J. A. Dumesic, *J. Catal.*, 102 (1986) 216.

97. T. Jin, H. Hattori and K. Tanabe, *Bull. Chem. Soc. Jpn.*, 55 (1982) 2279.

98. K. Tanabe, M. Itoh and K. Morishige, in "*Preparation of Catalysts*", B. Delmon, P. A. Jacobs and G. Poncelet, Eds., Elsevier, Amsterdam, (1976) p. 65.

99. K. Shibata, T. Kiyoura, J. Kitagawa, T. Sumiyoshi and K. Tanabe, *Bull. Chem. Soc. Jpn.*, 46 (1973) 2985.

100. M. Ai, *J. Catal.*, 40 (1975) 318.

101. M. Ai, *Bull. Chem. Soc. Jpn.*, 49 (1976) 1328.

102. K. Tanabe, T. Sumiyoshi, K. Shibata, T. Kiyoura and I. Kitagawa, *Bull. Chem. Soc. Jpn.*, 47 (1974) 1064.

103. H. Miyata, K. Kohno, T. Ono, T. Ohno and F. Hatayama, *J. Mol. Catal.*, 86 (1990) 731.

104. A. Corma, V. Fornes, M. I. Juan Rajadell and J. M. Lopez Nieto, *Appl. Catal. A: Gen.*, 116 (1994) 151.

105. A. Clearfield, G. P. D. Serrete and A. H. Khazi-Syed, *Catal. Today*, 20 (1994) 295.

106. R. T. Sanderson, "*Chemical Bonds and Bond Energy*", Academic Press, New York (1976) p.75.

107. F. Lonyi, J. Valyon, J. Engelhardt and P. Mizukami, *J. Catal.*, 160 (1997)279.

108. F. Arena, R. Dario and A. Parmaliana, *Appl. Catal. A: Gen.*, 170 (1998) 127.

109. Y-Y. Huang, B-Y. Zhao and Y-C. Xie, *Appl. Catal. A: Gen.*, 171 (1998) 65.

110. S. J. Decanio, J. R. Sohn, P. O. Paul and J. H. Lunsford, *J. Catal.*, 101 (1986) 132.

111. A. Corma and B. W. Wojciechowski, *Catal. Rev. Sci. Eng.*, 24 (1982) 1.

112. J. W. Ward, *J. Catal.*, 9 (1967) 225.

113. W. Przystajko, R. Fieddorow and I. G. Dalla Lana, *Appl. Catal.*, 15 (1985) 265.

114. H. Pines, "*The chemistry of catalytic hydrocarbon conversions*", Academic Press, New York (1981) p.85.

115. P. M. Boorman, R. A. Kydd, Z. Sarbak and A. Somogyvari, *J. Catal.*, 96 (1985) 115.

116. P. M. Boorman, R. A. Kydd, Z. Sarbak and A. Somogyvari, *J. Catal.*, 100 (1986) 287.

117. H. Miyata, K. Fujii and T. Ono, *J. Chem. Soc. Faraday Trans.*, 1 (84) (1988) 3121.

118. H. Miyata, H. Nishiguchi and T. Ono, *Chem. Express*, 3 (1988) 243.

119. J. Le Barrs, J. C. Vedrine, A. Auroux, S. Trautman and M. Eaerns, *Apppl. Catal. A. Gen.*, 119 (1994) 341.

120. M. M. Khader, *J. Mol. Catal. A. Chem.*, 104 (1995) 97.

121. J. H. Lunsford, H. Sang, S. M. Campbell, C. H.Liang and R. G.Anthony, *Catal. Lett.*, 27 (1994) 305.

Chapter 4

Friedel-Crafts Alkylation of Arenes

ABSTRACT

Catalyzed aromatic Friedel-Crafts alkylation is a very important industrial process and would become even more so if the noxious homogeneous catalysts in current use, which are sources of pollution, industrial hazard and equipment corrosion, could be replaced by a non-corrosive solid acid catalyst. The present study has undertaken the Friedel-Crafts benzylation of aromatics over the supported vanadia systems as well as its sulfated analogues. Under the optimized reaction conditions, these catalysts are found to be very effective and considerably more selective than the conventional homogeneous Lewis acid catalysts. The investigation of vanadia systems-catalyzed benzylation of benzene, toluene and *o*-xylene with benzyl chloride revealed that the catalytic activity and product selectivity are sensitive to the precise reaction parameters and can be related to the Lewis acidity of the systems. The reaction is found to be very clean and produces the desired monoalkylated product with very high yield.

4.1 INTRODUCTION

The Friedel-Crafts alkylation reactions are of great interest due to their importance and common use in synthetic and industrial chemistry[1]. The alkylation is traditionally performed with alkyl halides using Lewis acid catalysts such as HF and $AlCl_3$ or with alcohols using Brönsted acids, typically H_2SO_4[2]. However, the homogeneous catalysts encounter major disadvantages like

corrosion, unfriendliness to environment because of the waste by-products induced by isomerization in the reaction and heavy expense due to the requirement of large excess of reagents. In view of these reasons, there was a long felt demand to substitute these reagents by less corrosive and environment friendly materials[3]. Intensive research in this direction revealed the materials in the form of solid acids developed from heteropolyacid[4], clays[5-9], zeolites[10], sulfated zirconia[11], transition metal cations[12], etc. These heterogeneous catalysts however, have shown drawbacks such as lower product selectivity, formation of higher amount of polyalkylated products and drastic reaction conditions.

The use of vanadia catalysts in the synthesis of fine chemicals is an increasing area of application and growing importance in recent years. By contrast, the utility of vanadia catalysts in the Friedel-Crafts alkylation of aromatic compounds has not been explored in sufficient detail. Hence we carried out a detailed study on the benzylation of arenes (benzene, toluene and *o*-xylene) by benzyl chloride over vanadia supported on SnO_2 and ZrO_2 as well as its sulfated analogues. The structural stability, catalytic activity and reusability of the systems have been checked. Since homogeneous Lewis acids often catalyze the Friedel-Crafts type reaction, the strong/Lewis acid sites on the surface of these metal oxides are expected to be of help in facilitating the reaction. The objective of this study is to enhance the conversion of aromatics and selectivity to the monoalkylated products, consequently to minimize the formation of polyalkylated products. In this part of the thesis, we report the results obtained in the alkylation under various reaction conditions and the effects of some catalyst variables on the catalyst performance. The results obtained over the vanadia systems are compared with the efficiency of the Lewis acid catalyst $AlCl_3$. A discussion about the mechanism of the reaction is also presented.

4.2 BENZYLATION OF ARENES WITH BENZYL CHLORIDE

The liquid-phase benzylation reaction was conducted by refluxing a mixture of aromatic compound (benzene, toluene or *o*-xylene) with alkylating agent, benzyl chloride in a required molar ratio at a particular temperature

using the experimental procedure given in section 2.6.1 of Chapter 2. The reaction always yielded a single major product under the present reaction conditions using the aromatic substrate in excess, which, due to the difficulty of identification as ortho or para, is named as monoalkylated product (MAP). Small peaks corresponding to polyalkylated products (PAP), the concentration of which corresponded to less than 5% of the total conversion of benzyl chloride were also identified and estimated by GC at a higher retention time in some cases. The product yield and selectivity was found to be considerably dependent on the reaction variables. So we optimized the reaction conditions separately for the three substrates. The performance of various samples was scanned under the optimized conditions so that a proper comparison of the catalyst efficiency could be made.

The catalytic activity was expressed as the percentage conversion (wt%) of benzyl chloride and is defined as the total percentage of benzyl chloride transformed in to the products. Assuming pseudo-first order reaction, the rate of benzyl chloride conversion (mmol g^{-1} h^{-1}) was calculated as the amount of benzyl chloride (mmol) converted per hour over 1 g of the catalyst. The selectivity to a product is expressed as the amount of that particular product divided by the amount of total products and multiplied by 100.

The observations of the investigation and the discussion of the results are presented under three main headings; I) Process optimization II) Catalyst efficiency of different systems III) Structural stability of the catalysts.

4.2.1 Process Optimization

The effect of reaction temperature, reaction time, catalyst concentration and substrate to benzyl chloride molar ratio on the catalyst performance was examined in order to optimize the conversion of benzyl chloride and selectivity to the monoalkylated product.

I. Effect of Temperature

The dependence of conversion of benzyl chloride (wt%) and the product distribution (%) on the reaction temperature is studied in the range 60-120°C

using T6 catalyst over the three substrates (Table 4.1). The influence of the reaction temperature on the rate of conversion (mmol $g^{-1} h^{-1}$) is given in Figure 4.1.

Table 4.1
Effect of temperature on benzylation of arenes.

Temperature (°C)	Substrate						
	Benzene		Toluene		*o*-Xylene		
	BC-C[a] (wt%)	MAP-S[b] (%)	BC-C (wt%)	MAP-S (%)	BC-C (wt%)	MAP –S (%)	PAP -S[c] (%)
60	4.3	100	5.5	100	26.6	100	-
70	8.4	100	13.5	100	31.9	100	-
80	15.2	100	24.7	100	39.3	100	-
90	-	-	29.6	100	53.2	100	-
100	-	-	36.1	100	88.1	97.8	2.2
110	-	-	48.7	100	92.7	95.6	4.4
120	-	-	-	-	100	92.5	7.5

[Amount of catalyst: 0.1 g (T6), Time: 1 h, Substrate: benzyl chloride molar ratio: 10: 1]
(a-benzyl chloride conversion, b-monoalkylated product selectivity, c- polyalkylated product selectivity)

Results:

From the data given in Table 4.1, it is clear that the temperature has a highly pronounced promotional effect on the conversion of benzyl chloride in Friedel-Crafts alkylation. The benzyl chloride conversion is found to increase gradually with the rise in temperature. Maximum conversion is found to be at the refluxing temperature in the case of benzene and toluene with 100% selectivity to the monoalkylated product. For *o*-xylene, at low temperatures, 100% selectivity to the monoalkylated product is observed. An increase in reaction temperature above 90°C though increases the conversion of benzyl chloride, results in a lowering of selectivity to the desired product.

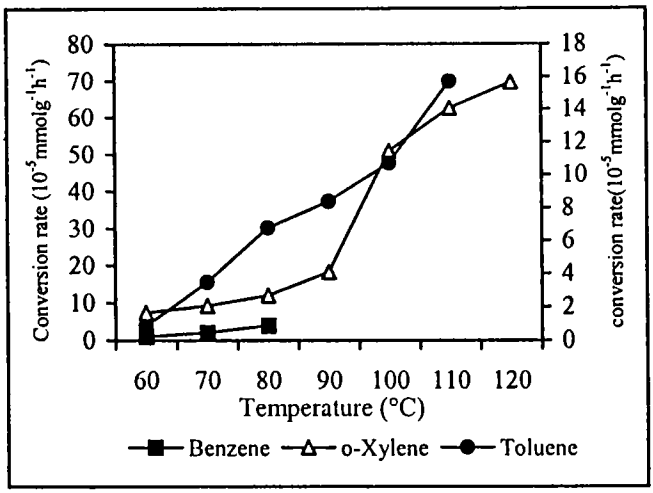

Figure 4.1

Dependence of conversion rate of benzyl chloride on temperature.

[Amount of catalyst: 0.1 g (T6), Time: 1 h, Substrate: benzyl chloride molar ratio: 10: 1]

A complete conversion of the benzylating agent is observed as the temperature reaches 120°C in this case. The results also reveal that the maximum conversion obtained in a typical run of reaction for I h at the refluxing temperature, is 15.2% for benzene and 48.7% for toluene. A complete conversion of benzyl chloride is observed even before reaching the refluxing temperature, when *o*-xylene is the substrate. But this happens at the expense of selectivity to the monoalkylated product. The conversion rate of benzyl chloride also increases gradually with the reaction temperature for the three substrates as evident from Figure 4.1. A much higher rate of benzyl chloride conversion is given by *o*-xylene when compared to benzene and toluene at all the temperatures in the range 60-120°C.

Discussion:

The reaction temperature seems to play a major role in deciding the catalytic activity and selectivity in Friedel-Crafts benzylation of arenes. From the above observations it is seen that the conversion of benzyl chloride increases linearly with temperature. This is probably due to the speedy desorption of the alkylated product from the catalyst surface as the temperature increases, which facilitates the further adsorption of reactant molecules, resulting in the increased

conversion of benzyl chloride. The increase in alkylation activity with temperature can also be ascribed to the increase in the intrinsic activity of the acid sites on the bare surface of the catalyst. However, the decrease in selectivity for monoalkyalted product in the case of *o*-xylene above 90°C may be due to the formation of consecutive products at higher temperatures. The results are in agreement with the literature report that the higher reaction temperature favours the consecutive alkylation, disproportionation and decarboxylation[13]. The decrease in selectivity to the monoalkylated product with increase in reaction temperature is also reported by Cseri *et al.*[14] over ion exchanged clays. It is reported that 'clayzic'- an ion-exchanged clay, can catalyze the Friedel-Crafts alkylation at room temperature[15-18]. Thus we believe that the activation energy for the above reaction over different catalyst is not the same.

II. Effect of Reaction Time

The reaction temperature is optimized as the corresponding refluxing temperature for benzene and toluene while it is set as 90°C for *o*-xylene. Taking 0.1 g of T6 catalyst, typical run was carried out for different reaction times with substrate to benzyl chloride molar ratio 10: 1. Figure 4.2 shows the percentage conversion of benzyl chloride plotted as a function of reaction time for the three substrates. Table 4.2 presents the product distribution with reaction time.

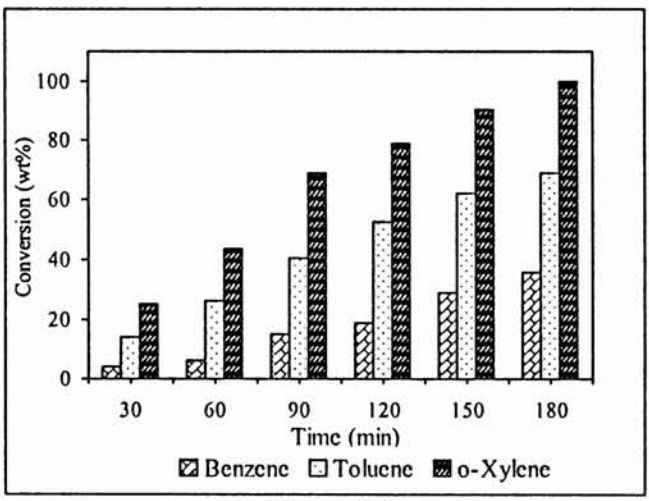

Figure 4.2
Conversion of benzyl chloride (wt%) -as a function of reaction time.

Table 4.2
Effect of reaction time on benzylation of arenes.

Time (min)	Product distribution (%)					
	Benzene[a]		Toluene[b]		*o*-Xylene[c]	
	MAP	PAP	MAP	PAP	MAP	PAP
30	100	-	100	-	100	-
60	100	-	100	-	100	-
90	100	-	100	-	99.3	0.7
120	100	-	98.9	1.1	98.1	1.9
150	100	-	98.3	1.7	95.4	4.6
180	100	-	97.4	2.6	93.8	6.2

[Amount of catalyst: 0.1 g (T6), Temperature: [a] 80°C; [b] 110°C ; [c] 90°C, Substrate: benzyl chloride molar ratio: 10: 1]

Results:

As shown in Figure 4.2, a continuous increase in the percentage conversion of benzyl chloride is registered with increase in reaction time for the three substrates. The variation in the product selectivity with time is also subjected to screening (Table 4.2). In the case of benzene, though the conversion is comparatively low, 100% selectivity to the monoalkylated product is observed even after 3 h of reaction run. Prolonged reaction time is found to generate undesirable products in the case of toluene and *o*-xylene. For toluene, at the beginning of the reaction, the percentage conversion is low and only monoalkylated product is detected up to 1.5 h of reaction time. After 1.5 h, secondary alkylation is also observed, resulting in low selectivity. The benzyl chloride conversion increases gradually and reaches 100% at 3 h reaction time at the expense of selectivity to the monoalkylated product for *o*-xylene. Polyalkylated products appear after 1 h reaction time in this case.

Discussion:

The results show that the reaction time also can have a deciding effect on the catalytic activity and product selectivity. The increase in conversion of benzyl chloride with time confirms the heterogeneity of the catalytic reaction. The observed order of reactivity of the various substrates in the benzylation reaction with reaction time is *o*-xylene > toluene > benzene, which is in perfect agreement with number of electron releasing alkyl groups attached to them. The benzylation is slow in the case of benzene where there are no methyl groups on the benzene ring. The inductive effect of methyl group makes the reaction more facile in the case of toluene and still higher for xylene due to the cumulative effect of the two methyl groups. Similar observations were made by Jun *et al.*[19] in Friedel- Crafts alkylation of aromatics over Al-impregnated mesoporous molecular sieves. Thus the optimum reaction time is selected as 2, 1.5 and 1 h for benzene, toluene and *o*-xylene respectively.

III. Influence of Catalyst Concentration

In heterogeneous catalysis the amount of catalyst plays a crucial role in determining the rate of the reaction. Table 4.3 displays the conversion of benzyl chloride and product distribution as a function of catalyst amount in benzylation of toluene. The catalyst concentration is varied by taking different amounts of T6 catalyst and keeping the amount of benzylating agent constant. The selected molar ratio is 10: 1 and the reaction is carried out at the refluxing temperature for 1.5 h.

Results:

Table 4.3 shows that the conversion of benzyl chloride is negligible in the absence of the catalyst. As the amount of catalyst is increased to 0.1 g, the percentage conversion changes from 2.3% to 49.4%. The conversion steeply increases with increase in catalyst concentration and reaches 100% when the amount is 0.35 g. The decrease in the selectivity to the monoalkylated product with high catalyst concentration is also worthy of note.

Table 4.3
Benzylation of toluene- Influence of catalyst concentration.

Amount of Catalyst (g)	Conversion (wt%)	Selectivity (%)	
		MAP	PAP
-	2.3	100	-
0.05	19.8	100	-
0.10	49.4	100	-
0.15	76.9	98.2	1.8
0.25	95.0	97.8	2.2
0.35	100	95.5	4.5

[Catalyst : T6, Toluene: benzyl chloride- molar ratio: 10: 1,
Time: 1.5 h, Temperature: 110°C.]

Discussion:

It can be seen from the above table that the amount of catalyst has an imperative function in the benzylation reaction. The product yield is found to be proportional to the amount of the catalyst taken establishing that the reaction proceeds through a pure heterogeneous mechanism. The optimum catalyst amount for the benzylation reaction is taken as 0.1 g for the effective performance. Singh *et al.*[20] studied the effect of catalyst concentration on zeolite catalyst and found similar results.

IV. Influence of Substrate to Benzyl Chloride Molar Ratio

In a set of experiments, the catalytic activity for T6 system is scanned by taking different molar ratios of substrates and benzyl chloride with already optimized conditions of temperature and reaction time. The ratios are changed keeping the amount of aromatic substrate constant. Figure 4.3 shows the effect of substrate to benzyl chloride molar ratio on conversion of benzyl chloride over the three substrates.

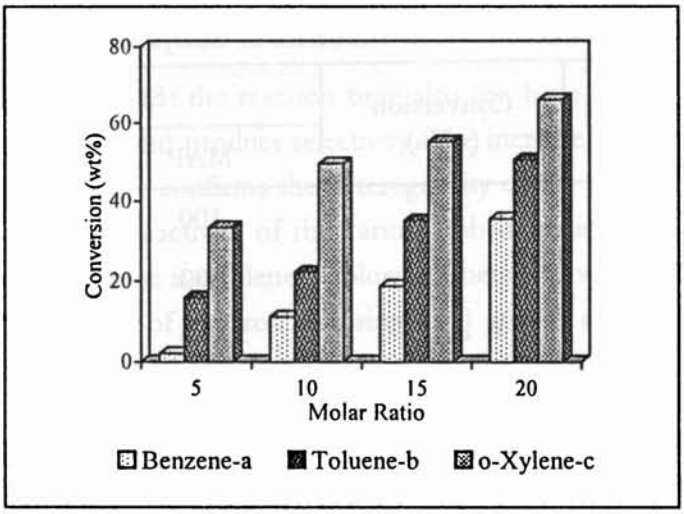

Figure 4.3
Effect of substrate to benzyl chloride molar ratio in benzylation of arenas. [Amount of catalyst: 0.1 g (T6), Temperature; Time: 80°C, 2 h (a); 110°C, 1.5 h (b); 90°C, 1 h (*c*)]

Results:

From Figure 4.3, it is apparent that the conversion of benzyl chloride is increased with the increase in the substrate to benzyl chloride molar ratio for the three substrates. i.e., increase in concentration of benzyl chloride in the reaction mixture reduce the product yield. However, at lower molar ratios, a significant amount of monoalkylted product is formed in the reaction mixture. Polyalkylated products are not observed at lower molar ratios for toluene and *o*-xylene. As the ratio changes from 10 to 15, the conversion is enhanced to a greater extent where the formation of polyalkylated products are also noticed. It is seen that the selectivity for the formation of monoalkylated product remains constant beyond the molar ratio of 10 in these cases. A higher molar ratio favours the high conversion of benzyl chloride in the case of benzene; polyalkylated products are not being formed even at a high molar ratio of 20.

Discussion:

Since the arene is taken in excess, the reaction is supposed to proceed *via* a pseudo unimolecular mechanism. The rate of the reaction, therefore, should vary with the concentration of the benzyl chloride alone. The results show that the benzylation is favoured with a lower concentration of benzylating agent. When the benzylating agent concentration is high (low arene to benzyl chloride molar ratio), there may be an enhanced poisoning effect by the alkylated products, which is strongly adsorbed on the catalyst surface[21]. This restricts further adsorption of the reactant molecules and thus reduces the conversion of benzyl chloride. The inhibition would be less significant for reaction mixtures richer in substrate concentration (high arene to benzyl chloride molar ratio), which helps to desorb the products formed from the catalyst surface easily. The observations are similar to those in benzylation of *o*-xylene over H-β [20] and toluene over H-Y[22] zeolites.

Optimized Conditions:

The substrate selectivity of the catalyst is of such an exquisite fine-tuning that it discriminates between benzene, toluene and *o*-xylene. This may be due to the different rates of chemisorption on to an inorganic solid and diffusion within the microporous solid in the absence of shape selectivity. The optimization procedure with T6 catalyst reveals that the reaction parameters have strong influence on the benzylation activity and product selectivity for V_2O_5-SnO_2 systems. The optimized reaction conditions are summarized in Table 4.4.

Table 4.4

Optimized conditions for benzylation –T6 system.

Substrate	Amount of Catalyst (g)	Molar Ratio	Reaction Temperature (°C)	Time of Reaction (h)
Benzene	0.1	15: 1	80	2
Toluene	0.1	10: 1	110	1.5
o-xylene	0.1	5: 1	90	1

We have done the optimization of the reaction parameters for V_2O_5-ZrO_2 systems following the same procedures taking Z6 as the representative. Similar trends as in the case of T6 are observed when we optimized the reaction temperature, time and molar ratio, though the Z6 system gave a slower conversion than T6. The optimized reaction conditions over Z6 system are given in Table 4.5.

Table 4.5

Optimized conditions for benzylation –Z6 system.

Substrate	Amount of catalyst (g)	Molar Ratio	Reaction Temperature (°C)	Time of Reaction (h)
Benzene	0.1	15: 1	80	3
Toluene	0.1	10: 1	110	2
o-Xylene	0.1	5: 1	100	1.5

4.2.2 Catalyst Efficiency of Different Systems

We have prepared four series of supported vanadia systems for the comparison of catalyst composition. The results and discussions are conveniently made under two groups for: (I) V_2O_5-SnO_2 series and (II) V_2O_5-ZrO_2 series. Individual metal oxides and the conventional homogeneous catalyst $AlCl_3$ were also looked for the catalytic reaction. Under optimized process parameters of temperature, time and molar ratio, the activity of all the prepared systems were tested for the benzylation of benzene, toluene and *o*-xylene. A detailed study correlating the acidity and benzylation activity of the catalyst system is also presented in this section.

I. V_2O_5-SnO_2 Series

Table 4.6 presents the results of benzylation of benzene, toluene and *o*-xylene using benzyl chloride over different vanadia promoted tin oxide systems and its sulfated series. The acid-base properties of metal oxide carriers can significantly affect the final selectivity of heterogeneous catalysts[23]. So an

attempt is made to correlate the catalytic activity with the acidic characteristics determined by different methods. Figures 4.4 to 4.6 show the correlation of benzylation activity of the systems with the acidity in benzylation of toluene. The increase in the percentage conversion is correlated with the increase in the strong acid sites (Figure 4.4) as revealed from TPD measurements. The variation in the activity of different systems also corresponds to the changes in Lewis acidity of the samples obtained by perylene adsorption studies and cumene conversion reaction (Figures 4.5 and 4.6).

Table 4.6
Activity of V_2O_5-SnO_2 systems in the benzylation of arenes.

System	Substrate						
	Benzene[a]	Toluene[b]			*o*-Xylene[c]		
	BC-C (wt%)	BC-C (wt%)	MAP -S (%)	PAP -S (%)	BC-C (wt%)	MAP -S (%)	PAP –S (%)
T0	-	10.9	100	-	18.8	100	-
T3	3.36	35.1	100	-	43.4	100	-
T6	18.8	49.4	100	-	56.9	100	-
T9	24.3	63.5	100	-	69.2	100	-
T12	30.1	74.5	98.4	1.6	75.7	98.3	1.7
T15	36.8	80.3	97.8	2.2	84.5	95.4	4.6
V	1.2	7.6	100	-	10.4	100	-
$AlCl_3$	-	76.6	83.4	16.6	92.6	67.1	32.9
ST0	10.5	25.3	100	-	38.1	100	-
ST3	22.1	43.5	100	-	49.9	100	-
ST6	31.5	51.9	100	-	78.6	97.3	2.7
ST9	60.2	94.6	95.2	4.8	100	91.2	8.8
ST12	43.6	89.5	97.6	2.4	91.8	93.5	6.5
ST15	39.5	86.0	98.5	1.5	89.3	95.6	4.4
SV	8.4	18.6	100	-	24.8	100	-

[Amount of Catalyst: 0.1 g, Temperature; Time; Molar ratio: [a] 80°C; 2 h; 15: 1, [b] 110°C; 1.5 h; 10: 1, [c] 90°C; 1 h; 5: 1.]

Results:

From the above table, it is evident that pure SnO_2 and V_2O_5 give very low conversions under the specified reaction conditions. However, satisfactory yield of diphenylmethane is obtained for most of the supported systems. An interesting observation is that only monoalkylated product is obtained in all the cases when benzene is used as the substrate. An enhanced conversion at the expense of monoalkylated product is observed in the case of toluene and *o*-xylene. The sulfated systems give comparatively higher benzyl chloride conversion for all the three substrates. Among the simple supported systems, the conversion gradually increased as the vanadia loading increased from 0 to 15%. In the case of sulfated systems the maximum activity is shown by ST9, thereafter the conversion declines. Although there is a decrease in selectivity to the monoalkyalted products in some cases, especially with sulfated systems, it is worthy to note that the selectivity in any of these cases is not going below 90%. The benzylation of aromatics over the systems in general give high yield of monoalkylated products, whereas $AlCl_3$ gives higher amounts of consecutive products. The selectivity for monoalkylated product obtained with $AlCl_3$ is 83.3 and 67.1% for toluene and *o*-xylene respectively (Table 4.6).

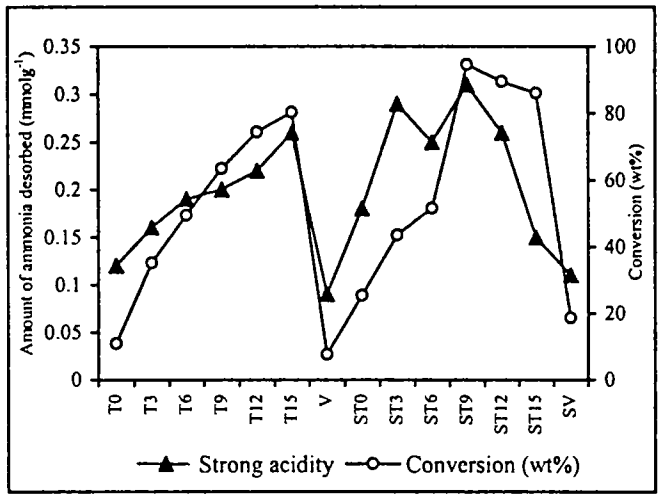

Figure 4.4
Catalytic activity correlated with the amount of strong acid sites obtained from ammonia TPD.

Figures 4.4 to 4.6 indicate that the catalytic activity of the systems ties nicely with the strong / Lewis acidity of the prepared systems. Considering the acid site distribution from the TPD measurements, the increase in the strong acid sites with increasing vanadia content is in agreement with the enhanced activity in the simple supported systems (Figure 4.4). Thus, strong acid sites may be considered to be involved in the Friedel-Crafts benzylation of arenes. Figure 4.5 shows that the catalytic activity of the system is in line with the amount of Lewis acid sites on the catalyst surface obtained from the limiting amount of perylene adsorbed. A comparison of the α-methylstyrene selectivity, which is proportional to the Lewis acidity of the systems, bolsters the above observation (Figure 4.6).

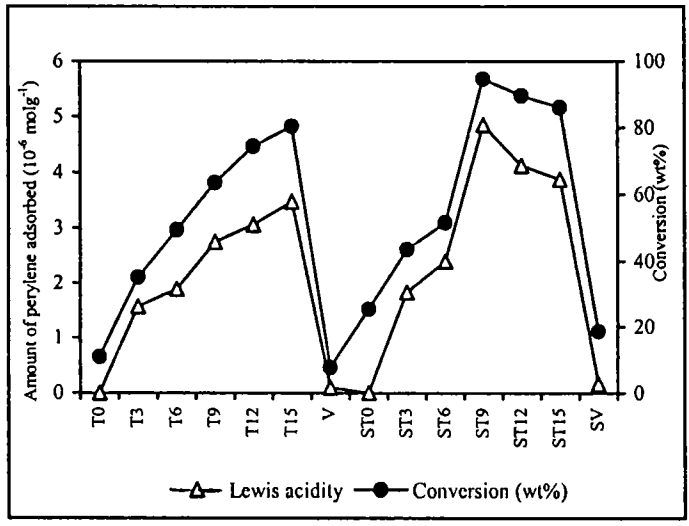

Figure 4.5
Catalytic activity correlated with the Lewis acidity determined by perylene adsorption method.

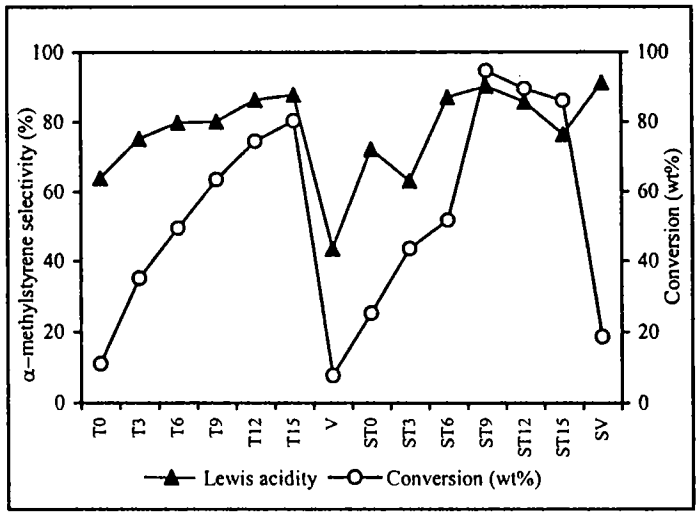

Figure 4.6
Catalytic activity correlated with α-methylstyrene- selectivity from cumene conversion reaction.

Discussion:

The benzylation over the catalysts under study is found very efficient with respect to both activity and selectivity. The impregnation of vanadia to the metal oxide support and the sulfate modification provoke a considerable synergistic effect leading to an enhanced activity. The metal oxide surface contains both Brönsted and Lewis acid sites and the above observations clearly indicate the dominating impact of Lewis acid sites for the benzylation reaction over the catalyst systems under consideration. The increased activity in the case of supported systems may be due to the enhancement of surface Lewis acidiy due to vanadia incorporation. The strength and amount of strong/Lewis sites increase by the introduction of sulfate anions leading to augmented surface acidity due to the electron withdrawing nature of sulfate groups. This explains the higher catalytic activity of the sulfated samples. Lower yields in the case of individual metal oxides are attributed to the low strength and amount of Lewis acid sites on the surface.

II. V_2O_5-ZrO_2 Series

Table 4.7 summarizes the experimental results of benzylation of aromatics with benzyl chloride over V_2O_5-ZrO_2 systems. The table also includes the results with $AlCl_3$ catalyst for comparison. Figures 4.7 to 4.9 demonstrate the correlation of catalytic performance with the surface acidity of the systems measured by different techniques. The percentage conversion is correlated with the amount of the strong acid sites (Figure 4.7) obtained from TPD measurements. Figures 4.8 and 4.9 give the comparison of the benzylation activity of different systems with the Lewis acidity obtained by perylene adsorption studies and cumene conversion reaction respectively.

Table 4.7
Activity of V_2O_5-ZrO_2 systems in the benzylation of arenes.

System	Substrate						
	Benzene[a]	Toluene[b]			*o*-Xylene[c]		
	BC-C (wt%)	BC-C (wt%)	MAP -S (%)	PAP -S (%)	BC-C (wt%)	MAP -S (%)	PAP -S (%)
Z0	-	9.5	100	-	12.6	100	-
Z3	2.5	29.5	100	-	36.4	100	-
Z6	18.1	76.1	99.3	0.7	89.3	98.4	1.6
Z9	13.8	30.9	100	-	64.7	100	-
Z12	10.1	19.4	100	-	48.1	100	-
Z15	6.8	16.7	100	-	39.2	100	-
V	1.2	7.6	100	-	10.4	100	-
$AlCl_3$	-	76.6	83.4	16.6	92.6	67.1	32.9
SZ0	26.5	100	94.6	5.4	100	91.2	8.8
SZ3	19.1	44.8	100	-	67.9	100	-
SZ6	41.5	88.6	98.2	1.8	100	93.7	6.3
SZ9	32.2	68.7	100	-	89.1	95.1	4.9
SZ12	23.6	37.5	100	-	71.8	98.6	1.4
SZ15	16.5	32.3	100	-	59.7	100	-
SV	8.4	18.6	100	-	50.3	100	-

[Amount of Catalyst: 0.1 g, Temperature; Time; Molar ratio: [a] 80°C; 3 h; 15: 1; [b] 110°C; 2 h; 10: 1, [c] 100°C; 1.5 h; 5: 1]

Results:

From Table 4.7, it is clear that although the pure metal oxides (ZrO_2 and V_2O_5) show comparatively negligible activity, the effect of benzylation activity of vanadia impregnated as well as its sulfated analogues is very dramatic. However, the reaction is found to be much slower when compared to the V_2O_5-SnO_2 systems. In this series, the highest conversion is given by catalyst with 6% vanadia loading among simple loaded and sulfate-modified systems. In the case of supported system, as the percentage loading increases up to 6%, the benzylation activity also increases and thereafter it declines.

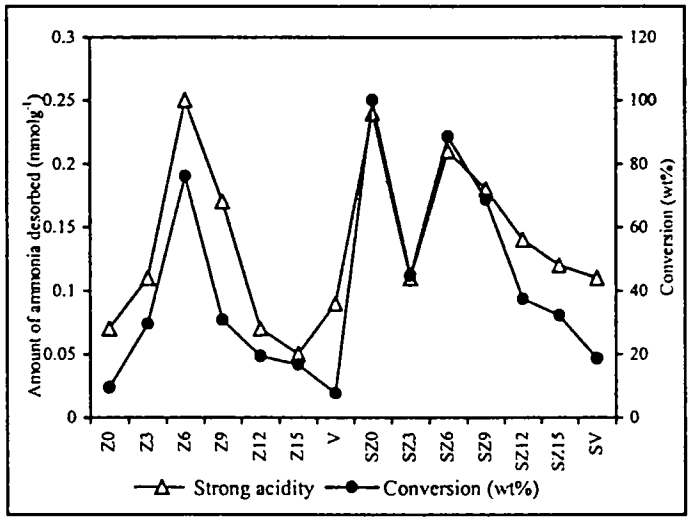

Figure 4.7
Catalytic activity correlated with the amount of strong acid sites determined from ammonia TPD method.

In sulfated series the trend is the same with much enhanced conversion with an exception of SZ0 giving 100% conversion of the benzylating agent. The selectivity for MAP is not going below 90% even with the catalyst systems, which give 100% conversion of benzyl chloride. A complete conversion of benzyl chloride is observed in the case of SZ0 and SZ3. Figure 4.7 reveals that percentage conversion for different systems are in agreement with the amount of strong acid sites as measured by the ammonia TPD method.

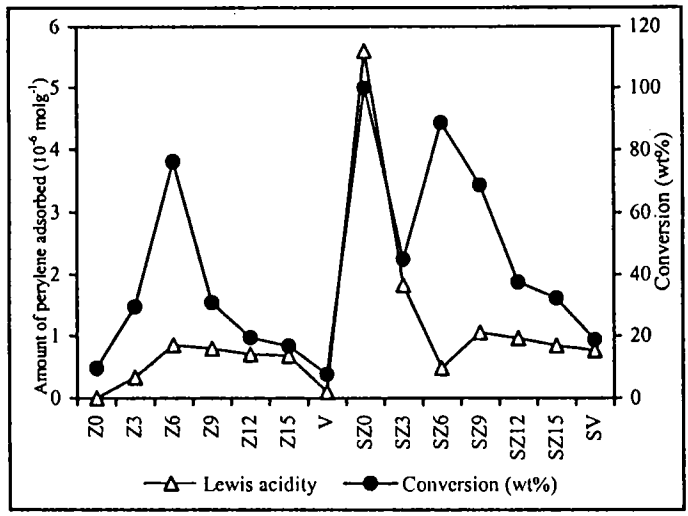

Figure 4.8
Catalytic activity correlated with the Lewis acidity determined from perylene adsorption.

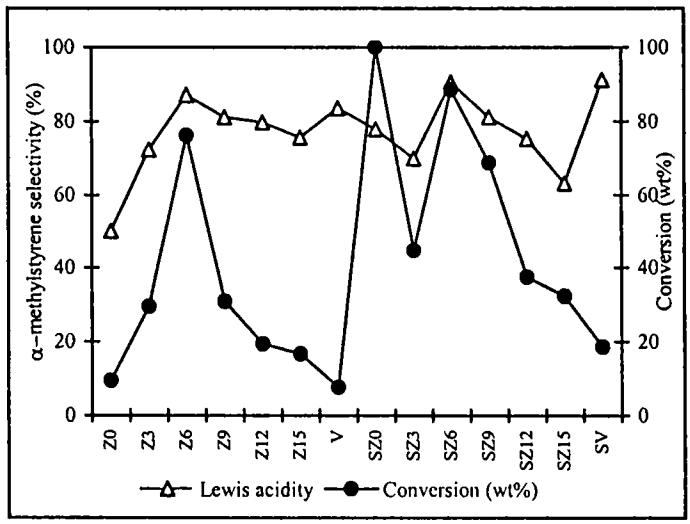

Figure 4.9
Catalytic activity correlated with α-methylstyrene selectivity obtained from cumene conversion reaction.

A good correlation could be sketched between the benzylation activity of different systems and the Lewis acidity values determined from the perylene adsorption data (Figure 4.8). The Lewis acidity trend predicted by α-methylstyrene selectivity from cumene conversion reaction also parallels the reactivity observed with the increase in the percentage of vanadium oxide (Figure 4.9).

Discussion:

The lower catalytic activity of these systems compared to the V_2O_5-SnO_2 systems may be due to the lower amount of acidity on the catalyst surface. This can be also related to the slower desorption processes of the product molecules from the surface of the catalysts. The highest conversion in the case of system with 6% vanadia loading may be attributed to the high surface area of the system as well as the greater surface acidity. The high conversion with lower monoalkylation selectivity given by SZ0 is agreeing with the high surface acidity created on zirconia surface by sulfate modification. Attempts to find a correlation between the catalytic activity and the acidic properties showed that surface Lewis acidity of the systems facilitates the benzylation reaction as in the case of V_2O_5-SnO_2 systems.

4.2.3 Structural Stability of the Catalysts

An important requisite for a heterogeneous catalyst for a better catalytic performance is the stability of its active sites under the reaction conditions. Major causes that can lead to the deactivation of a catalyst include the disruption of the crystalline structure and changes in chemical composition during the reaction. In benzylation reactions with benzyl chloride, the by-product formed is HCl, the interaction of which can leach out metal cation, from the metal oxide catalyst. This will destroy the structural stability of the system. The leached metal cation in solution can enhance the reaction rate too whereby the pure heterogeneity of the reaction is lost. Another factor that seriously affect the stability of the catalyst is the moisture sensitivity, one of the disadvantages of the commonly practiced homogeneous catalysts in Friedel-Crafts reactions. The regeneration of the catalyst after several repeated reaction runs also gives an idea

about the stability of the system towards a particular reaction. Thus, it becomes important to test the influence of moisture adsorption, metal leaching on the catalytic activity and regeneration ability of the present systems. T6 and Z6 were taken as the representative samples for these investigations.

I. Effect of Moisture

In order to study the effect of moisture on the catalyst, the catalysts stored in a desiccator saturated with water vapour at room temperature for 48 h were used for benzylation of toluene. The reactions were carried out at 110°C for 3 h by taking toluene/benzyl chloride molar ratio of 10. For comparison, parallel runs were conducted using fresh catalyst. The results are presented in Figure 4.10.

Another method was also adopted to check the influence of moisture on the catalytic activity; a known amount of water was injected to the reaction mixture before starting the reaction. The effect was also studied by changing the concentration of water in the mixture. The results obtained for benzylation of toluene over T6 system is given in Figure 4.11.

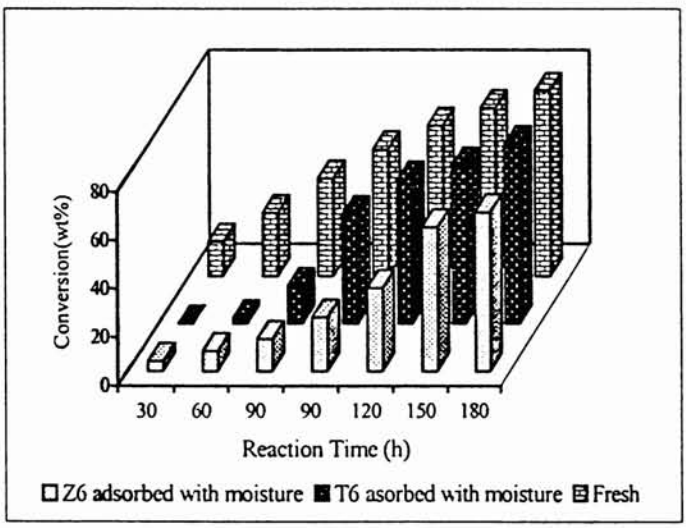

Figure 4.10
Benzylation of toluene –Influence of moisture.
[Amount of catalyst: 0.1 g, Toluene: benzyl chloride molar ratio: 10:1, Time: 3 h]

Results:

From Figure 4.10, it can be seen that the percentage conversion of benzyl chloride gradually increases as a function of reaction time and reaches 76.5% after a reaction time of 3 h, when fresh catalyst is used. The conversion is negligible even after one hour of reaction in presence of the moisture-adsorbed catalyst. Thus existence of an induction period for the benzylation reaction due to the presence of adsorbed moisture on the catalyst is clear and the period is found to be higher for T6 system than Z6 system.

However, after the induction period, reaction proceeds with almost the same rate. When we add water to the reaction mixture (Figure 4.11), the induction period is found to increase and the period is prolonged with the concentration of the water. In contrast to the observation with adsorbed water vapour on the catalyst surface, the presence of water in the reaction mixture reduces the reaction rate considerably even after the induction period. The conversion never reaches the same value as that of the fresh catalyst without moisture in this case.

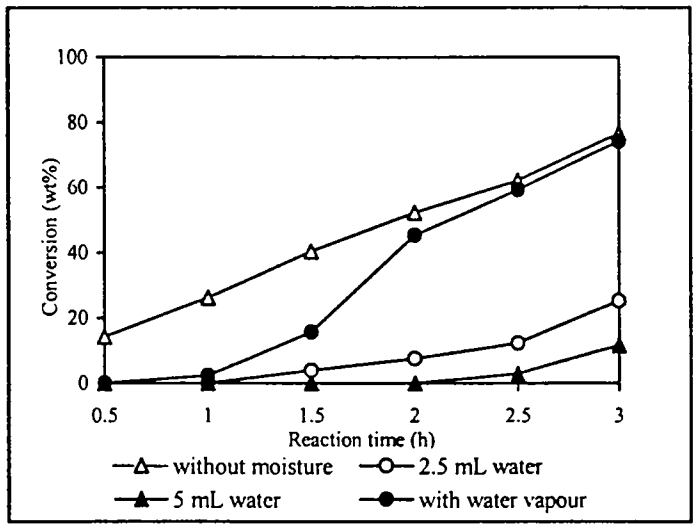

Figure 4.11
Influence of moisture in benzylation of toluene.

Discussion:

From the above results, it is unambiguous that there is a time period for which the catalyst is inactive towards the reaction, when it is adsorbed with moisture. The moisture gets adsorbed on the active sites on the catalyst surface and prevents the interaction of benzyl chloride molecule with these sites. Induction period is the time required for replacing the adsorbed moisture by the reactants to start the catalytic reaction[24]. Once the sites are freed from moisture, they are active towards the desired reaction. Thus, though the moisture initially blocks the active sites, after the induction period, the reaction rate is as in the case of fresh catalyst itself. Hence we conclude that the catalyst systems are active even in the presence of moisture.

However, the presence of added water in the reaction mixture results in a loss of catalytic activity. The benzyl chloride molecule finds it difficult to replace the water molecule when the concentration of water in the reaction mixture is high. This may be correlated with the reversible transformation of the Lewis acid sites into Brönsted acid sites upon exposure to moisture. A lowering of the percentage conversion goes together with a decrease in the Lewis acidity. From these observations it can be inferred that the Lewis acid sites are catalyzing the reaction. The induction period due to the presence of moisture was also reported by Choudhary *et al.*[24] over Si-MCM-41 supported Ga_2O_3 and In_2O_3. The negative effect of the presence of water in the benzylation mixture on the catalytic activity is also reported for Ga-Mg-hydrotalcite anionic clay[25].

II. Effect of Metal Leaching

An ever-popular subject of concern associated with solid acid catalysts is the leaching phenomenon and the question about the true nature of catalytic reaction (homogeneous or heterogeneous). Leaching can occur during a catalyzed reaction without an induction period and the nature of reaction may gradually change from heterogeneous to homogeneous without any indications in the reaction profile[26]. To prove the heterogeneous character of the reactions, the solid catalyst was removed by filtration after a particular time from the

reaction mixture at the reaction temperature. The filtration with filter paper at room temperature is avoided since by this the homogeneous active species readsorb completely on the catalyst particles on cooling, some remaining centers may effectively adsorb on the filter paper[27]. The mother liquor is then monitored for further reaction.

The leaching probability of T6 and Z6 were measured in benzylation of toluene at the refluxing temperature of 110°C. The catalyst was removed from the reaction mixture after I h and the filtrate was again subjected for reaction at the same conditions for one more hour. The reaction was monitored at regular intervals of 30 minutes. The results are shown in Table 4.8. The filtrate was further subjected to qualitative analysis for testing the presence of leached metal ions.

Table 4.8
Effect of metal leaching in benzylation of toluene with benzyl chloride.

Catalyst	Time (min)	Conversion (wt%)	Selectivity (%)	
			MAP	PAP
T6	60	30.7	100	-
	90*	32.1	100	-
	120*	32.5	100	-
Z6	60	54.8	97.4	2.6
	90*	56.9	98.5	1.5
	120*	57.2	98.6	1.4

[Amount of catalyst: 0.1 g, Temperature110°C, Toluene: benzyl chloride molar ratio: 10: 1]
(*The filtrate is tested for leaching after 1 h reaction.)

Results:

Table 4.8 shows the benzyl chloride conversion obtained in benzylation of toluene at 110°C. The conversion at the time of catalyst filtration is 30.7% and 54.8% for T6 and Z6 respectively. After the removal of the catalyst,

though the reaction is continued for one more hour, no noticeable change in the conversion is obtained in both the cases. The qualitative analysis of the filtrate also confirmed the absence of any metal ion in the filtrate.

Discussion:

From the results it is clear that metal ions are not leaching from the metal oxide surface during benzylation reaction. The qualitative analysis also supports this observation implying the chemical identity and structural stability of the systems. The investigations also reveal the true heterogeneous nature of the reaction over supported vanadia catalysts. Deng *et al.*[26] studied the stability of V, Ti and Si containing catalysts in the oxidation of different substrates. According to them, leaching strongly depends on the reaction conditions. Leaching of vanadium has been reported in liquid phase oxidation reactions over titanium oxide supported vanadium oxide[28], molecular sieves[29], V-doped zeolite[30].

III. Catalyst Regeneration

One of the major objectives guiding the development of solid acid catalysts includes the easy separation of final products from the reaction mixture and efficient catalyst recovery. The recycling of the used catalyst for the same reaction is also a measure of catalyst structural stability. The reusability of our catalyst systems was subjected to investigation, taking T6 and Z6 as representative systems. The catalyst was removed by filtration from the reaction solution, washed thoroughly with acetone and then dried and calcined at 550°C for 5 h. The same catalyst was again used for carrying out subsequent runs under similar reaction conditions. To check the structural change of the catalyst during the reaction, the XRD spectrum of the used catalyst was taken. Table 4.9 displays the conversion of benzyl chloride obtained for toluene benzylation using regenerated T6 catalyst during a five times recycling process. The same catalyst after regeneration is used in the reaction after each cycle. The XRD of the reused catalysts after recycling are given in Figures 4.12 and 4.13.

Table 4.9
Regeneration of catalyst

No: of cycles		1	2	3	4	5
Conversion (wt%)	T6	49.4	47.5	44.1	35.6	23.9
	Z6	39.6	38.4	26.2	19.5	15.9

[Amount of catalyst: 0.1 g, Time: 1.5 h, Toluene: Benzyl chloride molar ratio: 10: 1, Reaction temperature: 110°C.]

Results:

Though negligible, a decrease in conversion of benzyl chloride is observed after the third recycling of the catalyst (Table 4.9). Figures 4.12 and 4.13 show that the crystalline phases as well as the intensities of the peaks remain intact even after the reaction for both T6 and Z6 systems.

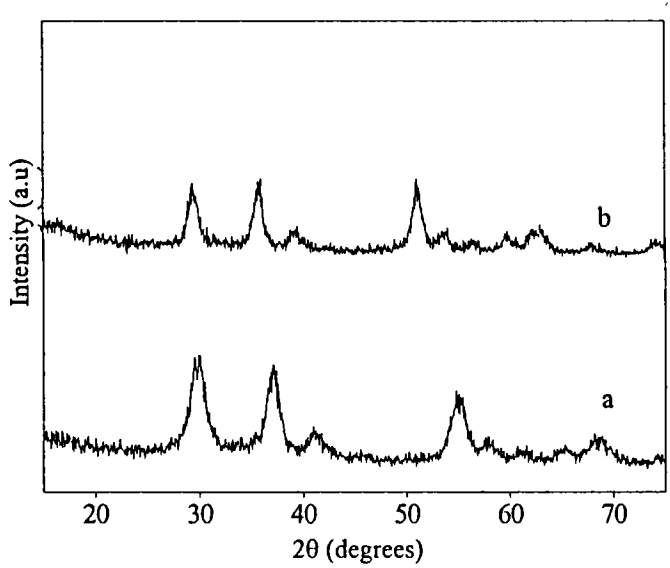

Figure 4.12
XRD patterns of T6 system (a) After reaction (b) Before reaction.

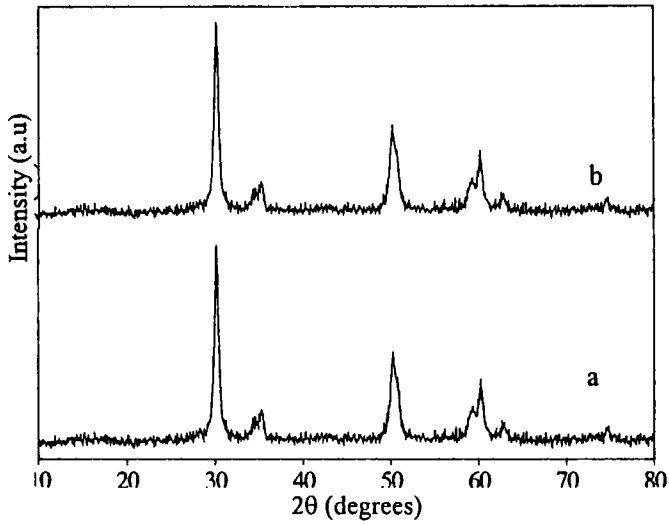

Figure 4.13
XRD patterns of Z6 system (a) After reaction (b) Before reaction

Discussion:

The XRD patterns of the used catalysts after regeneration retained all the distinctiveness of the fresh catalyst, symptomatic of the fact that there is no structural collapse of the system forming different crystalline phases during the reaction. No remarkable fall in the activity could be monitored even after three successive regenerations. However, the decrease becomes more pronounced as the cycles are repeated. This suggests that the catalyst systems are resistant to rapid deactivation in benzylation reactions.

Mechanism of the Reaction

Different authors have proposed explanations of the origin of active sites in solid acid catalysts for the benzylation of aromatics. On investigating the benzylation of anisole over 'Clayzic', Barlow *et al.*[31] reported that the reaction is catalyzed by Bronsted sites below the temperature, 40°C. An equilibrium exists between Bronsted and Lewis sites in the temperature range

40-65°C and above that the reaction proceeds under Lewis acid sites predominantly. While studying the benzylation of methylbenzenes, Rhodes *et al.*[32] found that the enhanced catalytic activity of adsorbed $ZnCl_2$ can be related to the increased accessibility of the Lewis sites to the reactant molecule. Ghorpade *et al.*[33] also showed that the Lewis acidity of $CuCr_{2-x}Fe_xO_4$ spinel catalysts is mainly responsible for the good catalyst performance in benzylation of benzene.

The catalytic activity studies on different vanadia promoted systems and its sulfated analogues also suggest the involvement of Lewis acid sites in the reaction. The progressive increase in the catalytic activity is well correlating with the amount of strong acid sites on the catalyst surface measured by TPD. The agreement of the results with the amount of Lewis acidity of the catalysts from two different techniques i.e, perylene adsorption and cumene cracking reaction also reinforce the suggestion. The detrimental influence of moisture confirms the dominating role of Lewis acidity in deciding the catalytic activity (Figure 4.10).

Friedel-Crafts alkylation reaction is an aromatic electrophilic substitution reaction in which a carbocation is formed by the complexation of alkyl halide with the catalyst. The carbocation then attacks the aromatic species whereby the reaction proceeds further. The formation of carbocation is thus an important step in the reaction mechanism. The benzyl chloride molecule may be polarized at the Lewis acidic centers present on the catalyst surface, which facilitates carbocation formation. The attack of the alkylating moiety on the aromatic ring then results in the formation of the diphenylmethane derivatives. The nonpolar nature of the substrate molecules also supports the formation of the electrophilic species by adsorption of benzyl chloride molecule on the catalyst surface. A plausible mechanism for the reaction can be represented schematically as shown in Figure 4.14.

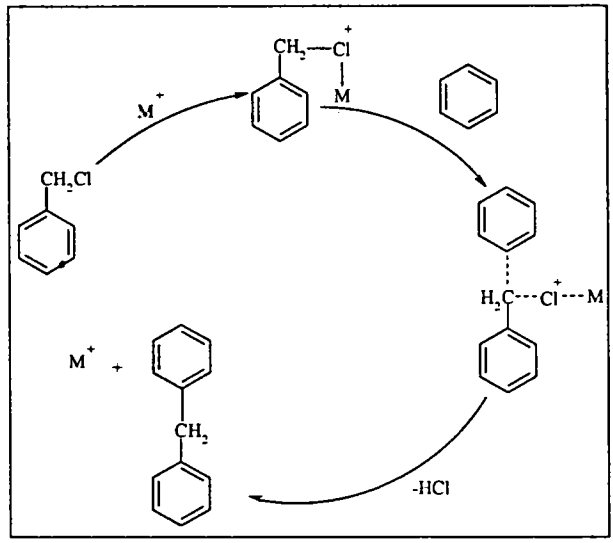

Figure 4.14
Mechanism of Friedel-Crafts benzylation using benzyl chloride showing the active involvement of Lewis acid sites.

4.3 CONCLUSIONS

The conclusions of the investigation can be summarized as:

- All the catalyst samples prepared by supporting vanadia on SnO_2 and ZrO_2 and its sulfated series serve as efficient Friedel-Crafts alkylation catalysts giving good activity and selectivity.
- Reaction variables such as temperature, reaction time substrate to alkylating agent molar ratio and catalyst concentration are critical factors influencing the activities of the systems. The activity of the systems is found to be increasing with the number of electron donor methyl groups present on the aromatic substrates.
- The yields obtained by the vanadia-based systems are comparable or even more when compared to those of the reported catalysts. The reaction is also found to be clean with negligible formation of polyalkylated products.
- The acidity plays an important role in the Friedel-Crafts alkyaltion. The evidences of the present study lead to the assumption that benzylation

reaction under the optimized conditions occurs exclusively on the surface Lewis acid sites.

- The results on the structural stability of the catalysts show that the vanadia-based systems are reusable and resistant to rapid deactivation in benzylation reaction even in the presence of moisture.

ꕥ ꕥ ꕥ

REFERENCES

1. G. A. Olah, "*Friedel-Crafts Chemistry*", Wiley, New York, 1973.
2. J. H. Clark, S. R. Cullen, S. J. Barlow and T. W. Bastock, *J. Chem. Soc. Perkin Trans.*, 2 (1994) 1117.
3. B. M. Chodhary, M. L. Kantam, M. Sateesh, K. K. Rao and P. L. Santhi, *Appl. Catal. A. Gen.*, 149 (1997) 257-264.
4. Y. Izumi, N. Natsume, H. Takamine, J. Tamoki and K. Urabe, *Bull. Chem. Soc. Jpn.*, 62 (1989) 2159.
5. A. Cornelis, C. Dony, P. Lazlo and K. M. Nsunda, *Tetrahedron Lett.*, 34 (1993) 529.
6. E. Herdeieckerhoff and W. Sutter, *Ger. Pat.*, 1 051 864 (1959).
7. J. Haydn and H. Holzrichter, *Ger. Pat.*, 1 089 168 (1960).
8. R. Stroh, J. Ebersberger, H. Haberland and W. Hahn, *Ger. Pat.*, 1 051 271 (1959).
9. R. Van Helden, C. F. Kohl and H. D. Scharf, *Brit. Pat.*, 1 110 029 (1968).
10. J. Strerte, *Clay Caly Miner.*, 34 (1986) 658.
11. G. D. Yadav, T. S. Thorat and P. S. Kumbhar, *Tetrahedron Lett.*, 34 (1993) 69.
12. P. Lazlo and A. Mathy, *Hel. Chem. Actal*, 70 (1987) 577.
13. P. Botella, A. Corma, J. M. Lopez Nieto, S. Valencia and R. Jacquot, *J. catal.*,195 (2000) 161.
14. T. Cseri, S. Bekassy, F. Figueras and S. Rizner, *J. Mol. Catal. A. Chem.*, 98 (1995) 101-107.
15. J. H. Clark, A. P. Kybett, D. J. Macquarrie, S. J. Barlow and P. Landon, *J. Chem. Soc. Chem. Comm.*, (1989) 1353.

16. S. J. Barlow, J. H. Clark, M. R. Darby, A. P. Kybett, P. Landon and K. Martin, *J. Chem. Researcher(s)*, (1991) 74.

17. N. Y. He, B. -L. Bao and Q. –H. Xu, *Stud. Surf. Sci.Catal.*, 105 (1997) 85.

18. N. Y. He, B. -L. Bao and Q. –H. Xu, *Chin. J. Chem.*, 15 (1997) 42.

19. B. Coq, V. Gourves and F. Figueras, *Appl. Catal. A.*, 100 (1993) 63.

20. A. P. Singh, B. Jacob and S. Sugunan, *Appl. Catal. A. Gen.*, 174 (1998) 51-60.

21. D. Rohan, C. Canaff, E. Romeafin and M. Guismet, *J. Catal.*,177 (1998) 2743.

22. S. Jun and R. Ryoo, *J. Catal.*, 195 (2000) 237-243.

23. K. Tanabe, *"Solid acids and bases and their catalytic properties"*, Academic Press, New York (1970) 103.

24. V. R. Choudhary, S. K. Jana and B. P. Kiran, *J. Catal.*, 192 (2000) 257-261.

25. V. R. Choudhary, S. K. Jana and A. B. Mandale, *Catal. Lett.*, 74 (2001) 95-98.

26. Y. Deng, C. Lettmann and W. F. Maier, *Appl. Catal. A. Gen.*, 214 (2001) 31-45.

27. D. L. Vanoppen, D. E. Devos, M. J. Genet, P. G. Rouxet and P. A. Jacobs, *Angew. Chem.*, 107 (1995) 635.

28. D. Rohan and B. K. Hodnett, *Appl. Catal. A. Gen.*, 151 (1997) 409.

29. B. J. Whittington and J. R. Anderson, *J. Phys. Chem.*, 97 (1993) 1032.

30. M. J. Haanepen, A. M. Elemans-Mehrimg and J. H. C. van Hoff, *Appl. Catal. A. Gen.*, 152 (1997) 203.

31. S. J. Barlow, T. W. Bastock, J. H. Clark and S. R. Cullen, *Tetrahedron Lett.*, 34 (1993) 3339.

32. C. N. Rhodes and D. R. Brown, *J. Chem. Soc. Faraday Trans.*, 89 (1993) 1387.

33. S. P. Ghorpade, V. S. Darshane and S. G. Dixit, *Appl. Catal. A. Gen.*, 166 (1998) 135-142.

Chapter 5

Beckmann Rearrangement of Cyclohexanone Oxime

ABSTRACT

The Beckmann rearrangement of cyclohexanone oxime is an important industrial reaction for the production of ε-caprolactam. The catalytic efficiency of the supported vanadia systems in the gas-phase Beckmann rearrangement of cyclohexanone oxime is presented in this chapter. The effect of various reaction parameters like temperature, flow rate, duration of run etc. are investigated in detail. The cyclohexanone oxime conversion and the ε-caprolactam selectivity are found to be dependent on the reaction conditions and the surface properties of the catalyst systems. The results of the investigation suggest that the acidity of the supported vanadia systems plays an imperative role in the activity and selectivity in the reaction. The total acidity is found to be the deciding feature of the activity in the case of V_2O_5-SnO_2 series while it is the medium strength acid site that has the major function in favor of V_2O_5-ZrO_2 systems.

5.1 INTRODUCTION

ε-Caprolactam, an important intermediate for the production of nylon-6, is industrially produced by the liquid-phase Beckmann rearrangement of cyclohexanone oxime using highly concentrated sulfuric acid as catalyst[1]. This process has several disadvantages such as the production of large amount of undesired ammonium sulfate as by product, and corrosion and environmental problems caused by the use of fuming sulfuric acid. To resolve these problems, a number of attempts have been made to use solid acid catalysts including

silica-alumina[2], tantalum oxides[3] and zeolites[4,5], in the vapour-phase Beckmann rearrangement of cyclohexanone oxime. Compared with the conventional liquid-phase method, this is an eco-friendly route since there is no inevitable salt formation (ammonium sulfate)[6]. However, the catalytic lifetime of these systems are too short and therefore they cannot be used in chemical industries. Furthermore, the yield of ε- caprolactam is insufficient and the deterioration of catalytic activities with time is substantial[3].

From the present work, we have found that supported vanadia catalysts and its sulfated analogues function as efficient heterogeneous catalysts for vapour-phase Beckmann rearrangement of cyclohexanone oxime. No report has been found so far in literature of the Beckmann rearrangement, catalyzed by vanadia-based systems. In this chapter, we report the observations of our study on vapour-phase Beckmann rearrangement of cyclohexanone oxime with V_2O_5-impregnated SnO_2 and ZrO_2 along with its sulfated series and attempt to rationalize the results on the basis of its physico-chemical properties.

5.2 BECKMANN REARRANGEMENT OF CYCLOHEXANONE OXIME

The vapour-phase Beckmann rearrangement of cyclohexanone oxime was carried out in a conventional fixed bed reactor and the experimental procedure is given in section 2.6.2 of Chapter 2. The reaction always yielded many products of which the major one estimated and identified by GC as ε-caprolactam. Among the various side products formed, only cyclohexanone was separately estimated while all the remaining minor products were set aside under one banner 'others' during the calculation of selectivities. The catalytic activity was expressed as the % conversion of cyclohexanone oxime and the selectivity for a product is expressed as the amount of the particular product divided by the total amount of products multiplied by 100. The percentage yield of ε-caprolactam and cyclohexanone were calculated by multiplying the total conversion with the selectivity of the particular product and then dividing by 100.

The results and discussion are conveniently done under two main headings; (I) Process optimization (II) Performance of different systems. The sulfated series of the samples were also tested for the catalytic activities. A comparative study was made with the pure oxide systems in each case.

5.2.1. Process Optimization

Vapour-phase reaction runs were performed under atmospheric pressure using benzene as the solvent. The process is extremely sensitive to reaction conditions. A detailed investigation on the optimization of the process is discussed below.

I. Effect of Temperature

Table 5.1 and Figure 5.1 show the effect of reaction temperature in the vapour-phase Beckmann rearrangement of cyclohexanone oxime. The reaction temperature was varied from 150 to 300°C for the rearrangement reaction over the representative sample, T6. The conversion of cyclohexanone oxime and selectivities for ε-caprolactam and cyclohexanone are given in the table. The variation of the caprolactam yield and the product selectivities with the increase in temperature is clear from the figure.

Table 5.1
Influence of reaction temperature on the
Beckmann rearrangement of cyclohexanone oxime.

Temperature (°C)	Conversion (wt%)	Selectivity (%)		
		ε-Caprolactam	Cyclohexanone	Others
150	8.6	28.3	-	71.7
200	55.8	42.2	3.5	54.3
250	83.4	80.4	12.5	7.1
300	100	55.1	39.6	5.3

[Amount of catalyst: 0.5 g (T6), Flow rate: 5mL h^{-1}, Reaction time: 2 h]

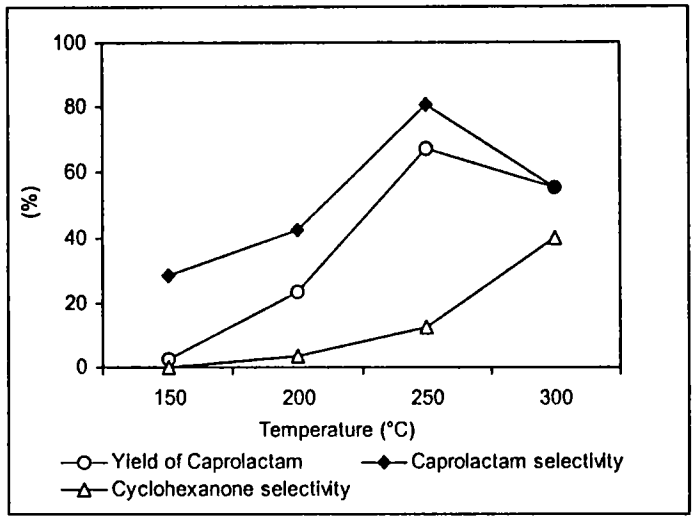

Figure 5.1
Influence of reaction temperature on the
Beckmann rearrangement of cyclohexanone oxime.

Results:

From the above table, it is clear that temperature has a marked influence on Beckmann rearrangement and the reaction proceeds effectively above 200°C. The reaction rate is found to increase drastically as we increase the temperature from 150 to 300°C. At 300°C, the conversion of oxime is 100% with ε-caprolactam selectivity 55.18%. The caprolactam selectivity is found to be maximum at 250°C; it decreases at higher temperature while there is a gradual increase in the cyclohexanone selectivity with temperature. At the high temperatures, the colour of the product solution is found to be yellow. The figure shows that the maximum yield of caprolactam with high selectivity is at 250°C. Further increase in temperature, though increases the catalytic activity, and does not improve either the caprolactam yield or its selectivity.

Discussion:

The promotional effect of temperature in vapour-phase Beckmann rearrangement of cyclohexanone oxime has been reported over various solid

acids such as silica-tantalum oxide[3], mesoporous molecular sieves[7,8] and titanium silicates[9]. Ushikubo *et al.*[3] reported the maximum conversion of cyclohexanone oxime and selectivities for caprolactam and cyclohexanone at 300°C over Ta_2O_5 with 4.3 wt% of SiO_2. The caprolactam selectivity decreased at higher temperatures. The suggested reason was an increased rate of side reaction at higher temperatures. Ko *et al.*[7] studied the temperature effect in Beckmann rearrangement over Al-MCM-41 molecular sieve in the range 300-400°C. They reported a remarkable increase in the oxime conversion with temperature from 300 to 400°C for a 4 h reaction run where the caprolactam selectivity varied only slightly. At temperatures above 370°C, the product selectivities were practically constant suggesting the high stability of caprolactam without successive reactions to yield side products. Murthy *et al.*[8] varied the temperature from 200-390°C in the rearrangement over Ti-SAPO-11 catalyst and found that the oxime conversion and lactam selectivity increase with temperature up to 390°C. Above 390°C, a lower selectivity was noticed for caprolactam which was accounted by the decomposition of caprolactam on the catalyst surface. Thankaraj *et al.*[9] reported an increase in conversion of oxime and selectivity for lactam production over titanium silicate with increase in the temperature in the range 250-350°C.

By comparing these results with the observations of the present work, we can conclude that the temperature has a positive effect on Beckmann rearrangement over vanadia- supported metal oxides in the range 150-250°C. Above 250°C, though the oxime conversion increases, a lower selectivity for ε-caprolactam is noticed and is expected to be due to the decomposition of caprolactam on the catalyst surface. The increase in cyclohexanone selectivity with reaction temperature suggests an increased rate of side reactions at higher temperature. The change in the colour of the product solution at higher temperature also supplements the formation of side products. Thus an optimum temperature of 250°C is selected for further investigations of the rearrangement reaction.

II. Effect of Feed Rate

A series of experiments were conducted at reaction temperature 250°C where the flow rate was varied from 4 to 7 mL h^{-1}. A typical activity profile of Beckmann rearrangement as a function of feed rate over T6 system is given in Figure 5.2. Table 5.2 presents the yield of caprolactam and cyclohexanone along with the product selectivities.

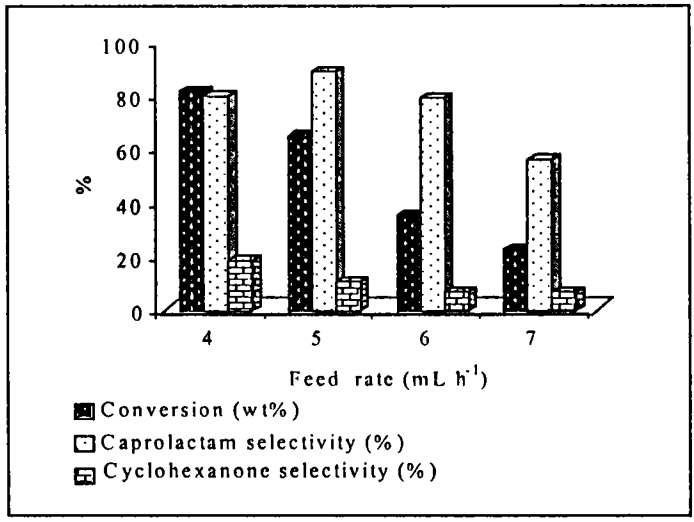

Figure 5.2
Effect of feed rate on oxime conversion and product selectivities.
[Amount of catalyst: 0.5 g (T6), Temperature: 250°C, Reaction time: 2 h]

Table 5.2
Effect of feed rate on yield and product distribution.

Feed rate (mL h^{-1})	Yield (wt%)		Selectivity (%)		
	ε-Caprolactam	Cyclohexa-none	ε-Caprolactam	Cyclohexa-none	Others
4	65.6	15.6	80.4	19.6	-
5	57.9	6.5	89.3	10.7	-
6	28.1	2.5	78.5	7.4	14.1
7	13.7	1.7	56.7	7.2	36.1

[Amount of catalyst: 0.5 g (T6), Temperature: 250°C, Reaction time: 2 h]

Results:

The feed rate has a highly pronounced detrimental effect on cyclohexanone oxime conversion and lactam selectivity as can be seen from Figure 5.2 and Table 5.2. The conversion decreases from 82.3% to 23.9% as the flow rate is increased from 4 to 7 mL h^{-1}. The selectivity of caprolactam shows an initial increase at 5 mL h^{-1}, reaches a maximum of 89.3% and then decreases. The cyclohexanone selectivity declines as we change the flow rate from 4 to 5 mL h^{-1} and it remains almost constant when the feed rate is varied from 6 to 7 mL h^{-1}. Table 5.2 clearly shows that both the caprolactam and cyclohexanone yields constantly decrease with the increase in the flow rate.

Discussion:

The feed rate alters the contact time and at high feed rate, the encounter of the reactants and products with catalyst surface will be less compared to that at lower feed rates. Thus a lower conversion is resulted at higher feed rates. The cyclohexanone oxime conversion and caprolactam yield decrease continuously due to the decrease in contact time of the oxime with the active sites of the catalysts. However, the selectivity to caprolactam is maximum (89.3%) at a flow rate of 5 mL h^{-1} suggesting an optimum velocity of the feed or caprolactam formation. The caprolactam selectivity decreases at higher flow rates indicating the possibility of competitive adsorption among the reactant and product molecules over the catalysts surface. The selectivity and yield of cyclohexanone decrease with the flow rate. This suggests that the contact time is insufficient for the side reactions to take place at higher feed rates. Thankaraj *et al.*[9] made similar observations on the effect of feed rate in vapour-phase Beckmann rearrangement of cyclohexanone oxime over titanium silicates.

III. Effect of Time On Stream

Another set of experiments was carried out to establish the stability of the systems to the deactivation processes. The performance of the reaction for a continuous 5 h run tests the susceptibility of deactivation of the catalyst. The products were collected and analyzed after every one hour. Figure 5.3 presents

the time course of Beckmann rearrangement over T6 and Z6 systems where cyclohexanone oxime conversion is plotted as a function of reaction time. The selectivity pattern obtained for caprolactam and cyclohexanone are separately shown in Figures 5.4 and 5.5. Table 5.3 compares the deactivation property of the reported catalysts with that of the newly developed catalyst.

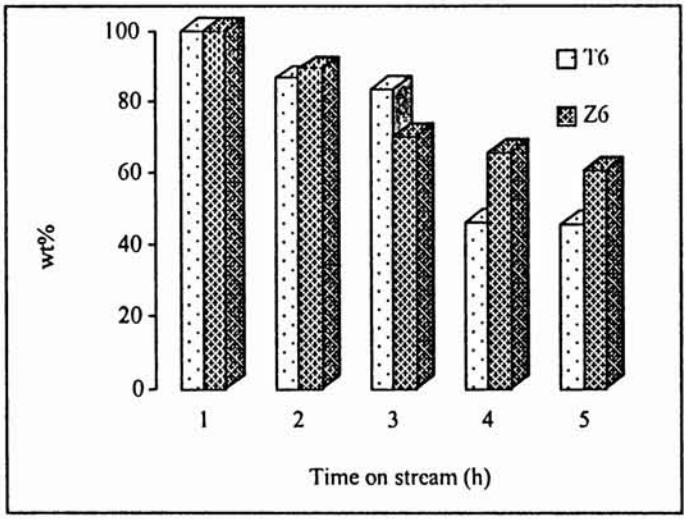

Figure 5.3
Oxime conversion as a function of time on stream (TOS)
over T6 and Z6 systems.
[Amount of catalyst: 0.5 g, Temperature: 250°C, Feed rate: 5 mL h^{-1}]

Results:

From Figure 5.3, it is seen that the activity of both T6 and Z6 systems continuously declines with reaction time. Initially the conversion is close to 100% in both the cases, but decreases to about 50% after five hours on stream. After 5 h run of the reaction, the conversion of oxime is found to be 45.6 % for T6, while it is 60.8% in the case of Z6. Though the oxime conversion decreases more or less with reaction time, no significant change in lactam selectivity is observed over the two catalyst systems.

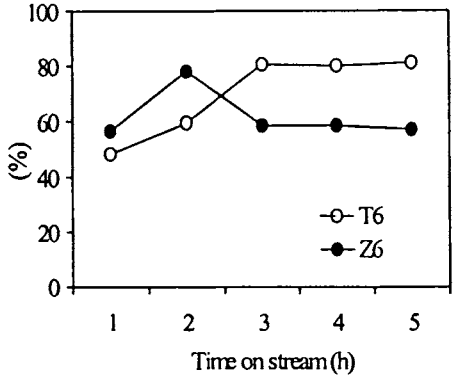

Figure 5.4
Caprolactam selectivity
with time on stream.

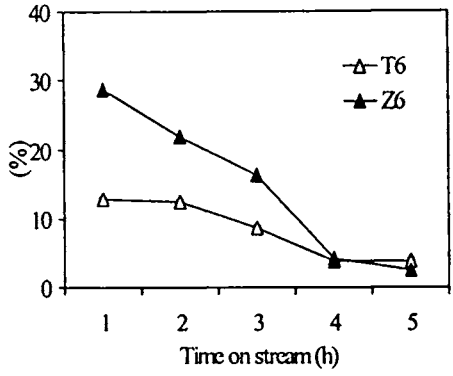

Figure 5.5
Cyclohexanone selectivity
with time on stream.

The selectivity to caprolactam changes during the first two hours and remains constant thereafter. However, the tin system shows a better selectivity (81%) to caprolactam even after 5 h when compared to the zirconia system, where the selectivity is 57.1%. The selectivity to cyclohexanone remains almost constant for the 5 h on stream in spite of the declining oxime conversion. All the catalysts are light coloured originally but after the reaction it turned black or grey.

Table 5.3
Comparison of time on stream study of various catalysts with T6 and Z6.

Catalyst system	Time on stream (h)	Oxime Conversion (wt%)	Lactam selectivity (%)
Al_2O_3/FSM-16[18]	5	17.5	47.1
B_2O_3/Al_2O_3[6]	10	62.3	89.2
Al-MCM-41[7]	15	39.8	72.6
SAPO-11[8]	5	76.9	43.7
ZSM-5 (90)[9]	5	69.6	48.9
ZSM-5 (300)[9]	5	90.9	64.6
B_2O_3/SiO_2[14]	4	11.1	35.6
T6	5	45.7	81.0
Z6	5	60.8	57.1

Discussion:

The lowering of activity with time on stream is a common problem associated with all reported solid acid catalyst type in vapour-phase Beckmann rearrangement. The literature suggests that zeolites with very high Si: Al ratios[9,10] are more resistant to this effect. Two main reasons have been suggested to account for the loss of activity: coke formation[11-13] and/or irreversible adsorption of basic by-products[4,5,14]. The adsorption of basic products is reported to be common with zeolites, while the reason for boria impregnated alumina catalysts is coke deposition[12,13]. These two mechanisms of loss of activity are classified as catalyst poisoning, since they involve the physical blocking of the active sites. This will be distinguished from deactivation, which will be defined as the loss of catalytic activity due to restructuring of the catalyst.

Mao *et al.*[6] studied the deactivation of B_2O_3/ TiO_2-ZrO_2 catalyst in the rearrangement and proposed coke deposition as the main reason for the decreased activity as the catalyst can be completely regenerated by burning off the coke. Curtin *et al.*[15] reported the details of study of loss of activity observed on a series of modified alumina catalysts, with particular emphasis to B_2O_3/ Al_2O_3. They showed that the oxime conversion after a period of 30 h on stream declined to almost zero. The selectivity to caprolactam increased initially, remained steady for approximately 10 h and declined significantly thereafter. The selectivity to cyclohexanone remained constant during the investigation. The selectivity pattern of caprolactam was suggested to be consistent with the role of dimerization and polymerization reaction in the mechanism of coke formation. Shouro *et al.*[16] investigated the desorption and reaction behaviour of ε-caprolactam, cyclohexanone oxime and the by-products of Beckmann rearrangement (5-cyanopentane, 5-cyano-pent-1-ene, cyclohexanone and 2-cyclohexene-1-one) on FSM-16 in detail and elucidated the formation mechanism of the by-products. Similar results were obtained by Corma and co-workers on H-Na-Y Zeolites[17].

Thus, observation of the present investigation on the effect of time on stream is consistent with the possibility of coke formation over the catalyst surface, which can be correlated with the significant decrease of oxime conversion over 5 h. The coke deposition may be either due to the eventual formation of carbonaceous deposits resulting from the reaction between the side products or arises from the polymerization of caprolactam[18]. There is ample evidence from present and other reported works that coke deposition and re-adsorption of basic reaction by-products play a part in catalyst poisoning in vapour-phase Beckmann rearrangement of cyclohexanone oxime. However, the Z6 system is found to be more resistant to deactivation process when compared to T6 system. A better selectivity to caprolactam of about 80% is given by T6 system even after 5 h of reaction time. The comparison of the deactivation susceptibility with other reported system reveals that these catalysts certainly lose their activity more rapidly than the zeolite catalyst with high Si: Al ratio[9], but are far better in its resistance to deactivation compaired to other metal oxide solid acids.

5.2.2 Performance of Different Catalyst Systems

A comparative evaluation of the catalytic activity of various vanadia catalysts in the vapour-phase Beckmann rearrangement is given in this section. Under optimized conditions of reaction temperature 250°C and flow rate 5 mL h^{-1}, all the prepared systems were tested for activity over a reaction time of 2 h. The performance of V_2O_5-SnO_2 and V_2O_5-ZrO_2 is given separately along with its sulfated sequences. An attempt to correlate the surface acidity and physical properties with the catalyst efficiency is done. A comparison between the two types of systems is also made to examine the support effects.

I. V_2O_5 - SnO_2 Systems

Table 5.4 shows the catalytic activities of various V_2O_5-SnO_2 catalysts together with its sulfated analogues for the vapour-phase Beckmann rearrangement.

Figure 5.6 presents the changes in acidity values obtained by ammonia TPD method with vanadia loading in the case of V_2O_5-SnO_2 systems. Table 5.6 gives the correlation between the oxime conversion and acidity values for the sulfate-modified catalysts. Table 5.7 summarizes the influence of surface area and pore volume on the product selectivity pattern over V_2O_5-SnO_2 systems.

Table 5.4
Activity of V_2O_5-SnO_2 systems in the vapour-phase Beckmann rearrangement of cyclohexanone oxime.

Catalyst	Conversion (wt%)	Selectivity (%)		
		ε-Caprolactam	Cyclohexanone	Others
T0	29.5	26.8	-	73.2
T3	62.7	42.5	7.8	49.7
T6	86.6	59.3	12.4	28.3
T9	90.4	78.8	19.0	2.2
T12	92.4	72.8	8.9	18.3
T15	96.5	58.7	7.2	34.1
V	13.3	40.8	-	59.2
ST0	59.3	25.5	1.9	72.6
ST3	94.7	32.2	8.7	59.1
ST6	98.4	48.7	9.6	41.7
ST9	100	61.2	4.3	34.5
ST12	96.7	56.5	4.2	38.1
ST15	90.7	57.7	1.4	42.1
SV	61.3	22.1	16.7	61.2

[Amount of catalyst: 0.5 g, Temperature: 250°C, Flow rate: 5 mL h^{-1}, TOS: 2 h]

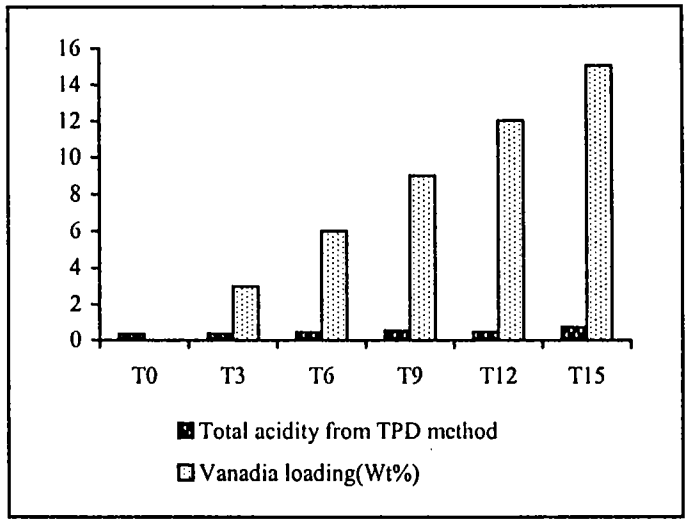

Figure 5.6
Variation of acidity with vanadia loading in unmodified V_2O_5-SnO_2 systems.

Table 5.5
Correlation of acidity values of sulfated systems from TPD measurements with activity.

Catalyst	ST0	ST3	ST6	ST9	ST12	ST15
Oxime conversion (wt%)	59.3	94.7	98.4	100	96.7	90.7
Total Acidity (mmol g^{-1})	0.85	1.07	1.19	1.37	1.06	1.33

Results:

From Table 5.4, it is clear that SnO_2 and V_2O_5 in the pure form are much less active in the Beckmann rearrangement than the supported catalysts. In the vanadia impregnated systems, as the loading of vanadia increases, the oxime conversion is found to increase. The maximum activity is shown by T15 system where the conversion is 96.5%. The selectivity of V_2O_5-SnO_2 catalysts is found to increase with vanadia loading, reaches a maximum and then decreases. The maximum selectivity obtained is 78.8% for system with 9% V_2O_5 loading.

Table 5.6
Influence of surface properties on the selectivity pattern of products.

Catalysts	Surface properties		Selectivity (%)	
	Surface area ($m^2 g^{-1}$)	Pore volume ($cm^3 g^{-1}$)	ε-Caprolactam	Cyclohexanone
T0	25	0.023	26.8	-
T3	49	0.054	42.5	7.8
T6	61	0.062	59.3	12.4
T9	83	0.081	78.8	19.0
T12	72	0.072	72.8	8.9
T15	67	0.064	58.7	7.2
ST0	79	0.081	25.5	1.9
ST3	87	0.086	32.2	8.7
ST6	95	0.096	48.7	9.6
ST9	118	0.109	61.2	4.3
ST12	89	0.092	56.5	4.2
ST15	74	0.072	57.7	1.4

All the sulfated systems show much higher activity than the simple loaded systems. However, the selectivity for caprolactam is comparatively low in these systems. The maximum activity is shown by ST6 where the conversion reaches 100%. From Figure 5.6, the total acidity of the supported systems is found to increase as the weight % of vanadia is increased from 0 to 15. Figure 5.6 and Table 5.5 reveal that the cyclohexanone conversion is in agreement with the total acidity of the catalyst measured by ammonia TPD method. Table 5.6 shows that the caprolactam and cyclohexanone selectivity depend strongly on the surface area and pore volume of the catalyst. The selectivity reaches maximum for the catalyst with highest surface area and pore volume.

Discussion:

The relationship between acidic properties and catalytic performance in vapour-phase Beckmann rearrangement has been studied by many researchers.

Curtin *et al.*[15] investigated the effect of amount of intermediate acid sites from ammonia TPD measurements on the activity and selectivity of the Beckmann rearrangement using B_2O_3/ Al_2O_3 catalysts. They reported that the excellent selectivity for caprolactam was exhibited by B_2O_3/ Al_2O_3 catalysts with largest concentration of intermediate strength acid sites. Ushikubo *et al.*[3] reported for the H-ZSM-5 zeolite modified by B_2O_3 that lactam selectivity improves with the increase of the ratio of weak acid sites to strong acid sites[19]. It has been reported that a relatively strong acid site (H_0<-5.6) of B_2O_3/ SiO_2 is responsible for the formation of caprolactam[20].

The results of our investigation on the catalytic performance of different V_2O_5-SnO_2 systems conclude that the presence of vanadium oxide on tin oxide surface significantly increases the catalyst performance in vapour-phase Beckmann rearrangement. The conversion of oxime depends on the total acidity of the systems while the selectivities for caprolactam and cyclohexanone seem to be effected by the surface area and the pore volume of the catalysts. The good agreement between the TPD results and conversion data suggests that all the surface acid sites irrespective of its strength, take part in the rearrangement reaction. The results disagree with the earlier reports where the active sites for cyclohexanone oxime conversion in Beckmann rearrangement were reported as intermediate strength acid sites.

The dependence of selectivity to the surface properties implies that there are some factors other than the surface concentration of acid sites, which determine the catalytic activity. The diffusion rate of caprolactam could depend on the pore structure and the fine pores seem to fill the effective role of diffusion. Similar observations were made by Ushikubo *et al.*[3]

The sulfated samples give higher conversion only at the expense of caprolactam selectivity. This may be due to the substantial amount of strong acid sites on the surface of sulfated systems. Oxime and/ or caprolactam seem to adsorb tightly on such strong acid sites and the Beckmann rearrangement is prevented from proceeding.

II. V_2O_5-ZrO_2 Systems

The catalytic performance of V_2O_5-ZrO_2 catalysts with various vanadia loadings and its sulfated analogues were examined at 250°C. The oxime conversion and the selectivity pattern obtained for the reaction is given in Table 5.7. Table 5.8 shows the correlation between the conversion and the amount of intermediate strength acid sites from TPD measurement.

Table 5.7
Activity of V_2O_5-ZrO_2 systems in the vapour-phase Beckmann rearrangement of cyclohexanone oxime.

Catalyst	Conversion (wt%)	Selectivity (%)		
		ε-Caprolactam	Cyclohexanone	Others
Z0	25.3	37.7	-	62.3
Z3	68.7	72.3	7.2	20.5
Z6	89.4	78.1	15.4	6.5
Z9	78.5	84.1	11.1	4.8
Z12	70.2	90.1	7.2	2.7
Z15	66.7	94.0	1.2	4.8
V	13.3	40.8	-	59.1
SZ0	100	32.5	12.7	54.8
SZ3	85.3	45.0	14.9	40.1
SZ6	100	38.1	13.6	48.3
SZ9	97.2	56.2	8.9	34.9
SZ12	90.8	61.3	4.6	34.1
SZ15	86.5	79.4	2.9	17.7
SV	61.3	22.2	16.7	61.1

[Amount of catalyst: 0.5 g, Temperature: 250°C, Flow rate: 5 mL h^{-1}, TOS: 2 h]

Results:

Table 5.7 shows that the cyclohexanone oxime conversion increases with vanadia loading, reaches a maximum and then decreases in the case of simple loaded as well as sulfated systems. From Table 5.8, it is clear that the amount

of medium strength acid sites is in correlation with the percentage of oxime conversion. The maximum conversion is obtained in the case of catalyst with 6% vanadium oxide loading in the sulfated and non-sulfated series. SZ0 showed 100% conversion at the expense of selectivity to caprolactam. However, the selectivity pattern obtained in the case of V_2O_5-ZrO_2 catalysts is quite different from that of V_2O_5-SnO_2 catalysts. Here, as the vanadia loading increases, the caprolactam selectivity increases and the lactam selectivity is maximum when the vanadia content is 15 wt%. Here again, the sulfated systems showed an enhanced conversion with low selectivity to caprolactam.

Table 5.8
Correlation of amount of medium strength acid sites from TPD measurements with activity.

Catalyst	Z0	Z3	Z6	Z9	Z12	Z15
Oxime conversion (wt%)	25.3	68.7	89.4	78.5	70.2	66.7
Medium Acidity (mmol g^{-1})	0.13	0.21	0.46	0.36	0.28	0.23
Catalyst	SZ0	SZ3	SZ6	SZ9	SZ12	SZ15
Oxime conversion (wt%)	100	85.3	100	97.2	90.8	86.5
Medium Acidity (mmol g^{-1})	0.67	0.28	0.63	0.55	0.31	0.27

Discussion:

Comparing the acidity pattern and the conversion percentage, it is clear that the intermediate strength acid sites are responsible for the reaction. The results are similar to the observations of Curtin *et al.*[15]. The selectivity pattern of caprolactam suggests that its formation is controlled by amount of vanadia present in the system rather than by the surface area or pore volume. The enhanced activity of the sulfated system is an indication of the presence of very strong acid sites over the catalyst surface. The increase in conversion may be due to an increased concentration of medium strength acid sites, created by sulfate modification, while the low selectivity is attributed to the presence of strong acid sites on the catalyst surface.

5.3 CONCLUSIONS

The following key points emerge from this study:

- Vapour-phase Beckmann rearrangement of cyclohexanone oxime occurres smoothly on the desirable and facile sites on the molecular structures of vanadia-based catalysts.
- Reaction variables such as temperature, feed rate and reaction time have strong influence on the oxime conversion and caprolactam selectivity.
- Good initial activity and high selectivity for caprolactam can be observed over both V_2O_5-SnO_2 and V_2O_5-ZrO_2 catalysts. However the oxime conversion declined significantly whereas the selectivity remained steady during 5 h reaction run. V_2O_5-ZrO_2 showed more resistance to catalytic deactivation than V_2O_5-SnO_2 systems.
- The acidity plays an important role in the Beckmann rearrangement. In the case of V_2O_5-SnO_2 systems the conversion of oxime is governed by the total acidity of the systems while the amount of medium strength acid sites are the active sites on V_2O_5-ZrO_2 catalysts.
- The selectivity pattern of caprolactam and cyclohexanone is in accordance with the surface area and pore volume of the catalyst when SnO_2 is the support. The selectivities are not at all influenced by the surface properties in the case of ZrO_2 based catalysts.

* * * * *

REFERENCES

1. J. E. Kent and S. Reigel, *Handbook of Industrial Chemical.*, 8th Edn., Vin Nostrand, New York, 1983, p. 402.
2. O. Immanuel, H. H. Scwarz, H. Starcke and W. Swooden, *Chem. Ing. Tech.*, 56 (1973) 612.
3. T. Ushikubo and K. Wada, *J. Catal.*, 148 (1994) 138.
4. P. S. Landis and P. B. Venuto, *J. Catal.*, 6 (1966) 245.

5. A. Aucejo, M. C. Burguet, A. Corma and V. Fornes, *Appl. Catal. A. Gen.*, 22 (1986) 187.
6. D. Mao, G. Lu, Q. Chen, Z. Xie and Y. Zhang, *Catal. Lett.*, Vol. 77, No. 1-3 (2001) 119-124.
7. A. N. Ko, C. C. Hung, C. W. Chen and K. H. Ouyang, *Catal. Lett.*, Vol. 71, No. 3-4 (2001) 219-224.
8. K. V. V. S. B. S R. Murthy, M. Chandrakala, S. J. Kulkarni and K. V. Raghavan, *Ind. J.Chem. Tech.*, Vol. 8 (2001) 368-370.
9. A. Thankaraj, S. Sivasanker, and P. Ratnasamy, *J. Catal.*, 137 (1992) 252-256.
10. S. Sato, N. Ishii, K. Hirose and S. Nakamura, *Stud. Surf. Sci. Catal.*, 28 (1986) 755.
11. Y. Izumi, S. Sato and K. Urabe, *Chem. Lett.*, 1649 (1983).
12. S. Sato, S. Hasebe, H. Sakurai, K. Urabe, and Y. Izumi, *Appl. Catal.*, 29 (1987) 107.
13. S. Sato, K. Urabe and Y. Izumi, *J. Catal.*, 102 (1986) 49-108.
14. M. C. Burguet, A. Aucejo and A. Corma, *Can. J. Chem. Eng.*, 64 (1987) 994.
15. T. Curtin, J, B. Mc Monagle, M. Ruwett and B. K. Hodnett, *J. Catal.*, 142 (1993) 172-181.
16. D. Shouro, Y. Ohya, S. Mishima and T. Nakajima, *Appl. Catal. A. Gen.*, 214 (2001) 59-67.
17. A. Corma, H. Garcia and J. Primo, *Zeolites*, 11 (1991) 593.
18. A. Ravve, "*Organic Chemistry of Macromolecules*", Dekker, New York (1967).
19. BASF. *Ger. Patent*, No. 1,227 028 (1967).
20. B.-Q. Xu, S.-B. Cheng, S. Jiang and Q.-M. Zhu, *Appl. Catal. A Gen.*, 188 (1999) 361.

Chapter 6

Selective Oxidations of Aromatics

ABSTRACT

Catalytic oxidation is widely employed in the manufacture of bulk chemicals from aromatics and more recently, as an environmentally attractive method for the production of fine chemicals. The present chapter and the results therein show a great versatility of vanadia-based catalysts in selective oxidation reactions of organic compounds. The chapter is divided into two sections. The first section depicts the liquid-phase oxidation of cyclohexanol using hydrogen peroxide as the oxidant over different vanadia systems and the effects of various operation parameters on the catalytic activity. The vapour-phase oxidative dehydrogenation of ethylbenzene was used to probe the reactivity of surface vanadium oxide. Various reaction parameters have been shown to direct the reaction selectively to styrene production, the results of which are presented in the second section. Both the reactions were found to be structure sensitive and the tetrahedral surface vanadium species played a vital role in the enhancement of the selective oxidation activity. An effort was made to relate the catalytic activity with the structure of the samples determined by different spectroscopic methods.

SECTION 1
OXIDATION OF CYCLOHEXANOL TO CYCLOHEXANONE

6.1 INTRODUCTION

Partial oxidation of cyclohexanol to cyclohexanone is extensively used as an important step in industrial processes for the production of polyamides, nylon 6,6, urethane foams, adipic acid, lubricating additives, etc[1]. The selective

formation of cyclohexanone without any by-products by a one-step process therefore will have great advantages economically and /or energetically. The oxidation and hydroxylation of organic compounds using molecular oxygen are not in common practice either in the laboratory or in the industry. Hydrogen peroxide is found to be a superior alternative as it is an efficient oxidizing agent, which yields water and oxygen only on decomposition[2,3]. Recently, many interesting liquid-phase oxidation reactions have been reported using hydrogen peroxide as co-oxidant over various heterogeneous catalysts. For example, liquid-phase benzene oxidation catalyzed by heteropolyacid systems[4,5], copper supported on metal oxides[6] and ion-impregnated MCM-41[7]. Wide ranges of heterogeneous catalysts such as metal oxides[8-10], molecular sieves[11,12], heteropolyacids[13], clays[14,15] and spinels[16] have been used for the liquid-phase hydroxylation of phenol. The oxidation of cyclohexanol to cyclohexanone using hydrogen peroxide as co-oxidant over vanadium containing heteropolyacids[17] is also reported.

The vanadia-based systems appear as promising catalysts, which are active and selective in various types of oxidation reactions of organic compounds comprising oxidative dehydrogenation, and reactions with the formation of oxygenated products[18]. Vanadium oxide catalysts in combination with various promoters are widely used for the selective oxidation of organic compounds[19]. In the present study, liquid-phase catalytic cyclohexanol oxidation has been attempted under a variety of reaction conditions over supported vanadium oxide catalysts using hydrogen peroxide as the oxidant. In this catalytic reaction, the surface structure of vanadium oxide species is found to exert a profound influence on the catalytic activity and selectivity. Therefore the nature of the active sites involved in the formation of selective oxidation product, as elucidated from spectroscopic techniques (FTIR, DR UV-VIS, ^{51}V NMR) will also be considered.

6.2 LIQUID-PHASE OXIDATION OF CYCLOHEXANOL

The oxydehydrogenation of cyclohexanol to cyclohexanone was probed in liquid-phase with the vanadia catalysts, where hydrogen peroxide was used as the

co-oxidant. The experiments were done and the products were analyzed by the procedures given in section 2.6.2 of Chapter 2. The reactions were carried out at different reaction temperatures with various cyclohexanol to hydrogen peroxide volume ratios and in a variety of solvents in order to optimize the reaction conditions. Furthermore, the reaction was performed by varying the concentration of hydrogen peroxide and solvent and the duration of reaction run. The only product identified by GC analysis was cyclohexanone for all the systems. Therefore the selectivity obtained was 100% in all the cases. The catalytic activity is expressed as the percentage conversion of cyclohexanol.

The observations of the present investigation and the possible explanation of the results are presented under two categories; I) Process optimization II) Performance of different catalyst systems. A plausible mechanism for the reaction is also proposed at the end of this section.

6.2.1 Process Optimization

Cyclohexanol oxidation carried out in liquid-phase under atmospheric pressure is found to be extremely sensitive to the variation in reaction conditions. Thus various experiments have been made to study the effect of operating parameters such as reaction temperature, time, cyclohexanol to hydrogen peroxide volume ratio, nature and concentration of solvent etc. for V_2O_5-SnO_2 and V_2O_5-ZrO_2 systems separately. The results of the observations are presented in the following part.

I. Effect of Solvent

It has been reported in several articles that the liquid-phase oxidation of alcohols are sensitive to the nature of the solvent used[20-22]. Therefore we employed different solvents such as water, methanol, isopropanol, acetonitrile and dioxane for the reaction. The influence of the solvent on the cyclohexanol conversion over T6 and Z6 systems is summarized in Figure 6.1. The reactions were carried out at 80°C for 2 h with cyclohexanol to hydrogen peroxide volume ratio 5. The volume of the solvent was fixed to be 5 mL.

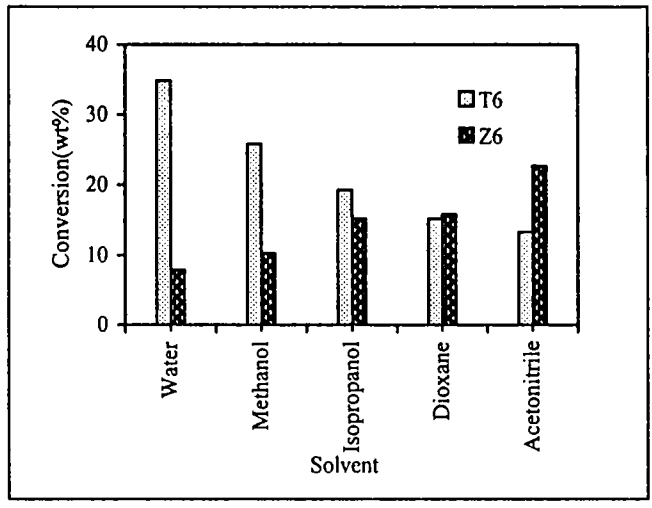

Figure 6.1
Influence of solvent on cyclohexanol oxidation reaction.
[Amount of catalyst: 0.1 g, Temperature: 80°C, Cyclohexanol/ H_2O_2 volume ratio: 5]

Results:

The catalytic reaction over T6 shows much higher conversion when water and methanol are used as the solvent. The conversion gradually decreases as the solvent is changed from isopropanol to acetonotrile. When dioxane is used as the solvent, the conversion is found to be in between that of isopropanol and acetonitrile. Thus, among all the solvent tested, water is found to be the best solvent for T6 system, which gives a conversion of 35% under the given reaction conditions. For Z6 system, the situation is found to be reversed. Acetonitrile is established to be an ideal solvent for Z6 system, with which the maximum conversion is obtained, (22.7%) whereas the conversion is only 7.9% with water.

Discussion:

The highest activity of T6 system with water as solvent can be ascribed to the strong adsorption of cyclohexanol on the catalyst surface in this solvent, which is driven by the non-ideality of water-alcohol solution[23]. It is also noticeable that the activity of the system varies with the polarity of the solvent.

As the polarity of the solvent increases, the conversion is also found to increase[20]. Among the different solvents studied the polarity is in the order, water > methanol > isopropanol > dioxane > acetonotrile. The cyclohexanol conversion also follows the same order as evident from Figure 6.1. The Z6 system shows an opposite effect with the polarity of the solvents. The maximum conversion obtained with acetonotrile indicates that solvent effect on different support materials will not be the same. Thus water is selected as the solvent for reactions with V_2O_5-SnO_2 systems whereas acetonitrile for further studies with V_2O_5-ZrO_2 systems.

II. Effect of Reaction Temperature

A set of experiments was done using T6 and Z6 systems for studying the influence of temperature. The reaction temperature was varied from 60 to 140°C with cyclohexanol to hydrogen peroxide volume ratio 5. The reactions were done in 5 mL of solvent (water for T6 and acetonitrile for Z6). The results are furnished in Figure 6.2.

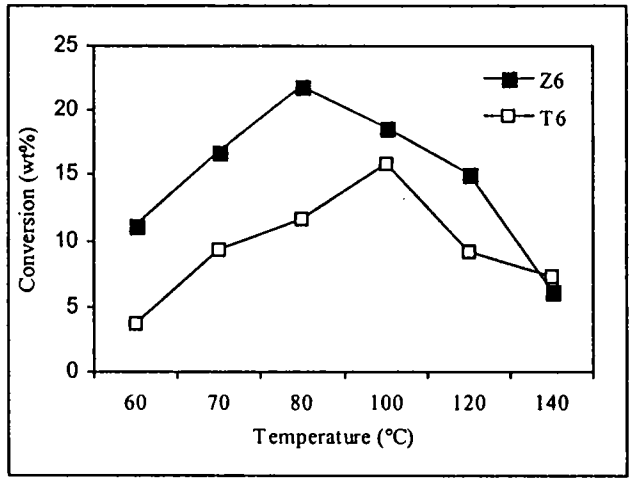

Figure 6.2
Effect of temperature on cyclohexanol oxidation reaction.
[Amount of catalyst: 0.1 g,, Cyclohexanol/ H_2O_2 volume ratio: 5, Solvent: 5 mL]

Results:

A gradual increase of conversion with reaction temperature, as usually sensible, is not observed here. The percentage conversion of cyclohexanol initially increases, reaches a maximum value and then declines for T6 as well as Z6 systems. However, the temperature, which gives the highest cyclohexanol conversion, is different for the two systems. For T6 system, the most favourable reaction temperature is found to be 100°C where as it is 80°C for Z6 system. As the temperature is increased above these values, the conversion is significantly reduced for both the systems.

Discussion:

The results show that the conversion of cyclohexanol is suppressed at higher reaction temperatures. This can be explained by the fact that higher temperature always favours the decomposition of hydrogen peroxide to molecular oxygen[24]. As the temperature is increased, the evaporation of the solvent along with the degree of decomposition of the hydrogen peroxide enhances and the net result is the decrease in cyclohexanol conversion. The observation of the decrease in percentage conversion of cyclohexanol with increasing temperature also suggests that the activation energy for hydrogen peroxide decomposition is lower than that for the selective oxidation of cyclohexanol[25].

III. Effect of Reaction Time

An appropriate reaction time is the main assurance for a perfect reaction. For optimizing the reaction time for the cyclohexanol oxidation, typical runs were carried out over T6 and Z6 with previously optimized conditions of temperature and solvent for 4 hours with cyclohexanol to hydrogen peroxide volume ratio, 5. The filtrate was collected from the reaction mixture at regular intervals of one hour for GC analysis. Figure 6.3 illustrates the conversion of cyclohexanol as a function of time.

Results:

From Figure 6.3, it becomes clear that the cyclohexanol conversion increases initially and after a particular time period, it remains almost a constant for both the systems. The maximum conversion of 34.5% for T6 system is reached in the first 1.5 h of reaction run and no detectable change is noticed by increasing the reaction time further. In the case of Z6 system, a higher reaction time of 2 h is required to achieve appreciable conversion of cyclohexanol.

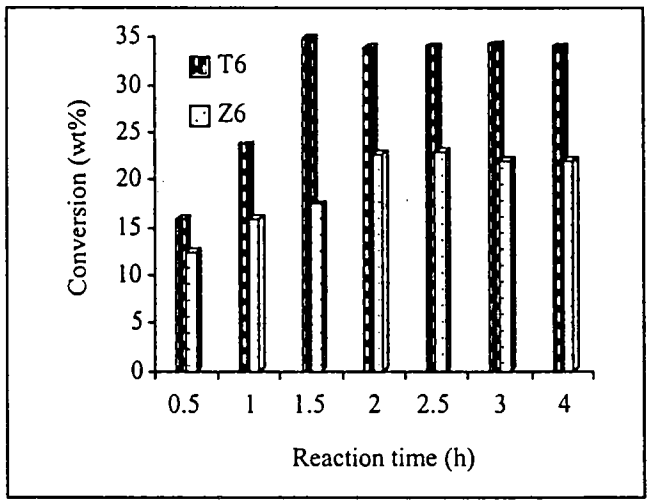

Figure 6.3
Effect of reaction time on cyclohexanol oxidation reaction.
[Amount of catalyst: 0.1 g, Cyclohexanol/ H_2O_2 volume ratio: 5, Solvent: 5 mL, Temperature: 100°C (T6); 80°C (Z6)]

Discussion:

The results show that an optimum reaction time is needed to get substantial cyclohexanol conversion. After a particular time period, the activity of the surface sites practically stops and thereafter the conversion remains the same with further increase in reaction time. This change in activity pattern may be attributed to the poisoning of the surface sites by the reaction products, which prevents the active sites from further reaction[26].

IV. Effect of Cyclohexanol to Hydrogen Peroxide Volume Ratio

Figure 6.4 depicts the selective oxidation activities of T6 and Z6 as a function of volume of hydrogen peroxide in the reaction mixture. The reactions were carried out under previously optimized conditions. Different volume ratios were selected keeping the amount of cyclohexanol as 5 mL and changing the volume of hydrogen peroxide from 1 to 5 mL.

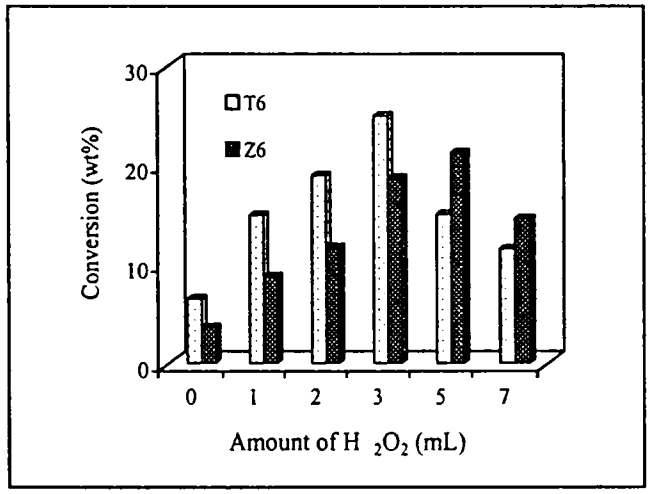

Figure 6.4
Variation of cyclohexanol conversion with amount of H_2O_2.
[Amount of catalyst: 0.1 g, Time; Solvent; Temperature: 1.5 h, 5 mL water, 100°C (T6) 2 h, 5 mL acetonitrile, 80°C (Z6)]

Results:

From the figure, it is found that the cyclohexanol conversion is sensitive to the variation in volume ratio of the two reactants. The cyclohexanol conversion in presence of hydrogen peroxide, is higher when compared to that in the absence of the oxidant. However, as the volume of hydrogen peroxide is increased from 1 to 7 mL, the conversion is also increases gradually and reaches a maximum value. Thereafter further addition of the oxidant significantly reduces the conversion percentage. The trend is similar for T6 as well as Z6 systems though different volumes of hydrogen peroxide are used up

to attain the maximum conversion. A volume of 3 mL is found to be the optimum for T6 system while it is 5 mL for of Z6 system.

Discussion:

From the figure, the presence of oxidant is found to be effective in the formation of cyclohexanone. However, it is observed that a large excess of hydrogen peroxide reduces the cyclohexanol conversion and thereby the product yield significantly. The probable reason for the lower conversion is that a large excess of hydrogen peroxide enhances its self-decomposition rather than the direct participation in selective oxidation of cyclohexanol[21]. The decreased conversion with higher amounts of hydrogen peroxide can also be explained as the negative influence of large amount of water accompanying the hydrogen peroxide sample[20]. Of course, this will be a trivial reason for the decrease in the conversion.

Optimized conditions:

The above observations and discussion of the results clearly reveal that in the liquid-phase oxidation of cyclohexanol using hydrogen peroxide over supported vanadia systems, the reaction conditions play a decisive role in determining the cyclohexanol conversion and product yield. The optimized reaction conditions obtained with T6 and Z6 as representative samples is summarized in Table 6.1.

Table 6.1
Optimized conditions for cyclohexanol oxidation.

System	Reaction conditions			
	Solvent	Temperature (°C)	Time (h)	Amount of H_2O_2 (mL)
T6	Water	100	1.5	3
Z6	Acetonitrile	80	2	5

6.2.2 Performance of Different Catalyst Systems

With the optimized reaction conditions presented in the first part, investigation of the oxidation activity of the vanadia-based systems was done.

We attempted to ascertain how the incorporation of various amounts of V_2O_5 into the support oxides and its surface modification by sulfate groups alter the structural properties as well as the oxidation activity, and examined whether or not the catalytic behaviour can be explained by the structure of the surface vanadium oxide species. The observations are given under two headings: (I) V_2O_5-SnO_2 systems and (II) V_2O_5-ZrO_2 systems.

I. V_2O_5-SnO_2 Systems

Table 6.2 presents the results of standard reactions carried out over V_2O_5-SnO_2 systems. The results include the activity profiles of the supported, sulfated and pure oxide systems. Under the optimized reaction conditions the cyclohexanol oxidation was done over all the prepared systems.

Table 6.2
Activity of V_2O_5-SnO_2 systems in cyclohexanol oxidation.

Systems	Conversion (wt%)	Systems	Conversion (wt%)
T0	3.1	ST0	5.7
T3	19.8	ST3	22.5
T6	34.8	ST6	36.6
T9	18.1	ST9	21.6
T12	7.2	ST12	13.7
T15	5.4	ST15	11.8
V	4.9	SV	5.9

[Amount of catalyst: 0.1 g, Time: 1.5 h, Solvent: 5 mL (water), Temperature: 100°C]

Results:

The results of the cyclohexanol oxidation over the V_2O_5-SnO_2 systems indicate that the single oxides and their sulfated analogues show poor activity. As vanadia is incorporated into the support oxide, the activity enhances to a greater extent. Maximum cyclohexanol conversion is observed for system with 6 wt% vanadium oxide content. The trend is the same in the case of sulfated series also. The highest conversion is found to be 34.8% and 36.6%

respectively for T6 and ST6. The conversion then reduces significantly with further increase in vanadium oxide content. The sulfate-modified systems show comparatively higher activity when compared to the unmodified samples.

Discussion:

From the results, it is clear that the catalytic oxidation of cyclohexanol to cyclohexanone can be accelerated by the addition of vanadium oxide to single oxide supports. According to Sachtler *et al.*[27,28], the activity and selectivity in oxidation reactions are determined by two factors namely the intrinsic activity of lattice oxygen and their availability. If only a limited number of lattice oxygen is available, the oxidation stops at a particular level to result partial oxidation products. In the supported systems, there is no large reservoir of bulk oxygen that is free to abstract many hydrogens. Thus the locally limited amount of reactive lattice oxygen may be the explanation for selective oxidation activity of the vanadia-based systems in the present study.

Since there are ample reports relating the acidity-basicity of supported vanadia catalysts with oxidation activity[29-33], we attempted to correlate the cyclohexanol oxidation activity with the acid-base properties of the systems, but failed to get any correlation between the two.

The different spectroscopic characterization like FTIR, DR UV-VIS and ^{51}V NMR of the prepared samples suggest the presence of appreciable amount of surface vanadium oxide, which exist as tetrahedral V^{5+} species in the low loaded samples. As the percentage loading of vanadia increases the fraction of tetrahedral species decreases and at higher vanadium oxide concentration V^{5+} is found to be present in an octahedral environment as in the case of crystalline V_2O_5. The presence of crystalline V_2O_5 was also detected at higher vanadia concentration.

The results reported by Trfiro *et al.*[34] on methanol oxidation claimed that V=O bond in the isolated tetrahedral vanadium oxide species is the active site whose labilization (reducibility) plays a crucial role in controlling the activity

and selectivity in oxidation reactions. According to them, the activity of the catalyst is directly connected with the metal-oxygen double bond which opens with the addition of hydrogen atom from the alcohol, which in turn leaves a free valence on the metal used for bonding with the dehydrogenated molecule. Miyata *et al.*[19] also reported that the weakening of V=O bond will be reflecting in the reactivity of surface V=O group in alcohol oxidation. According to the results on ethanol oxidation, they concluded that the V=O bond in a tetrahedral surface species will be more easily reduced than that an octahedral unit or crystalline V_2O_5. A similar perception can be applied in the case of cyclohexanol oxidation reaction with supported vanadia systems.

Thus a very good correlation can be obtained between the enhanced activity and the fraction of tetrahedral surface vanadium oxide species. In regions of low vanadium oxide content up to 6 wt% as described above, the activity of V-Sn oxides for selective oxidation of cyclohexanol will increase with increase in vanadium content. Above 6 wt% loading the octahedral surface species fraction increases, where a considerable amount of vanadium oxide consists of crystalline vanadia. Accordingly, a further increase in vanadium oxide content is expected to cause an increase in fraction of crystalline V_2O_5 which will result in a decrease in activity. Thus with increasing vanadia loading the activity will rise from a small value of pure SnO_2, passes through a maximum and then decreases. A similar trend observed in the sulfated analogues also, the slight higher activity of the sulfated series may be attributed to the higher surface area and induced oxidation activity by the surface sulfate groups.

II. V_2O_5-ZrO_2 Systems

The catalytic activity of different V-Zr oxides and its sulfated counterparts have been screened for liquid-phase cyclohexanol oxidation under optimized reaction conditions and the results are summarized in Table 6.3.

Table 6.3
Activity of V_2O_5-ZrO_2 systems in cyclohexanol oxidation.

Systems	Conversion (wt%)	Systems	Conversion (wt%)
Z0	4.5	SZ0	7.3
Z3	17.8	SZ3	30.5
Z6	13.9	SZ6	18.3
Z9	12.8	SZ9	15.4
Z12	10.3	SZ12	12.8
Z15	9.4	SZ15	10.2
V	4.9	SV	5.9

[Amount of catalyst: 0.1 g, Time: 2 h, Solvent: 5 mL (acetonotrile), Temperature: 80°C]

Results:

The results show that pure oxides and are with very low activity produce only small amount of cyclohexanone. As vanadium oxide is deposited on the support, a noticeable change in activity is observed. The cyclohexanol conversion increases from 4.5% to 17.8% when the vanadia weight percentage is changed from 0 to 3 as evident from Table 6.3. Further increase in vanadia loading has a negative effect on the catalytic activity. Thus, the maximum conversion is obtained for catalyst with 3 wt% vanadia and thereafter the conversion declines. Similar trend is observed with the sulfate modified series with comparatively higher conversion.

Discussion:

As in the case of V_2O_5-SnO_2 systems the strength of the terminal V=O bond in the active surface vanadia species has been proposed to be the main factor controlling the reactivity of V_2O_5-ZrO_2 systems also. The validity of the proposal is supported by the results of spectroscopic investigation of the prepared systems. Examination of the data (Table 6.3) reveals that the low-vanadia loaded samples, which possess higher fraction of isolated tetrahedral

surface vanadia species have higher cyclohexanol conversion rate. The activity changes dramatically at higher vanadium oxide content indicating that the surface structure has changed which affects the reaction. At higher concentration of vanadia, the fraction of inactive crystalline vanadia increases reducing the cyclohexanol conversion. Here also the enhanced activity of the sulfate-doped systems can be explained by the additional oxidizing property of the sulfate groups present on the catalyst surface.

Mechanism of the Reaction

The common feature of all vanadia-based catalysts is the presence of VO_x groups. Vanadium ions in these units can be present in tetrahedral, octahedral and square pyramidal environment. The separation of VO_x units can effectuated by dispersion of vanadia phase on oxide supports when vanadium loading is low. It is generally accepted that a very low loadings the surface vanadium oxide species is present as tetrahedral isolated species, whereas with increase in the loading, octahedral VO_x species forming chains of V-O-V appear[18]. The formal valence state of vanadium in VO_4 tetrahedra, VO_6 octahedra and V_2O_5 is +5. The surface of the vanadia-based systems exhibits cationic center (V^{5+}) linked in different manners to the anionic oxide centers. The V-O groups are present in V-O-V or V-O-M^{n+}units and in V=O terminal vanadyl groups sticking out of the surface. In many oxidation reactions, surface oxide ions have been proposed as the sites capable of abstracting H atom in the form of a proton[35]. Hence the activity is dependent on the nucleophilicity of the catalyst oxygen[36,37]. Therefore the nucleophilicity will be higher for oxygen bound to V^{5+} ion in VO_4 tetrahedra when compared to V_2O_5 or VO_6 octahedral units. The active species bound to the catalyst surface after the abstraction of hydrogen atom can desorb or undergo further reaction forming the oxygenated product. The plausible mechanism of cyclohexanol oxidation over tetrahedral surface vanadium oxide species is depicted in Figure 6.5.

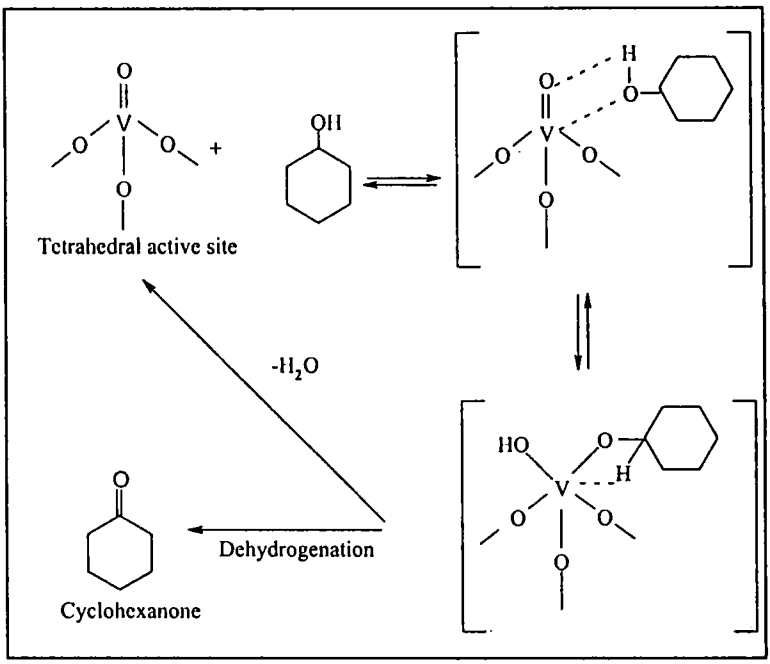

Figure 6.5
Plausible reaction mechanism for cyclohexanol oxidation.

6.3 CONCLUSIONS

The summary of the results of the various studies is presented below:

- The vanadia supported on SnO_2 and ZrO_2 and their sulfate-modified analogues are found to catalyze the liquid-phase oxydationn of cyclohexanol with considerable activity for cyclohexanone formation. The reaction gives 100% selectivity to cyclohexanone over all the systems.
- The results on the influence of reaction variables such as temperature, solvent, reaction time, and amount of oxidant show that these factors play an imperative role in deciding the catalytic efficiency and each parameter has an optimum value in order to acquire conversion maximum.
- The agreement between the catalytic activity and the surface concentration of vanadium oxide suggests that the difference in catalytic

behaviour of the supported vanadia systems can be related to the structural difference of surface active species of vanadium.

- No correlation is found between the acid-base character and the catalytic performance of the oxide systems.
- Structural characterization results of the presently developed systems confirm the active sites to be V^{5+} ions in tetrahedral environment, the reducibility of which is the main factor in the reaction mechanism of cyclohexanol oxidation. The maximum activity in T6, ST6, Z3 and SZ3 appear to be explicable on the concept of maximum dispersion of the active species over the support at these vanadia loadings.

SECTION 2
OXIDATIVE DEHYDROGENATION OF ETHYLBENZENE

6.4 INTRODUCTION

Styrene is one of the fundamental materials for the industrial production of many synthetic rubbers and numerous thermoplastics. This monomer is commercially manufactured by the catalytic dehydrogenation of ethylbenzene[1,2]. The process for dehydrogenation, although selective for styrene, has some inherent limitations. The reaction which is endothermic and energy intensive usually gives very low conversion and requires high temperatures (> 600°C) which bring about several cracking reactions[3]. Moreover, several problems, such as coke formation, thermodynamic constraints and release of large amount of wasted energy in the form of steam also remain[4]. Energy saving dehydrogenation processes that are more economical are therefore highly desirable. Thus oxidative dehydrogenation of ethylbenzene has attracted much attention, which is a potential alternative for the manufacture of styrene at low temperature, without thermodynamic restrictions on the yield. Various catalysts have been reported as efficient for the oxidative dehydrogenation of lower alkanes[5-14], cyclohexane[15] and ethylbenzene[16-18]reaction. Moreover, it was shown that several metal oxide systems display improved catalytic performances in oxidative

dehydrogenation reactions[19-25]. Here, the process is favoured at low temperatures and the presence of oxygen inhibits the carbon deposition prevalent in non-oxidative routes.

Recent reviews outline the importance of supported vanadium oxide catalysts in several oxidative dehydrogenation reactions[12]. In addition to the role of the support, the vanadium oxide loading on a specific oxide support is also found to be crucial in determining the activity and selectivity in such reactions[26]. Hence we examined the catalytic performance of vanadia promoted SnO_2 and ZrO_2 as well as their sulfated analogues for the oxidative dehydrogenation of ethylbenzene in presence of air. Addition of vanadium oxide to these supports as well as the surface sulfate modification gave an enhanced rate for the reaction. A detailed study of the nature and structure of the active surface vanadium species seems important to obtain correlation between the optimum catalytic activity and content of vanadium in the bulk frame of the oxide and also in understanding the role of vanadium in the enhancement of catalytic activity. A detailed representation of process optimization by studying the effect of reaction temperature, flow rate and time on stream is also included in this section.

6.5 OXIDATIVE DEHYDROGENATION OF ETHYLBENZENE

The oxidative dehydrogenation of ethylbenzene over the vanadia catalysts was performed in vapour-phase and the general experimental and analytical procedure is given in section 2.6.2 of Chapter 2. A blank run (with no catalyst in the reactor) was carried out at 450°C with no catalyst in the reactor, which indicated negligible thermal reaction. The influence of temperature, feed rate and the time on stream was also investigated in detail in order to optimize the reaction conditions. All the catalytic reactions were done in presence of air. GC analysis showed styrene as the major product along with minor quantities of toluene and benzene. The oxidative dehydrogenation of ethylbenzene produced a considerable amount of carbon

oxides also, which are formed by the complete oxidation of the organics. The conversion of ethylbenzene and selectivities of the products were calculated in the following manner:

Ethylbenzene (EB) conversion (%) = (mols of EB converted/mols of EB fed) X 100

Selectivity to a product (%) = (mols of product formed/mols of EB converted) X 100

Selectivity to carbon oxides (%) = (Mass balance) X 100

The goals of the investigations were two-fold; optimizing the reaction conditions and screening of catalytic activity of different catalysts, which is correlated with the properties of the systems. The results and discussion are given under two headings; I) Process optimization II) Catalyst comparison

6.5.1 Process Optimization

The reactions were performed under atmospheric pressure and the reaction conditions found to play an imperative role in deciding the catalytic activity and product distribution. So before carrying out the reaction over all the catalyst systems, it becomes highly essential to fix the optimum parameters for the reaction. Hence the effect of operating parameters such as reaction temperature, feed rate, and time on stream has been the subject of preliminary investigation.

I. Effect of Temperature

In order to study the temperature influence on the oxidative dehydrogenation of ethylbenzene, a set of reactions were performed over T6 system in the temperature range from 300 to 550°C. The air flow rate and flow rate of ethylbenzene were maintained at 25 mL min^{-1} and 6 mL h^{-1} respectively. The activity and selectivity pattern obtained is presented in Table 6.4.

Table 6.4
Effect of reaction temperature on conversion and product selectivity in oxidative dehydrogenation of ethylbenzene.

Temperature (°C)	Conversion (wt%)	Selectivity (%)			
		Styrene	Toluene	Benzene	C-oxides
300	4.9	57.5	-	26.6	15.9
350	14.1	96.3	-	1.5	2.2
400	16.8	88.1	-	1.6	10.3
450	31.7	89.5	-	3.7	6.8
500	54.0	64.5	15.6	16.2	3.7
550	85.0	47.7	23.8	26.3	2.2

[Amount of catalyst: 0.5 g (T6), Air flow rate: 25 mL min^{-1}, Flow rate: 6 mL h^{-1}]

Results:

The results of dehydrogenation over T6, as a function of temperature show an increasing trend for ethylbenzene conversion. However, the styrene selectivity increases first in the temperature range 300-350°C and thereafter it decreases. At higher temperatures, considerable amount of side products (benzene and toluene) is formed. The selectivities for these minor products is maximum at 550°C. The selectivity to styrene is maximum at 350°C (96.3%), but the ethylbenzene conversion at this temperature is only 14.1%. A comparatively high selectivity of ethylbenzene (89.5%) with minimum amounts of side products is observed at 450°C. As the temperature is raised in steps from 450 to 550°C, the styrene selectivity falls from 89% to 47%, and the amount of benzene and toluene formed shows an enhancement with the increase in temperature. The selectivity to carbon oxides is found to decrease with rise in reaction temperature.

Discussion:

From the data it is clear that the conversion of ethylbenzene increases with reaction temperature, while the selectivity exhibits a considerable variation. The reaction of ethylbenzene to styrene is endothermic with

ΔH = 124.9 KJ/mol[27]. Hence an increase in temperature will always favour the reaction. However, the decrease in selectivity of styrene observed at higher temperatures may be due to the higher rate of disproportionation reaction, which is again supported by the higher amount of benzene and toluene formed at these temperatures[28]. From the results, 450°C is fixed as the optimum temperature of the reaction for further investigations. Several researchers[3,4,22,29-31] have investigated the effect of reaction temperature on ethylbenzene dehydrogenation and the current observations are similar to the earlier reports.

II. Influence of Flow Rate

Flow rate is another important parameter that has an influence on the reactivity, in the case of gas-phase reactions. For studying the effect of flow rate on ethylbenzene conversion and product selectivity, five flow rates (4, 5, 6, 7 and 8 mL h^{-1}) were selected. The reactions were done over T6 system at 450°C, maintaining the air flow rate at 25 mL min^{-1}. The typical run was performed for a reaction time of 2 h. The results obtained are depicted in Figure 6.6.

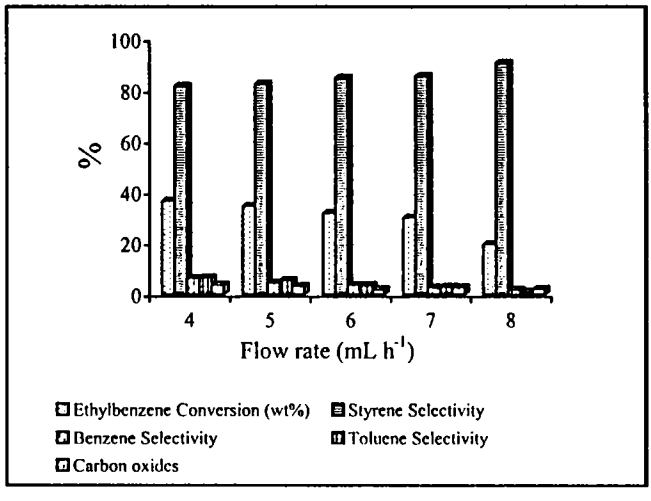

Figure 6.6
Effect of feed rate on conversion and product selectivity in oxidative dehydrogenation of ethylbenzene.
[Amount of catalyst: 0.5 g (T6), Air flow rate: 25 mL min^{-1}, Temperature: 450°C]

Results:

Figure 6.6 shows that the conversion is maximum at lower flow rates and it is adversely affected by the increase in flow rate. As the flow rate is increased from 4 to 8 mL h^{-1}, the ethylbenzene conversion drastically decreases from 36.5 to 19.5%. However, the selectivity for styrene remains more or less constant with increase in the feed rate. The maximum styrene selectivity of 90.4% is observed to be at 8 mL h^{-1}. The formation of carbon oxides is observed only at the initial runs of the reaction. The benzene and toluene selectivities are also found to be decreasing as the flow rate increases.

Discussion:

From the figure, it is clear that higher feed rate decreases the ethylbenzene conversion to a great extent. This may be due to the fact that with the increase in flow rate, the contact time of the reactants with the catalyst surface is decreased. At higher feed rates, reactants will not get enough time to get adsorbed on the catalyst surface and this will result in a reduced percentage conversion of ethylbenzene. Thus higher the residence time, higher is the probability of reactive adsorption leading to a higher conversion of ethylbenzene. However, high selectivity for styrene at high feed rates may be due to the prevention of re-adsorption of styrene on catalyst surface, there by preventing its conversion to unwanted products. The possibility of product re-adsorption and production of more oxygenated products are feasible at lower flow rates, which leads to poor selectivity[3,4,31]. So an intermediate flow rate of 6 mL h^{-1} is selected for further activity measurements.

III. Influence of Time On Stream

Another set of experiments was carried out to evaluate the stability of the systems with reaction time. In order to test the deactivation of the prepared systems, we carried out the reaction continuously for 6 hours at 450°C and the reaction mixture was analyzed at intervals of one hour. The feed rate and air flow rate were maintained at 6 mL h^{-1} and 25 mL min^{-1} respectively. Typical

activity profiles for T6 and Z6 systems as a function of time on stream are shown in Figures 6.7 and 6.8.

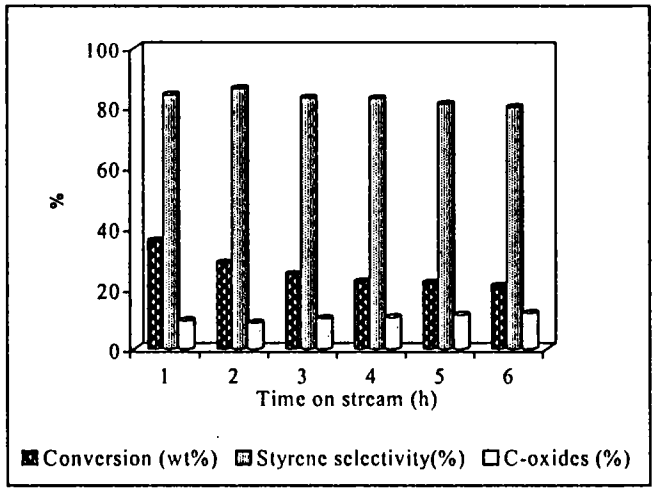

Figure 6.7
Effect of time on stream in oxidative dehydrogenation of ethylbenzene over T6.
[Amount of catalyst: 0.5 g (T6), Air flow rate: 25 mL min^{-1},
Temperature: 450°C, Feed rate: 6mL h^{-1}]

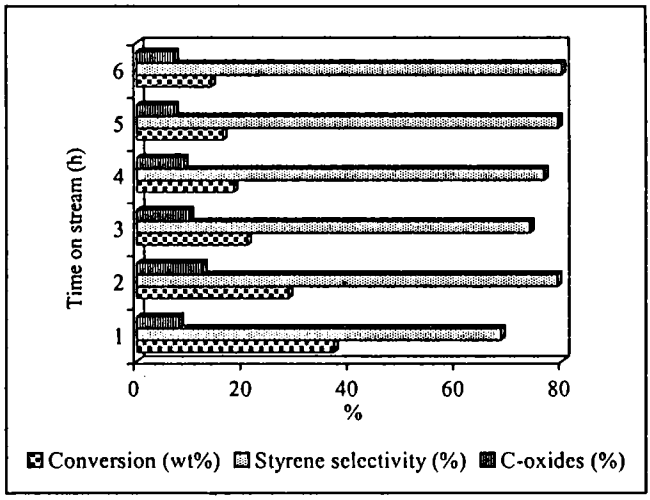

Figure 6.8
Effect of time on stream in oxidative dehydrogenation of ethylbenzene over Z6.
[Amount of catalyst: 0.5 g (Z6), Air flow rate: 25 mL min^{-1},
Temperature: 450°C, Feed rate: 6mL h^{-1}]

Results:

The results show (Figures 6.7 and 6.8) that the reactivity of the catalyst systems decreases to some extent in the first three hours and thereafter it remains more or less constant. The selectivity towards styrene and carbon oxides shows little change even after 6 h of reaction run. The maximum styrene selectivity obtained is 86.5% in the case of T6 system while it is 79.9% for Z6 system. The catalyst systems turned dark grey after 6 h continuously on stream. The original colour of the systems can be regained by regenerating the catalysts at 550°C for 5 hours.

Discussion:

The results clearly indicate that the vanadia-supported systems possess reasonable selectivity in oxidative dehydrogenation reaction during the 6 h reaction run. The deactivation observed may be due to the reduction of the metal ions present on the catalyst surface; the higher valence state of vanadium ions is not maintained during the prolonged reaction time[4]. The metal ions reduced during the reaction are reoxidized by the external supply of oxygen providing a long-term catalytic selectivity to the systems. The dark colour of the systems after continuous use may be due to the carbon deposited which can be burned off by treating the catalysts at higher temperatures[3,20].

6.5.2 Catalyst Comparison

In order to compare catalytic performance of different systems for the oxidative dehydrogenation of ethylbenzene we carried out the reaction under optimized conditions over all the prepared systems. The results of the observations are separately given for V_2O_5-SnO_2 and V_2O_5-ZrO_2 systems.

I. V_2O_5-SnO_2 Systems

The results obtained for oxidative dehydrogenation over V_2O_5-SnO_2 series are presented in Table 6.5. Pure metal oxides (SnO_2 and V_2O_5) are also

screened for catalytic activity. The variation of conversion and selectivity to the products with vanadium oxide loading is presented in Figure 6.9.

Table 6.5
Oxidative dehydrogenation activity of V_2O_5-SnO_2 systems.

Catalyst	Conversion (wt%)	Selectivity (%)			
		Styrene	Toluene	Benzene	C-oxides
T0	22.84	78.98	8.84	6.05	6.13
T3	25.48	80.02	3.81	7.03	9.14
T6	36.53	86.21	2.05	2.53	8.76
T9	32.65	74.93	5.3	12.57	7.14
T12	26.40	84.81	4.40	3.63	7.15
T15	24.05	83.63	5.65	3.24	6.15
V	31.45	5.88	11.8	21.02	67.19
ST0	33.47	72.27	17.54	3.47	5.38
ST3	35.63	86.50	5.08	4.29	4.13
ST6	36.59	85.49	4.95	4.18	4.02
ST9	35.53	72.46	8.41	17.7	3.98
ST12	30.45	85.25	4.24	4.59	7.70
ST15	25.53	78.96	6.19	4.97	9.87
SV	35.8	4.56	5.18	3.00	58.5

[Amount of catalyst: 0.5 g, Air flow rate: 25 mL min^{-1}, Temperature: 450°C, Feed rate: 6 mL h^{-1}]

Results:

From Table 6.5, it is noticeable that all the systems show remarkable activity and selectivity in oxidative dehydrogenation reaction. Styrene is the selective product along with small amounts of toluene, benzene and carbon oxides as non-selective products. Among the vanadia supported systems, as the percentage loading of vanadium oxide increases, the catalytic activity along with styrene selectivity increases, reaches a maximum at 6% loading and thereafter decreases. The variation of activity follows the same trend in simple

as well as sulfate modified systems (Figure 6.9). Though pure vanadia gives a comparatively high conversion, the styrene selectivity of vanadia is found to be very low, which is evident from the higher percentage of carbon oxides formed. The sulfate modification has a positive influence on the catalytic activity of supported systems towards the reaction. Here also the maximum catalytic activity and selectivity for styrene is shown by ST6 system.

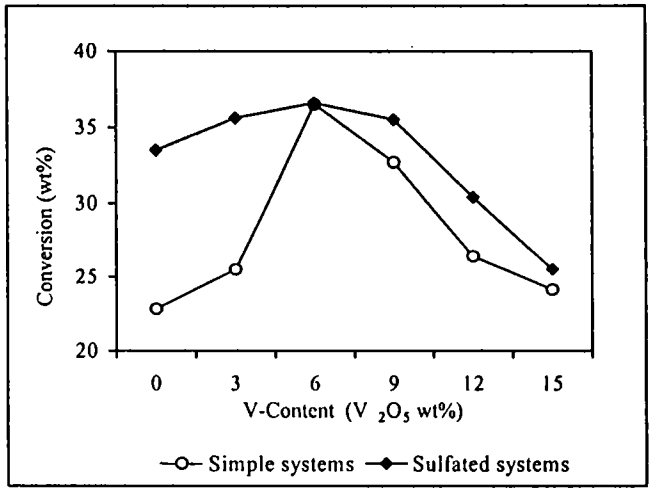

Figure 6.9
Variation of ethylbenzene conversion as a function of vanadium oxide content.

Discussion:

From the data and figure, it is obvious that the activity of V_2O_5-SnO_2 systems in selective oxidative dehydrogenation of ethylbenzene is greatly influenced by the presence of vanadium oxide as well as sulfate ions on the surface. The selective oxidation activity of pure vanadia is too low indicating that it catalyzes the complete oxidation of ethylbenzene leading to more oxygenated products as evident from the higher percentage of carbon oxides formed. Addition of vanadia to tin oxide induces remarkable oxidation activity while selectivity of styrene is also enhanced. This indicates that the presence of

a metal oxide support is indispensable for vanadia in the selective oxidative dehydrogenation reaction.

Tagawa *et al*[17]. have showed that both acidic and basic sites are required for the oxidative dehydrogenation reactions. The oxidative dehydrogenation activity in correlation with surface acidity and basicity was also reported by Brozyana *et al.*[32] and Kania *et al.*[20] Acidity determination using different independent methods of our systems showed that due to the vanadium oxide addition, the acidity of the catalyst systems is enhanced and the sulfate modification again increased the acidity. No correlation could be obtained between the acid-base properties and oxidation activity of the systems. Campelo *et al.*[33] proposed that acid-base sites on $AlPO_4$ –supported nickel catalysts do not exhibit catalytic activity in the oxidative dehydrogenation of alkylbenzens. So an attempt was made to correlate the structure of vanadium oxide species dispersed on the catalyst surface and the catalytic activity.

The supported vanadia catalysts have been characterized by various techniques like FTIR, DR UV-VIS and solid-state NMR and the results are given in different sections of Chapter 3. Characterization studies of V_2O_5-SnO_2 systems have shown that the surface vanadium oxide species exist as isolated tetrahedral at low vanadium loaded samples. With increasing vanadium oxide content above 6 wt%, the tetrahedral species aggregates forming chains or bidimensional arrays. At higher surface coverages, the V^{5+} progressively becomes six coordinated (octahedral geometry) in an environment similar to metavanadates or decavanadates. The appearance of V_2O_5 crystallites is also observed at high vanadium oxide coverages. In fact, several studies carried out with Raman[34-38] and ^{51}V NMR[38-41] spectroscopies indicate that in vanadia supported on both alumina and titania catalysts, the V-environment goes from tetrahedral at low coverages to octahedral at high coverages.

There are many reports on vanadia-based systems where the isolated tetrahedral V^{5+} species are proven to be the active and selective sites for oxidative dehydrogenation reactions[5,9,10,42,43]. From the reports it is accepted

that surface vanadium oxide in tetrahedral coordination is the one, which catalyzes the reaction. Further evidence is provided from the studies of Corma *et al.*[44] who reported comparatively high oxidative dehydrogenation activity and selectivity for orthovanadates, in which vanadium is in tetrahedral environment. In oxidation reactions, surface oxygen is proposed as the site capable of abstracting H atom as H ion to form an OH group[45]. The activity therefore depends on the nucleophilicity of the oxygen of the active site. The oxygen attached to a V^{5+} ion in tetrahedral geometry is found to be highly nucleophilic[42], which favours the selective oxidation of the reactants. Bulk vanadium oxide is known to possess a vast reservoir of oxygen, which becomes highly mobile when the oxide is in partially reduced state. Normally, this mobile lattice oxygen is capable to achieve selective oxidation, but at the very high temperature used for the reaction it can cause overoxidation[26].

Comparison of the results of the present investigation and the earlier reports concludes the importance of coordination number and structure of the surface vanadium species in the oxidative dehydrogenation of ethylbenzene. In the V_2O_5-SnO_2 systems the feature that permits to obtain moderate selectivities to styrene at relatively high ethylbenzene conversion is mainly the isolated tetrahedral vanadium oxide units. At low vanadium oxide loadings, up to 6 wt%, isolated tetrahedral species predominates leading to high activity and selectivity. However, on catalysts with vanadium loading above 6 wt% in which octahedral V^{5+} species with V=O bonds as in V_2O_5 is mainly observed which show poor selectivity and activity. The highly active isolated tetrahedral units may be dispersed on the surface of the catalyst, the monolayer coverage of which may be completed at 6 wt% vanadia loading. As the percentage of vanadium oxide still increases, crystallites of V_2O_5 may be formed which reduces the selective oxidation property and produces mainly carbon oxides[35].

II.V_2O_5-ZrO_2 Systems

The catalyst efficiencies of V_2O_5-ZrO_2 systems as well as their sulfate-modified series in oxidative dehydrogenation of ethylbenzene are given in

Table 6.6. The ethylbenzene conversion obtained as a function of surface concentration of vanadium oxide is presented in Figure 6.10.

Results:

From Table 6.6, it is perceptible that the selectivity-conversion trend in the oxidative dehydrogenation over V_2O_5-ZrO_2 systems is quite similar to that of V_2O_5-SnO_2 systems. The activity and styrene selectivity increases until the surface concentration of vanadium oxide is 3 wt% and thereafter decreases for both the simple and sulfated systems. The addition of vanadia to ZrO_2 increases the activity and selectivity significantly. The selectivity of the supported systems for dehydrogenation is also much higher than that of pure V_2O_5. The sulfated systems show slightly higher activity when compared to the unmodified samples.

Table 6.6

Oxidative dehydrogenation activity of V_2O_5-ZrO_2 systems.

Catalyst	Conversion (wt%)	Selectivity (%)			
		Styrene	Toluene	Benzene	C-oxides
Z0	11.16	83.42	3.16	2.77	7.10
Z3	28.25	85.23	7.90	4.39	2.48
Z6	19.36	79.92	7.31	5.05	7.72
Z9	16.42	80.69	5.79	9.38	4.14
Z12	16.1	80.37	5.22	6.83	7.58
Z15	14.13	82.25	5.82	6.53	5.35
V	31.45	5.88	11.8	21.02	67.19
SZ0	26.88	79.56	8.54	7.04	4.86
SZ3	30.27	86.85	4.13	3.11	5.91
SZ6	29.08	68.60	16.44	9.42	5.54
SZ9	26.31	85.54	5.68	4.91	3.84
SZ12	19.2	82.29	4.58	4.43	8.69
SZ15	19.15	80.52	7.21	5.64	6.99
SV	35.8	4.56	5.18	3.00	58.5

[Amount of catalyst: 0.5 g, Air flow rate: 25 mL min^{-1}, Temperature: 450°C, Feed rate: 6 mL h^{-1}]

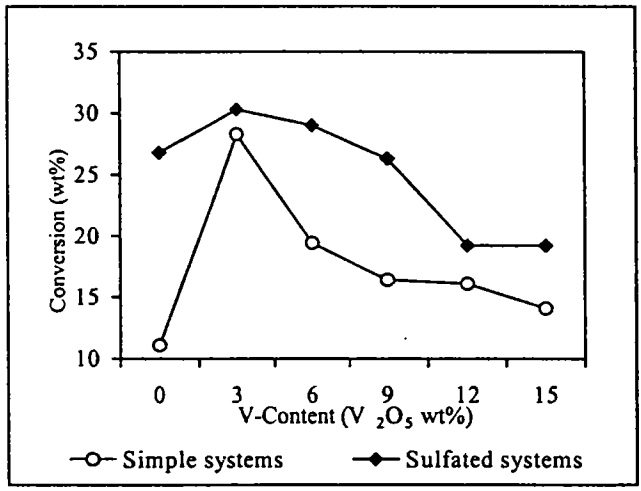

Figure 6.10
Variation of ethylbenzene conversion as a function of vanadium oxide content.

Discussion:

The activity and selectivity patterns of V_2O_5-ZrO_2 systems show that the results are comparable to those of V_2O_5-SnO_2 systems. No correlation can be found in support of any of the previous proposals that the activity is strongly influenced by the acid-base character of the catalysts. Efforts aimed at relating the structure of the dispersed vanadia to its activity suggest that the local environment and the surface concentration of vanadium oxide have a vital role in deciding the activity and selective oxidation capacity. Analysis of catalytic and spectroscopic data suggests that isolated tetrahedral units highly dispersed on the ZrO_2 surface are the active and selective sites in ethylbenzene oxidative dehydrogenation. The styrene selectivity is maximum at 3 wt% vanadia loading for which there is maximum dispersion of the tetrahedral units. At higher vanadium oxide loadings, the activity and selectivity decrease monotonically, which may be due to the presence of higher fraction of octahedral surface species. On ZrO_2 support, there may be rapid formation of multiplayer structure of vanadia as a consequence of the weak interaction of the support and the dispersed vanadium oxide[46,47]. Therefore, at vanadia loading above

3 wt%, octahedral or crystalline V_2O_5 may be formed as the concentration of vanadia exceeds the theoretical monolayer.

Mechanism of the Reaction

Comparison of the most effective supported vanadium oxide catalysts in oxidative dehydrogenation of ethylbenzene from literature with the present systems suggests that a higher activity and selectivity can be obtained at vanadium oxide loading below the theoretical monolayer of active species. In addition, for most of these catalysts, tetrahedral V^{5+} units on the surface are proposed to be the active sites in the oxidative dehydrogenation reaction as they are the main species present at submonolayer coverage as evident from the spectroscopic characterization. The appearance of octahedral V^{5+} species, on the other hand, favours the non-selective oxidation products[48].

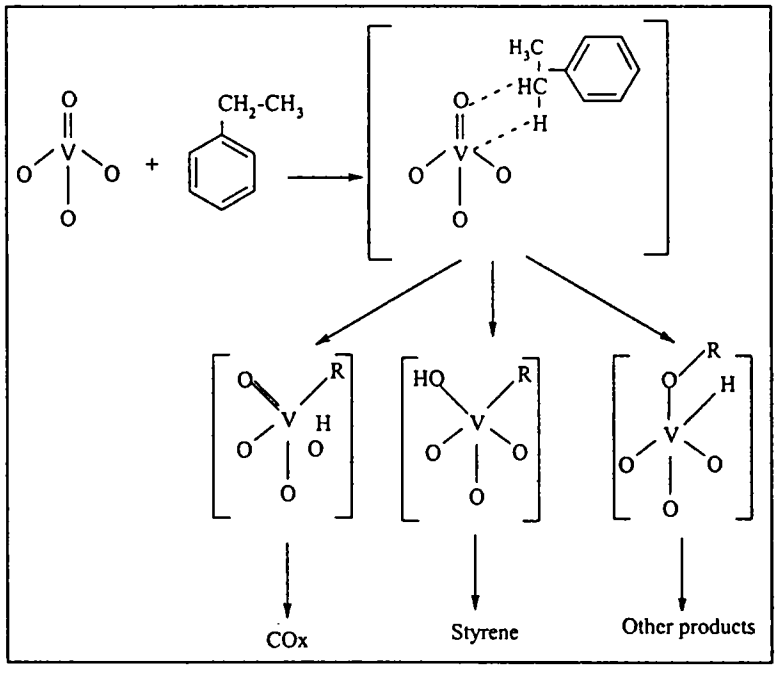

Figure 6.11
Possible reaction mechanism for oxidative dehydrogenation on isolated VO_4 units.

Figure 6.11 shows the possible mechanism proposed for ethylbenzene activation and dehyrogenation on isolated tetrahedral VO_4 units[49,50]. According to this scheme, the first H abstraction occurs from a secondary carbon atom which gives rise to different possible intermediates. The second H-abstraction from these intermediates can give styrene, Oxygen containing partial oxidation products or carbon oxides. In this mechanism, both the V=O double bond character and strength of V-O-M oxygen bond are essential factors in the final product distribution.

6.6 CONCLUSIONS

The conclusions of the investigation can be summarized as:

- Supported vanadia catalysts undertaken for the present study afford high activity and selectivity in oxidative dehydrogenation of ethylbenzene to give styrene in presence of air.
- The catalytic behaviour is influenced by the reaction parameters like temperature, feed rate and time on stream significantly. Catalyst deactivation with reaction time is ascribed to coke deposition and reduction of the active metal ions.
- For ethylbenzene/styrene reaction a clear correlation exists among the activity, selectivity and vanadium oxide content of the systems. The addition of vanadia to the support metal oxide promotes the selective oxidation activity. The rate of the reaction is increased with vanadia loading. After a particular concentration vanadium oxide, the activity and selectivity attenuate. The sulfate modification of the supported surface gives additional enhancement of catalytic efficiency.
- The catalytic data indicate that the surface species present in the reaction are essentially the same for V_2O_5-SnO_2 and V_2O_5-ZrO_2 systems. The spectral characterization with FTIR, DR UV-VIS and ^{51}V NMR techniques gives the implication that V^{5+} ions in tetrahedral coordination is the active sites for oxidative dehydrogenation reaction. The bulk V_2O_5

present at high vanadia loading is not likely to take part in the reaction, which on the other hand, reduces the selectivity to the desired product. The sulfate modification increases the surface area of the samples, thereby resulting in a high dispersion of the surface active species.

REFERENCES

SECTION 1

1. K. U. Ingold, *Aldrichimica*, 22 (1989) 69.
2. D. Rohan and B. K. Hodnett; *Appl. Catal.*, 151 (1997) 409.
3. R. Raja and P. Ratnaswamy; *Appl. Catal.*, 143 (1996) 145.
4. F. Matsuda, K. Inoue and K. Kato, *Jap. Pat.*, H06-116187 (1994).
5. F. Matsuda, K. Inoue and K. Kato, *Jap. Pat.*, H06-192150 (1994).
6. K. Ohtani, S. Nishiyama, T. Suruya and M. Masai, *J.Catal.*, 155 (1995) 158.
7. J. Okamura, S. Nishiyama, T. Suruya and M. Masai, *J. Mol. Catal. A. Chem.*, 135 (1998) 133.
8. A. Njnibeako; *Prepr. Can. Symp. Catal.*,5 (1997) 170.
9. T. A. Tatarinova; *Katal. Kal.*, 23 (1985) 54.
10. S. Goldstein, G. Czapski and J. Robani; *J. Phys. Chem.*, 98 (1994) 6586.
11. A. Thankaraj, R. Kumar and P. Ratnaswamy; *Appl.Catal.*, 57 (1990) L1.
12. J. S. Reddy and S. Sivasankar; *Catal. Lett.*,11 (1992) 241.
13. D. P. Serrano, H. X. Liand and M. E. Davis; *J. Chem. Soc Chem. Commun.*, (1992) 745.
14. M. A. Camblor, A. Corma, A. Martinez and J. Perez–Pariente; *J. Chem. Soc. Chem. Commun.*, (1992) 589.
15. J. F. Yu, Y. Yang and T. H. Wu; *Chem. J. Chin. Univ.*, 17 (1996) 126.
16. Y. Yang, J. F. Yu, T. H. Wu and J. Z. Sun, *Chin. J. Catal.*, 18 (1997) 126.
17. V. Indira, P. A. Joy, N. Alekar, S. Gopinatahn and C. Gopinathan, *Ind. J. Chem.*, 36A (1997) 687-692.

18. B. Gryzybowska-Swierskosz, *Appl. Catal. A. Gen.*, 157 (1997) 409-420.

19. Y. Nakagawa, T. Ono, H. Miyata and Y. Kubokawa, *J. Chem. Soc. Faraday Trans.*, 1 (1983) 79, 2929-2936.

20. R. Yu, F. Xiao, D. Wang, T. Sun, Y. Liu, G. Pang, S. Feng, S. Qui, R. Xu and C. Fang, *Catal. Today*, 51 (1999) 39.

21. A. Tuel, S. Mohssa-Khouzami, Y. Ben Tarrit and C. Naccache, *J. Mol. Catal.*, 68 (1991) 45.

22. R. Neumann and M. Levin-Elad, *Appl. Catal. A. Gen.*, 122 (1995) 85.

23. S. I. Saudler, *"Chemical and Engineering Thermodynamica"*, 2nd Edn, Elsevier (1992).

24. A. Dubey, R. Rives and S. Kannan, *Fifteenth Ind. Nat. Symp. on Catal.*, Pune, India (2000).

25. R. Yu, F. Xiao, D. Wang, G. Pang, S. Feng, S. Qiu and R. Xu; *Catal. Lett*, 49 (1997) 49.

26. C. B. Lui, Z. Zhang, X. G. Yang and Y. Wu; *J. Chem. Soc. Commun.*, (1996) 1019.

27. W. M. H. Sachtler and N. H. De Boer, *Proc. 3rd Int. Con. on Catal.*, Amsterdam, Wiley, New York (1965) 240.

28. W. M. H. Sachtler, G. J. H. Dorgelo, J. Fahrenfort, and J. H. Voorhoev, *Proc. 4th Int. Con. on Catal.*, Moscow, B. A. Kazanski Edn., Adler, New York (1968) 454.

29. M. Ai and S. Sakurai, *Nippon Kagaku Kaishi* (1973) 200.

30. M. Ai and S. Sakurai, *Bull. Chem. Soc. Jpn.*, 47 (1974) 3074.

31. M. Ai, *7th Sanka-hanno (oxidation) meeting*, Noyaga (1973) 98.

32. M. Ai, *J. Catal.*, 40 (1975) 318.

33. M. Ai and S. Sakurai, *Bull. Chem. Soc. Jpn.*, 49 (1976) 1328-1334.

34. F. Trifiro and I. Pasaquon, *J. Catal.*, 12 (1968) 412.

35. A. Bielanski and J. Haber, *"Oxygen in Catalysis"*, Marcel Dekker, New York (1991).

36. V. A. Zazhigalov, J. Haber, J. Stoch, I. V. Bacherikova, G. A. Komashko and A. I. Pyatnitskaya, *Appl. Catal. A.*, 134 (1996) 225.

37. J. Haber, R. Tokarz and M. Witko, in *"Heterogeneous Hydrocarbon Oxidation"*, B. K. Warren, S. T. Oyama Eds., ACS symposium series, 638 (1996) 246.

REFERENCES

SECTION 2

1. J. Jarecki and M. Konopka; *Prezm. Chem.*, 57 (1978) 226.
2. W. W. Kaeding; *Catal. Rev.*, 8 (1973) 307.
3. G. Edwin Vrieland, *J. Catal.*, 111 (1988) 1-13.
4. Y. Sakurai, T. Suzuki, N.-O. Ikenaga and T. Suzuki, *Appl. Catal. A. Gen.*, 192 (2000) 281-288.
5. T. Blasco, A. Galli, J. M. Lopez Neito and F. Trifiro, *J. Catal.*, 169 (1997) 203.
6. M. Puglisi, E. Frusteri, V. Sokoluvskii and A. Parmaliana, *Catal. Lett.*, 41 (1996) 41.
7. T. Blasco, J. M. Lopez Nieto, A. Dejoz and M. I. Vazquez, *J. Catal.*, 157 (1995) 271.
8. M. A. Chaar, D. Patel and H. H. Kung, *J. Catal.*, 109 (1988) 463.
9. J. G. Eon, R. Olier and J. C. Volta, *J. Catal.*, 145 (1994) 318.
10. H. H. Kung and M. C. Kung, *Appl.Catal.A.*, 157 (1997) 105.
11. M. A. Chaar, D. Patel, M. C. Kung and H. H. Kung, *J. Catal.*, 105 (1987) 483.
12. E. A. Mamedov and V. C. Corberan, *Appl.Catal.A.*, 127 (1995) 1.
13. W. Ueda, S. W. Lin and I. Tohomoto, *Catal. Lett.*, 44 (1997) 241.
14. F. Cavani and F. Trifiro, *Catal. Today*, 24 (1995) 307.
15. H. H. Kung and M. C. Kung, *J. Catal.*, 128 (1991) 287.
16. W. Oganowski, T. Hanuza, H. Drulis, W. Mista and L. Malalik, *Appl.Catal.A.*, 136 (1996) 143.
17. T. Tagawa, H. Hattori and Y. Murakami, *J. Catal.*, 75 (1982) 66.
18. W. Oganowski, T. Hanuza and L. Kepinski, *Appl.Catal.A.*, 171 (1998) 145.
19. P. Galli, A. La Ginestra, P. Patrono, M. A. Massucci, C. Ferragina, P. Ciambelli and G. Bagnasco, *Italian Pat.* N. 21587 A/ 86 (1986)
20. W. Kania and K. Jurczyk, *Appl. Catal.*, 61 (1990) 35.
21. G. C. Grunewald and R. S. Drago, *J. Mol. Catal.*, 68 (1981) 33-41.
22. R. Fiedorow, W. Pryystajko and M. Sopa, *J. Catal.*, 58 (1990) 227-233.

23. A. Miyokoshi, A. Veno and M. Ichikawa, *Appl.Catal.A.Gen.*, 219 (2001) 249-258.

24. W. P. Addiego, C. A. Estrada, D. W. Goodman and M. P. Rosynek, *J. Catal.*, 146 (1994) 407-414.

25. T. Hattori, H. Niwa and A. Satsuma, *Appl.Catal.*, 50 (1989) 11-15.

26. T. Blasco and J. M. Lopez Nieto, *Appl.Catal.A.Gen.*, 127 (1995) 117-142.

27. E. H. Lee, *Catal.Rev.*, 8 (1973) 285.

28. N. J. Jabaratinam, M. Eswaramoorthy and V. Krisnasamy, *Appl. Catal. A.*, 145 (1996) 57.

29. T. Badstube, H. Papp, R. Dziembaj and P. Kustrowski, *Appl.Catal.A.Gen.*, 204 (2000) 153-165.

30. A. Cortes and J. L. Seoane, *J. Catal.*, 34 (1974) 7-12.

31. G. Bagnasco, P. Ciambelli, A. La Ginestra and P. Patrono, *Appl.Catal.*, 68 (1991) 69-79.

32. K. Brozyana and Z. Dziewiecki, *Appl.Catal.*, 35 (1987) 211-216.

33. F. M. Bautista, J. M. Campelo, a. Garcia, D. Luna and J. M. Marinas, *J. Catal.*, 107 (1987) 181-194.

34. F. Roozeboom, M. C. Mittelmeijer-Hazeleger, J. A. Mailijn, J. Medema, V. H. J. de Beer and P. J. Gellings, *J. Phys. Chem.*, 84 (1980) 2783.

35. J. M. Lopez Nieto, G. Kremenic and J. L. G. Fierro, *Appl.Catal.*, 61 (1990) 235.

36. G. T. Went, S. T. Oyama and A. T. Bell, *J. Phys. Chem.*, 94 (1990) 4240.

37. I. E. Wachs, F. D. Hardcastle and S. S. Chan,"*Spectroscopy*", 8 (1) (1986) 30.

38. L. R. Costumer, B. Taouk, M. Le Meur, E. Payen, M. Guelton and J. Grimbolt, *J. Phys. Chem.*, 92 (1988) 1230.

39. H. Eckert and I. E. Wachs, *J. Phys. Chem.*, 93 (1989) 6769.

40. W. S. Chang, Y. S. Chen and B. L. Yang, *Appl.Catal.A.*, 124 (1995) 221.

41. O. B. Lapina, V. M. Mastikhin, L. G. Simonova and Y. O. Bulgakova, *J. Mol. Catal.*, 69(1991) 61.

42. O. B. Lapina, V. M. Mastikhin, A. A. Subin, V. N. Kraslinikov and K. I. Zamaraev, *Progr. NMR Spectosc.*, 245 (1992) 457.

43. D. Patel, P. J. Andersen and H. H. Kung, *J. Catal.*, 125 (1990) 132.

44. A. Corma, J. M. Lopez Nieto, N. Paredes, M. Parez, Y. Shen, H. Cao and L. Suib, *Stud. Surf. Sci.*, 72 (1992) 213.

45. A. Bielanski and J. Haber, "*Oxygen in Catalysis*", Marcel Dekker, New York (1991).

46. U. Schart, M. Scrami-Marth, A. Wokaun and A. Baiker, *J. Chem. Soc. Faraday Trans.*, 87 (1991) 3299.

47. J. R. Sohn, S. G. Cho, Y. I. Pae and S. Hayashi, *J. Catal.*, 159 (1996) 170.

48. A. Corma, J. M. Lopez Nieto, N. Paredes, M. Parez and A. Lopez Agudo, *J. Catal.*, 95 (1985) 520.

49. H. H. Kung, *Adv. Catal.*, 40 (1994) 1.

50. G. Busca, *Catal. Today*, 27 (1996) 457.

Chapter 7

Summary and Concluding Remarks

ABSTRACT

Three main research objectives form the basis of the work presented in this thesis; i) preparation of highly active and selective vanadia supported metal oxide catalysts and its sulfated analogues for the acid catalyzed as well as selective oxidation reactions; ii) characterization of the supported vanadia catalysts and determination of the surface acidity; iii) determination of the catalytic activity of the catalysts towards industrially important reactions like Friedel-Crafts alkylation, Beckmann rearrangement and oxidative dehydrogenation of ethylbenzene and cyclohexanol oxidation. This final chapter deals with a summary of the results described in the preceding chapters of this thesis. Suggestions for further research in this field are also proposed.

7.1 SUMMARY

Supported vanadium oxide catalysts have found wide commercial application in a variety of industrial chemical processes. Vanadium oxides catalysts in combination with various promoters are widely used for several reactions including oxidation, ammoxidation and selective catalytic reductions. Further more, these catalysts are active in the oxidative dehydrogenation reactions. Some metal oxides, when sulfated, develop the ability to catalyze reactions characteristic of very strong acid catalysts at low temperature. Therefore sulfated oxides are considered as potential alternatives to

environmentally harmful mineral acids such as HF, $AlCl_3$, H_2SO_4 etc. used for acid catalyzed reactions. Studies carried out on promoters such as oxides and sulfates showed that they improve catalytic activity and selectivity to a great extent. However, notwithstanding this long periods of commercial applications, the currently used supported vanadia catalysts have several drawbacks such as poor reproduction of the synthesis, high production costs, a long and difficult activation procedure and deactivation under reaction conditions.

Our idea was to develop supported vanadia systems using metal oxide promoters like SnO_2 and ZrO_2 in order to overcome the drawbacks of the currently used systems. The sulfate modification of the samples was also done to enhance the surface acidity so that they can replace the environmental unfriendly catalysts in acid catalyzed reactions. These systems were expected to show superior characteristic over the bulk vanadia catalysts or the individual support metal oxides in selective oxidation capacity. Therefore the employment of the presently developed supported systems in acid catalyzed as well as selective oxidation reactions is promising. The well-dispersed vanadia phase on a support material would open new opportunities for a detailed characterization of the surface species. Besides promoting a variety of acid catalyzed reactions, sulfation is also observed to affect the physical properties of the catalyst surface, which is always an important consideration in heterogeneously catalyzed processes, where the reactions occur on the surfaces. Thus, the prime intention of the present project was the synthesis and systematic investigation of the physico-chemical properties of some vanadium oxide promoted tin oxide and zirconia systems along with it sulfated series. Though different methods of preparing the catalysts are available in literature, the widely employed wet impregnation method was used for preparing the present systems. The supported metal oxides and sulfate-modified compositions have also been evaluated in several reactions with industrial relevance. The characterization and catalytic activity results were compared with that of pure metal oxides and simple sulfated metal oxide systems. The chapters of this thesis are dedicated to the several aspects of supported vanadia

on SnO_2 and ZrO_2 and its sulfated analogues giving emphasis to its preparation, comparison of characterization results and screening of the catalytic performance obtained. The chapter-wise organization of the thesis is as follows.

Chapter 1 covers a brief literature review on vanadia supported and sulfated metal oxide systems. The effect of vanadia promotion and sulfate doping on the physico-chemical characteristics and catalytic properties is included in this chapter. The mechanism of acidity generation and nature of acidity in sulfated metal oxide systems is discussed in detail. The effect of incorporation of a second metallic species is also reviewed. This chapter also includes literature survey on heterogeneous Friedel-Crafts alkyaltion, Beckmann rearrangement and oxidative dehydrogenation reactions. Determination of surface acidity by different techniques, including surface electron-accepting properties by electron donors and cumene test reaction are the additional features of the chapter.

Chapter 2 is devoted to a complete description of the materials used in the present work and the experimental techniques employed for the catalyst characterization. The preparation methods adopted are described in detail. The experimental details for the evaluation of catalytic activity are also incorporated in this chapter.

Chapter 3 describes the physico-chemical characteristics of the catalyst systems. The catalyst systems were characterized by surface area and pore volume measurements, XRD analysis, thermal studies and IR spectroscopy. The elemental composition was revealed by EDX analysis. Selected samples were also analyzed by ^{51}V NMR, Diffuse Reflectance UV-VIS spectroscopies and Scanning Electron Microscopy (SEM). Surface acidic properties of the prepared samples were examined by three independent techniques namely ammonia TPD, perylene adsorption and Cumene conversion reaction.

Chapter 4 focuses on the application of the catalytic systems for Friedel-Crafts benzylation reaction. Benzylation of aromatics (benzene, toluene and *o*-xylene) was achieved using benzyl chloride as the alkylating reagent. The influence of different reaction parameters on the catalytic activity and selectivity was subjected to investigation. The reusability of the catalytic systems was also checked. Attempt has been made to correlate the catalytic activity with the surface acidic properties of the catalyst systems and plausible mechanisms have been drawn out based on the experimental observations.

Chapter 5 illuminates the application of supported vanadia systems and its sulfated analogues as efficient catalysts for the vapour-phase Beckmann rearrangement of cyclohexanone oxime, an industrially important reaction for the production of ε-caprolactam. Here also, the variation in the catalytic activity and product selectivity with experimental parameters has been taken care of.

Chapter 6 narrates the catalytic test results of selective oxidation reactions such as liquid-phase oxidation of cyclohexanol to cyclohexanone and vapour-phase oxidative dehydrogenation of ethylbenzene. The catalytic activity and selectivity of all the systems were screened after optimizing the reaction conditions. There was also an attempt to correlate the results obtained with the nature of surface vanadium oxide active species presented by the characterization results.

The key points emerging from the investigations are given at the end of each chapter as conclusions.

Chapter 7 presents the summary and important general conclusions of the present work.

7.2 CONCLUSIONS

The conclusions that can be drawn from the present investigation are the following.

- Vanadia incorporation and sulfate modification improve the physico-chemical characteristics and surface properties of pure tin and zirconium oxides. The major outcome includes enhancement of surface area and stabilization of the catalytically active tetragonal phase. The surface area increases with vanadia loading, reaches a maximum and then decreases.
- Vanadia incorporation and sulfate modification decrease the particle size significantly and is clear from the SEM analysis. While the non-sulfated samples are thermally stable at very high temperatures, the sulfated systems are found to be stable only up to 700°C due to the decomposition of the sulfate groups.
- Different characterization techniques like FTIR, ^{51}V NMR and DR UV-VIS identify the surface vanadia as mono-oxo species, which is found to be existing as isolated tetrahedra in the low loaded samples. The presence of octahedral vanadium oxide species along with crystalline vanadia is prominent in high vanadia containing samples.
- The surface acidic properties of the supports considerably improve upon vanadia addition and also due to the surface modification by sulfate anions. Good correlation is observed among the surface acidities measured by the three independent techniques such as ammonia TPD, perylene adsorption and vapour-phase cumene cracking reaction.
- Friedel-Crafts alkylation reaction of arenes using benzyl chloride as the alkylating agent, is taking place very efficiently over the prepared systems. A very high selectivity to the monoalkylated product is obtained in all the cases. Thorough analysis of the acidity values obtained by different techniques and the benzylation reaction data indicates the involvement of the Lewis acid sites in the reaction.
- Supported vanadia systems and its sulfated analogues prove to be efficient catalysts for vapour phase Beckmann rearrangement of cyclohexanone oxime leading to the formation of ε-caprolactam. In this case conversion

of cyclohexanone oxime is observed to be a function of the acidity of the system.

- Cyclohexanol oxidation proceeds efficiently over all the systems. All systems exhibit 100% selectivity to cyclohexanone, which is indicative of the selective oxidation capacity of the developed catalysts.
- Vapour-phase oxidative dehydrogenation of ethylbenzene over the catalytic systems results in the formation of styrene with high selectivity. Parameters like reaction temperature, molar ratio, feed rate, etc. profoundly influence the catalytic activity and product selectivity.

Future Outlook

An overview of catalysis by transition metal oxides in general and supported vanadia catalysts in particular reveals that we have been able to prepare and design catalysts for achieving proposed targets by adopting ingenious and innovative scientific approach. In the three years of this Ph.D. research work, we have learned a lot about the nature of supported vanadia catalysts using SnO_2 and ZrO_2 metal oxide supports. The results of the present investigations reveal that there can be ample scope for planning strategic research for the preparation and development of supported vanadia with other support materials and its application for the production of olefins by oxidative dehydrogenation of alkanes, methanol and formaldehyde by partial oxidation of methane and industrially important nitriles by ammoxidation of alkyl aromatics/ heteroaromatic hydrocarbons and also for selective catalytic reduction (SCR) of NO_x with ammonia. Since the present systems are found to be very effective for Friedel-Crafts and Beckmann rearrangement reactions, which are acid-catalyzed, work can be extended to study various industrially important acid-catalyzed alkylations and rearrangements of other aromatic molecules. Beckmann rearrangement with these systems can be designed to get hydrocarbostyril derivatives of indanones, which are the key intermediate for developing neuotransmitters.